

Response to the referee comments on the manuscript originally titled “Evaluating the value of a network of cosmic-ray probes for improving land surface modelling” by Baatz et al. on behalf of all co-authors submitted to *Hydrology and Earth System Sciences – Discussion*.

We thank the Editor for his guidance through the revision process.

We thank the reviewers for their time reviewing the manuscript and their suggestions for improving the manuscript. We appreciate their constructive comments and changed the manuscript in the following main points:

- All comments of the reviewers were addressed throughout the manuscript
- Three new experiments with four instead of nine cosmic ray neutron sensors were conducted
- Two new experiments with the FAO soil map were conducted
- These additional five experiments were addressed/included in Abstract, Introduction, Methods, Results & Discussion, Conclusion
- “Discussion” was merged into results section; now “Results and discussion”
- The Tables with detailed site-wise results were moved into the Annex, and two shorter summarizing Tables were included instead. This reduces length and increases readability of the results section.
- Introduction and Results were shortened, as suggested by the reviewers
- Discussion was improved including results on evapotranspiration and new important references

The title of the manuscript was changed as suggested by Referee #1 and #3 to “Evaluation of a cosmic-ray neutron sensor network for improved land surface model prediction”.

Sincerely,

Roland Baatz and co-authors

Text formats:

**Referee – bold**

Answer of the authors – non-bold

**Reviewer 1**

**Received and published: 14 September 2016**

#### **GENERAL COMMENTS**

The manuscript is well written and clear. The topic is of interest for the HESS readership as cosmic-ray probes represent a relatively new technology for ground measuring soil moisture over large areas. Therefore, we need to assess the impact of this new technology for improving land surface modelling. The paper describes several assimilation experiments in which soil moisture data from cosmic-ray probes are used for improving soil moisture modelling through CLM land surface model. Results are (quite) well described and clearly structured. However, in my opinion, several aspects should be improved/changed before the publication. I reported below a list of the general comments to be addressed with also the specification of their relevance.

Thank you for your positive evaluation and for your time reviewing this manuscript. We carefully address your comments in the following.

**1) MAJOR: Some of the results shown in the paper are well-known. I am aware that it is important to show real-world experiments, mainly by considering new technology, but the main results given in the paper were already reported in several previous studies: a) the assimilation of ground-based soil moisture data is able to improve soil moisture modelling, b) the joint state-parameter assimilation is better than the state assimilation only, and c) the assimilation is more effective when soil texture information are wrong (i.e., there's larger room for improvement). I believe that the paper results need to be published, but I would like to see some new findings that can be obtained by using the same material (data and modelling) presented in the paper.**

Thank you, we understand that the novelty of this paper needs to be more clearly pointed out. The main novelty is the use of the cosmic ray probe to measure soil moisture at the intermediate scale and update soil moisture at the larger catchment scale. Although it is true that points a, b and c have been demonstrated in other papers, this has never been done for the cosmic ray probe at the larger catchment scale. We added now begin the abstract with:

Page 1 line 5: "In this study, the potential of a network of CRNS installed in the 2354 km<sup>2</sup> Rur catchment (Germany) for estimating soil hydraulic parameters and improving soil moisture states was tested."

CRNS, catchment wide, used for parameter updates, this is clearly novel.

Another key finding was pointed out in the abstract, where we quantified the possible improvement of soil moisture prediction using a land surface model:

Page 2 line 11-14: “For the FAO soil map and the biased soil map soil moisture predictions improved strongly to a root mean square error of  $0.03 \text{ cm}^3/\text{cm}^3$  for the assimilation period and  $0.05 \text{ cm}^3/\text{cm}^3$  for the evaluation period. Improvements were limited by the measurement error of CRNS ( $0.03 \text{ cm}^3/\text{cm}^3$ ). “

Demonstrating a way to propagate CRNS measurements into horizontal space using the local ensemble transform Kalman Filter is novel. The improved parameterization in catchment space was not demonstrated before. Therefore we state in the abstract:

Page 2 line 15-17: “The results demonstrate that assimilated data of a CRNS network can improve the characterization of soil moisture content at the catchment scale by updating spatially distributed soil hydraulic parameters of a land surface model.”

**For instance:**

**A) What are the results if only one (or two) cosmic-ray probes are assimilated? In the real world it is expected that the number of probes will be limited and, hence, the use of a limited number of probes is surely of great interest.**

Thank you for the suggestion. Many further (synthetic) studies are possible, but a publication generally has limited space available. However, we add to the manuscript three additional simulation experiments with a smaller number (four) of cosmic ray neutron sensors for assimilation. This allows verification at the five remaining cosmic ray neutron sensors. Please see the manuscript for further details.

**B) What is the impact in terms of fluxes? In section 4.6 a comparison of annual evapotranspiration maps without and with the assimilation is carried out, but simply showing that the resulting maps are different.**

Thank you. We agree that the figure demonstrates an impact of soil moisture and soil parameter updates on latent heat flux during the evaluation period. We added more information to the caption:

Page 35 line 1: “Annual evapotranspiration (ET) is shown in the year 2013 (evaluation period, no assimilation). This figure demonstrates the impact of parameter updates (PAR-S80-10 and PAR-BK50-10) in comparison to open loop (OL-S80) and reference soil map (OL-BK50). ET changes in the North but not as much in the South.”

**However, it is obvious that changing soil moisture will change evapotranspiration. Is it possible to perform an independent validation by using data about the actual evapotranspiration in the basin? Or likely by using discharge observations? I believe that some new results should be included in the paper (even though I am aware that authors are usually reluctant to perform additional analyses). Moreover, the results in terms of soil moisture simulation should be synthetized (see Comment 5).**

We agree that a comparison to evapotranspiration (ET) observations would be beneficial. However, a comparison of catchment ET or observed ET at a representative number of sites is beyond the scope of this paper because uncertainties in upscaling of ET are large. Impacts on ET are discussed in a paragraph:

Page 20 line 25-page21: “Additionally, the impact of soil parameter estimates on ET is different in the North of the catchment compared to the South. While ET in the North of the catchment was impacted by

the estimated soil properties during the evaluation period 2013 for PAR-S80-10, ET in the South was not as much impacted by estimated soil properties. This is related to the fact that in the North ET is moisture limited in summer, whereas in the South this is not moisture limited but energy limited. Therefore, ET in the North is sensitive to variations in soil hydraulic parameter values, whereas in the South this is not the case. In the South, ET is sensitive to model forcings like incoming shortwave radiation. Nearing et al. (2016) came to the conclusion that soil parameter uncertainty dominates soil moisture uncertainty and forcing uncertainty dominates ET uncertainty. Our findings in the southern part of the catchment support their conclusion, but in the northern part of the catchment soil parameter uncertainty strongly affect ET. Hence particularly in the northern part of the catchment, further observations such as ET measurements are desirable for further improving the land surface model. These additional observations could be used for future land surface model benchmarking (Best et al., 2015) or for more constrained parameter estimates (Shi et al., 2015)."

**2) MAJOR: The description of the data assimilation experiments should be improved. As usually, a number of subjective choices were made in the setup of the data assimilation experiments, and these choices may have a significant impact on the results. For instance, a fixed error for soil moisture estimates from cosmic-ray probes is considered (0.03 cm<sup>3</sup>/cm<sup>3</sup>). Similarly, the perturbation factors for input data (precipitation and shortwave radiation) and parameters (10 and 30%) are arbitrarily selected. A sensitivity analysis on these choices should be carried out. It might be that different choices produce very different results.**

Thank you for these constructive suggestions. We agree that a number of assumptions needed to be made. The assumption on the measurement error for the soil water content was thoroughly evaluated and more details can be found in our earlier papers on this (e.g., Bogaen et al., 2013; Baatz et al., 2014; Baatz et al., 2015). We feel that there is no need to repeat experiments with other values for the measurement error given the earlier work:

Page 13 line 24: "Based on previous work (Baatz et al., 2015), the SWC retrieval uncertainty for CRNS was estimated to be 0.03 cm<sup>3</sup>/cm<sup>3</sup> while fluctuations in the measurement standard deviation, related to the non-linear relation between observed neutron intensity and SWC, were assumed negligible."

However, we agree that perturbation of meteorological forcings and soil hydraulic parameters are subject to larger uncertainty. We applied a 10% and 30% perturbation and think covers adequately the uncertainty with respect to texture. Simulations were not strongly affected by the magnitude of the soil perturbations:

Page 15 line 25-28: "The  $E_{RMS}$  and bias for simulations with 10 % and 30 % perturbation of soil texture only showed very small differences (smaller than 0.01 cm<sup>3</sup>/cm<sup>3</sup>)."

We feel that the applied perturbations are realistic and the difference in the two applied perturbations was already large.

We also already tested two different magnitudes of perturbation of precipitation, including a 50% and 100% error but this did not affect the simulation results:

Page 13 line 23: "In this work, only results for precipitation perturbation with  $\sigma = 0.5$  will be shown as results for  $\sigma = 1.0$  were similar."

The simulations are also CPU-intensive. We expect that an extension of the experiments for further magnitudes of perturbation would not supply significant additional insights.

**3) MODERATE: Similarly as above, the selection of one single biased soil texture map is arbitrary. Why only one soil map? Why 80% of sand content and 10% of clay content is selected? What is the average sand and clay content percentage in the basin? Again, a sensitivity analysis is needed. Otherwise, it might be that a very large error in the soil map is used to highlight the positive impact of assimilating soil moisture data. What happens for a less biased map? This aspect should be clarified.**

Thank you for this suggestion. In the revised version, we include a simulation with a third (FAO) soil map that may be close to the expected values of the BK50 soil map. Table 1 shows the sand content at the nine sites for the BK50 soil map. We added information on catchment wide average sand and clay content, and what was the motivation to select the biased soil map as initial soil map in part of the simulation experiments:

Page 12 line 15-18: "Alternative simulations were also performed with the FAO soil map of the global Harmonized World Soil Database (FAO, 2012) and with a biased soil texture with a fixed sand content of 80 % and clay content of 10 % (S80 soil map). Average sand and clay content are 22.5% and 21.4% for the BK50 soil map and 39% and 22% for the FAO soil map. The FAO soil map and the biased soil map represent large error with respect to the soil properties of the BK50 soil map."

The new simulation results with the FAO soil map are discussed in detail.

**4) MINOR: In CLM the subsurface lateral flow is not considered. It has an impact on soil moisture simulation and, mainly, on the capability to modify soil moisture simulations at unmonitored locations. Therefore, I expect that the assimilation of in situ soil moisture data will have a local effect. However, the jackknifing data assimilation experiments show that the assimilation produces significant changes also at unmonitored locations. Why does it happen? I believe it should be clarified in the paper.**

Thank you for this detail. It is correct that CLM does not consider subsurface lateral flow. The updates of soil moisture in space depend on spatial correlations of soil moisture. In this study, spatial correlations of soil moisture are the consequence of spatial correlations of the atmospheric forcings, spatial correlations of soil hydraulic parameters and their interaction with the land surface model. Atmospheric reanalysis data and the soil map provided a good basis for the imposed spatial correlation structure. The imposed

spatial correlation structures on the perturbations determine to a large extent the soil moisture updates in space. We added:

Page 17 lin 27-29: "Spatial improvements are possible by spatial correlation structures of atmospheric forcings, soil hydraulic parameters and soil moisture which are taken into account by the local ensemble transform Kalman filter."

**5) MINOR: In sections 4.2 and 4.5, too many details are provided in the description of the results for each single site. I suggest focusing on the most important results to improve their readability. Also, discussion section is too generic, especially the first paragraph. In the specific comments, I added some corrections and suggestions that should be implemented. On this basis, I believe the paper deserves to be published only after a major revision.**

Results section and discussion section were shortened and sharpened, also taking into account the detailed comments of reviewer #3. We also merged the Results and Discussion section into one section for more fluent reading.

**SPECIFIC COMMENTS (P: page, L: line or lines) Title: The paper, in the current version, demonstrates that the assimilation of soil moisture data from cosmic-ray probes is able to improve soil moisture modelling, not "land surface modelling" (e.g., evapotranspiration or discharge fluxes). Therefore, I suggest changing the title. Abstract: The abstract should include information on the location of the study area and on the employed data assimilation technique.**

Thank you.

We changed the title to:

"Evaluation of a cosmic-ray neutron sensor network for improved land surface model prediction."

We now include the employed data assimilation technique and the location of the study area in the abstract:

Page 2 line 4-9: "In this study, the potential of a network of CRNS installed in the 2354 km<sup>2</sup> Rur catchment (Germany) for estimating soil hydraulic parameters and improving soil moisture states was tested. Data measured by the CRNS were assimilated with the local ensemble transform Kalman filter in the Community Land Model v. 4.5."

**P4, L7: Formatting error for Kurtz et al. (2016). Please correct.**

Thank you. We corrected this.

**P5, L19: It should be COSMIC in place of COMIC.**

Thank you. We corrected this.

**P12, L11: Is  $\sigma=0.5$  considered for perturbing precipitation in all the assimilation**

**experiments? Please clarify.**

Yes. We agree that this was slightly unclear and moved the sentence to the right position in the text.

**P12, L25: It should be “four data assimilation scenarios” in place of “six assimilation scenarios”.**

Thank you. We changed this:

Page 15 line 10: “Presented are results for the open loop scenarios with the BK50, FAO and S80, and data assimilation scenarios.”

**P19, L18-19: This sentence is too broad, please modify.**

Thank you. We agree and changed the sentence to:

Page 22 line 6-8: “Hence, this study represents a way forward towards the integration of CRNS information in the calibration or real-time updating of land surface models. “

## Anonymous Referee #2

Received and published: 23 September 2016

### GENERAL COMMENTS

The authors present an interesting and important study on investigating the benefits of integrating CRNP in data assimilation to improve atmospheric/land surface modeling. While I am not a data assimilation expert, this clearly seems to be a path forward on showing the importance and utilizing long-term monitoring networks for societal benefits. This is a novel study on using a network of CRNP to improve catchment water and energy balance. The authors show the utility of a network on CRNP on improving SWC states and soil parameter estimates in areas with poor or low meteorological coverage and soil information. While the paper is generally well written the authors missed some key references to put this work into proper context. In particular, the recent paper on the Plumber experiment of LSMs (Best 2015) and follow up paper on information content (Nearing 2016) should be discussed in light of this papers major findings. With these additional modifications the paper is appropriate for publication in HESS.

Thank you for your positive evaluation and reviewing this manuscript. We added two suggested references relevant to the manuscript. Please see below.

#### Major Comments.

1. The recent paper by Best (2015) on the plumbing of LSMs needs to be discussed in the introduction and discussion. In addition, the follow up paper by Nearing (2016) on discussing the information content of LSMs is critical. Most notably, their findings on the importance parameterization, model physics, and boundary conditions affecting the partitioning of sensible and latent heat, and comparisons between a SWC benchmark are important. The authors need to discuss these results and how their findings agree or disagree with Best (2015) and Nearing (2016). (e.g. Pg. 3 L 12, Pg. 17 L 13, conclusions). Without this it is hard to place this work in its proper context for critical evaluation. 2. The work of Avery (2016) should also be discussed given the importance of soil and vegetation parameters discussed in this manuscript. This and point 1 will help update the referencing to be most up to date. (e.g. Pg. 10 L 25, Pg. 18 L 18).

Thank you. We agree that the study of Nearing et al. (2016) and Best et al. (2015) is related to this work. We add to the discussion:

Page 20 line 31-page21: "Nearing et al. (2016) came to the conclusion that soil parameter uncertainty dominates soil moisture uncertainty and forcing uncertainty dominates ET uncertainty. Our findings in the southern part of the catchment support their conclusion, but in the northern part of the catchment soil parameter uncertainty strongly affect ET. Hence particularly in the northern part of the catchment, further observations such as ET measurements are desirable for further improving the land surface model. These additional observations could be used for future land surface model benchmarking (Best et al., 2015) or for more constrained parameter estimates (Shi et al., 2015)."

We also found the reference of Avery et al. (2016) being useful and added:

Page 10 line 19: "This would require calibration data throughout the catchment which is only feasible using spatially distributed data sets (e.g. Avery et al., 2016)."

**Minor Comments:**

**Pg 4. L 6. The cases illustrate a way. . .**

Thank you. We changed this.

**Pg 4. L 15-16. Sentence is awkward please revise.**

Thank you. We rephrased:

Page 4 line 32-page5: "They showed that the nonlinear character of the soil moisture retention characteristic is critical for joint state-parameter estimation in data assimilation systems and showed that the Particle Filter is an interesting alternative for soil hydraulic parameter estimation for 1D problems."

**Referecnes:**

**Avery, W., C. Finkenbiner, T. E. Franz, T. Wang, A. L. Nguy-Roberston, A. Suyker, T. Arkebauer, and F. Munoz-Arriola. 2016. Incorporation of globally available datasets into the roving cosmic-ray neutron probe method for estimating field-scale soil water content. HESS 20: 3859-3872. doi:10.5194/hess-20-3859-2016.**

**Best, M. J., G. Abramowitz, H. R. Johnson, A. J. Pitman, G. Balsamo, A. Boone, M. Cuntz, B. Decharme, P. A. Dirmeyer, J. Dong, M. Ek, Z. Guo, V. Haverd, B. J. J. Van den Hurk, G. S. Nearing, B. Pak, C. Peters-Lidard, J. A. Santanello, L. Stevens, and N. Vuichard. 2015. The Plumbing of Land Surface Models: Benchmarking Model Performance. J. Hydrometeorol. 16:3: 1425-1442. doi:10.1175/jhm-d-14-0158.1.**

**Nearing, G. S., D. M. Mocko, C. D. Peters-Lidard, S. V. Kumar, and Y. L. Xia. 2016. Benchmarking NLDAS-2 Soil Moisture and Evapotranspiration to Separate Uncertainty Contributions. J. Hydrometeorol. 17:3: 745-759. doi:10.1175/jhm-d-15-0063.1.**

**Anonymous Referee #3**

**Received and published: 27 September 2016**

## **GENERAL COMMENTS**

The presented manuscript applies time-series data from 9 cosmic-ray neutron stations to the land-surface model CLM in the Rur catchment. The authors assimilate the data using an ensemble Kalman filter technique to update states and parameters of their model. The added value of training data in years 2011 to 2012 is assessed (1) by testing the model performance in year 2013, (2) by testing the model adaption capabilities to an invalid soil map, and (3) by jackknifing single stations from the training period. The application of the cosmic-ray neutron method in large-scale models is one of the challenges in state-of-the-art hydrology and thus the present study is worth to be published in the scope of HESS after major revision.

Thank you for your positive evaluation. We sincerely appreciate your time reviewing the manuscript. We carefully addressed your suggestions and comments to further strengthen the manuscript.

### **1 Evaluating the overall quality**

Large parts of the manuscript are written in the style of a protocol, by listing lots of other publications who used similar approaches, by mentioning tools that were used, and by reporting every step of the performed analysis. However, I believe that scientific articles should be entitled to challenge their own strategy by discussing alternative methods, by justifying their selection of tools and decisions, and by explaining the corresponding implications. I would thus recommend to rewrite and extend major parts of the introduction and method section. Therein, some literature reviews are unnecessary and probably unrelated to the study and can be omitted or need further explanation (see line-by-line comments). Here, I would suggest to follow the guideline that cited papers should be discussed, and not just mentioned. Other parts concerning the data integration and the SWC model need to be described in more detail. I would further recommend to reduce the detail of the results section, which is hard to follow without proper discussion, and thus to merge it with the discussion section. The results of the study were well structured and described, but are not entirely novel, and not sufficient to provide answers to all research questions raised by the authors. For example, to assess the value of a CRNS network of certain density to the performance of a land-surface model, various fractions of the 9 stations should be tested as requested by Referee #1.

We shortened and sharpened the indicated parts of the manuscript to further increase its readability. Where appropriate, we added additional discussion to the mentioned references. In the revised version we state more clearly, how the research questions were answered by this study.

As pointed out in the answer to Referee #1, new simulations were run with a more limited number of cosmic-ray neutron sensors (4) to emphasize the additional value of a network of CRNS using five CRNS for evaluation and with a third soil map.

Furthermore, the study uses some questionable assumptions, like a constant error of soil moisture data (although neutron measurement uncertainty highly varies with wetness condition), or the

assimilation of SWC data assuming homogeneous vertical profiles and no changes of seasonal biomass (see line-by-line comments for details). Another questionable approach is to allow static site-specific parameters to be variable in time, e.g., hydraulic conductivity or soil porosity.

Thank you. We address these questions exhaustively in the line-by-line comments in the following pages.

This is highly counter-intuitive and should be discussed with respect to uncertain data and/or model conceptualization. I agree to most of the general comments made by Referee #1 and will thus compensate the previous reviews by detailed line-by-line comments below.

## 2 Line-by-line comments, scientific questions/issues, and technical corrections

- Title (“Evaluating the value of a network of cosmic-ray probes for improving land surface modelling”): I’d suggest to remove “the value of” to simplify the title. Furthermore, state observations usually do not improve a model, they rather improve model results, e.g. predictions.

Thank you for this suggestion. We agree and suggest to change the title towards:

“Evaluation of a cosmic-ray neutron sensor network for improved land surface model prediction”

### Page 2

- L1: “Land surface models can model”: bad phrasing, replace “can model” e.g. by “describe”.

We changed this to “describe”.

- L3: “CRP”, please use the newly accepted abbreviation CRNS (cosmic-ray neutron sensing/sensor) with regards to the recent 5th COSMOS workshop.

We agree and changed this throughout the manuscript.

- L14: improve readability, split in two sentences.

Thank you, we did split the sentence.

- L18: please add a statement about the impact of your findings for the scientific community.

The impact on the scientific community can only crystalize after publication. The expected scientific impact is highly speculative and in my opinion not suitable for the abstract.

We conclude the abstract with the key finding summarizing the detailed results of the study in a general way and think this is sufficient for the abstract:

“The results demonstrate that assimilated data of a CRNS network can improve the characterization of soil moisture content at the catchment scale by updating spatially distributed soil hydraulic parameters of a land surface model.”

- L21-22: this sentence needs a reference.

We added: Brutsaert, W.: Hydrology : an introduction, Cambridge University Press, Cambridge ; New York, xi, 605 p. pp., 2005.

- L24: " and is "→ “while it is”

We changed this.

- **L27-28: the given number of references here appears to overwhelm the statement and its low relevance to your paper. Please use only the 1 or 2 most important citations.**

We agree and removed some references of less relevance.

- **L30-31: Please discuss the alternatives in more detail to strengthen your decision to use CRNS technology. Were space-borne remote-sensing products assimilated to LSMs before? Why wasn't it successful? What about the use of airborne products with higher resolution and depth? You could also mention point-scale or large-scale soil moisture monitoring networks which have been used for evaluation of land surface models.**

These methods were successful in some cases, but have deficiencies particularly in respect to dense vegetation as mentioned here:

Page 2 line 31-page3: "Soil moisture measured by space-borne remote sensing technologies provides information over large areas but is strongly affected by vegetation and surface roughness (e.g. Temimi et al., 2014). Therefore, in this paper an alternative source for soil moisture information is explored which can measure soil moisture more accurately under dense vegetation (Bogena et al., 2013)."

We mention successful applications of remote sensing data e.g. here:

Page 3 line 27: "Reichle et al. (2002) performed a synthetic experiment using L-band microwave observations of the Southern Great Plains Hydrology Experiment (Jackson et al., 1999) to analyse the effect of ensemble size and forecast errors."

And here:

Page 3 line 32-page4: "More recently, state updates with the EnKF were tested for the Soil Moisture Ocean Salinity (SMOS, Kerr et al., 2012) mission. De Lannoy and Reichle (2016) assimilated SMOS temperature brightness and soil moisture retrievals into a land surface model with large improvements in surface soil moisture."

Following your previous argumentation on limiting the introduction to relevant publications, we constrain the introduction to cosmic-ray neutron sensors, mentioning alternative techniques. Additionally, we give a limited overview on important literature of earlier work done particularly on methods used in this study.

- **L31: "not reliable for areas with dense vegetation": a paper by the same first author recently found that CRNS is also influenced by dense vegetation. Is it more reliable?**

Yes, CRNS are more accurate under dense vegetation than remote sensing products. We added:

Page 2 line 31: "Soil moisture measured by space-borne remote sensing technologies provides information over large areas but is strongly affected by vegetation and surface roughness (e.g. Temimi et al., 2014). Therefore, in this paper an alternative source for soil moisture information is explored which can measure soil moisture more accurately under dense vegetation (Bogena et al., 2013)."

- **L33: the selection of citations for this statement appears to be random/unrelated. If you want to provide references for the "intermediate scale", Zreda 2008 and Köhli 2015 might be appropriate.**

We state this more precise now:

Page 3 line 3-5: “Cosmic-ray neutron sensors (CRNS) measure fast neutron intensity at an intermediate scale of ~15 ha (Kohli et al., 2015;Zreda et al., 2008) which is the desired application scale of land surface models (Ajami et al., 2014;Chen et al., 2007;Shrestha et al., 2014).”.

- **L34: “desired application scale of land surface models”:** please make the reader happy by finally providing concrete information. What is the scale? Are you talking about centimeters or lightyears? Please do not use citations inflationary and do not keep them untouched. How do the three citations help you to support your argumentation?

Thank you, we are precise by now stating the observation scale (15ha, see comment before), but the model resolution is stated in the methods section which is common sense in literature of hydrologic modelling.

### Page 3

- **L1: omit “fast” as it repeats with the next sentence.**

In accordance with your following comment, we prefer to stay clear and keep “fast”:

Page 3 line 5-8: “Fast neutrons originate from collisions of secondary cosmic particles from outer space with terrestrial atoms. Fast neutrons in turn are moderated most effectively by hydrogen because the mass of a neutron is similar to that of a nucleus of the hydrogen atom.”

- **L3: add “fast” to make clear that the sensor measures the non-moderated neutrons.**

We added “fast”.

- **L4: “15 ha”, your SWC range seems to be 10 to 40%, which leads to an approximate CRNS footprint of 7 to 14 ha following Köhli 2015, excluding vegetation and altitude influence. You could write “maximum area of 15 ha” to circumvent mentioning this variability.**

Thank you for the suggestion. We see your point, however, the newest research is not always carved into stone and figures are evolving as research continues and is discussed. Take for example the all very recent publications that address the cosmic ray neutron sensor footprint defined to 300m radius (Zreda et al., 2008), 300m radius and less (Desilets and Zreda, 2013, on the footprint specifically) and 200m radius and less (Kohli et al, 2015 on the footprint specifically).

However, this is not a major focus of this study. We changed to:

Page 3 line 4: “intensity at an intermediate scale of ~15 ha (Kohli et al., 2015;Zreda et al., 2008)”

- **L6: omit “Desilets and Zreda, 2013” as it does only marginally address heterogeneous averaging. Franz 2013a is already a great reference to this topic, Köhli 2015 also touched this.**

We agreed and changed to:

Page 3 line 11: “are averaged over a larger area (Franz et al., 2013a; Kohli et al., 2015).”

- **L8: Bogena et al. 2013 did not perform simulations to the penetration depth. Instead, Franz et al. 2012 (doi:10.1029/2012WR01187) and Köhli et al. 2015 provided simulations that both support these values.**

We changed this:

Page 3 line 12-15: "Vertical measurement depth ranges from a maximum of ~70 cm under completely dry conditions and decreases to roughly ~12 cm under wet conditions (e.g. 40 vol. % soil moisture) (Kohli et al., 2015; Franz et al., 2012)."

- **L11: add a reference for COSMOS-UK, Evans et al. 2016, 10.1002/hyp.10929**

Thank you. We added:

Page 3 line 17: "and the British COSMOS-UK (Evans et al., 2016)."

- **L13-15: please rephrase to make clear what data assimilation is and is not.**

Thank you. We rephrased:

Page 2 line 28: "Data assimilation of soil moisture provides a way to improve imperfect land surface model predictions. Here, soil moisture measurements are used to update model predictions by optimally considering the uncertainty of model initial conditions, model parameters and model forcings. "

- **L15: It is not clear why you choose EnKF. Please at least mention other techniques and provide reasons for your choice. The sentence further should be moved to the end of the paragraph after you have introduced the history of DA.**

We added:

Page 3 line 23: "The EnKF is much less CPU intensive compared to alternative methods such as the particle filter (e.g. Montzka et al., 2011) because for high dimensional problems the EnKF requires a much smaller ensemble size to achieve reasonable good predictions. "

We considered moving the 'sentence further', but find it is located well at that spot.

- **L16-34: This historical overview appears to be unnecessary in the context of your study. Neither do you explain what things like "four-dimensional variational DA" are, nor is the relation to your work described. Furthermore, citations are used inflationary again. Please reduce this paragraph to the key publications which support your study. Also think about moving certain studies about ensemble size, multiple time steps, and other filtering approaches to the methodology section, where you need justification for your approach.**

Thank you. We shortened the literature review slightly, but include previous work on state updates and joint state-parameter updates.

- **L30-32: Just to emphasize the previous comment, these lines particularly carry no information for non-experts due to the lack of explanation.**

Thank you. We removed this section out.

Page 4

- **L1-19: As stated before, the whole literature review appears to be random and irrelevant to your work. Or at least the relations are not explained. For example, work from Montzka 2011;2013 and Han 2014b appear to be of some relevance for you, prior to others.**

The literature review puts this work into the context of soil moisture data assimilation and the joint state-parameter estimation. We may be too broad for you in this literature review but may not be too broad for other reviewers who desire a literature review.

- **L23-24: “Its capability to propagate surface soil moisture information into the deeper soil column was analyzed by Rosolem et al. (2014)”, what does this sentence mean?**

We rephrase:

Page 5 line 21-25: “The surface soil moisture information was propagated into greater soil depth than only the measurement depth using COSMIC in combination with data assimilation (Rosolem et al., 2014).”

- **L26: “The COSMIC operator”, third repetition as a sentence starter.**

We reformulated

- **L27-29: combine those sentences: “neutron observations have been used to update states (. . . ) and hydraulic parameters (. . . )”**

We considered to combine the sentences but it is better as is:

Page 5 line 24-28: “Neutron counts measured by CRNS have been used in data assimilation studies to update model states (Han et al., 2015; Rosolem et al., 2014). Soil hydraulic parameters were also updated by assimilation of neutron counts in one synthetic study (Han et al., 2016), showing its feasibility.”

- **L29: “showed” → “demonstrated”**

We changed.

- **L29-30: be more correct in phrasing. Rephrase that Villarreyes 2014 used a different model, but also estimated hydr. parameters by inversion.**

We state:

Page 5 line 27: “CRNS were also used for inverse estimation of soil hydraulic parameters of the Hydrus-1D model (Villarreyes et al., 2014).”

- **Han 2016 did so too, using support from neutron data, but neutron assimilation alone does not “update” a hydraulic parameter.**

We rephrase:

Page 5 line 24: “Soil hydraulic parameters were also updated by assimilation of neutron counts in one synthetic study (Han et al., 2016), showing its feasibility.”

- **L31: “This work further explores”, omit “further”. Until now it is not clear what this work does, you only told stories about work of others. Please summarize which of the presented approaches you are picking up and what scientific novelty you add.**

“This work further...” links to the previous paragraph and the meaning of “further” means to expand the work that has been done by the community, not necessarily by the authors themselves. It is placed correctly in this context.

## Page 5

- **L3-4: “the soil moisture characterization at the larger catchment scale”, what exactly is meant by these terms, and how do you measure improvement?**

Thank you. We removed “larger” and hope this is clearer now.

- **L4: “how dense the CRP network should be”, do you answer this question?**

Thank you. We removed this question, as this should be addressed in a synthetic study and is most probably catchment specific.

- **L7-8: “soil maps and atmospheric forcings show spatial correlations over larger distances”, this is an interesting point, please provide reference. Isn’t the largescale heterogeneity of soil maps only an artefact of soil data scarcity?**

These correlations are generated by large scale atmospheric processes, geomorphology, vegetation, and last but not least anthropogenic activities such as land use. We added three relevant references:

Page 6 line 6-9: “On the other hand, soil moisture, soil maps and atmospheric forcings show spatial correlations over larger distances (Kirkpatrick et al., 2014;Korres et al., 2015) which suggests that CRNS measurements potentially carry important information to update soil moisture contents for larger regions (e.g. Han et al., 2012).”

- **L9: “10 stations”, do you assimilate all 10, or just 9?**

Thank you. We corrected this, it is nine stations.

- **L15: “feasibility of the updated large scale soil hydraulic parameters”, how can a parameter be feasible? Please clarify your novel research question.**

We removed “of the feasibility”.

- **L18-19: The sentences can be omitted as being obvious.**

We prefer to keep these sentences.

## Page 6

- **L6: correct wording, a “process” can not be “solved”**

We rephrased:

Page 7 line 10: “Some of the key processes which are modelled by CLM are radiative transfer...”

- **L10: “Oleson et al. (2013) provide further details on CLM4.5”, redundant information with regard to L5-6.**

Thank you. We removed this sentence.

- **L10-12: provide reasons why you artificially limit the scope and complexity of your study. What process would a “biogeochemical module” have added and why are they not important here compared to a prescribed LAI?**

This would be beyond the scope of this study as invoking the biogeochemical module would require a model spin-up of 1000 years for the catchment. It would have allowed to model vegetation development

dynamically and model the biomass development. It was however already explained elsewhere in this response letter that little additional gain is expected from this, which would not have balanced the great additional complexity introduced in the modelling process. We added:

Page 7 line 15-19: "To limit the scope and complexity of this study, CLM was run using satellite phenology e.g. prescribed leaf area index data and the biogeochemical module turned off. The biogeochemical module allows CLM to model the vegetation development dynamically, but it requires a large spin-up of 1000 years and little additional gain is expected for this study from these additionally modelled processes."

- **L14: please finally (after lots of references in the introduction) provide concrete information about the grid size in your study (the reader is still lost between centimeters and lightyears)**

In hydrologic literature it is common to provide the numbers for the model setup in the corresponding section. We added there:

Page 12line 10-11: "The model of the Rur catchment was spatially discretized by rectangular grid cells of 0.008 degree size (~750 m)."

- **L23: use standard format for functions,  $k[z] \rightarrow k(z)$**

Thank you, changed

- **L24: format  $z \rightarrow z$**

We modified.

- **L24: what is the difference between "soil moisture" and SWC? Why are you using the expression  $\theta$  here, while SWC is used elsewhere (e.g., eqs. 24 and 25)?**

Thank you. Agreed. We changed the term SWC in Eqs. 24 and 25.

- **L25: use the more convenient expression  $k_{\text{sat}}(z)$ ,**

We agree and modified it.

- **L26 (eq. 1):**

– format  $k[z] \rightarrow k(z)$ ,

Agreed.

– rewrite  $k_{\text{sat},z} \rightarrow k_{\text{sat}}(z)$  as this is a functional relationship. In contrast, indexing a state variable  $\theta_i$  is ok.

We agree and modified it.

– omit occurrences of 0.5 since  $\frac{0.5}{0.5} \approx 1$ ,

Agreed.

– case conditions (e.g.,  $1 < i < N \dots$ ) are usually preceded by a comma in each line

We added comma.

– the curly bracket on the right is not common in multi-case equations.

Thank you. We removed it.

- **eq. 3 and 5: reformat sand → sand, same for clay.**

This was changed.

- **L6: “whereas”, split sentence here.**

Thank you. We will split the sentence.

- **eqs. 9 and 10: this is a single equation, requiring only a single equation number, and a multi-case alignment using a curly bracket**

Thank you, this was modified.

- **L12: reformat mm → mm,**

This was corrected

- **whole page: please motivate the reader why these details are important for your research question. Also provide information where all these empirical (fixed) parameters (or regression coefficients) are coming from. Is the underlying theory so well understood that no uncertainties or further dependencies are required?**

We agree that this is important. We added motivation to this section:

Page 9 line 24-29: “The joint state-parameter estimation used in this study updates soil texture and organic matter in CLM. Hence, parameter estimates directly determine soil hydraulic properties in CLM. The following equations describe how soil texture and organic matter define the soil hydraulic properties in CLM such as porosity, hydraulic conductivity, the empirical exponent  $B$  and soil matric potential.”

#### Page 8

- **L4: “COSMIC parameterizes interactions”. The interactions are parameterized by the underlying physical cross-section data. COSMIC rather parameterizes the neutron transport.**

We rephrased:

Page 9 line 9: “COSMIC parameterizes neutron transport within the soil subsurface and was calibrated against the more complex Monte Carlo Neutron Particle model MCNPx (Pelowitz, 2005).”

- **L7-8: Repetition from the introduction.**

We removed.

- **L10: “high energy neutrons are reduced” → “the number of high energy neutrons is reduced”**

We modified as suggested.

- **L11: “with less energy in each soil layer”, misleading/unphysical. Fast neutrons typically evaporate with constant energy.**

We modified:

Page 9 line 14: “ In the soil, the number of high energy neutrons is reduced by interactions within the soil leading to generation of fast neutrons in each soil layer.”

- **L12: rewrite “soil interaction”, as fast neutrons predominantly interact with the water.**

Agreed. However, bulk density plays a major role in parameterizing COSMIC.

We changed to:

“...interactions within the soil...”

- **L16-22 and eq. 14: this part can be omitted, since it is already well described in papers from Shuttleworth and Baatz, and does not add to the message of this paper. If you decide not to omit it, replace  $\theta$  in eq. 14 to avoid confusion with soil moisture.**

Thank you. We replaced  $\theta$  accordingly.

- **L22: explain to the reader how the 300 soil layers in COSMIC communicate with the 10 soil layers from CLM.**

We rephrased:

Page 10 line 13-14: “In this study, the contribution of each CLM soil layer was used to calculate the weighted CLM SWC retrieval corresponding to the vertical distribution of simulated SWC in each grid cell.”

And

Page 10 line 16-18: “Measured neutron intensity of CRNS was used to inversely determine a CRNS SWC retrieval as by Baatz et al. (2014) assuming a homogeneous vertical SWC distribution. Then, the weighted CLM SWC retrieval is used in the data assimilation scheme to relate the CRNS SWC retrieval to the model state.”

Further explanation is given in the next section on data assimilation.

- **L26: what is a “COSMIC soil surface”?**

We rephrase: “the soil surface in COSMIC”

- **L25ff: it looks like you are not assimilating neutrons, but reiterating SWC from neutron data. The whole paragraph creates a great confusion about what the difference is between SWC, CLM SWC, weighted CLM SWC, and CRP SWC. In contrast to other less relevant paragraphs in this section, this part is highly unclear and simultaneously highly important to understand the most important part of your model. Please rephrase the whole paragraph and clarify to the reader what exactly you do, and why (i.e., why not assimilating N directly?)**

It is stated several times that SWC retrievals are assimilated updated and not neutron data e.g.:

Page 10 line 16-18: “Then, the weighted CLM SWC retrieval is used in the data assimilation scheme to relate the CRNS SWC retrieval to the model state.”

The first sentence of this paragraph states what observation is assimilated:

Page 10 line 26-27: “To further expand the work of Han et al. (2016), this study uses the local ensemble transform Kalman filter (LETKF) (Hunt et al., 2007) to assimilate SWC retrievals by CRNS into the land surface model CLM. “

We then clearly state what is updated in CLM:

Page 10 line 28-29: “Updates were calculated either for SWC states or jointly for SWC states and soil parameters depending on the experiment setup.”

We also added to the previous paragraph why SWC retrievals were assimilated, and not neutron flux:

Page 10 line 16-24: “Measured neutron intensity of CRNS was used to inversely determine a CRNS SWC retrieval as by Baatz et al. (2014) assuming a homogeneous vertical SWC distribution. Then, the weighted CLM SWC retrieval is used in the data assimilation scheme to relate the CRNS SWC retrieval to the model state. Alternatively, neutron flux data could be assimilated directly within the catchment. This would require calibration data throughout the catchment which is only feasible using spatially distributed data sets (e.g. Avery et al., 2016). However, high stands of biomass are a major factor for calibration in the Rur catchment (Baatz et al., 2015) and estimates of biomass come along with high uncertainties. To circumvent introducing these additional uncertainties, SWC retrievals are assimilated in this study. Changes in on-site biomass were assumed negligible.”

#### Page 9

- **L5-10: Your paper is not a protocol. Again, it is described what you are using and who else used it, but the reader is left with the question why you (and others) made this decision. Shortly explain advantages of your strategy and why it serves your research question better than others.**

Thank you. We now state:

Page 10 line 26: “To further expand the work of Han et al. (2016), this study uses the local ensemble transform Kalman filter (LETKF) (Hunt et al., 2007) to assimilate SWC retrievals by CRNS into the land surface model CLM. “

We also argue:

Page 3 line 22-25: “The EnKF is much less CPU intensive compared to alternative methods such as the particle filter (e.g. Montzka et al., 2011) because for high dimensional problems the EnKF requires a much smaller ensemble size to achieve reasonable good predictions.”

- **L11: what is  $f$  in  $\vec{x}^f$ ?**

We added at page 11 line 3: “ $f$  marks the model prediction or forecast before the update”

- **L19: confusing typesetting. Is it  $\bar{H}$  as a function of the COSMIC model, or is  $\bar{H}$  identical with the COSMIC operator?**

We now state:

Page 11 line 11-13: “the observation operator  $H$  (COSMIC) is applied on the measured neutron intensity in order to obtain the expected weighted SWC retrieval at each of the observation locations for each of the stochastic realizations” to explain that  $H$  is neither identical nor a function.

- **eq. 19: do not use  $T$  as a symbol for transposition, there is a reserved symbol for this:  $\bar{Y}^T$ .**

Thank you. We change  $T$  to the reserved symbol.

## Page 10

- **L18: redundant sentence.**

The sentence was removed.

- **L20: why these values? is it comparable with the catchment-mean texture? If your question is, what impact a rough and uncertain soil map in data scarce region would have, wouldn't it be more reasonable to smooth out the existing soil map to a very rough degree, rather than using a completely arbitrary soil map?**

Thank you for your questions. We did calculations with the globally available but coarse FAO soil map for the revised version of the manuscript (see responses to reviewer #1).

We add information on catchment wide average sand and clay content, and what was the motivation to select the biased soil map as initial soil map in part of the simulation experiments:

Page 12 line 15-24: "Alternative simulations were also performed with the FAO soil map of the global Harmonized World Soil Database (FAO, 2012) and with a biased soil texture with a fixed sand content of 80 % and clay content of 10 % (S80 soil map). Average sand and clay content are 22.5% and 21.4% for the BK50 soil map and 39% and 22% for the FAO soil map. The FAO soil map and the biased soil map represent large error with respect to the soil properties of the BK50 soil map. The FAO soil map and S80 soil map simulations allow evaluating the joint state-parameter estimation approach because given the expected bias, we can evaluate to what extent the soil properties are modified by the data assimilation. This is important because in many regions across the Earth a high resolution soil map is not available. Land surface models are applied for those regions, for example in the context of global simulations, and hence might be strongly affected by the error in soil properties."

The new simulation results and discussion on the FAO soil map simulations were added.

## Page 11

- **L3-5: omit physical units (they are irrelevant in this context).**

Omitted as suggested.

- **L8-11: How do you justify the perturbation of physical soil parameters like porosity and texture?**

**Does the uncertainty of the soil map justify the huge variation ranges applied in this work? Are models allowed to adapt their physical basement to hydrological data (which also show uncertainty)?**

Perturbation of physical soil parameters like porosity and texture is a general standard procedure in data assimilation and numerous papers use this approach mentioned in the introduction of joint state-parameter estimation.

With the perturbation we account for uncertainty in these soil parameters. One of the main relevant sources of uncertainty in our modelling here is the uncertainty with respect to the soil parameters. The variation ranges are not so huge, considering that CLM assumes a single set of pedotransfer functions being valid throughout the globe. We added:

Page 13 line 12: "Soil texture perturbation considers that in CLM a single set of pedotransfer functions is assumed to be valid throughout the globe while usually pedotransfer functions are specific for regions

(e.g. Patil and Singh, 2016). In other words, the perturbation of soil texture also covers the uncertainty in the pedotransfer function itself.”

- **L15: omit “=”**

We agree and modified.

- **How was the CRP SWC uncertainty determined? Assuming a constant CRNS error is not physical and might have substantial influence on the results (to be tested). For example, the error of neutron observations  $N$  is  $pN$ , while  $N$  can almost double from very wet to very dry conditions, which leads to a variation of the neutron uncertainty by 30%. This can propagate through the non-linear relation to soil moisture in such a way that your observed SWC is significantly more uncertain in wet periods compared to dry periods. Consequently, the DA approach should give more weight to dry periods during assimilation.**

This is a good point. The uncertainty of the neutron count intensity can be modelled by the Poisson distribution, and sampling this distribution and processing it through the non-linear equation which links neutron count intensity and weighted soil water content, allows deriving the measurement error in terms of SWC, also as function of SWC. This was not done here and we used results from earlier work that focused explicitly on estimating the measurement standard deviation of SWC. Based on this work we assume a fixed measurement standard deviation of  $0.03 \text{ cm}^3/\text{cm}^3$  here. We added:

Page 13 line 24-27: “Based on previous work (Baatz et al., 2015), the SWC retrieval uncertainty for CRNS was estimated to be  $0.03 \text{ cm}^3/\text{cm}^3$  while fluctuations in the measurement standard deviation, related to the non-linear relation between observed neutron intensity and SWC, were assumed negligible.”

## Page 12

- **L16: Why do you use RMSE, although many alternative measures are accepted as state-of-the-art measures for time series evaluation, e.g., KGE or NSE, in order to assess bias, deviation, and correlation simultaneously?**

RMSE is a standard measure used in the data assimilation community, whereas NSE is not standard. KGE is indeed an interesting measure which was however not considered here.

- **eqs. 23 and 24: reformat  $SWC \rightarrow SWC$ , same with RMSE and bias, as those are single multi-letter variables, not products of multiple single-letter variables. Following this style guide, rewrite  $E_{RMS} \rightarrow E_{RMS}$ . You can even omit “RMS” since E is the only error used in this work. This would improve readability of the results section.**

Thank you for the suggestion. We reformatted the equation.

## Page 16

- **L17-26: It is argued that changes in SWC states have impact to simulated ET flux. However, only for state-parameter updates (L19). Why is ET not affected by (SWC) state updates only?**

No, we did not argue this. The impact on ET was explored in less detail, partly because ET is most of the year close to potential ET, especially in the southern part of the catchment (hills). For illustration

purposes, we showed here the impact on ET by comparing open loop simulations and simulations with joint state-parameter updating.

- **L32: “to  $E_{RMS}$ -values”, omit “-”**

Thank you, agreed.

#### Page 17

- **L9: if precipitation data from COSMO\_DE was used, why was this information omitted in the method section (only mentioning DWD)?**

We added this now to the method section.

- **L26: replace “fast” with “quickly”.**

Thank you. Done.

#### Page 18

- **L10-23: This question already needs an answer in the method section, I’d suggest to move the whole paragraph.**

We agree and moved the paragraph to the method section.

- **L10-23: I cannot follow the argumentation. Baatz et al. 2014 suggested a correction function for neutron counts based on vegetation estimates.**

Baatz et al. (2016) suggested such a correction function.

**In your model, you already have LAI data every month, implementation of the correction functions in the model would probably be straight forward. Furthermore, to convert neutron data to SWC, some vegetation correction would be necessary, too.**

LAI is not modelled dynamically (predicted) by CLM, but is a model forcing. In addition, LAI data from satellite are not as accurate (bias, scale mismatch) and the conversion from LAI to biomass is also affected by significant uncertainty. We do not expect additional gain from assimilating neutron count intensity instead of converted neutron count intensity.

The conversion of neutron data to SWC does not require vegetation correction per-se. If on-site calibration is done (which was the case for all nine locations) seasonal biomass changes are normally negligible. If biomass changes are not negligible (fast growing crops), at the sites more precise information on biomass is needed than at other catchment locations. Therefore the translation of neutron counts into SWC is reliable at the sites, and SWC can be interpolated dynamically afterwards with data assimilation. It is unclear what extra information can be gained if neutron count intensity is assimilated, given the less precise information on for example biomass at other locations in the catchment.

**Third, assimilating CRP SWC assumes homogeneous vertical SWC profiles (before iteration), this assumption would be unnecessary if neutrons would be assimilated directly. I am afraid that this topic**

**is more complex and needs further discussions and tests. It would be most convincing if you could show that neutron assimilation indeed gives different results than CRP SWC assimilation.**

This would be ideal but should be subject of another study. We clarify the paragraph, put it into the method section and rephrased:

Page 10 line 16: “Measured neutron intensity of CRNS was used to inversely determine a CRNS SWC retrieval as by Baatz et al. (2014) assuming a homogeneous vertical SWC distribution. Then, the weighted CLM SWC retrieval is used in the data assimilation scheme to relate the CRNS SWC retrieval to the model state. Alternatively, neutron flux data could be assimilated directly within the catchment. This would require calibration data throughout the catchment which is only feasible using spatially distributed data sets (e.g. Avery et al., 2016). However, high stands of biomass are a major factor for calibration in the Rur catchment (Baatz et al., 2015) and estimates of biomass come along with high uncertainties. To circumvent introducing these additional uncertainties, SWC retrievals are assimilated in this study. Changes in on-site biomass were assumed negligible.”

• **L27: “neutron flux intensity”, do you mean flux or intensity or both?**

Thank you. We removed intensity.

• **L27: “Although . . . only available at few locations”, write more positively. Neutron data was available at up to 9 locations, which was intended to be the amazing novelty compared to other catchments!**

Thank you. We removed this part of the sentence.

## **Figures**

### **1. South → south, same with North.**

Thank you, we considered but according to Bryan A. Garner “The Oxford Dictionary of Usage and Style” (2000) Oxford University Press:

“The words north, south, east and west should not be capitalized when used to express directions <we went north>. They are properly capitalized when used as nouns denoting regions of the world or of a country <Far East> <the South>.

But when a directional word appears as an adjective before a geographic proper name, it is lower case <eastern United States> <southern Italy>. If, however, the adjective is part of the proper name, it should be capitalized <North Dakota> <East Anglia>.”

In this study, the North of the catchment is a geographic region. Hence, we keep “the North” and “the South”.

### **2. Please add grid lines**

We added horizontal grid lines.

### **3. Please add grid lines**

We added horizontal grid lines.

### **4. Please add grid lines**

We added horizontal grid lines.

**5. It is hard to distinguish two black lines with different meaning. Further indication of the expected “true” sand content (given by the soil map or soil samples) would be helpful to evaluate these plots.**

We added a marker for the value of the BK50 soil map.

**6. This figure is not understandable without the text. Please shortly provide information about the B parameter in the caption to understand the message of this figure.**

We added information to the caption.

**7. replace  $k(\text{sat}) \rightarrow k_{\text{sat}}$ . It would be interesting to also show the evolution of the soil porosity parameter together with an indication of its measured value. Why does hydraulic conductivity (and probably also porosity) vary over time at individual sites? Those are expected to be constant physical parameters of the sites. In my opinion this is a serious flaw of the DA approach used here.**

Thank you. We replaced  $k_{\text{sat}}$ . We rephrase the figure caption to be more clear:

Page 32 line 3-6: “At nine sites, estimates of percentage sand content are shown for simulations with parameter update: PAR-S80-30 (green), PAR-S80-10 (light green), PAR-BK50-30 (red), PAR-BK50-10 (light red), jk8-S80-\* (black) and jk8-BK50-\* (black). The value of the BK50 soil map is marked at the second y-axis.”

The period with parameter updates should be considered as calibration period where parameters are allowed to change. Notice also that simulations were made for a verification period with constant parameters (estimated during the assimilation period). We would like therefore to stress the importance of the evaluation period with temporally constant (estimated) parameter values.

**8. The purpose of this figure is not clear, as no observation data is provided to evaluate the model performance with respect to simulated latent heat.**

Thank you. We rephrased the caption:

Page 35 line 2-6: “Annual evapotranspiration (ET) is shown in the year 2013 (evaluation period, no assimilation). This figure demonstrates the impact of parameter updates (PAR-S80-10 and PAR-BK50-10) in comparison to open loop (OL-S80) and reference soil map (OL-BK50). ET changes in the North but not as much in the South.”

## Tables

**1. what is C3? Replace “non arctic” with “non-arctic”, probably add a citation to the caption for plant functional types.**

C3 is a type of carbon fixation.

We added:

Page 36 line 1: “CLM plant functional type (Bonan et al., 2002)”

And removed “non” as there is not “arctic grass” in the catchment.

**3. improve readability by increasing font weight (boldness) for particularly good cases below an RMSE threshold, which is a common strategy in many journals.**

Thank you for the suggestion. We added:

Page 40 line 5: "The best cases are marked bold."

**4. same as 3. Rephrase the last sentence.**

Thank you. We rephrased.

**5. same as 4.**

Thank you. We rephrased.

Anonymous Referee #4

Received and published: 10 October 2016

## GENERAL COMMENTS

### OVERALL QUALITY

The paper by Baatz et al. (2016-432) describes an effort to use soil moisture data from nine closely-spaced (2000 km<sup>2</sup>) cosmic-ray probes (CRPs) with data assimilation scheme to improve the assessment of soil moisture in land-surface models. The goal is worthy and the execution is thorough. The results are significant: (1) the joint state (soil moisture) and parameter (soil properties, like sand percentage) estimation within data assimilation scheme produces better results than just state estimation; (2) in absence of soil data and meteorological data, CRPs alone can improve data assimilation results. On that account, the paper is suitable for publication in HESS.

Thank you for the positive overall evaluation of the manuscript. We appreciate your effort in reviewing the manuscript. In the forthcoming revision we will consider each of your suggestions and expand the discussion to answer the questions raised.

**However, I am less certain about the significance of these results in light of the finding that the parameters change in time and in many cases never converge. This is only possible if the parameters are fitting parameters rather than physical parameters. So we end up with better results, but possibly only by statistical manipulation rather than by improved understanding of the physics. Is this progress? I would like to see at least some discussion of this issue in the paper in its final form.**

We will expand the discussion on this issue in the revised version of the manuscript. Regarding the change of parameters, those should be considered as parameter estimates. Notice also that simulations were made for a verification period with constant parameters (estimated in the assimilation period). Regarding uncertainty of parameters and the fact that those are not

We added possible reasons and discussion:

Page 19 line 26: “Temporally not stable parameter estimates imply that there may be multiple or seasonal optimal parameter values. This is also supported by the findings of the temporal behaviour of site average  $E_{RMS}$  (**Error! Reference source not found.**) e.g. during the evaluation period when in the dry summer 2013 the  $E_{RMS}$  peaks for the PAR-S80-30 simulation. In this context, it is important to mention that many possible error sources were not subject to calibration in this study but could be crucial for an even better modelled soil moisture and more reliable soil parameter estimation. In this study we only considered uncertainty of soil parameters, but also vegetation parameters are uncertain. Also a number of other CLM-specific hydrologic parameters (e.g. decay factor for subsurface runoff and maximum subsurface drainage) strongly influence state variables in CLM and hence show potential for optimization (Sun et al., 2013). Considering this uncertainty from multiple parameters could give a better parameter uncertainty characterization (Shi et al., 2014). Precipitation is also an important forcing for hydrologic modelling. For this study, precipitation data from the COSMO\_DE re-analysis were used. A product which optimally combines precipitation estimates from radar and gauge measurements is expected to give better precipitation estimates than the reanalysis. This could improve the soil moisture characterization and also potentially lead to better parameter estimates. Further improvements and constraining of parameter uncertainty is also possible using multivariate data assimilation with observations such as latent heat flux (e.g. Shi et al., 2014). Also other error sources related to the model structure play a significant role. These options should be subject of future investigations. “

## **SPECIFIC COMMENTS**

**Why are RMSE and bias discussed separately if they are essentially the same information? One is computed on squares of differences and therefore has a positive sign; the other is computed on differences and therefore has a sign. Wouldn't the bias suffice? If you keep both, please explain why they are both needed and how they are different.**

We add a motivation for using bias as second error measurement:

Page 15 line 4-5: "The second evaluation measurement in this study is the bias which is, in contrast to the  $E_{RMS}$ , a measure for systematic deviation."

**How are the results evaluated? What is the gold standard for soil properties? Pedotransfer functions? What is it for soil moisture? At some of the sites extensive networks of TDR probes exists. Would it be possible to include TDR data in the evaluation?**

Thank you for the suggestions.

TDR probes work on a scale of few  $dm^3$  which is significantly smaller than the scale of the land surface model ( $1 km^2$ ). Hence, TDR probes are not suitable for a direct evaluation whereas cosmic-ray neutron sensors (CRNS) measure soil moisture at an equivalent scale.

**While TDRs are hardly the gold standard in soil moisture measurements, they would provide independent soil moisture data. By the same token, have soil properties been measured at some of the sites? Using the pedotransfer functions to derive unsaturated hydraulic conductivities is hardly the gold standard, and hard to defend.**

Using pedotransfer functions is common sense in land surface modeling such as the land surface model used in this study (CLM) or the Noah land surface model. Those models need to be calibrated by some sort of measurements which are scale consistent data measured by cosmic-ray neutron sensors in this study.

**I suggest that the authors make at least some effort to provide independent data on soil moisture and hydraulic properties.**

We note that soil moisture measurements by CRNS were already independent from the prediction of the land surface model during the verification period. Soil hydraulic properties at the desired scale of the land surface model were not measured.

We also acknowledge that measurements on evapotranspiration would be desirable, but those are not in the scope of this paper which focuses on soil moisture predictions:

Page 21 line 2-6: "Hence particularly in the northern part of the catchment, further observations such as ET measurements are desirable for further improving the land surface model. These additional observations could be used for future land surface model benchmarking (Best et al., 2015) or for more constrained parameter estimates (Shi et al., 2015)."

## **TECHNICAL CORRECTIONS**

**Please, see the annotated pdf manuscript.**

For technical corrections we refer to the annotated pdf manuscript.

## References

- Ajami, H., McCabe, M. F., Evans, J. P., and Stisen, S.: Assessing the impact of model spin-up on surface water-groundwater interactions using an integrated hydrologic model, *Water Resour Res*, 50, 2636-2656, 10.1002/2013wr014258, 2014.
- Avery, W. A., Finkenbiner, C., Franz, T. E., Wang, T. J., Nguy-Robertson, A. L., Suyker, A., Arkebauer, T., and Munoz-Arriola, F.: Incorporation of globally available datasets into the roving cosmic-ray neutron probe method for estimating field-scale soil water content, *Hydrol Earth Syst Sc*, 20, 3859-3872, 10.5194/hess-20-3859-2016, 2016.
- Baatz, R., Bogen, H. R., Hendricks Franssen, H. J., Huisman, J. A., Qu, W., Montzka, C., and Vereecken, H.: Calibration of a catchment scale cosmic-ray probe network: A comparison of three parameterization methods, *J Hydrol*, 516, 231-244, <http://dx.doi.org/10.1016/j.jhydrol.2014.02.026>, 2014.
- Baatz, R., Bogen, H. R., Hendricks Franssen, H. J., Huisman, J. A., Montzka, C., and Vereecken, H.: An empirical vegetation correction for soil water content quantification using cosmic ray probes, *Water Resour Res*, 51, 2030-2046, 10.1002/2014WR016443, 2015.
- Best, M. J., Abramowitz, G., Johnson, H. R., Pitman, A. J., Balsamo, G., Boone, A., Cuntz, M., Decharme, B., Dirmeyer, P. A., Dong, J., Ek, M., Guo, Z., Haverd, V., Van den Hurk, B. J. J., Nearing, G. S., Pak, B., Peters-Lidard, C., Santanello, J. A., Stevens, L., and Vuichard, N.: The Plumbing of Land Surface Models: Benchmarking Model Performance, *J Hydrometeorol*, 16, 1425-1442, 10.1175/Jhm-D-14-0158.1, 2015.
- Bogen, H. R., Huisman, J. A., Baatz, R., Hendricks-Franssen, H. J., and Vereecken, H.: Accuracy of the cosmic-ray soil water content probe in humid forest ecosystems: The worst case scenario, *Water Resour Res*, 49, 10.1002/wrcr.20463, 2013.
- Chen, F., Manning, K. W., LeMone, M. A., Trier, S. B., Alfieri, J. G., Roberts, R., Tewari, M., Niyogi, D., Horst, T. W., Oncley, S. P., Basara, J. B., and Blanken, P. D.: Description and evaluation of the characteristics of the NCAR high-resolution land data assimilation system, *J Appl Meteorol Clim*, 46, 694-713, 10.1175/Jam2463.1, 2007.
- De Lannoy, G. J. M., and Reichle, R. H.: Assimilation of SMOS brightness temperatures or soil moisture retrievals into a land surface model, *Hydrol Earth Syst Sc*, 20, 4895-4911, 10.5194/hess-20-4895-2016, 2016.
- FAO, I., ISRIC, ISSCAS, J: Harmonized World Soil Database v1.2, Rome, Italy, 2012.
- Franz, T. E., Zreda, M., Ferre, T. P. A., Rosolem, R., Zweck, C., Stillman, S., Zeng, X., and Shuttleworth, W. J.: Measurement depth of the cosmic ray soil moisture probe affected by hydrogen from various sources, *Water Resour Res*, 48, Artn W08515, 2012.
- Han, X., Li, X., Franssen, H. J. H., Vereecken, H., and Montzka, C.: Spatial horizontal correlation characteristics in the land data assimilation of soil moisture, *Hydrol Earth Syst Sc*, 16, 1349-1363, 10.5194/hess-16-1349-2012, 2012.
- Han, X., Franssen, H. J. H., Rosolem, R., Jin, R., Li, X., and Vereecken, H.: Correction of systematic model forcing bias of CLM using assimilation of cosmic-ray Neutrons and land surface temperature: a study in the Heihe Catchment, China, *Hydrol. Earth Syst. Sci.*, 19, 615-629, 10.5194/hess-19-615-2015, 2015.
- Han, X., Franssen, H.-J. H., Bello, M. Á. J., Rosolem, R., Bogen, H., Alzamora, F. M., Chanzy, A., and Vereecken, H.: Simultaneous Soil Moisture and Properties Estimation for a Drip Irrigated Field by Assimilating Cosmic-ray Neutron Intensity, *J Hydrol*, <http://dx.doi.org/10.1016/j.jhydrol.2016.05.050>, 2016.
- Hunt, B. R., Kostelich, E. J., and Szunyogh, I.: Efficient data assimilation for spatiotemporal chaos: A local ensemble transform Kalman filter, *Physica D*, 230, 112-126, DOI 10.1016/j.physd.2006.11.008, 2007.

Jackson, T. J., Le Vine, D. M., Hsu, A. Y., Oldak, A., Starks, P. J., Swift, C. T., Isham, J. D., and Haken, M.: Soil moisture mapping at regional scales using microwave radiometry: The Southern Great Plains Hydrology Experiment, *IEEE T Geosci Remote*, 37, 2136-2151, Doi 10.1109/36.789610, 1999.

Kerr, Y. H., Waldteufel, P., Richaume, P., Wigneron, J. P., Ferrazzoli, P., Mahmoodi, A., Al Bitar, A., Cabot, F., Gruhier, C., Juglea, S. E., Leroux, D., Mialon, A., and Delwart, S.: The SMOS Soil Moisture Retrieval Algorithm, *IEEE T Geosci Remote*, 50, 1384-1403, Doi 10.1109/Tgrs.2012.2184548, 2012.

Kirkpatrick, J. B., Green, K., Bridle, K. L., and Venn, S. E.: Patterns of variation in Australian alpine soils and their relationships to parent material, vegetation formation, climate and topography, *Catena*, 121, 186-194, 10.1016/j.catena.2014.05.005, 2014.

Kohli, M., Schron, M., Zreda, M., Schmidt, U., Dietrich, P., and Zacharias, S.: Footprint characteristics revised for field-scale soil moisture monitoring with cosmic-ray neutrons, *Water Resour Res*, 51, 5772-5790, 10.1002/2015WR017169, 2015.

Korres, W., Reichenau, T. G., Fiener, P., Koyama, C. N., Bogen, H. R., Comelissen, T., Baatz, R., Herbst, M., Diekkruger, B., Vereecken, H., and Schneider, K.: Spatio-temporal soil moisture patterns - A meta-analysis using plot to catchment scale data, *J Hydrol*, 520, 326-341, 10.1016/j.jhydrol.2014.11.042, 2015.

Montzka, C., Moradkhani, H., Weihermuller, L., Franssen, H. J. H., Canty, M., and Vereecken, H.: Hydraulic parameter estimation by remotely-sensed top soil moisture observations with the particle filter, *J Hydrol*, 399, 410-421, DOI 10.1016/j.jhydrol.2011.01.020, 2011.

Nearing, G. S., Mocko, D. M., Peters-Lidard, C. D., Kumar, S. V., and Xia, Y. L.: Benchmarking NLDAS-2 Soil Moisture and Evapotranspiration to Separate Uncertainty Contributions, *J Hydrometeorol*, 17, 745-759, 10.1175/Jhm-D-15-0063.1, 2016.

Patil, N. G., and Singh, S. K.: Pedotransfer Functions for Estimating Soil Hydraulic Properties: A Review, *Pedosphere*, 26, 417-430, 10.1016/S1002-0160(15)60054-6, 2016.

Pelowitz, D. B.: MCNPX user's manual, version 5, Rep. LA-CP-05-0369, Los Alamos National Laboratory, Los Alamos LA-CP-05-0369, 2005.

Reichle, R. H., McLaughlin, D. B., and Entekhabi, D.: Hydrologic data assimilation with the ensemble Kalman filter, *Mon Weather Rev*, 130, 103-114, Doi 10.1175/1520-0493(2002)130<0103:Hdawte>2.0.Co;2, 2002.

Rosolem, R., Hoar, T., Arellano, A., Anderson, J. L., Shuttleworth, W. J., Zeng, X., and Franz, T. E.: Translating aboveground cosmic-ray neutron intensity to high-frequency soil moisture profiles at sub-kilometer scale, *Hydrol. Earth Syst. Sci.*, 18, 4363-4379, 10.5194/hess-18-4363-2014, 2014.

Shi, Y. N., Davis, K. J., Zhang, F. Q., Duffy, C. J., and Yu, X.: Parameter estimation of a physically based land surface hydrologic model using the ensemble Kalman filter : A synthetic experiment, *Water Resour Res*, 50, 706-724, 10.1002/2013wr014070, 2014.

Shi, Y. N., Davis, K. J., Zhang, F. Q., Duffy, C. J., and Yu, X.: Parameter estimation of a physically-based land surface hydrologic model using an ensemble Kalman filter: A multivariate real-data experiment, *Adv Water Resour*, 83, 421-427, 10.1016/j.advwatres.2015.06.009, 2015.

Shrestha, P., Sulis, M., Masbou, M., Kollet, S., and Simmer, C.: A Scale-Consistent Terrestrial Systems Modeling Platform Based on COSMO, CLM, and ParFlow, *Mon Weather Rev*, 142, 3466-3483, 10.1175/Mwr-D-14-00029.1, 2014.

Sun, Y., Hou, Z., Huang, M., Tian, F., and Leung, L. R.: Inverse modeling of hydrologic parameters using surface flux and runoff observations in the Community Land Model, *Hydrol Earth Syst Sc*, 17, 4995-5011, 10.5194/hess-17-4995-2013, 2013.

Temimi, M., Lakhankar, T., Zhan, X. W., Cosh, M. H., Krakauer, N., Fares, A., Kelly, V., Khanbilvardi, R., and Kumassi, L.: Soil Moisture Retrieval Using Ground-Based L-Band Passive Microwave Observations in Northeastern USA, *Vadose Zone J*, 13, 10.2136/vzj2013.06.0101, 2014.

Villarreyes, C. A. R., Baroni, G., and Oswald, S. E.: Inverse modelling of cosmic-ray soil moisture for field-scale soil hydraulic parameters, *Eur J Soil Sci*, 65, 876-886, 10.1111/ejss.12162, 2014.

Zreda, M., Desilets, D., Ferre, T. P. A., and Scott, R. L.: Measuring soil moisture content non-invasively at intermediate spatial scale using cosmic-ray neutrons, *Geophys Res Lett*, 35, 10.1029/2008GL035655, 2008.



## Evaluating the value of a network of cosmic-ray probes for improving land surface modelling

Roland Baatz<sup>1,2</sup>, Harrie-Jan Hendricks Franssen<sup>1,2</sup>, Xujun Han<sup>1,2</sup>, Tim Hoar<sup>3</sup>, Heye R. Bogaen<sup>1</sup> and Harry Vereecken<sup>1,2</sup>

5 <sup>1</sup>Agrosphere (IBG-3), Forschungszentrum Jülich GmbH, 52425 Jülich, Germany.

<sup>2</sup>HPSC-TerrSys, 52425 Jülich, Germany.

<sup>3</sup>NCAR Data Assimilation Research Section, Boulder, CO, USA.

*Correspondence to:* Roland Baatz (r.baatz@fz-juelich.de)



**Abstract:** Land surface models can model matter and energy fluxes between the land surface and atmosphere, and provide a lower boundary condition to atmospheric circulation models. For these applications, accurate soil moisture quantification is highly desirable but not always possible given limited observations and limited subsurface data accuracy. Cosmic-ray probes (CRPs) offer an interesting alternative to indirectly measure soil moisture and provide an observation that can be assimilated into land surface models for improved soil moisture prediction. Synthetic studies have shown the potential to estimate subsurface parameters of land surface models with the assimilation of CRP observations. In this study, the potential of a network of CRPs for estimating subsurface parameters and improved soil moisture states is tested in a real-world case scenario using the local ensemble transform Kalman filter with the Community Land Model. The potential of the CRP network was tested by assimilating CRP-data for the years 2011 and 2012 (with or without soil hydraulic parameter estimation), followed by the verification year 2013. This was done using (i) the regional soil map as input information for the simulations, and (ii) an erroneous, biased soil map. For the regional soil map, soil moisture characterization was only improved in the assimilation period but not in the verification period. For the biased soil map, soil moisture characterization improved in both periods strongly from a bias of  $0.11 \text{ cm}^3/\text{cm}^3$  to  $0.03 \text{ cm}^3/\text{cm}^3$  (assimilation period) and from  $0.12 \text{ cm}^3/\text{cm}^3$  to  $0.05 \text{ cm}^3/\text{cm}^3$  (verification period) and the estimated soil hydraulic parameters were after assimilation closer to the ones of the regional soil map. Finally, the value of the CRP network was also evaluated with jackknifing data assimilation experiments. It was found that the CRP network is able to improve soil moisture estimates at locations between the assimilation sites from a  $E_{\text{RMS}}$  of  $0.12 \text{ cm}^3/\text{cm}^3$  to  $0.06 \text{ cm}^3/\text{cm}^3$  (verification period), but again only if the initial soil map was biased.

## 20 1 Introduction

Soil water content (SWC) is a key variable of land surface hydrology and has a strong control on the partitioning of net radiation between latent and sensible heat flux. Knowledge of SWC is relevant for the assessment of plant water stress and agricultural production, as well as runoff generation as a response to precipitation events (Vereecken et al., 2008; Robinson et al., 2008). In atmospheric circulation models, SWC is important as a lower boundary condition and is calculated as a state variable in land surface models. Coupling of atmospheric circulation models and land surface models allows quantifying the role of soil moisture on atmospheric processes such as soil moisture-precipitation feedbacks (Koster et al., 2004; Eltahir, 1998) and summer climate variability and drought (Oglesby and Erickson, 1989; Sheffield and Wood, 2008; Seneviratne et al., 2006; Bell et al., 2015). It is therefore important to improve the modelling and prediction of SWC, but this is hampered by model deficiencies and lack of high quality data (Vereecken et al., 2016). Soil moisture measured by ground-based remote sensing technologies provides information over large areas (e.g. Ajami et al., 2014). However, space-born remote sensing supplies only information on the upper few centimeters, and data are not reliable for areas with dense vegetation. Therefore, in this paper an alternative source for soil moisture information is explored. Cosmic-ray probes (CRPs) measure fast neutron intensity which allows estimating SWC at an intermediate scale (Zreda et al., 2008; Desilets et al., 2010; Cosh et al., 2016; Lv et al., 2014) which is closer to the desired application scale of land surface models (Ajami et al., 2014; Chen et al.,



7;Shrestha et al., 2014). **Fast neutrons originate from moderation of secondary cosmic particles from outer space by**  
**terrestrial atoms.** These particles are mainly fast neutrons, which are moderated most effectively by hydrogen **because of the**  
**similar atomic mass.** Therefore, the corresponding neutron intensity measured by CRPs strongly depends on the amount of  
hydrogen within the CRP footprint, allowing for a continuous non-invasive soil moisture estimate over an area of ~15 ha  
5 (Kohli et al., 2015). The spatial **extend** of this measurement is desirable as it matches with the desired grid cell size of a land  
surface model (Crow et al., 2012) and **small scale heterogeneities are averaged over a larger area** (Franz et al., 2013a; Desilets  
and Zreda, 2013). Vertical measurement depth ranges from a maximum of ~70 cm under completely dry conditions and  
decreases to roughly ~12 cm under wet conditions (e.g. 40 vol. % soil moisture) (Bogena et al., 2013). Worldwide several  
CRP networks exist, like the North American **COSMOS network (Zreda et al., 2012), the German CRP network (Baatz et**  
10 **al., 2014) installed in the context of the TERENO infrastructure measure (Zacharias et al., 2011) and the Australian**  
**COSMoZ network (Hawdon et al., 2014).**

**moisture data assimilation** provides a way to improve imperfect land surface model predictions with measured soil  
moisture data by merging model predictions and data, and can consider the uncertainty of initial conditions, model  
15 parameters and model forcings. Ensemble Kalman Filtering (EnKF) is one of the most commonly applied data assimilation  
methods (Evensen, 1994; Burgers et al., 1998). ~~Soil moisture data assimilation has been the subject of intensive study for  
more than a decade now. An early contribution was provided by Houser et al. (1998) who assimilated remotely sensed soil  
moisture observations from a microwave radiometer into a land atmosphere transfer scheme using four-dimensional  
variational data assimilation. Rhodin et al. (1999) assimilated soil moisture data for a four day period in order to obtain an  
20 improved characterization of the lower boundary condition for an atmospheric circulation model. They also used a  
variational data assimilation approach.~~ More recently, the Ensemble Kalman Filter (Reichle et al., 2002a; Dunne and  
Entekhabi, 2005; Crow, 2003), the Extended Kalman Filter (Draper et al., 2009; Reichle et al., 2002b), four-dimensional  
variational methods (Hurkmans et al., 2006) and the Local Ensemble Transform Kalman Filter (Han et al., 2015; Han et al.,  
2013) were applied for updating soil moisture states in land surface models. Reichle et al. (2002a) performed a synthetic  
25 experiment using L-band microwave observations of the Southern Great Plains Hydrology Experiment (Jackson et al., 1999)  
to analyze the effect of ensemble size and prediction error. Dunne and Entekhabi (2005) showed that an Ensemble Kalman  
Smoother approach, where data from multiple time steps was assimilated to update current and past states, can yield a  
reduced prediction error compared to a pure filtering approach.

30 More recent work addressed joint state-parameter estimation in hydrologic land surface models with data assimilation  
methods. **Joint state-parameter estimation with EnKF is possible** by an augmented state vector approach (Chen and Zhang,  
2006), a dual approach (Moradkhani et al., 2005) or an approach with an additional external optimization loop (Vrugt et al.,  
2005). Pauwels et al. (2009) optimized soil hydraulic parameters of a land surface model with synthetic aperture radar data.  
Lee (2014) used Synthetic Aperture Radar soil moisture data to estimate soil hydraulic properties at the Tibetan plateau



using the EnKF and a Soil Vegetation Atmosphere Transfer model. Bateni and Entekhabi (2012) assimilated land surface temperature with an Ensemble Kalman Smoother and achieved a better estimate of the partitioning of energy between sensible and latent heat fluxes. Han et al. (2014b) updated soil hydraulic parameters of the Community Land Model (CLM) by assimilation of synthetic brightness temperature data with the Local Ensemble Transform Kalman Filter (LETKF) (Hunt et al., 2007). Shi et al. (2014) used the Ensemble Kalman Filter for a synthetic multivariate data assimilation problem with a land surface model and then applied it to real data (Shi et al., 2015). The cases illustrated a way to use real world data for estimating several parameters in hydrologic land models. (Kurtz et al., 2016) developed a particular CPU-efficient data assimilation framework for the coupled land surface-subsurface model TerrSysMP (Shrestha et al., 2014). They successfully updated  $2 \times 10^7$  states and parameters in a synthetic experiment. Whereas these studies were made with land surface models, also in soil hydrological applications recently data assimilation was used to estimate soil hydraulic parameters. Early work was by Wu and Margulis (2011, 2013) in the context of real-time control of waste water reuse in irrigation. Erdal et al. (2014) investigated the role of bias in the conceptual soil model and explored bias aware EnKF as a way to deal with it. Erdal et al. (2015) focused on handling of strong -Gaussianity of the state variable in EnKF under very dry conditions. Montzka et al. (2013;2011) explored the role of the particle filter for handling non-Gaussianity in soil hydrology data assimilation. They showed that the ability of a data assimilation system to correct the soil moisture state and estimate hydraulic parameters strongly depends on the nonlinear character of the soil moisture retention characteristic. Song et al. (2014) worked on a modified iterative filter to handle the non-linearity and non-Gaussianity of data assimilation for the vadose zone. For a further literature review on data assimilation in the context of hydrological and land surface models we refer to Reichle (2008) and Montzka et al. (2012).

20

Shuttleworth et al. (2013) developed the Cosmic Ray Soil Moisture Interaction Code (COSMIC), which is a forward operator to be applied for assimilating neutron intensity observations from CRPs. The COSMIC code was evaluated for several sites (Baatz et al., 2014;Rosolem et al., 2014). Its capability to propagate surface soil moisture information into the deeper soil column was analyzed by Rosolem et al. (2014). The COSMIC operator was successfully implemented in the Data Assimilation Research Testbed (Rosolem et al., 2014) to allow for state updating by the Ensemble Adjustment Kalman Filter (Anderson, 2001). The COSMIC operator was implemented in a python interface that couples the land surface model CLM and the LETKF for joint state parameter updating (Han et al., 2015). Neutron counts measured by CRP have been used in data assimilation studies to update model states (Han et al., 2015;Rosolem et al., 2014). Soil hydraulic parameters were also updated by assimilation of neutron counts (Han et al., 2016), but only for a synthetic study which showed its feasibility. CRPs were also used for inverse estimation of soil hydraulic parameters of the Hydrus-1D model (Villarreyes et al., 2014).

30

This work further explores the value of measured neutron intensity by CRPs to improve modelling of terrestrial systems at the catchment scale (Simmer et al., 2015) using a land surface model.  ~~compared to existing work~~ the main novelties are:



(i) Data from a network of nine CRPs were assimilated in the Community Land Model version 4.5 (CLM) with an evaluation of the information gain by this assimilation at the larger catchment scale. Until now evaluations with CRPs were made for a single location, but not for a complete network of CRPs. It is a very important question whether CRPs can also improve the soil moisture characterization at the larger catchment scale and how dense the CRP network should be. The high variability of soil moisture at a short distance could potentially limit the CRP measurement value and make updating of soil moisture contents further away from the sensor meaningless. On the other hand, soil maps and atmospheric forcings show spatial correlations over larger distances which suggests that CRP measurements potentially carry important information to update soil moisture contents for larger regions. If it is found that CRP networks with a density like in this study (10 stations per 2354 km<sup>2</sup>) can improve soil moisture content characterization at the larger catchment scale, this is of high relevance and importance for agricultural applications, flood prediction and protection, and regional weather prediction (Whan et al., 2015;Koster et al., 2004;Seneviratne et al., 2010). The main research question addressed in this paper is therefore whether a CRP network of the density in this study can improve large scale soil moisture characterization by state and parameter updates.

(ii) Soil hydraulic parameters were updated together with the soil moisture states in a real-world case study at the larger catchment scale. The study in this paper also allows some evaluation of the feasibility of the updated large scale soil hydraulic parameters.

In the following paragraphs are presented the model site and the measurements (2.1), the Community land Model and its parameterization (2.2), the MIC forward model (2.3) and the data assimilation procedure (2.4).

## 2 Materials and methods

### 2.1 Site description and measurements

model domain, the Rur catchment (2354 km<sup>2</sup>), is situated in western Germany and illustrated in Fig. 1. Most prominent vegetation types are agricultural land use (mainly in the North), grassland, and coniferous and deciduous forest. The altitude varies between 15 m a.s.l. in the flat northern part and 690 m a.s.l. in the hilly southern part. Precipitation, evapotranspiration and land use follow the topography. Annual precipitation ranges between less than 600 mm in the North 200 mm in the hilly South (Montzka et al., 2008). Annual potential evapotranspiration varies between 500 mm in the South and 700 mm in the North (Bogena et al., 2005). The Rur catchment CRP network comprises nine CRPs (CRS1000, HydroInnova LLC, 2009) which were installed in 2011 and 2012 (Baatz et al., 2014). Climate and soil texture of the CRP sites can be found in Table 1. The CRPs were calibrated in the field using gravimetric soil samples. At each site, 18 soil samples were taken along three circles with distances of 25, 75 and 175 meters from the CRP, six samples evenly distributed along each circle. Each sample was extracted with a 50.8 x 300 mm round HUMAX soil corer (Martin Burch AG, Switzerland). The samples were split into 6 sub-samples with 5 cm length each and oven dried at 105 °C for 48 hours to measure dry soil bulk density and soil moisture. Ice water was determined for each site using a heat conductivity detector. Soil bulk density, soil moisture,



Ice water and hour averaged measured neutron intensity were used to determine poration parameters specific for each CRP and the COSMIC operator.

## 2.2 Community land model and parameterization

5 The Community Land Model version 4.5 (CLM) was the land surface model of choice for simulating water and energy exchange between the land surface and the atmosphere (Oleson et al., 2013). Some of the key processes which are solved by CLM are radiative transfer in the canopy space, interception of precipitation by the vegetation and evaporation from intercepted water, water uptake by vegetation and transpiration, soil evaporation, photosynthesis, as well as water and energy flow in the subsurface. SWC in CLM is influenced by precipitation, infiltration into the soil, water uptake by vegetation, surface evaporation and surface and subsurface runoff. Oleson et al. (2013) provide further details on CLM4.5. To limit the scope and complexity of this study, CLM was run using satellite phenology, e.g. prescribed leaf area index data and the biogeochemical module turned off.

15 The spatial domain is discretized by rectangular grid cells by CLM. Each grid cell may have several types of land cover: Lake, urban, vegetated, wetland, and glacier. The vegetated part of the grid cell can be covered by several plant functional types which are all linked to a single soil column. The soil column is vertically discretized by ten soil layers and five bedrock layers. Layer thickness increases exponentially from 0.007 m at the surface to 2.86 m for layer 10. Vertical water flow in is modelled by the 1D Richards equation. Soil hydraulic parameters are determined from sand and clay content using pedotransfer functions for the mineral soil fraction (Clapp and Hornberger, 1978; Cosby et al., 1984), and organic matter content for the organic soil fraction (Lawrence and Slater, 2008).

25 The following equations describe how soil texture and organic matter define the soil hydraulic properties in CLM such as porosity, hydraulic conductivity, the empirical exponent  $B$  and soil matric potential. Hydraulic conductivity ( $k[z]$  in mm/s) at the depth  $z$  between two layers ( $i$  and  $i+1$ ) is a function of soil moisture ( $\theta$  in  $\text{m}^3/\text{m}^3$  in layers  $i$  and  $i+1$ ), saturated hydraulic conductivity ( $k_{sat}$  in mm/s at  $z$ ), saturated soil moisture ( $\theta_{sat}$  in  $\text{m}^3/\text{m}^3$ ) and the empirical exponent  $B$ :

$$= \begin{cases} \phi_{ice} k_{sat,z} \left[ \frac{0.5(\theta_i + \theta_{i+1})}{0.5(\theta_{sat,i} + \theta_{sat,i+1})} \right]^{2B_i+3} & 1 \leq i \leq N_{levsoi} - 1 \\ \phi_{ice} k_{sat,z} \left( \frac{\theta_i}{\theta_{sat,i}} \right)^{2B_i+3} & i = N_{levsoi} \end{cases} \quad 1$$

where  $\phi_{ice}$  is the ice impedance factor. The ice impedance factor was implemented to simplify an increased tortuosity of water flow in a partly frozen pore space. It is calculated with  $\phi_{ice} = 10^{-\Omega F_{ice}}$  using the resistance factor  $\Omega = 6$  and the frozen fraction of soil porosity  $F_{ice} = \theta_{ice}/\theta_{sat,i}$ . Soil hydraulic properties are calculated separately for the mineral (*min*) and organic matter (*om*) soil components. Total porosity  $\theta_{sat,i}$  is calculated using the fraction of organic matter ( $f_{om,i}$ ) with:



$$\theta_{sat,i} = (1 - f_{om,i})\theta_{sat,min,i} + f_{om,i}\theta_{sat,om} \quad 2$$

where the organic matter porosity is  $\theta_{sat,om} = 0.9$  and sand content in % determines the mineral soil porosity  $\theta_{sat,min}$  as:

$$\theta_{sat,min} = 0.489 - 0.00126 \times \%sand \quad 3$$

Analogous, the exponent  $B$  is calculated with

$$B_i = (1 - f_{om,i})B_{min,i} + f_{om,i}B_{om} \quad 4$$

Where  $B_{om} = 2.7$  is the organic exponent and the mineral exponent  $B_{min,i}$  is determined by clay content in % with:

$$B_{min,i} = 2.91 + 0.159 \times \%clay \quad 5$$

Saturated hydraulic conductivity is calculated for a connected and an unconnected fraction of the grid cell with:

$$k_{sat}[z_i] = (1 - f_{perc})k_{sat,uncon}[z_i] + f_{perc,i}k_{sat,om}[z_i] \quad 6$$

- 5 where  $f_{perc,i}$  is the fraction of a grid cell where water flows with saturated hydraulic conductivity of the organic matter ( $k_{sat,om}[z_i]$  in mm/s) through the organic material only, the so called connected flow pathway, whereas the saturated hydraulic conductivity of the unconnected part ( $k_{sat,uncon}[z_i]$  in mm/s) depends on organic and mineral saturated soil hydraulic conductivity:

$$k_{sat,uncon} = (1 - f_{perc}) \left( \frac{1 - f_{om}}{k_{sat,min}} + \frac{f_{om} - f_{perc}}{k_{sat,om}} \right)^{-1} \quad 7$$

where saturated hydraulic conductivity for mineral soil is calculated from the grid cell sand content as:

$$k_{sat,min}[z_i] = 0.0070556 \times 10^{-0.884 + 0.0153 \times \%sand} \quad 8$$

- 10 The fraction  $f_{perc}$  is calculated with:

$$f_{perc} = 0.908 \times (f_{om} - 0.5)^{0.139} \quad f_{om} \geq 0.5 \quad 9$$

$$f_{perc} = 0 \quad f_{om} < 0.5 \quad 10$$

Soil matric potential (mm) is defined as function of saturated soil matric potential (mm) with:

$$\psi_i = \psi_{sat,i} \left( \frac{\theta_i}{\theta_{sat,i}} \right)^{-B_i} = [(1 - f_{om,i})\psi_{sat,min,i} + f_{om,i}\psi_{sat,om}] \left( \frac{\theta_i}{\theta_{sat,i}} \right)^{-B_i} \quad 11$$

where saturated organic matter matric potential is  $\psi_{sat,om} = -10.3 \text{ mm}$  and saturated mineral soil matric potential is calculated from sand content as:

$$\psi_{sat,min,i} = -10.0 \times 10^{1.88 - 0.0131 \times \%sand} \quad 12$$



### 2.3 Cosmic-ray forward model

SWC retrievals were calculated from neutron intensity observations with the Cosmic-ray Soil Moisture Interaction Code COSMIC (Shuttleworth et al., 2013) following calibration results and the procedure of Baatz et al. (2014). COSMIC parameterizes interactions between neutrons and atoms in the subsurface, relevant for soil moisture estimation. COSMIC was calibrated against the more complex Monte Carlo Neutron Particle model MCNPx (Pelowitz, 2005) and needs considerably less CPU-time than the MCNPx model. The reduced CPU-time need and the physically based parameterization make COSMIC a suitable data assimilation operator. The code was tested at multiple sites for soil moisture determination (Baatz et al., 2014; Rosolem et al., 2014) and analyzed in detail by Rosolem et al. (2014).

COSMIC assumes that a number of high energy neutrons enter the soil. In the soil, high energy neutrons are reduced by interaction with the soil leading to the production of fast neutrons with less energy in each soil layer. Before surfacing, fast neutrons are produced again by interaction (Shuttleworth et al., 2013). The number of neutrons  $N_{CRP}$  that reaches the CRP can be summarized in a single integral as

$$N_{CRP} = N_{COSMIC} \int_0^{\infty} \left\{ A(z) [\alpha \rho_s(z) + \rho_w(z)] \exp \left( - \left[ \frac{m_s(z)}{L_1} + \frac{m_w(z)}{L_2} \right] \right) \right\} \cdot dz \quad 13$$

where  $N_{COSMIC}$  is an empirical coefficient that is CRP specific and needs to be estimated by calibration,  $A(z)$  is the integrated average attenuation of fast neutrons,  $\alpha = 0.404 - 0.101 \times \rho_s$  is the site specific empirical coefficient for the creation of fast neutrons by soil,  $\rho_s$  is the dry soil bulk density in  $\text{g/cm}^3$ ,  $\rho_w$  is the total soil water density in  $\text{g/cm}^3$ ,  $m_s$  and  $m_w$  are the mass of soil and water, respectively, per area in  $\text{g/cm}^2$ .  $L_1 = 162.0 \text{ g cm}^{-2}$  and  $L_2 = 129.1 \text{ g cm}^{-2}$  are empirical coefficients that were estimated using the MCNPx code (Shuttleworth et al., 2013). The integrated average attenuation of fast neutrons  $A(z)$  can be found numerically by solving

$$A(z) = \left( \frac{2}{\pi} \right) \int_0^{\pi/2} \exp \left( \frac{-1}{\cos(\theta)} \left[ \frac{m_s(z)}{L_3} + \frac{m_w(z)}{L_4} \right] \right) \cdot d\theta \quad 14$$

where  $\theta$  is the angle along a vertical line below the CRP detector to the element that contributes to the attenuation of fast neutrons,  $L_3 = -31.65 + 99.29 \times \rho_s$  is determined from soil bulk density and  $L_4 = 3.16 \text{ g cm}^{-2}$  is another empirical coefficient estimated using the MCNPx code (Shuttleworth et al., 2013). The COSMIC operator is discretized into 300 vertical layers of one cm thickness up to a depth of three meters. For each CLM grid cell in the model domain, simulated SWC is used to generate a SWC retrieval using the COSMIC code. Simulated SWC is handed from the CLM simulation history files to the COSMIC operator. Given the vertical SWC distribution of the individual CLM soil column, COSMIC internally calculates the contribution of each layer to the simulated neutron intensity signal at the COSMIC soil surface. In this study, the contribution of each layer was used to calculate the weighted CLM SWC retrieval corresponding to the vertical distribution of simulated SWC in each grid cell. Measured neutron intensity of CRPs was used to inversely



determine a CRP SWC retrieval as by Baatz et al. (2014) assuming a homogeneous vertical SWC distribution. Then, the weighted CLM SWC retrieval is used in the data assimilation scheme to relate the CRP SWC retrieval to the model state.

## 2.4 Data assimilation

5 This study uses the local ensemble transform Kalman filter (LETKF) (Hunt et al., 2007) to assimilate SWC retrievals by CRPs into the land surface model CLM. Besides other Ensemble Kalman Filter variants, the LETKF is applied in atmospheric sciences (Liu et al., 2012; Miyoshi and Kunii, 2012), ocean science (Penny et al., 2013) and also in land surface hydrology (Han et al., 2014a; Han et al., 2015). Updates were calculated either for states or jointly for states and parameters. For state updates only, the LETKF was used as proposed by Hunt et al. (2007). Calculations were made for an ensemble of  
 10 model simulations which differed related to variations in model forcings and input parameters. The states of the different ensemble members are indicated by  $\mathbf{x}_i^f$  where  $i=1, \dots, N$  and  $N$  is the number of ensemble members. The individual state vectors  $\mathbf{x}_i^f$  contain the CLM-simulated SWC of the ten soil layers and the vertically weighted SWC retrieval obtained with the COSMIC operator. For each grid cell, a vector  $\mathbf{X}^f$  can be constructed which contains the deviations of the simulated states with respect to the ensemble mean  $\bar{\mathbf{x}}^f$  :

$$\mathbf{X}^f = [\mathbf{x}_1^f - \bar{\mathbf{x}}^f, \dots, \mathbf{x}_N^f - \bar{\mathbf{x}}^f] \quad 15$$

15 In case of joint state-parameter updates, a state augmentation approach was followed (Hendricks Franssen and Kinzelbach, 2008; Han et al., 2014b). In this case, the augmented model state vector  $\mathbf{X}^f$  is constructed from the weighted SWC, and the grid cell's sand, clay and organic matter content.

In order to relate the measured neutron intensity with the simulated SWC of CLM, the observation operator  $\mathbf{H}$  (COSMIC) is  
 20 applied on the measured neutron intensity in order to obtain the expected weighted SWC retrieval for each of the stochastic realizations:

$$\mathbf{y}_i^f = \mathbf{H}(\mathbf{x}_i^f) \quad 16$$

The ensemble realizations of the modelled SWC retrieval  $\mathbf{y}_1^f$  to  $\mathbf{y}_N^f$  with respect to the ensemble mean  $\bar{\mathbf{y}}^f$  are stored in the vector  $\mathbf{Y}^f$ :

$$\mathbf{Y}^f = [\mathbf{y}_1^f - \bar{\mathbf{y}}^f, \dots, \mathbf{y}_N^f - \bar{\mathbf{y}}^f] \quad 17$$

The observation error correlation was reduced in space by the factor  $f_{red}$  using the spherical model:

$$f_{red} = 1 - (1.5 \times d/d_{max}) + (0.5 \times [d/d_{max}]^3) \quad 18$$

25 where  $d$  is the distance to the observation and  $d_{max} = 40km$  is the maximum observation correlation length, about half the size of the catchment. Only SWC retrievals within the maximum observation correlation length were used for assimilation.



This leads to a ‘localized’ size of  $\mathbf{Y}^f$  and the observation error covariance matrix  $\mathbf{R}$ . The intermediate covariance matrix  $\mathbf{P}^a$  (also called analysis error covariance matrix) is calculated according to:

$$\mathbf{P}^a = [(\mathbf{N} - 1)\mathbf{I} + \mathbf{Y}^{fT}\mathbf{R}^{-1}\mathbf{Y}^f] \quad 19$$

In addition, the mean weight vector  $\bar{\mathbf{w}}^a$  is obtained as follows:

$$\bar{\mathbf{w}}^a = \mathbf{P}^a \mathbf{Y}^{fT} \mathbf{R}^{-1} (\mathbf{y}^0 - \bar{\mathbf{y}}^f) \quad 20$$

where  $\mathbf{y}^0$  is CRP SWC retrieval. In the ensemble space, a perturbation matrix  $\mathbf{W}^a$  is calculated from the symmetric square root of  $\mathbf{P}^a$ :

$$\mathbf{W}^a = [(\mathbf{N} - 1)\mathbf{P}^a]^{1/2} \quad 21$$

The final analysis  $\mathbf{X}^a$  is obtained from:

$$\mathbf{X}^a = \bar{\mathbf{x}}^f + \mathbf{X}^f [\bar{\mathbf{w}}^a + \mathbf{W}^a] \quad 22$$

A more detailed description of the LETKF can be found in (Hunt et al., 2007) and details on the implementation of the LETKF in combination with CLM are given by (Han et al., 2015).

## 10 3 Model and Experiment Setup

### 3.1 Model Setup

In this study, discretization and parameterization of the hydrological catchment was done on the basis of high resolution data. The Rur catchment domain is spatially discretized by rectangular grid cells of 0.008 degree size (~750 m). The model time step was set to hourly. Land cover was assumed to consist of vegetated land units only, and a single plant functional type (PFT) for each grid cell was defined. The plant functional types were derived from a remotely sensed land use map using RapidEye and ASTER data with 15 m resolution (Waldhoff, 2012). Sand content, clay content and organic matter content were derived from the high resolution regional soil map BK50 (Geologischer Dienst Nordrhein-Westfalen, 2009). The BK50 soil map provides the high resolution soil texture for the catchment and is the most detailed soil map available for the defined region. As an alternative, simulations were also performed for a biased soil texture distribution with a fixed sand content of 80 % and clay content of 10 % (S80 soil map). This represents a large error with respect to the expected true soil properties. It allows evaluating the joint state-parameter estimation approach because given the expected bias, we can evaluate whether and to what extent the soil properties are modified by the data assimilation to be closer to the available high resolution soil map. In addition, in many regions across the Earth a high resolution soil map is not available and land surface models which are applied for those regions, for example in the context of global simulations, might be strongly affected by the error in soil properties. As tested how this impacted the simulation results. Maximum saturated fraction, a surface parameter which is used for runoff generation, was calculated from a 10 meter digital elevation model (GmbH, 2010). Leaf area index data were derived from monthly averaged Moderate Resolution Imaging Spectrometer data



(MODIS). CLM was supplied with hourly atmospheric forcing data from a reanalysis data set for the years 2010 to 2013 from the German Weather Service (DWD). The data was downscaled from a resolution of 2.8 km<sup>2</sup> to the CLM resolution using linear interpolation based on Delaunay triangulation. Forcing data include precipitation in mm/s, incident solar and longwave radiation in W/m<sup>2</sup>, air temperature in K, air pressure in hPa, wind speed in m/s and relative humidity in kg/kg at the lowest atmospheric level.

### 3.2 Model ensemble

Uncertainty was introduced into the regional CLM model by perturbed soil parameters and forcings. Contents of sand, clay and organic matter were perturbed with spatially correlated noise from a uniform sampling distribution with mean zero and standard deviation 10 % or 30 % (Han et al., 2015). By perturbing texture, soil parameters are also perturbed through the pedotransfer functions used in CLM as specified in Sect. 2.2. Precipitation ( $\sigma = 1.0$ ; lognormal distribution) and shortwave radiation ( $\sigma = 0.3$ ; lognormal distribution) were perturbed with multiplicative noise with mean equal to one. Longwave radiation ( $\sigma = 20 \text{ W m}^{-2}$ ) and air temperature ( $\sigma = 1\text{K}$ ) were perturbed with additive noise. The forcing perturbations were imposed with correlations in space (5 km) using a fast Fourier transform. Correlation in time was introduced with an AR(1)-model with autoregressive parameter=0.33. These correlations and standard deviations were chosen based on previous data assimilation experiments (Reichle et al., 2010; Kumar et al., 2012; De Lannoy et al., 2012; Han et al., 2015). In this work, only results for precipitation perturbation with  $\sigma = 0.5$  will be shown as results for  $\sigma = 1.0$  were similar. An ensemble size of 95 realizations was used in the simulations. Based on previous work (Baatz et al., 2015), the SWC retrieval uncertainty for CRPs was estimated to be 0.03 cm<sup>3</sup>/cm<sup>3</sup>.

### 3.3 Experiment set-up

All simulation experiments in this study used initial conditions from a single five year spin-up run. For the five year spin-up run, a single forcing data set of the year 2010 was repeatedly used as atmospheric input. The soil moisture regime became stable after five years spin-up period, and additional spin-up simulations would not affect soil moisture in the consecutive years. After this five year spin-up, soil parameters and forcing data of the consecutive years were perturbed. From 1<sup>st</sup> Jan. 2011 onwards, CLM was propagated forward with an ensemble of 95 realizations. On 20<sup>th</sup> Mar. 2011, the first SWC retrieval was assimilated and assimilation of SWC retrievals continued until 31<sup>st</sup> Dec. 2012. From 1<sup>st</sup> January 2013 to 31<sup>st</sup> December 2013 the model was propagated forward without data assimilation but with an ensemble of 95 realizations. The year 2013 was used exclusively as evaluation period for data assimilation experiments.

In total, 26 simulation experiments were carried out using different setups (Table 2). Two open loop simulations were run for the BK50 soil map (OL-BK50) and the S80 soil map (OL-S80), respectively, without data assimilation and soil parameter perturbation of 30 %. These simulations are referred to as reference runs for the respective soil map. Simulation results of data assimilation runs were compared to the reference runs for quantification of data assimilation benefits. Simulations were



done with joint state-parameter estimation (PAR-), two for the S80 soil map (PAR-S80-) and two for the BK50 soil map (PAR-BK50-), for which soil texture was perturbed by 10 % and 30 %. Two simulations were done with state updates only for the BK50 soil map (Stt-BK50) and the S80 soil map (Stt-S80), where soil texture was perturbed by 30 %. These eight simulations form the basic set of experiments.

5

Besides the data assimilation experiments also a larger number of jackknifing simulations was run to evaluate the data assimilation performance. These simulations allow evaluating the impact of the CRP network to improve SWC characterization at other locations, without CRP. In a jackknife experiment, data from eight CRP locations were assimilated and one CRP was excluded from the assimilation for evaluation purpose. At the evaluation location, simulated SWC (which is affected by the assimilation of the other eight probes) was compared to CRP SWC retrievals. For jackknife simulations, the perturbation of soil texture was set to 30 % and precipitation perturbation was done with  $\sigma = 0.5$ . States and parameters at these sites were jointly updated, and simulations were made using the BK50 and the S80 soil maps as input. Therefore, a total of 18 jackknife simulations (jk-S80-\* and jk-BK50-\*) was performed (two soil maps times nine different simulations leaving away one CRP at a time).

15

Simulation results were evaluated with the root mean square error s:

$$RMSE = \sqrt{\frac{\sum_{t=1}^n (SWC_{t,CLM} - SWC_{t,CRP})^2}{n}} \quad 23$$

where  $n$  is the total number of time steps,  $SWC_{t,CLM}$  is the CLM SWC retrieval at time step  $t$  and  $SWC_{t,CRP}$  is the CRP SWC retrieval at time step  $t$ . In case SWC was assimilated at the corresponding time step,  $SWC_{t,CLM}$  is SWC prior to assimilation.

In the case the  $E_{RMS}$  is estimated at a single point in time over all CRPs available, the number of time steps  $n$  can be replaced by the number of CRPs available. The second evaluation measurement in this study e bias:

$$bias = \frac{\sum_{t=1}^n (SWC_{t,CLM} - SWC_{t,CRP})}{n} \quad 24$$

## 4 Results

### 4.1 General Results

Table 3 summarizes the performance statistics in terms of  $E_{RMS}$  for the assimilation period (2011 and 2012). Presented are results for the open loop scenario and six data assimilation scenarios. Errors of open loop simulations are higher for the S80-simulation than for the BK50-simulation at all sites but Merzenhausen. At Merzenhausen  $E_{RMS}$  was  $0.054 \text{ cm}^3/\text{cm}^3$  for the S80 soil map and  $0.067 \text{ cm}^3/\text{cm}^3$  for the BK50 soil map. Open loop simulations with the S80 soil map resulted in  $E_{RMS}$ -values above  $0.10 \text{ cm}^3/\text{cm}^3$  at five of nine sites. At all sites data assimilation results with the S80 soil map improved SWC compared to the open loop simulations. This was also the case for the BK50 soil map simulations at all sites but Aachen



where  $E_{RMS}$  was larger than for the open loop run. In general, data assimilation improved simulations more for the S80 soil map ( $E_{RMS}$  reduced by  $0.079 \text{ cm}^3/\text{cm}^3$ ) than for the BK50 soil map ( $E_{RMS}$  reduced by  $0.01 \text{ cm}^3/\text{cm}^3$ ). Room for improvement with the BK50 soil map runs was more limited because of the smaller open loop errors. Nevertheless, after state updating alone the BK50 soil map still gave smaller errors than the S80 soil map. However, joint state-parameter estimation further improved simulation results by reducing  $E_{RMS}$ -values and the parameter updating resulted in similar  $E_{RMS}$ -values for the BK50 ( $0.028 \text{ cm}^3/\text{cm}^3$ ) and S80 soil map ( $0.03 \text{ cm}^3/\text{cm}^3$ ). The  $E_{RMS}$  for simulations with 10 % and 30 % perturbation of soil texture values  not show very different results.

The temporal course of soil moisture in 2011 at the two sites Gevenich and Merzenhausen is shown in Fig. 2. The figure  illustrates that SWC at both sites was lower with the S80 soil map than with the BK50 soil map. ~~In Gevenich and Merzenhausen,~~  mean open loop SWC in 2011 was  $0.17 \text{ cm}^3/\text{cm}^3$  for the S80 soil map at both sites and  $0.27 \text{ cm}^3/\text{cm}^3$  for the BK50 soil map at both sites. CRP measurements at Merzenhausen started in May 2011. In the data assimilation runs SWC was immediately affected at the Merzenhausen and Gevenich sites as soon as Merzenhausen CRP SWC retrievals were assimilated. The simulated SWC for the PAR-S80-30 data assimilation run increased as compared to the S80 open loop simulation. The first observation at Gevenich was recorded on July 7<sup>th</sup>, 2011. By that date, the simulated CLM SWC retrieval was already close to the CRP SWC retrieval at the Gevenich site (Fig. 2) due to SWC updates which showed to have a beneficial impact. Fig. 2 also shows that the  50 open loop run was close to the observed SWC at both sites, even without data assimilation.

Fig. 3 shows the temporal course of SWC from January 2011 to December 2013 at Heinsberg and Wildenrath. Assimilation and evaluation results are shown for the case of joint state-parameter updates (PAR-S80-30), only state updates (Stt-S80), open loop (OL-S80) and CRP SWC retrievals. At Heinsberg, results show that assimilated SWC was closer to the CRP SWC retrieval when both states and parameters were updated (PAR-S80-30) than if only states were updated (Stt-S80). This is the case in the assimilation period and in the evaluation period. At the beginning of the evaluation period, the Stt-S80 simulation shows an increase in bias between modeled CLM SWC retrievals and CRP SWC retrieval within the first few days of 2013. The bias of Stt-S80 remained throughout the evaluation period. In contrast, modeled SWC during the evaluation period was close to the CRP SWC retrieval if parameters were previously updated (PAR-S80-30).

The CRP at Wildenrath started operating on May 7<sup>th</sup>, 2012. SWC retrievals at other CRPs were assimilated already from May 2011 onwards and affected SWC at Wildenrath (Fig. 3). Until May 2012, Fig. 3 shows assimilated SWC (Stt-S80 and PAR-S80-30) was higher than open loop SWC. However, no SWC retrievals were available at the Wildenrath site for comparison during this period. When SWC retrievals from the CRP at Wildenrath became available and were assimilated into the model, assimilated (Stt-S80 and PAR-S80-30) and open loop (OL-S80) SWC were close to CRP SWC retrievals. This was the case throughout the remaining assimilation and evaluation period. These results suggest that the high sand



content of the biased soil map is not far from the optimal sand content at Wildenrath. Therefore, at Wildenrath, the high sand content of both soil maps (60 % and 80 %) resulted in good modeling results already for the open loop runs. This suggests that before May 2012, simulated SWC of the open loop runs with either soil map represented more realistic SWC than assimilated SWC during this period. This will be discussed further in the discussion section.

5

## 4.2 Verification period

The year 2013 was the verification year without data assimilation.  $E_{\text{RMS}}$  values for the evaluation period 2013 are reported in Table 4. On the one hand, BK50 data assimilation runs with joint state-parameter estimation resulted in improved SWC at three out of the nine sites compared to open loop BK50-runs. For the other six sites results worsened compared to the corresponding BK50 open loop run.  $E_{\text{RMS}}$  values increased from an average of  $0.041 \text{ cm}^3/\text{cm}^3$  (OL-BK50) over all sites to  $0.047 \text{ cm}^3/\text{cm}^3$  (PAR-BK50-30). On the other hand, for the S80 soil map, all sites except Wildenrath had significantly reduced  $E_{\text{RMS}}$  values for the case of data assimilation including parameter updating compared to the S80 open loop run. For the S80 simulations, average  $E_{\text{RMS}}$  over all sites for 2013 was on average  $0.12 \text{ cm}^3/\text{cm}^3$  for the open loop run and  $0.04 \text{ cm}^3/\text{cm}^3$  for the run including data assimilation. In case only states were updated (Stt-S80 and Stt-BK50),  $E_{\text{RMS}}$  was also slightly reduced (compared to open loop runs) for the majority of sites during the evaluation period in 2013. On average, this reduction was  $0.016 \text{ cm}^3/\text{cm}^3$  for the S80 soil map (Stt-S80) and  $0.002 \text{ cm}^3/\text{cm}^3$  for the BK50 soil map (Stt-BK50). At sites, where  $E_{\text{RMS}}$  was larger for data assimilation runs with state updating (compared to open loop runs), the increase was only  $0.001 \text{ cm}^3/\text{cm}^3$ .

Bias calculated on the basis of a comparison of hourly SWC measured by CRP and simulated for 2013 is reported in Table 5. The average bias for the S80 open loop run is  $0.11 \text{ cm}^3/\text{cm}^3$  while it is  $0.02 \text{ cm}^3/\text{cm}^3$  for the BK50 open loop run. Bias of the BK50 open loop run was positive at Merzenhausen, Gevenich, Heinsberg, and Aachen, and it was negative at Rollesbroich, Kall, RurAue, and Wuestebach. Bias was zero at Wildenrath for the BK50 open loop run. Bias of the S80 open loop run was negative at all sites indicating that modeled SWC was higher than measured SWC. Joint state-parameter updates reduced the absolute bias on average to  $0.03 \text{ cm}^3/\text{cm}^3$  (PAR-S80-30) and  $0.02 \text{ cm}^3/\text{cm}^3$  (PAR-S80-10) for the S80 soil map. In case of the BK50 soil map, the bias in 2013 increased to  $0.03 \text{ cm}^3/\text{cm}^3$  by joint state-parameter updates. State updates without parameter updates reduced the biases only marginally to  $0.01 \text{ cm}^3/\text{cm}^3$  for the BK50 soil map and to  $0.09 \text{ cm}^3/\text{cm}^3$  for the S80 soil map. This indicates that state updates also can slightly improve SWC-characterization in the verification period due to improved initial conditions.

30

## 4.3 Temporal evolution of mean $E_{\text{RMS}}$

Fig. 4 shows the temporal evolution of the hourly  $E_{\text{RMS}}$  calculated for all nine CRPs.  $E_{\text{RMS}}$  was highest for the S80 open loop run and lowest for the PAR-S80-30 simulation. State updates did not improve modeled SWC as much as joint state-parameter updates improved modeled SWC. The  $E_{\text{RMS}}$  in case of Stt-S80 also falls behind the  $E_{\text{RMS}}$  of the BK50 open loop



run through most of the time. Joint state-parameter updates for the S80 soil map improved the  $E_{RMS}$  throughout most of the time compared to the open loop simulations based on the BK50 and S80 soil maps. During the assimilation period 2011-2012, the PAR-S80-30 simulation performed best out of the four simulations. During the evaluation period 2013, OL-BK50 and PAR-S80-30 performed equally well except in summer 2013 when the PAR-S80-30 simulation yielded much higher  $E_{RMS}$ -values than the BK50 open loop run.

#### 4.4 Jackknife simulations

The jackknife simulations investigated the impact of the network of CRPs for improving estimates of SWC at locations between the CRPs, outside the network. The errors shown in Table 4 refers to the two open loop simulations (for the S80 soil map and the BK50 soil map) and the 18 jackknife simulations. All simulations with the S80 soil map resulted in an improved  $E_{RMS}$  in the jackknife simulations compared to the open loop simulation, except for Wildenrath. In all cases the  $E_{RMS}$  was smaller than  $0.10 \text{ m}^3/\text{m}^3$ . Error reduction was smaller at sites where the open loop error was smaller. At sites with large open loop  $E_{RMS}$ , the assimilation could reduce the  $E_{RMS}$  by 50 % or more. In case of the BK50 soil map, the jackknife simulations resulted in  $E_{RMS}$ -values below  $0.10 \text{ m}^3/\text{m}^3$  at all sites. However, in this case only at Merzenhausen the  $E_{RMS}$  was reduced during the data assimilation period. At Wildenrath, the  $E_{RMS}$  was highest for jk-BK50 ( $0.091 \text{ m}^3/\text{m}^3$ ) and jk-S80 ( $0.095 \text{ m}^3/\text{m}^3$ ). The average absolute bias for the jackknife experiments was  $0.04 \text{ cm}^3/\text{cm}^3$  for both soil maps, BK50 and S80, in the evaluation period 2013 (Table 5). Hence, bias in the jk-S80-\* simulations improved compared to the open loop run but not in the jk-BK50-\* simulations, where bias was already small.

#### 4.5 Temporal evolution of parameters

The temporal evolution of the percentage sand content during the assimilation period for the nine CRP sites is shown in Fig. 5 for PAR-S80-30, PAR-S80-10, PAR-BK50-30, PAR-BK50-10, jk-S80-30\* and jk-BK50-30\*. Time series start on March 20<sup>th</sup>, 2011, the date of the first assimilated CRP SWC retrieval at Wuestebach. Wuestebach and sites within the influence sphere of Wuestebach (Aachen, Kall and Rollesbroich) show also a change in sand content from this date onwards. All other sites show a change in sand content in May 2012 when Rollesbroich and Merzenhausen start operating and their data is assimilated.  sites show variability in sand content over time. Wuestebach, Kall, RurAue, Rollesbroich and Heinsberg show some peaks in the time series. Merzenhausen, Aachen, Gevenich, and Wildenrath show a smoother course compared to  other sites. Sand levels approach a constant site-specific value for the sites Merzenhausen (45 %), Kall (30 %), Gevenich (41 %), RurAue (30 %), Heinsberg (42 %) and Wildenrath (62 %) with a reasonable spread amongst the experiments. The spread in estimated sand content for the sites Wuestebach, Aachen and Rollesbroich is larger, and it seems not to have stabilized at the end of the assimilation. Sand content estimates of the jackknife simulations was close to the sand content of the other data assimilation experiments with joint state-parameter estimation at the sites Merzenhausen, Gevenich, RurAue and Heinsberg. Evolution of the sand content for the jackknife simulations showed larger deviations from the sand content estimated by other data assimilation experiments for the sites Wuestebach, Kall, Aachen, Rollesbroich and Wildenrath.



The soil hydraulic parameter  $B$  and saturated hydraulic conductivity are shown in Fig. 6 and Fig. 7 for PAR-S80-30, PAR-S80-10, PAR-BK50-30, PAR-BK50-10, jk-S80-30\* and jk-BK50-30\*. Updates of soil hydraulic parameters start in March and May 2011 with the assimilation of SWC retrievals depending on the location. The  $B$  parameter increases for all simulations. Throughout the whole assimilation period  $B$  varies considerably within short time intervals. The total range of the  $B$  parameter is between 2.7 and 14 at all sites. At the sites Merzenhausen, Kall, Aachen, Gevenich and Rollesbroich, it generally ranges between 6 and 10. At Wuestebach, Heinsberg and RurAue,  $B$  ranges most of the time between 8 and 12, and at Wildenrath,  $B$  is below 8. Initial saturated hydraulic conductivity is rather high ( $k_{sat} > 0.015$  mm/s) in case of high sand content i.e. for the S80 soil map, and rather low ( $k_{sat} < 0.005$  mm/s) in case of low sand content i.e. for the BK50 soil map. In case of the S80 soil map, at all sites except Wildenrath, high initial saturated hydraulic conductivity decreases quickly by parameter updates to values below 0.01 mm/s. The initial spread in  $k_{sat}$  values amongst the simulation scenarios decreases at most sites. At Wuestebach, Merzenhausen, Aachen, Gevenich, RurAue and Heinsberg, the spread is rather small particularly at the end of the assimilation period, while at Wildenrath  $k_{sat}$  ranges from 0.005 to 0.015 for individual experiments at the end of the assimilation period. The discussion section will elaborate more on this.

15

#### 4.6 Latent heat and sensible heat

Latent heat flux or evapotranspiration (ET) is another important diagnostic variable of the CLM model and of importance for atmospheric models. Results of the data assimilation experiments showed that soil texture updates altered soil moisture states significantly. In Fig. 8 it is shown that joint state-parameter estimation also altered ET. Fig. 8 shows ET within the evaluation period 2013 across the whole catchment for four simulations. On the one hand, ET was similar for both open loop simulations in the South of the catchment. On the other hand, ET in the North was up to 80 mm per year lower for the S80 open loop run compared to the BK50 open loop run. Regarding open loop runs, the differences can be linked to the drier soil conditions in case OL-S80 compared OL-BK50 simulation results. For PAR-S80-10, ET increased by up to 40 mm per year in the Northern part of the catchment through data assimilation. The differences between open loop ET and data assimilation ET were larger for the S80 soil map than for the BK50 soil map. This could be related to the larger update in SWC in case of the S80 scenario compared to the BK50 scenario.

## 5 Discussion

The applied data assimilation scheme improved soil moisture characterization in the majority of simulation experiments with the regional Community Land Model (CLM). During 2011 and 2012, the biased S80 soil map gave a  $E_{RMS}$  up to  $0.17 \text{ cm}^3/\text{cm}^3$  (at Rollesbroich) in the open loop simulation which left plenty of room for improvements. The soil map BK50 led to  $E_{RMS}$ -values in open loop simulations below  $0.05 \text{ cm}^3/\text{cm}^3$  which left little room for error reduction considering the measurement error of  $0.03 \text{ cm}^3/\text{cm}^3$ . For the simulations starting with 80 % sand content, sand content was closer to the values of the BK50 soil map after joint state-parameter estimation. However, the temporal evolution of the updated soil



texture and the soil hydraulic parameters was not stable. Temporal fluctuations imply that there may be multiple or seasonal optimal parameter values. This is also supported by the findings of the temporal behavior of  $E_{RMS}$  during the evaluation period e.g. when in the dry summer 2013 the  $E_{RMS}$  peaked in the PAR-S80-30 simulation. Many possible error sources were not subject to calibration in this study but they could be crucial for an even better soil moisture and more stable soil parameter estimation. In this study we only considered uncertainty of soil parameters, but also vegetation parameters are uncertain. Also a number of other CLM-specific hydrologic parameters (e.g. decay factor for subsurface runoff and maximum subsurface drainage) strongly influence state variables in CLM and hence show also potential for optimization. Considering this uncertainty could give a better uncertainty characterization. Precipitation is an important forcing for the model calculations and its estimate could be improved. For this study, precipitation data from the COSMO\_DE re-analysis were used. A product which optimally combines gauge measurements and precipitation estimates from radar could give better precipitation estimates. This could improve the soil moisture characterization and also potentially lead to better parameter estimates. Also other error sources like the ones related to the model structure play a significant role. This should be subject of future investigation.

Evaluation simulations for 2013 led to partly improved and partly deteriorated  $E_{RMS}$  values when the BK50 soil map was used as prior information on the soil hydraulic properties. The simulations with the S80 soil map on the contrary showed an improved soil moisture characterization in all simulation scenarios and the updated soil hydraulic parameter estimates for those simulations approached the values of the BK50 soil map. These results indicate that the soil hydraulic parameters derived from the BK50 soil map were already well suited for soil moisture predictions and updating soil texture and soil parameters could not improve further the results.  $E_{RMS}$  values for simulations with state updates only (Stt-BK50 and Stt-BK50) in 2013 imply the beneficial role of state updates only. However, the improvements in the evaluation period by state updates (without parameter values) are small compared to the improvements obtained by joint state-parameter estimation. This illustrates the benefits of joint state-parameter updates compared to state updates only, and that soil moisture states are strongly determined by soil hydraulic parameters. It also illustrates that the improved characterization of soil moisture states in the assimilation period which results in improved initial states for the verification period loses its influence in the verification period fast over time.

The jackknife simulations illustrated that a network of CRPs can improve modeled SWC if the soil map information is not sufficient. Temporal evolution of subsurface parameters of the jackknife simulations (e.g. jk-S80-\*) was close to the evolution of parameter estimates by other simulations (e.g. PAR-S80-10). Parameter estimates at jackknife test sites were inferred from multiple surrounding CRP sites, while updates at sites with CRP information were strongly inferred from single site information. A comparison of parameter estimates at the end of the assimilation period indicates that initial soil parameterization has a limited effect on the resulting parameter estimates. Parameter estimates of jk-BK50-30\* and jk-S80-30\* are close together at the end of the assimilation period. The CRP network led to improved results for the jackknife



evaluation simulations in case of the biased soil map. This suggests that assimilation of CRP data is particularly useful for regions with little information on subsurface parameters. We expect a tradeoff between the initial uncertainty on soil moisture content (related to the quality of the soil map and meteorological data) and the density of a CRP network. In case of a large uncertainty, like in regions with limited information about soils and a low density of meteorological stations, a sparse network of probes can already be helpful for improving soil moisture characterization. On the other hand, in regions with a high density of meteorological stations and a high resolution soil map it can be expected that a high resolution CRP network is needed to further lower the error of soil moisture characterization. Further experiments in other regions with networks of CRPs are needed to get more quantitative information about this.

A question that remains to be answered is whether it is more beneficial to assimilate neutron counts measured by CRPs directly or to assimilate CRP SWC retrievals derived from the neutron counts, as done in this study. Fast neutron intensity measured by CRPs is also affected by vegetation. Neutron count rate decreases with increasing biomass because of the hydrogen content in vegetation (Baatz et al., 2015). Seasonal biomass changes at a single site have a rather small impact on neutron intensity compared to differences between grass land site and a forest site (Baatz et al., 2015). Therefore, using measured neutron flux directly in a data assimilation framework in a catchment with different vegetation types would require to account for the effects of vegetation types on neutron intensity. Hence, vegetation estimates for each grid cell would be necessary. At present, there are two methods that include biomass in the CRP calibration process (Baatz et al., 2015; Franz et al., 2013b) but both methods naturally require accurate biomass estimates, which are typically not available. Besides the uncertainty associated with CRP methods using biomass in the calibration process, biomass estimates also come along with high uncertainties. Therefore, in the case of a catchment with different vegetation types, it is desirable to circumvent the use of biomass estimates, and assimilate directly SWC retrievals obtained at the observation sites instead of assimilating neutron intensity. Therefore, this study uses CRP SWC retrievals in the data assimilation scheme assuming that seasonal changes of biomass can be neglected.

## 6 Conclusions and Outlook

This study demonstrates the benefits of assimilating data from a network of nine cosmic-ray probes (CRP) in the land surface model CLM version 4.5. Although information on neutron flux intensity was only available at few locations in the catchment, the local ensemble transform Kalman filter (LETKF) allows updating of soil water content (SWC) at unmonitored locations in the catchment considering model and observation uncertainties. Joint state-parameter estimates improved soil moisture estimates during the assimilation and during the evaluation period. The  $E_{\text{RMS}}$  and bias for the soil moisture characterization reduced strongly for simulations initialized with a biased soil map and approached values similar to the ones obtained when the regional soil map was used as input to the simulations.  $E_{\text{RMS}}$ -values in simulations with a regional soil map were not improved, because open loop simulation results were already close to the observations. The beneficial results of joint state-parameter updates were confirmed by additional jackknife experiments. This real-world case



study on assimilating CRP SWC retrievals into a land surface model shows the potential of CRP networks to improve subsurface parameterization in regional land surface models, especially if prior information on soil properties is limited. In many areas of the world, less detailed soil maps are available than the high resolution regional soil map applied in this study. In these areas, more advanced sub-surface characterization is possible using CRP measurements and the data assimilation framework presented in this study.

For now, CRP neutron intensity observations were not assimilated directly. In future studies it would be desirable to use the COSMIC operator for assimilating neutron intensity observations directly. However, in this case the impact of biomass on the CRP measurement signal would have to be taken into account. Therefore, it is desirable to further develop the COSMIC operator to include the impact of biomass on neutron intensities. Using the biogeochemical module of CLM would then allow to characterize local vegetation states as input for the measurement operator. Remotely sensed vegetation states are another option to characterize vegetation states as input for the measurement operator. Both methods require additional field measurements for the verification of vegetation state estimates. The further extension of the data assimilation framework would also enable the estimation of additional sub-surface parameters. The impact of other sub-surface parameters such as subsurface drainage parameters and the surface drainage decay factor on SWC states and radiative surface fluxes has already been shown (Sun et al., 2013). Estimation of these parameters is desirable because of the inherent uncertainty of these globally tuned parameters. However, estimation of soil texture and organic matter content was demonstrated to be already beneficial for improved SWC modeling. Hence, this study represents a way forward towards the integration of CRP information in the calibration of large scale weather prediction models.

## 20 Data Availability

Most data presented in this study are freely available via the TERENO data portal TEODOOR (<http://teodoor.icg.kfa-juelich.de/>). Atmospheric data were licensed by the German Weather Service (DWD), and the BK50 soil map was licensed by the Geologischer Dienst Nordrhein-Westfalen.

## Acknowledgements

25 We gratefully acknowledge the support by the SFB-TR32 "Pattern in Soil-Vegetation-Atmosphere Systems: Monitoring, Modelling and Data Assimilation" funded by the Deutsche Forschungsgemeinschaft (DFG) and TERENO (Terrestrial Environmental Observatories) funded by the Helmholtz-Gemeinschaft. The authors also gratefully acknowledge the computing time granted by the John von Neumann Institute for Computing (NIC) and provided on the supercomputer JURECA at Jülich Supercomputing Centre (JSC).

30



## 7 References

- Ajami, H., McCabe, M. F., Evans, J. P., and Stisen, S.: Assessing the impact of model spin-up on surface water-groundwater interactions using an integrated hydrologic model, *Water Resour Res*, 50, 2636-2656, 10.1002/2013wr014258, 2014.
- Anderson, J. L.: An ensemble adjustment Kalman filter for data assimilation, *Mon Weather Rev*, 129, 2884-2903, Doi 10.1175/1520-0493(2001)129<2884:Aeakff>2.0.Co;2, 2001.
- 5 Baatz, R., Bogena, H. R., Hendricks Franssen, H. J., Huisman, J. A., Qu, W., Montzka, C., and Vereecken, H.: Calibration of a catchment scale cosmic-ray probe network: A comparison of three parameterization methods, *J Hydrol*, 516, 231-244, <http://dx.doi.org/10.1016/j.jhydrol.2014.02.026>, 2014.
- Baatz, R., Bogena, H. R., Hendricks Franssen, H. J., Huisman, J. A., Montzka, C., and Vereecken, H.: An empirical vegetation correction for soil water content quantification using cosmic ray probes, *Water Resour Res*, 51, 2030-2046, 10.1002/2014WR016443, 2015.
- 10 Bateni, S. M., and Entekhabi, D.: Surface heat flux estimation with the ensemble Kalman smoother: Joint estimation of state and parameters, *Water Resour Res*, 48, Artn W08521 10.1029/2011wr011542, 2012.
- Bell, J. E., Leeper, R. D., Palecki, M. A., Coopersmith, E., Wilson, T., Bilotta, R., and Embler, S.: Evaluation of the 2012 Drought with a Newly Established National Soil Monitoring Network, *Vadose Zone J*, 14, 10.2136/vzj2015.02.0023, 2015.
- 15 Bogena, H. R., Herbst, M., Hake, J. F., Kunkel, R., Montzka, C., Pütz, T., Vereecken, H., and Wendland, F.: MOSYRUR - Water balance analysis in the Rur basin., in: *Schriften des Forschungszentrums Jülich. Reihe Umwelt/Environment*, Jülich, 2005.
- Bogena, H. R., Huisman, J. A., Baatz, R., Franssen, H. J. H., and Vereecken, H.: Accuracy of the cosmic-ray soil water content probe in humid forest ecosystems: The worst case scenario, *Water Resour Res*, 49, 5778-5791, Doi 10.1002/Wrcr.20463, 2013.
- 20 Burgers, G., van Leeuwen, P. J., and Evensen, G.: Analysis scheme in the ensemble Kalman filter, *Mon Weather Rev*, 126, 1719-1724, Doi 10.1175/1520-0493(1998)126<1719:Asitek>2.0.Co;2, 1998.
- Chen, F., Manning, K. W., LeMone, M. A., Trier, S. B., Alfieri, J. G., Roberts, R., Tewari, M., Niyogi, D., Horst, T. W., Oncley, S. P., Basara, J. B., and Blanken, P. D.: Description and evaluation of the characteristics of the NCAR high-resolution land data assimilation system, *J Appl Meteorol Clim*, 46, 694-713, 10.1175/Jam2463.1, 2007.
- 25 Chen, Y., and Zhang, D. X.: Data assimilation for transient flow in geologic formations via ensemble Kalman filter, *Adv Water Resour*, 29, 1107-1122, 10.1016/j.advwatres.2005.09.007, 2006.
- Clapp, R. B., and Hornberger, G. M.: Empirical Equations for Some Soil Hydraulic-Properties, *Water Resour Res*, 14, 601-604, Doi 10.1029/Wr014i004p00601, 1978.
- Cosby, B. J., Hornberger, G. M., Clapp, R. B., and Ginn, T. R.: A Statistical Exploration of the Relationships of Soil-Moisture Characteristics to the Physical-Properties of Soils, *Water Resour Res*, 20, 682-690, Doi 10.1029/Wr020i006p00682, 1984.
- 30 Cosh, M. H., Ochsner, T. E., McKee, L., Dong, J. N., Basara, J. B., Evett, S. R., Hatch, C. E., Small, E. E., Steele-Dunne, S. C., Zreda, M., and Sayde, C.: The Soil Moisture Active Passive Marena, Oklahoma, In Situ Sensor Testbed (SMAP-MOISST): Testbed Design and Evaluation of In Situ Sensors, *Vadose Zone J*, 15, 10.2136/vzj2015.09.0122, 2016.
- Crow, W. T.: Correcting land surface model predictions for the impact of temporally sparse rainfall rate measurements using an ensemble Kalman filter and surface brightness temperature observations, *J Hydrometeorol*, 4, 960-973, 2003.
- 35 Crow, W. T., Berg, A. A., Cosh, M. H., Loew, A., Mohanty, B. P., Panciera, R., de Rosnay, P., Ryu, D., and Walker, J. P.: Upscaling Sparse Ground-Based Soil Moisture Observations for the Validation of Coarse-Resolution Satellite Soil Moisture Products, *Rev Geophys*, 50, Artn Rg2002 Doi 10.1029/2011rg000372, 2012.
- 40 De Lannoy, G. J. M., Reichle, R. H., Arsenault, K. R., Houser, P. R., Kumar, S., Verhoest, N. E. C., and Pauwels, V. R. N.: Multiscale assimilation of Advanced Microwave Scanning Radiometer-EOS snow water equivalent and Moderate Resolution Imaging Spectroradiometer snow cover fraction observations in northern Colorado, *Water Resour Res*, 48, Artn W01522 Doi 10.1029/2011wr010588, 2012.
- Desilets, D., Zreda, M., and Ferre, T. P. A.: Nature's neutron probe: Land surface hydrology at an elusive scale with cosmic rays, *Water Resour Res*, 46, 10.1029/2009WR008726, 2010.
- 45 Desilets, D., and Zreda, M.: Footprint diameter for a cosmic-ray soil moisture probe: Theory and Monte Carlo simulations, *Water Resour Res*, 49, 3566-3575, Doi 10.1002/Wrcr.20187, 2013.
- Draper, C. S., Mahfouf, J. F., and Walker, J. P.: An EKF assimilation of AMSR-E soil moisture into the ISBA land surface scheme, *J Geophys Res-Atmos*, 114, 10.1029/2008JD011650, 2009.
- 50 Dunne, S., and Entekhabi, D.: An ensemble-based reanalysis approach to land data assimilation, *Water Resour Res*, 41, Artn W02013 10.1029/2004wr003449, 2005.
- Eltahir, E. A. B.: A soil moisture rainfall feedback mechanism 1. Theory and observations, *Water Resour Res*, 34, 765-776, Doi 10.1029/97wr03499, 1998.
- Erdal, D., Neuweiler, I., and Wollschlager, U.: Using a bias aware EnKF to account for unresolved structure in an unsaturated zone model, *Water Resour Res*, 50, 132-147, 10.1002/2012wr013443, 2014.



- Erdal, D., Rahman, M. A., and Neuweiler, I.: The importance of state transformations when using the ensemble Kalman filter for unsaturated flow modeling: Dealing with strong nonlinearities, *Adv Water Resour*, 86, 354-365, 10.1016/j.advwatres.2015.09.008, 2015.
- Evensen, G.: Sequential Data Assimilation with a Nonlinear Quasi-Geostrophic Model Using Monte-Carlo Methods to Forecast Error Statistics, *J Geophys Res-Oceans*, 99, 10143-10162, Doi 10.1029/94jc00572, 1994.
- 5 Franz, T. E., Zreda, M., Ferre, T. P. A., and Rosolem, R.: An assessment of the effect of horizontal soil moisture heterogeneity on the area-average measurement of cosmic-ray neutrons, *Water Resour Res*, 49, 6450-6458, Doi 10.1002/Wrcr.20530, 2013a.
- Franz, T. E., Zreda, M., Rosolem, R., and Ferre, T. P. A.: A universal calibration function for determination of soil moisture with cosmic-ray neutrons, *Hydrol Earth Syst Sc*, 17, 453-460, DOI 10.5194/hess-17-453-2013, 2013b.
- GmbH, s.: Digital Elevation Model 10 without anthropogenic landfo<sub>RMS</sub>, 2010.
- 10 Han, X., Franssen, H. J. H., Montzka, C., and Vereecken, H.: Soil moisture and soil properties estimation in the Community Land Model with synthetic brightness temperature observations, *Water Resour Res*, 50, 6081-6105, 10.1002/2013WR014586, 2014a.
- Han, X., Franssen, H. J. H., Rosolem, R., Jin, R., Li, X., and Vereecken, H.: Correction of systematic model forcing bias of CLM using assimilation of cosmic-ray Neutrons and land surface temperature: a study in the Heihe Catchment, China, *Hydrol. Earth Syst. Sci.*, 19, 615-629, 10.5194/hess-19-615-2015, 2015.
- 15 Han, X., Franssen, H.-J. H., Bello, M. Á. J., Rosolem, R., Bogena, H., Alzamora, F. M., Chanzy, A., and Vereecken, H.: Simultaneous Soil Moisture and Properties Estimation for a Drip Irrigated Field by Assimilating Cosmic-ray Neutron Intensity, *J Hydrol*, <http://dx.doi.org/10.1016/j.jhydrol.2016.05.050>, 2016.
- Han, X. J., Franssen, H. J. H., Li, X., Zhang, Y. L., Montzka, C., and Vereecken, H.: Joint Assimilation of Surface Temperature and L-Band Microwave Brightness Temperature in Land Data Assimilation, *Vadose Zone J*, 12, Doi 10.2136/Vzj2012.0072, 2013.
- 20 Han, X. J., Franssen, H. J. H., Montzka, C., and Vereecken, H.: Soil moisture and soil properties estimation in the Community Land Model with synthetic brightness temperature observations, *Water Resour Res*, 50, 6081-6105, 10.1002/2013WR014586, 2014b.
- Hawdon, A., McJannet, D., and Wallace, J.: Calibration and correction procedures for cosmic-ray neutron soil moisture probes located across Australia, *Water Resour Res*, 50, 5029-5043, 10.1002/2013WR015138, 2014.
- Hendricks Franssen, H. J., and Kinzelbach, W.: Real-time groundwater flow modeling with the Ensemble Kalman Filter: Joint estimation of states and parameters and the filter inbreeding problem, *Water Resour Res*, 44, Artn W09408  
 25 Doi 10.1029/2007wr006505, 2008.
- Houser, P. R., Shuttleworth, W. J., Famiglietti, J. S., Gupta, H. V., Syed, K. H., and Goodrich, D. C.: Integration of soil moisture remote sensing and hydrologic modeling using data assimilation, *Water Resour Res*, 34, 3405-3420, Doi 10.1029/1998wr900001, 1998.
- Hunt, B. R., Kostelich, E. J., and Szunyogh, I.: Efficient data assimilation for spatiotemporal chaos: A local ensemble transform Kalman filter, *Physica D*, 230, 112-126, Doi 10.1016/j.physd.2006.11.008, 2007.
- 30 Hurkmans, R., Paniconi, C., and Troch, P. A.: Numerical assessment of a dynamical relaxation data assimilation scheme for a catchment hydrological model, *Hydrol Process*, 20, 549-563, 10.1002/hyp.5921, 2006.
- Jackson, T. J., Le Vine, D. M., Hsu, A. Y., Oldak, A., Starks, P. J., Swift, C. T., Isham, J. D., and Haken, M.: Soil moisture mapping at regional scales using microwave radiometry: The Southern Great Plains Hydrology Experiment, *Ieee T Geosci Remote*, 37, 2136-2151,  
 35 Doi 10.1109/36.789610, 1999.
- Kohli, M., Schron, M., Zreda, M., Schmidt, U., Dietrich, P., and Zacharias, S.: Footprint characteristics revised for field-scale soil moisture monitoring with cosmic-ray neutrons, *Water Resour Res*, 51, 5772-5790, 10.1002/2015WR017169, 2015.
- Koster, R. D., Dirmeyer, P. A., Guo, Z. C., Bonan, G., Chan, E., Cox, P., Gordon, C. T., Kanae, S., Kowalczyk, E., Lawrence, D., Liu, P., Lu, C. H., Malyshev, S., McAvaney, B., Mitchell, K., Mocko, D., Oki, T., Oleson, K., Pitman, A., Sud, Y. C., Taylor, C. M., Versegny, D.,  
 40 Vasic, R., Xue, Y. K., Yamada, T., and Team, G.: Regions of strong coupling between soil moisture and precipitation, *Science*, 305, 1138-1140, DOI 10.1126/science.1100217, 2004.
- Kumar, S. V., Reichle, R. H., Harrison, K. W., Peters-Lidard, C. D., Yatheendradas, S., and Santanello, J. A.: A comparison of methods for a priori bias correction in soil moisture data assimilation, *Water Resour Res*, 48, Artn W03515  
 Doi 10.1029/2010wr010261, 2012.
- 45 Kurtz, W., He, G. W., Kollet, S. J., Maxwell, R. M., Vereecken, H., and Franssen, H. J. H.: TerrSysMP-PDAF version 1.0): a modular high-performance data assimilation framework for an integrated land surface-subsurface model, *Geosci Model Dev*, 9, 1341-1360, 10.5194/gmd-9-1341-2016, 2016.
- Lawrence, D. M., and Slater, A. G.: Incorporating organic soil into a global climate model, *Clim Dynam*, 30, 145-160, 10.1007/s00382-007-0278-1, 2008.
- 50 Lee, J. H.: Spatial-Scale Prediction of the SVAT Soil Hydraulic Variables Characterizing Stratified Soils on the Tibetan Plateau from an EnKF Analysis of SAR Soil Moisture, *Vadose Zone J*, 13, 10.2136/vzj2014.06.0060, 2014.
- Liu, J. J., Fung, I., Kalnay, E., Kang, J. S., Olsen, E. T., and Chen, L.: Simultaneous assimilation of AIRS Xco(2) and meteorological observations in a carbon climate model with an ensemble Kalman filter, *J Geophys Res-Atmos*, 117, Artn D05309  
 10.1029/2011jd016642, 2012.
- 55 Ly, L., Franz, T. E., Robinson, D. A., and Jones, S. B.: Measured and Modeled Soil Moisture Compared with Cosmic-Ray Neutron Probe Estimates in a Mixed Forest, *Vadose Zone J*, 13, 10.2136/vzj2014.06.0077, 2014.



- Miyoshi, T., and Kunii, M.: The Local Ensemble Transform Kalman Filter with the Weather Research and Forecasting Model: Experiments with Real Observations, *Pure Appl Geophys*, 169, 321-333, 10.1007/s00024-011-0373-4, 2012.
- Montzka, C., Canty, M., Kunkel, R., Menz, G., Vereecken, H., and Wendland, F.: Modelling the water balance of a mesoscale catchment basin using remotely sensed land cover data, *J Hydrol*, 353, 322-334, DOI 10.1016/j.jhydrol.2008.02.018, 2008.
- 5 Montzka, C., Moradkhani, H., Weihermuller, L., Franssen, H. J. H., Canty, M., and Vereecken, H.: Hydraulic parameter estimation by remotely-sensed top soil moisture observations with the particle filter, *J Hydrol*, 399, 410-421, 10.1016/j.jhydrol.2011.01.020, 2011.
- Montzka, C., Pauwels, V. R. N., Franssen, H. J. H., Han, X. J., and Vereecken, H.: Multivariate and Multiscale Data Assimilation in Terrestrial Systems: A Review, *Sensors-Basel*, 12, 16291-16333, 10.3390/s121216291, 2012.
- Montzka, C., Grant, J. P., Moradkhani, H., Franssen, H. J. H., Weihermuller, L., Drusch, M., and Vereecken, H.: Estimation of Radiative Transfer Parameters from L-Band Passive Microwave Brightness Temperatures Using Advanced Data Assimilation, *Vadose Zone J*, 12, 10.2136/vzj2012.0040, 2013.
- 10 Moradkhani, H., Sorooshian, S., Gupta, H. V., and Houser, P. R.: Dual state-parameter estimation of hydrological models using ensemble Kalman filter, *Adv Water Resour*, 28, 135-147, 10.1016/j.advwatres.2004.09.002, 2005.
- Nordrhein-Westfalen, G. D.: Informationssystem Bodenkarte 50, 1:50000, 2009.
- 15 Oglesby, R. J., and Erickson, D. J.: Soil-Moisture and the Persistence of North-American Drought, *J Climate*, 2, 1362-1380, Doi 10.1175/1520-0442(1989)002<1362:Smatpo>2.0.Co;2, 1989.
- Oleson, K., Lawrence, D. M., Bonan, G. B., Drewniak, B., Huang, M., Koven, C. D., Levis, S., Li, F., Riley, J. M., Subin, Z. M., Swenson, S., Thornton, P. E., Bozbiyik, A., Fisher, R., Heald, C. L., Kluzek, E., Lamarque, J.-F., Lawrence, P. J., Leung, L. R., Lipscomb, W., Muszala, S. P., Ricciuto, D. M., Sacks, W. J., Sun, Y., Tang, J., and Yang, Z.-L.: Technical description of version 4.5 of the Community Land Model (CLM), NCAR Technical Note NCAR/TN-503+STR, 420, 10.5065/D6RR1W7M, 2013.
- 20 Pauwels, V. R. N., Balenzano, A., Satalino, G., Skriver, H., Verhoest, N. E. C., and Mattia, F.: Optimization of Soil Hydraulic Model Parameters Using Synthetic Aperture Radar Data: An Integrated Multidisciplinary Approach, *Ieee T Geosci Remote*, 47, 455-467, 10.1109/Tgrs.2008.2007849, 2009.
- Pelowitz, D. B.: MCNPX user's manual, version 5, Rep. LA-CP-05-0369, Los Alamos National Laboratory, Los Alamos LA-CP-05-0369, 25 2005.
- Penny, S. G., Kalnay, E., Carton, J. A., Hunt, B. R., Ide, K., Miyoshi, T., and Chepurin, G. A.: The local ensemble transform Kalman filter and the running-in-place algorithm applied to a global ocean general circulation model, *Nonlinear Proc Geoph*, 20, 1031-1046, 10.5194/npg-20-1031-2013, 2013.
- Reichle, R. H., McLaughlin, D. B., and Entekhabi, D.: Hydrologic data assimilation with the ensemble Kalman filter, *Mon Weather Rev*, 130, 103-114, Doi 10.1175/1520-0493(2002)130<0103:Hdawte>2.0.Co;2, 2002a.
- 30 Reichle, R. H., Walker, J. P., Koster, R. D., and Houser, P. R.: Extended versus ensemble Kalman filtering for land data assimilation, *J Hydrometeorol*, 3, 728-740, Doi 10.1175/1525-7541(2002)003<0728:Evekff>2.0.Co;2, 2002b.
- Reichle, R. H.: Data assimilation methods in the Earth sciences, *Adv Water Resour*, 31, 1411-1418, 10.1016/j.advwatres.2008.01.001, 2008.
- 35 Reichle, R. H., Kumar, S. V., Mahanama, S. P. P., Koster, R. D., and Liu, Q.: Assimilation of Satellite-Derived Skin Temperature Observations into Land Surface Models, *J Hydrometeorol*, 11, 1103-1122, Doi 10.1175/2010jhm1262.1, 2010.
- Rhodin, A., Kucharski, F., Callies, U., Eppel, D. P., and Wergen, W.: Variational analysis of effective soil moisture from screen-level atmospheric parameters: Application to a short-range weather forecast model, *Q J Roy Meteor Soc*, 125, 2427-2448, Doi 10.1256/Smsqj.55904, 1999.
- 40 Robinson, D. A., Campbell, C. S., Hopmans, J. W., Hornbuckle, B. K., Jones, S. B., Knight, R., Ogden, F., Selker, J., and Wendroth, O.: Soil moisture measurement for ecological and hydrological watershed-scale observatories: A review, *Vadose Zone J*, 7, 358-389, Doi 10.2136/Vzj2007.0143, 2008.
- Rosolem, R., Hoar, T., Arellano, A., Anderson, J. L., Shuttleworth, W. J., Zeng, X., and Franz, T. E.: Translating aboveground cosmic-ray neutron intensity to high-frequency soil moisture profiles at sub-kilometer scale, *Hydrol. Earth Syst. Sci.*, 18, 4363-4379, 10.5194/hess-18-45 4363-2014, 2014.
- Seneviratne, S. I., Luthi, D., Litschi, M., and Schar, C.: Land-atmosphere coupling and climate change in Europe, *Nature*, 443, 205-209, Doi 10.1038/Nature05095, 2006.
- Seneviratne, S. I., Corti, T., Davin, E. L., Hirschi, M., Jaeger, E. B., Lehner, I., Orlowsky, B., and Teuling, A. J.: Investigating soil moisture-climate interactions in a changing climate: A review, *Earth-Science Reviews*, 99, 125-161, http://dx.doi.org/10.1016/j.earscirev.2010.02.004, 2010.
- 50 Sheffield, J., and Wood, E. F.: Global trends and variability in soil moisture and drought characteristics, 1950-2000, from observation-driven Simulations of the terrestrial hydrologic cycle, *J Climate*, 21, 432-458, 10.1175/2007JCLI1822.1, 2008.
- Shi, Y. N., Davis, K. J., Zhang, F. Q., Duffy, C. J., and Yu, X.: Parameter estimation of a physically based land surface hydrologic model using the ensemble Kalman filter : A synthetic experiment, *Water Resour Res*, 50, 706-724, 10.1002/2013wr014070, 2014.



- Shi, Y. N., Davis, K. J., Zhang, F. Q., Duffy, C. J., and Yu, X.: Parameter estimation of a physically-based land surface hydrologic model using an ensemble Kalman filter: A multivariate real-data experiment, *Adv Water Resour*, 83, 421-427, 10.1016/j.advwatres.2015.06.009, 2015.
- 5 Shrestha, P., Sulis, M., Masbou, M., Kollet, S., and Simmer, C.: A Scale-Consistent Terrestrial Systems Modeling Platform Based on COSMO, CLM, and ParFlow, *Mon Weather Rev*, 142, 3466-3483, 10.1175/Mwr-D-14-00029.1, 2014.
- Shuttleworth, J., Rosolem, R., Zreda, M., and Franz, T.: The COsmic-ray Soil Moisture Interaction Code (COSMIC) for use in data assimilation, *Hydrol Earth Syst Sc*, 17, 3205-3217, DOI 10.5194/hess-17-3205-2013, 2013.
- Simmer, C., Thiele-Eich, I., Masbou, M., Amelung, W., Bogena, H., Crewell, S., Diekkruger, B., Ewert, F., Franssen, H. J. H., Huisman, J. A., Kemna, A., Klitzsch, N., Kollet, S., Langensiepen, M., Lohnert, U., Rahman, A. S. M. M., Rascher, U., Schneider, K., Schween, J., Shao, Y. P., Shrestha, P., Stiebler, M., Sulis, M., Vanderborght, J., Vereecken, H., van der Kruk, J., Waldhoff, G., and Zerenner, T.: MONITORING AND MODELING THE TERRESTRIAL SYSTEM FROM PORES TO CATCHMENTS The Transregional Collaborative Research Center on Patterns in the Soil-Vegetation-Atmosphere System, *B Am Meteorol Soc*, 96, 1765-1787, 10.1175/Bams-D-13-00134.1, 2015.
- 10 Song, X. H., Shi, L. S., Ye, M., Yang, J. Z., and Navon, I. M.: Numerical Comparison of Iterative Ensemble Kalman Filters for Unsaturated Flow Inverse Modeling, *Vadose Zone J*, 13, 10.2136/vzj2013.05.0083, 2014.
- 15 Sun, Y., Hou, Z., Huang, M., Tian, F., and Leung, L. R.: Inverse modeling of hydrologic parameters using surface flux and runoff observations in the Community Land Model, *Hydrol Earth Syst Sc*, 17, 4995-5011, 10.5194/hess-17-4995-2013, 2013.
- Temimi, M., Lakhankar, T., Zhan, X. W., Cosh, M. H., Krakauer, N., Fares, A., Kelly, V., Khanbilvardi, R., and Kumassi, L.: Soil Moisture Retrieval Using Ground-Based L-Band Passive Microwave Observations in Northeastern USA, *Vadose Zone J*, 13, 10.2136/vzj2013.06.0101, 2014.
- 20 Vereecken, H., Huisman, J. A., Bogena, H., Vanderborght, J., Vrugt, J. A., and Hopmans, J. W.: On the value of soil moisture measurements in vadose zone hydrology: A review, *Water Resour Res*, 44, Artn W00d06  
Doi 10.1029/2008wr006829, 2008.
- Vereecken, H., Schnepf, A., Hopmans, J. W., Javaux, M., Or, D., Roose, D. O. T., Vanderborght, J., Young, M. H., Amelung, W., Aitkenhead, M., Allison, S. D., Assouline, S., Baveye, P., Berli, M., Bruggemann, N., Finke, P., Flury, M., Gaiser, T., Govers, G., Ghezzehei, T., Hallett, P., Franssen, H. J. H., Heppell, J., Horn, R., Huisman, J. A., Jacques, D., Jonard, F., Kollet, S., Lafolie, F., Lamorski, K., Leitner, D., McBratney, A., Minasny, B., Montzka, C., Nowak, W., Pachepsky, Y., Padarian, J., Romano, N., Roth, K., Rothfuss, Y., Rowe, E. C., Schwen, A., Simunek, J., Tiktak, A., Van Dam, J., van der Zee, S. E. A. T. M., Vogel, H. J., Vrugt, J. A., Wohling, T., and Young, I. M.: Modeling Soil Processes: Review, Key Challenges, and New Perspectives, *Vadose Zone J*, 15, 10.2136/vzj2015.09.0131, 2016.
- 25 Villarreyes, C. A. R., Baroni, G., and Oswald, S. E.: Inverse modelling of cosmic-ray soil moisture for field-scale soil hydraulic parameters, *Eur J Soil Sci*, 65, 876-886, 10.1111/ejss.12162, 2014.
- Vrugt, J. A., Diks, C. G. H., Gupta, H. V., Bouten, W., and Verstraten, J. M.: Improved treatment of uncertainty in hydrologic modeling: Combining the strengths of global optimization and data assimilation, *Water Resour Res*, 41, Artn W01017  
10.1029/2004wr003059, 2005.
- 30 Waldhoff, G.: Enhanced land use classification of 2009 for the Rur catchment, in, TR32DB, 2012.
- Whan, K., Zscheischler, J., Orth, R., Shongwe, M., Rahimi, M., Asare, E. O., and Seneviratne, S. I.: Impact of soil moisture on extreme maximum temperatures in Europe, *Weather and Climate Extremes*, 9, 57-67, <http://dx.doi.org/10.1016/j.wace.2015.05.001>, 2015.
- Wu, C. C., and Margulis, S. A.: Feasibility of real-time soil state and flux characterization for wastewater reuse using an embedded sensor network data assimilation approach, *J Hydrol*, 399, 313-325, 10.1016/j.jhydrol.2011.01.011, 2011.
- 40 Wu, C. C., and Margulis, S. A.: Real-Time Soil Moisture and Salinity Profile Estimation Using Assimilation of Embedded Sensor Datastreams, *Vadose Zone J*, 12, 10.2136/vzj2011.0176, 2013.
- Zacharias, S., Bogena, H., Samaniego, L., Mauder, M., Fuss, R., Putz, T., Frenzel, M., Schwank, M., Baessler, C., Butterbach-Bahl, K., Bens, O., Borg, E., Brauer, A., Dietrich, P., Hajnsek, I., Helle, G., Kiese, R., Kunstmann, H., Klotz, S., Munch, J. C., Papen, H., Priesack, E., Schmid, H. P., Steinbrecher, R., Rosenbaum, U., Teutsch, G., and Vereecken, H.: A Network of Terrestrial Environmental Observatories in Germany, *Vadose Zone J*, 10, 955-973, Doi 10.2136/Vzj2010.0139, 2011.
- Zreda, M., Desilets, D., Ferre, T. P. A., and Scott, R. L.: Measuring soil moisture content non-invasively at intermediate spatial scale using cosmic-ray neutrons, *Geophys Res Lett*, 35, 10.1029/2008GL035655, 2008.
- 45 Zreda, M., Shuttleworth, W. J., Zeng, X., Zweck, C., Desilets, D., Franz, T., and Rosolem, R.: COSMOS: the COsmic-ray Soil Moisture Observing System (vol 16, pg 4079, 2012), *Hydrol Earth Syst Sc*, 17, 1065-1066, DOI 10.5194/hess-17-1065-2013, 2012.
- 50



## Figures

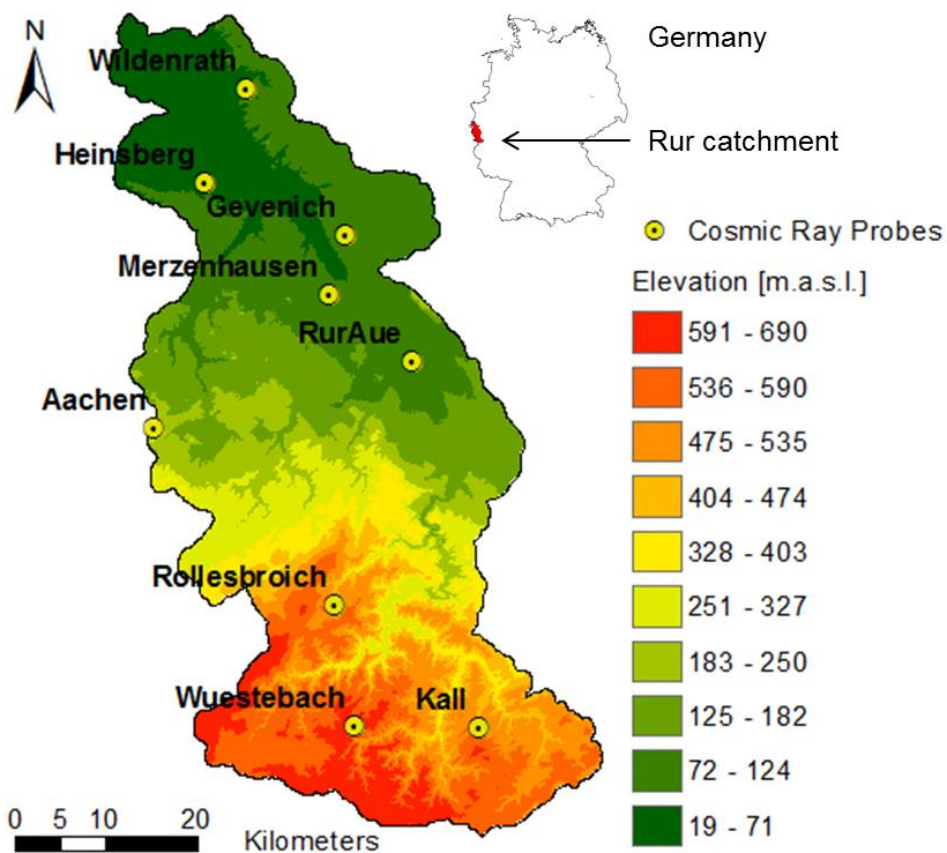


Fig. 1. Map of the Rur catchment and locations of the nine cosmic-ray probes. The hilly South of the catchment is prone to more rainfall,  
5 lower average temperatures and less potential evapotranspiration than the North of the catchment.

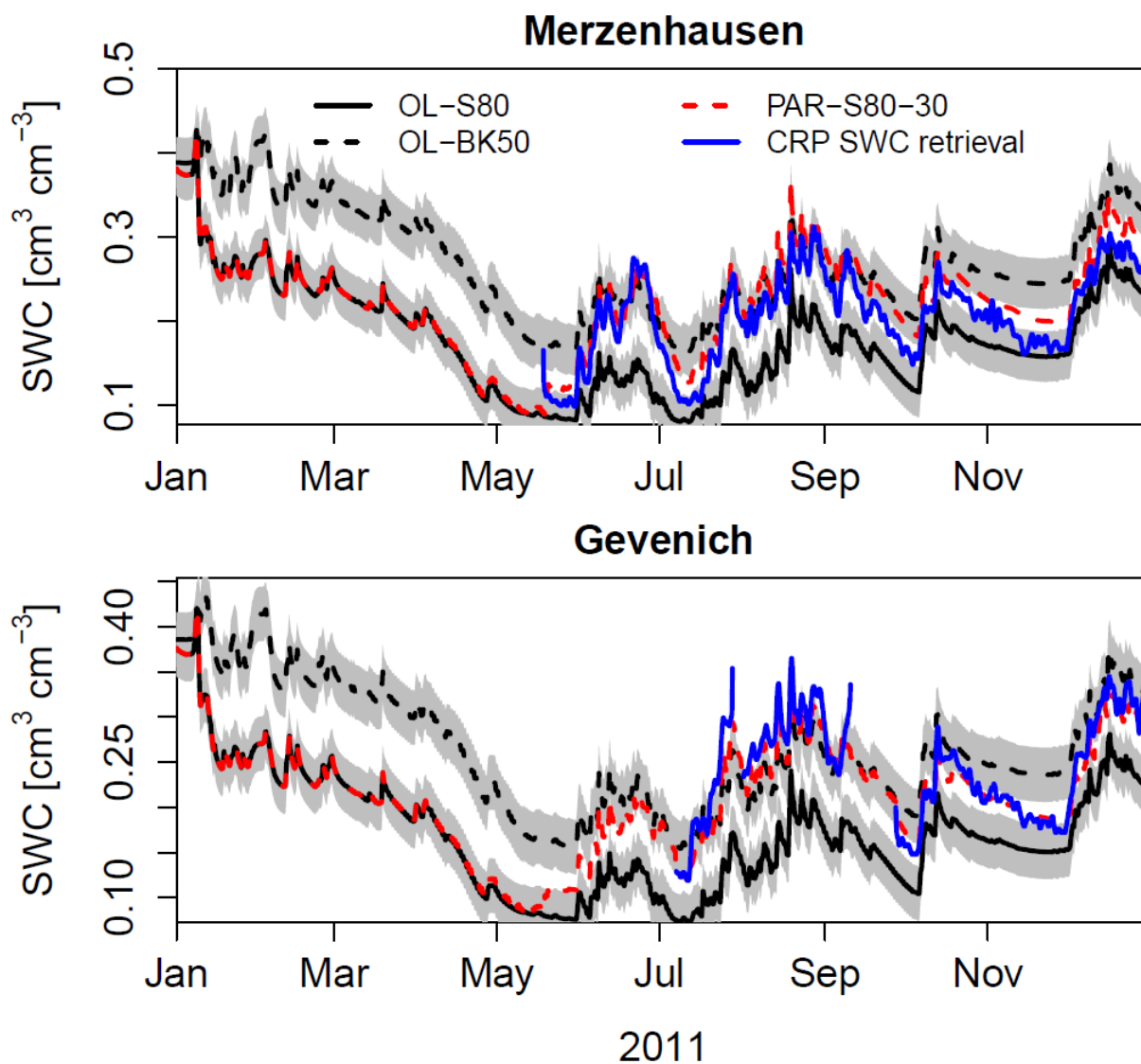


Fig. 2. Temporal evolution of simulated SWC, calculated with open loop (OL-\*) simulations and data assimilation including parameter updating (PAR-S80-30), together with the CRP soil water content retrieval (SWC) during the first year of simulation at the sites Merzenhausen and Gevenich. Simulated SWC was vertically weighted using the COSMIC operator to obtain the appropriate SWC corresponding to the CRP SWC retrieval.

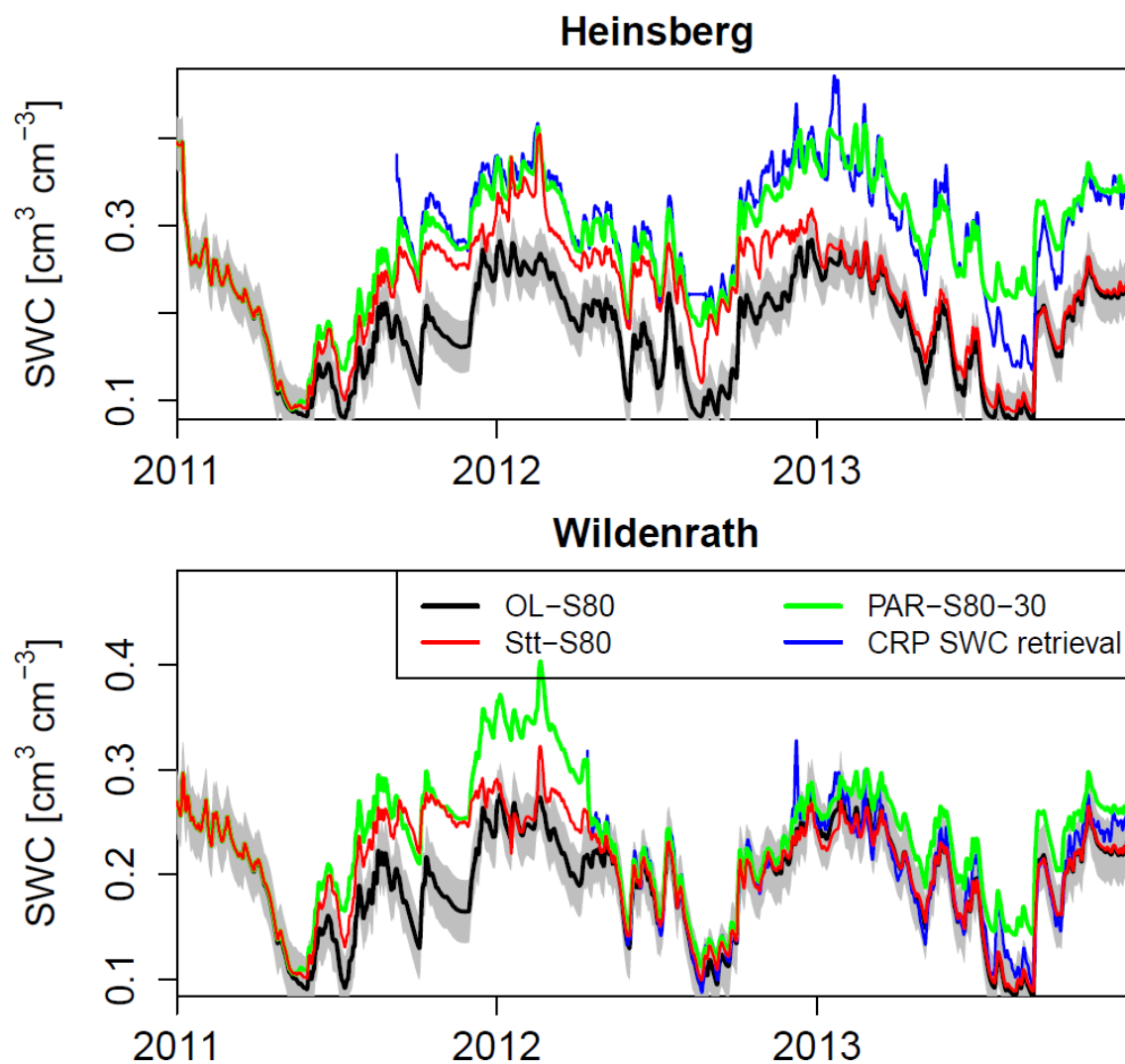


Fig. 3. Temporal evolution of simulated SWC retrievals, calculated with open loop (OL-S80), data assimilation with state update only (Stt-BK50), and data assimilation including parameter updating (PAR-S80-30), together with the CRP soil water content (SWC) retrieval at the sites Heinsberg and Wildenrath for the data assimilation period 2011 and 2012, and the evaluation period 2013. Simulated SWC was vertically weighted to obtain the appropriate SWC corresponding to the CRP SWC retrieval.

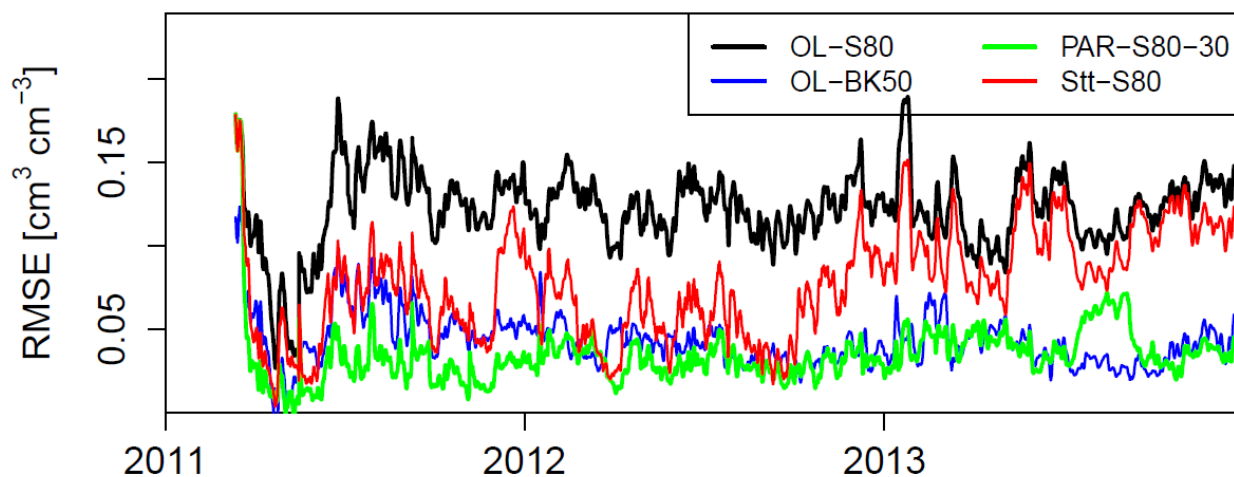


Fig. 4. Temporal evolution of root mean square error ( $E_{RMS}$ ) for hourly SWC retrievals.  $E_{RMS}$  is calculated hourly for nine CRP's for open loop runs for soil maps S80 and BK50, joint state-parameter updates (PAR-S80-30) and state updates only (Stt-S80) during the assimilation period (2011 and 2012) and verification period (2013).

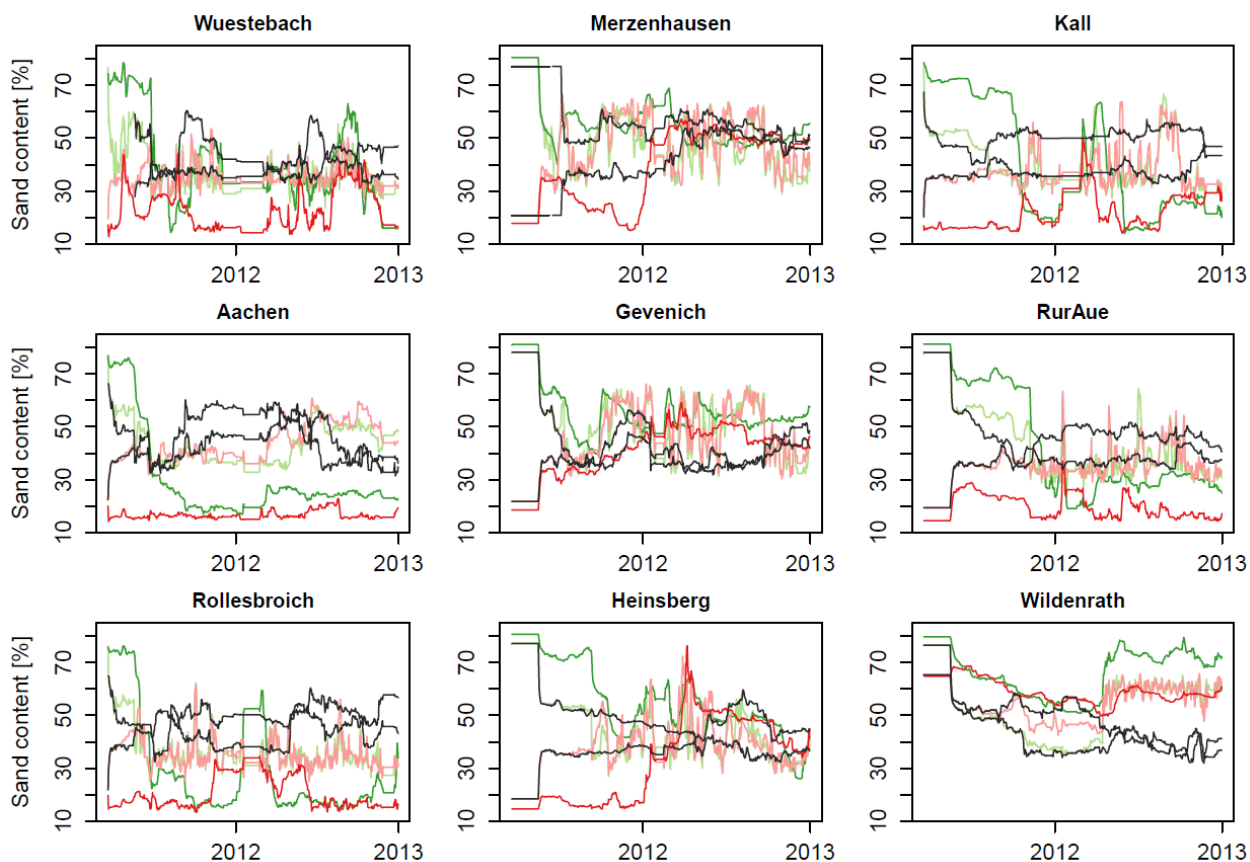


Fig. 5. Temporal evolution of the percentage sand content for simulations with parameter update: PAR-S80-30 (green), PAR-S80-10 (light green), PAR-BK50-30 (red), PAR-BK50-10 (light red), jk-S80-30\* (black) and jk-BK50-30\* (black).

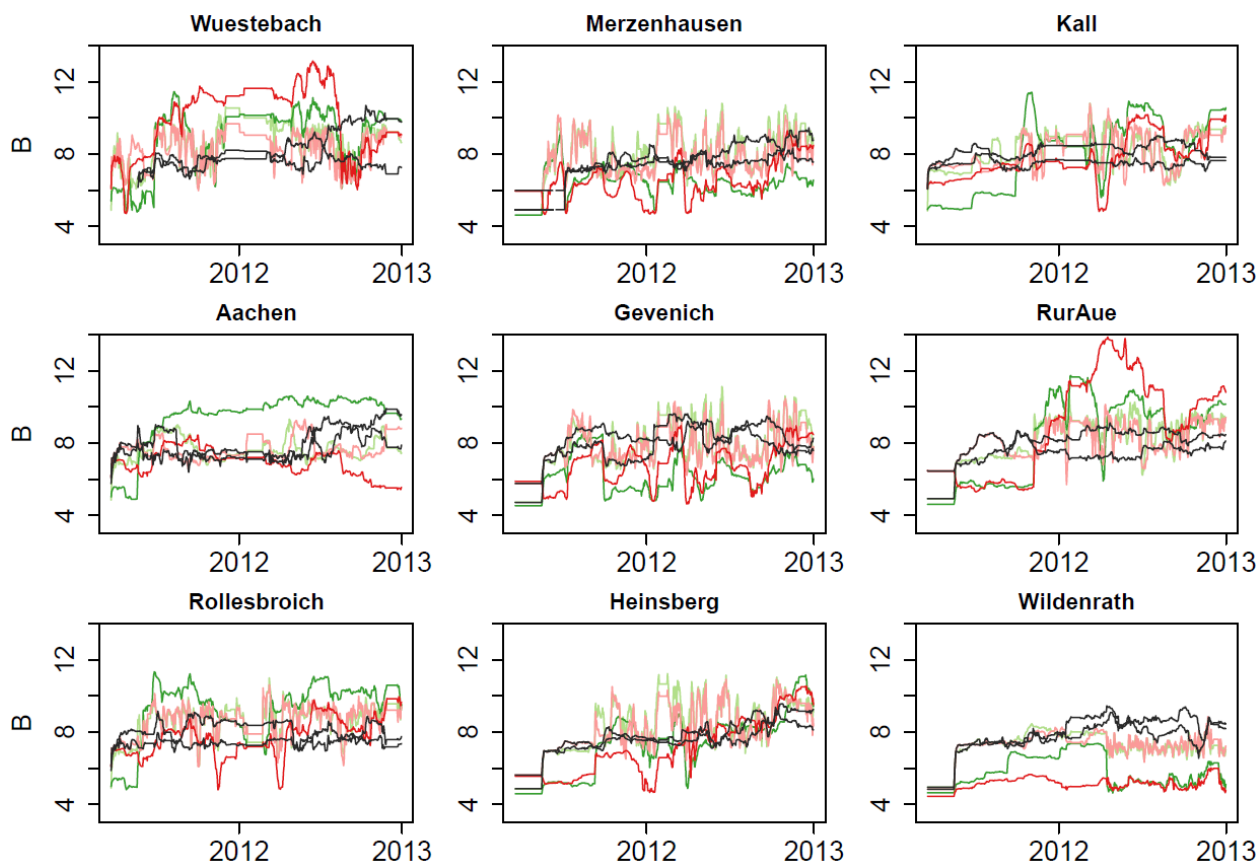


Fig. 6. Temporal evolution of the B parameter (top 15cm) for simulations with parameter update: PAR-S80-30 (green), PAR-S80-10 (light green), PAR-BK50-30 (red), PAR-BK50-10 (light red), jk-S80-30\* (black) and jk-BK50-30\* (black).

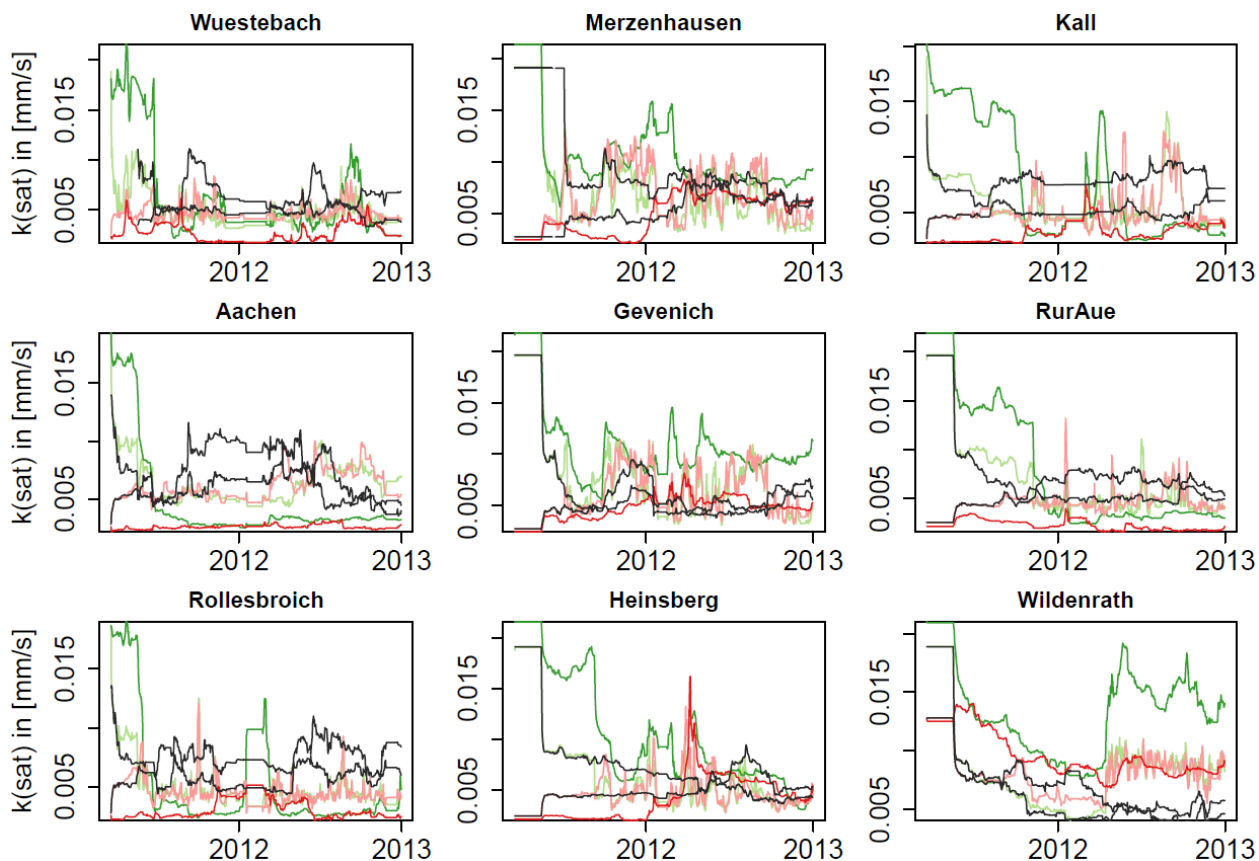


Fig. 7. Temporal evolution of saturated hydraulic conductivity (top 15cm) for simulations with parameter update: PAR-S80-30 (green), PAR-S80-10 (light green), PAR-BK50-30 (red), PAR-BK50-10 (light red), jk-S80-30\* (black) and jk-BK50-30\* (black).

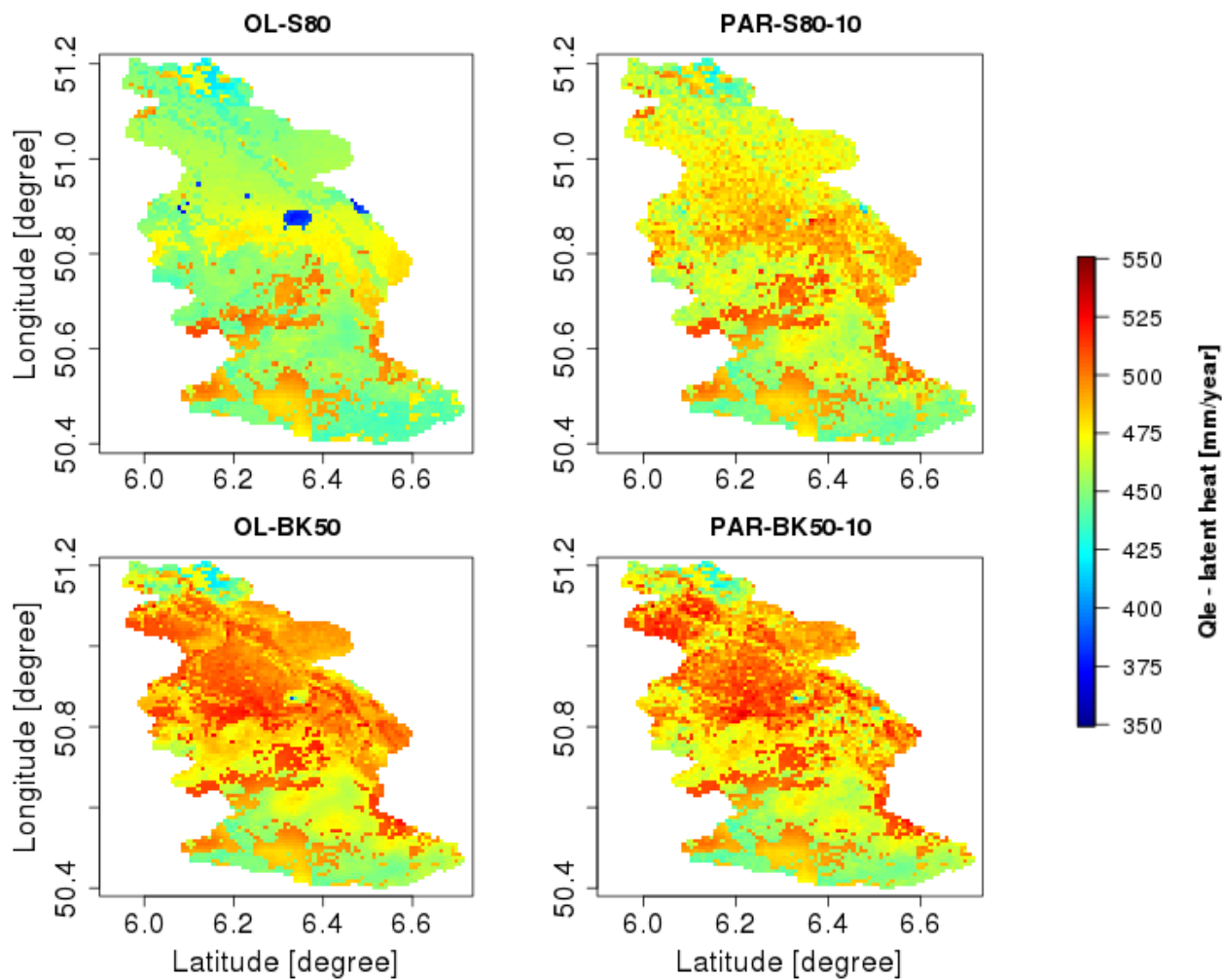


Fig. 8. Annual evapotranspiration in the evaluation period (year 2013) for simulations OL-S80, OL-BK50, PAR-S80-10 and PAR-BK50-10.



## Tables

Table 1: Site information on elevation (m.a.s.l.), average annual precipitation (mm/year), CLM plant functional type, sand content (%), clay content (%), and the date of the first SWC retrieval assimilated.

Name	m.a.s.l.	Precip.	Plant functional type	Sand	Clay	Date of first assimilation
Aachen	232	952	Crops	22	23	13.01.2012
Gevenich	108	884	Crops	22	20	07.07.2011
Heinsberg	57	814	Crops	18	19	09.09.2011
Kall	504	935	C3 non arctic grass	20	22	15.09.2011
Merzenhausen	94	825	Crops	21	22	19.05.2011
Rollesbroich	515	1307	C3 non arctic grass	22	23	19.05.2011
RurAue	102	743	C3 non arctic grass	19	26	08.11.2011
Wildenrath	76	856	Broadleaf deciduous temperate tree	65	12	07.05.2012
Wuestebach	605	1401	Needleleaf evergreen temperate tree	19	23	20.03.2011



5 Table 2: Overview of simulation scenarios: Open loop (OL-\*) with variation in the soil map BK50 or S80, data assimilation run with state update (Stt) or joint state- and parameter update (PAR) with variation in the soil map perturbation (-10 or -30), and jackknife evaluation runs (jk-S80-1 to 9, and jk-BK50-1 to 9).

Simulation Code	Soil Perturbation		Sand Content		Update	
	10	30	BK50	80 % fix	State	Parameter
OL-BK50		+	+			
OL-S80		+		+		
Stt-BK50		+	+		+	
Stt-S80		+		+	+	
PAR-BK50-30		+	+		+	+
PAR-BK50-10	+		+		+	+
PAR-S80-30		+		+	+	+
PAR-S80-10	+			+	+	+
jk-BK50-1 to 9		+	+		+	+
jk-S80-1 to 9		+		+	+	+



Table 3:  $E_{\text{RMS}}$  ( $\text{cm}^3/\text{cm}^3$ ) at CRP sites for open loop runs and different data assimilation scenarios, for the assimilation period (2011 and 2012).

2011 & 2012	Rollesbroich	Merzenhausen	Gevenich	Heinsberg	Kall	RurAue	Wuestebach	Aachen	Wildenrath	Average $E_{\text{RMS}}$
OL-BK50	0.054	0.067	0.039	0.035	0.042	0.027	0.041	0.032	0.017	0.039
Stt-BK50	0.033	0.041	0.021	0.022	0.030	0.024	0.038	0.023	0.017	0.028
PAR-BK50-10	0.036	0.036	0.019	0.021	0.033	0.025	0.035	0.045	0.015	0.029
PAR-BK50-30	0.031	0.034	0.018	0.019	0.027	0.023	0.040	0.044	0.016	0.028
jk-BK50-*	0.070	0.058	0.073	0.035	0.048	0.050	0.053	0.050	0.091	0.059
OL-S80	0.170	0.053	0.081	0.117	0.149	0.158	0.065	0.169	0.020	0.109
Stt-S80	0.104	0.020	0.037	0.051	0.083	0.056	0.060	0.086	0.018	0.057
PAR-S80-10	0.032	0.038	0.024	0.023	0.033	0.023	0.036	0.048	0.015	0.030
PAR-S80-30	0.029	0.035	0.018	0.019	0.027	0.023	0.039	0.068	0.016	0.030
jk-S80-*	0.082	0.038	0.063	0.026	0.062	0.034	0.038	0.073	0.095	0.057



Table 4:  $E_{RMS}$  ( $\text{cm}^3/\text{cm}^3$ ) at CRP-sites for open loop, data assimilation and jackknife simulations on the basis of a comparison with CRP SWC retrievals during the verification period (2013). For each jackknife simulation only one  $E_{RMS}$  is reported: The  $E_{RMS}$  of the location that is meant for evaluation.

Year 2013	Rollesbroich	Merzenhausen	Gevenich	Heinsberg	Kall	RurAue	Wuestebach	Aachen	Wildenrath	Average $E_{RMS}$
OL-BK50	0.044	0.065	0.036	0.027	0.048	0.038	0.048	0.042	0.017	0.041
Stt-BK50	0.041	0.054	0.034	0.027	0.049	0.038	0.048	0.041	0.018	0.039
PAR-BK50-10	0.068	0.062	0.036	0.038	0.056	0.056	0.043	0.058	0.017	0.048
PAR-BK50-30	0.052	0.061	0.035	0.033	0.068	0.048	0.043	0.048	0.035	0.047
jk-BK50-*	0.036	0.047	0.028	0.025	0.042	0.031	0.040	0.054	0.106	0.045
OL-S80	0.157	0.062	0.106	0.115	0.160	0.154	0.099	0.167	0.019	0.115
Stt-S80	0.100	0.063	0.107	0.106	0.099	0.146	0.097	0.158	0.020	0.100
PAR-S80-10	0.060	0.039	0.043	0.040	0.064	0.043	0.052	0.060	0.019	0.047
PAR-S80-30	0.049	0.059	0.037	0.036	0.053	0.032	0.046	0.047	0.035	0.044
jk-S80-*	0.079	0.046	0.042	0.036	0.059	0.038	0.063	0.044	0.105	0.057



Table 5: Bias ( $\text{cm}^3/\text{cm}^3$ ) at CRP-sites for open loop, data assimilation and jackknife simulations compared to CRP SWC retrievals during the verification period (2013). For each jackknife simulation only one bias is reported: The bias of the location that is meant for evaluation.

Year 2013	Rollesbroich	Merzenhausen	Gevenich	Heinsberg	Kall	Rur-Aue	Wuestebach	Aachen	Wildenrath	Mean absolute bias
OL-BK50	-0.03	0.06	0.01	0.00	-0.02	0.00	-0.02	0.01	0.00	0.02
Stt-BK50	-0.01	0.04	0.00	0.00	-0.01	-0.01	-0.02	0.00	0.00	0.01
PAR-BK50-10	0.06	0.05	0.01	0.02	0.04	0.04	0.02	-0.04	0.00	0.03
PAR-BK50-30	0.03	0.05	0.00	0.02	0.04	0.03	-0.01	-0.03	0.03	0.03
jk-BK50-*	-0.02	0.04	0.01	-0.01	-0.03	-0.02	-0.03	-0.05	0.11	0.04
OL-S80	-0.17	-0.05	-0.08	-0.12	-0.15	-0.16	-0.09	-0.17	-0.01	0.11
Stt-S80	-0.09	-0.05	-0.10	-0.10	-0.08	-0.14	-0.09	-0.15	-0.01	0.09
PAR-S80-10	0.03	0.05	-0.01	0.02	0.03	0.01	-0.01	-0.03	0.03	0.02
PAR-S80-30	0.04	0.02	-0.03	0.02	0.05	0.03	0.03	-0.04	-0.01	0.03
jk-S80-*	-0.07	0.03	0.02	0.02	-0.04	-0.02	-0.04	-0.03	0.10	0.04

5

~~Evaluating the value~~Evaluation of a ~~network of~~ cosmic-ray  
~~probes~~neutron sensor network for ~~improving~~improved land  
surface ~~modelling~~model prediction

**Style Definition:** Caption: Font:  
Calibri, 11 pt

5 Roland Baatz<sup>1,2</sup>, Harrie-Jan Hendricks Franssen<sup>1,2</sup>, Xujun Han<sup>1,2</sup>, Tim Hoar<sup>3</sup>, Heye ~~R.~~Reemt  
Bogena<sup>1</sup> and Harry Vereecken<sup>1,2</sup>

<sup>1</sup>Agrosphere (IBG-3), Forschungszentrum Jülich GmbH, 52425 Jülich, Germany.

<sup>2</sup>HPSC-TerrSys , 52425 Jülich, Germany.

<sup>3</sup>NCAR Data Assimilation Research Section, Boulder, CO, USA.

**Formatted:** English (U.K.)

10 *Correspondence to:* Roland Baatz (r.baatz@fz-juelich.de)

**Abstract:** Land surface models can model matter and energy fluxes between the land surface and atmosphere, and provide a lower boundary condition to atmospheric circulation models. For these applications, accurate In-situ soil moisture quantification is sensors provide highly desirable accurate but not always possible given limited observations and limited subsurface data accuracy. Cosmic ray probes (CRPs) offer an interesting alternative to indirectly measure very local soil moisture and provide an observation that can be assimilated into land surface models for improved measurements while remotely sensed soil moisture prediction. Synthetic studies have shown the potential to estimate subsurface parameters of land surface models with the assimilation of CRP observations is strongly affected by vegetation and surface roughness. In contrast, Cosmic-Ray Neutron Sensors (CRNS) allow highly accurate soil moisture estimation at the field scale which could be valuable to improve land surface model predictions. In this study, the potential of a network of CRPs/CRNS installed in the 2354 km<sup>2</sup> Rur catchment (Germany) for estimating subsurface soil hydraulic parameters and improved/improving soil moisture states is/was tested in a real world case scenario using. Data measured by the CRNS were assimilated with the local ensemble transform Kalman filter within the Community Land Model. The potential of the CRP network was tested by assimilating CRP data v. 4.5. Data of four, eight and nine CRNS were assimilated for the years 2011 and 2012 (with ~~or~~ and without soil hydraulic parameter estimation), followed by the verification year 2013, without data assimilation. This was done using (i) the regional soil map/high resolution soil map, (ii) the FAO soil map and (iii) an erroneous, biased soil map as input information for the simulations, and (ii) an erroneous, biased soil map. For the regional soil map, soil moisture characterization was only improved in the assimilation period but not in the verification period. For the FAO soil map and the biased soil map, soil moisture characterization/predictions improved in both periods strongly from to a  $E_{RMS}$  root mean square error of  $0.11 \text{ cm}^3/\text{cm}^3$  to  $0.03 \text{ cm}^3/\text{cm}^3$  (for the assimilation period) and from  $0.12 \text{ cm}^3/\text{cm}^3$  to  $0.05 \text{ cm}^3/\text{cm}^3$  (verification for the evaluation period) and the estimated soil hydraulic parameters were after. Improvements were limited by the measurement error of CRNS ( $0.03 \text{ cm}^3/\text{cm}^3$ ). The positive results obtained with data assimilation closer to the ones of of nine CRNS were confirmed by the regional soil map. Finally, the value of the CRP network was also evaluated with jackknifing data-jackknife experiments with four and eight CRNS used for assimilation experiments. It was found that the CRP network is able to improve soil moisture estimates at locations between the assimilation sites from. The results demonstrate that assimilated data of a  $E_{RMS}$ -CRNS network can improve the characterization of soil moisture content at the catchment scale by updating spatially distributed soil hydraulic parameters of  $0.12 \text{ cm}^3/\text{cm}^3$  to  $0.06 \text{ cm}^3/\text{cm}^3$  (verification period), but again only if the initial soil map was biased a land surface model.

Formatted: English (U.K.)

Formatted: English (U.K.)

Formatted: English (U.K.)

Formatted: English (U.K.)

## 1 Introduction

Soil water content (SWC) is a key variable of land surface hydrology and has a strong control on the partitioning of net radiation between latent and sensible heat flux- (Brutsaert, 2005). Knowledge of SWC is relevant for the assessment of plant water stress and agricultural production, as well as runoff generation as a response to precipitation events (Vereecken et al., 2008; Robinson et al., 2008). In atmospheric circulation models, SWC is important as a lower boundary condition ~~and while it~~ is calculated as a state variable in land surface models. Coupling of atmospheric circulation models and land surface models allows quantifying the role of soil moisture on atmospheric processes such as soil moisture-precipitation feedbacks (Koster et al., 2004; Eltahir, 1998) and summer climate variability and drought (Seneviratne et al., 2006; Oglesby and Erickson, 1989; Sheffield and Wood, 2008; Seneviratne et al., 2006; Bell et al., 2015). It is therefore important to improve the modelling and prediction of SWC, ~~but this is hampered by~~. Data assimilation of soil moisture provides a way to improve imperfect land surface model deficiencies and predictions. Here, soil moisture measurements are used to update model predictions by optimally considering the uncertainty of model initial conditions, model parameters and model forcings. However, there is a lack of high quality soil moisture data (Vereecken et al., 2016). Soil moisture measured by space-~~borne~~ remote sensing technologies provides information over large areas (e.g. Temimi et al., 2014). ~~However, space born remote sensing supplies only information on the upper few centimeters, but is strongly affected by vegetation, and data are not reliable for areas with dense vegetation-surface roughness (e.g. Temimi et al., 2014).~~ Therefore, in this paper an alternative source for soil moisture information is explored- which can measure soil moisture more accurately under dense vegetation (Bogena et al., 2013). Cosmic-ray ~~probes (CRPs)~~ neutron sensors (CRNS) measure fast neutron intensity ~~which allows estimating SWC~~ at an intermediate scale of ~15 ha (Kohli et al., 2015; Zreda et al., 2008; Desilets et al., 2010; Cosh et al., 2016; Lv et al., 2014) which is ~~closer to~~ the desired application scale of land surface models (Ajami et al., 2014; Chen et al., 2007; Shrestha et al., 2014). Fast neutrons originate from ~~moderation collisions~~ of secondary cosmic particles from outer space ~~by with~~ terrestrial atoms. ~~These particles are mainly fast~~ Fast neutrons, ~~which in turn~~ are moderated most effectively by hydrogen because ~~of the mass of a neutron is similar atomic mass to that of a nucleus of the hydrogen atom.~~ Therefore, the corresponding fast neutron intensity measured by ~~CRPs~~ CRNS strongly depends on the amount of hydrogen within the ~~CRP~~ CRNS footprint, allowing for a continuous non-invasive soil moisture estimate ~~over an area of ~15 ha (Kohli et al., 2015).~~ at the field scale. The spatial ~~extend~~ extent of this measurement is desirable as it matches with the desired grid cell size of a high resolution land surface model (Crow et al., 2012) and small scale heterogeneities are averaged over a larger area (Franz et al., 2013a; Desilets and Zreda, 2013; Kohli et al., 2015). Vertical measurement depth ranges from a maximum of ~70 cm under completely dry conditions and decreases to roughly ~12 cm under wet conditions

Formatted: English (U.S.)

(e.g. 40 vol. % soil moisture) (~~Bogena et al., 2013~~). ~~Worldwide several CRP~~(Kohli et al., 2015; Franz et al., 2012). Worldwide several CRNS networks exist, like the North American COSMOS network (Zreda et al., 2012), the German ~~CRP~~CRNS network (Baatz et al., 2014) installed in the context of the TERENO infrastructure measure (Zacharias et al., 2011) ~~and~~, the Australian COSMoZ network (~~Hawdon et al., 2014~~)(Hawdon et al., 2014) and the British COSMOS-UK (Evans et al., 2016).

~~Soil moisture~~In this work, fast neutron intensity data assimilation providesmeasured by CRNS are assimilated in a ~~way~~land surface model, to evaluate the impact those data can have to improve ~~imperfect soil moisture characterization and~~ land surface model predictions ~~with measured soil moisture data by merging model predictions and data, and can consider the uncertainty of initial conditions, model parameters and model forcings.~~ The Ensemble Kalman Filtering (EnKF) is one of the most commonly applied data assimilation methods (Evensen, 1994; Burgers et al., 1998). ~~Soil moisture data assimilation has been the subject of intensive study for more than a decade now. An early contribution was provided by Houser et al. (1998) who assimilated remotely sensed soil moisture observations from a microwave radiometer into a land atmosphere transfer scheme using four dimensional variational data assimilation. Rhodin et al. (1999) assimilated soil moisture data for a four day period in order to obtain an improved characterization of the lower boundary condition for an atmospheric circulation model. They also used a variational data assimilation approach. More recently, the~~The EnKF is much less CPU intensive compared to alternative methods such as the particle filter (e.g. Montzka et al., 2011) because for high dimensional problems the EnKF requires a much smaller ensemble size to achieve reasonable good predictions. The Ensemble Kalman Filter (Reichle et al., 2002a; Dunne and Entekhabi, 2005; Crow, 2003; De Lannoy and Reichle, 2016), ~~and variants like~~ the Extended Kalman Filter (Draper et al., 2009; Reichle et al., 2002b), ~~four dimensional variational methods (Hulkmans et al., 2006)~~ and the Local Ensemble Transform Kalman Filter (Han et al., 2015; Han et al., 2013) were applied for updating soil moisture states in land surface models. Reichle et al. (2002a) performed a synthetic experiment using L-band microwave observations of the Southern Great Plains Hydrology Experiment (Jackson et al., 1999) to ~~analyze~~analyse the effect of ensemble size and ~~prediction error~~forecast errors. Dunne and Entekhabi (2005) showed that an Ensemble Kalman Smoother approach, where data from multiple time steps was assimilated to update current and past states, can yield a reduced prediction error compared to a pure filtering approach. More recently, state updates with the EnKF were tested for the Soil Moisture Ocean Salinity (SMOS, Kerr et al., 2012) mission. De Lannoy and Reichle (2016) assimilated SMOS temperature brightness and soil moisture retrievals into a land surface model with large improvements in surface soil moisture. However, localized error patterns were not captured well enough and locally optimized EnKF error parameters would improve prediction results further.

More recent work addressed joint ~~state-parameter estimation~~updating of model states and parameters in hydrologic and land surface models with data assimilation methods. Joint state-parameter estimation with EnKF is possible by an augmented state vector approach (Chen and Zhang, 2006), a dual approach (Moradkhani et al., 5 2005) or an approach with an additional external optimization loop (Vrugt et al., 2005). In the augmented state vector approach, parameters are included in the state vector and are updated via cross-covariances between states and parameters. The cross-covariances are estimated from the ensemble. In the dual approach, first parameters are updated by data assimilation, and the assimilation step is repeated with the updated parameters to update also the states by data assimilation. In the approach with an external optimization loop the parameters are not updated by EnKF, but in an external optimization loop. Pauwels et al. (2009) ~~optimized~~were one of the first to optimize soil hydraulic parameters of a land surface model ~~with~~by data assimilation, assimilating synthetic aperture radar data. Lee (2014) used Synthetic Aperture Radar soil moisture data to estimate soil hydraulic properties at the Tibetan plateau using the EnKF and a Soil Vegetation Atmosphere Transfer model. Bateni and Entekhabi (2012) assimilated land surface temperature with an Ensemble Kalman Smoother and achieved a better estimate of the 15 partitioning of energy between sensible and latent heat fluxes. Han et al. (~~2014b~~2014) updated soil hydraulic parameters of the Community Land Model (CLM) by assimilation of synthetic brightness temperature data with the Local Ensemble Transform Kalman Filter (LETKF) (Hunt et al., 2007)- and showed the potential of this approach for improving land surface states and fluxes like evapotranspiration. Shi et al. (2014) used the Ensemble Kalman Filter for a synthetic multivariate data assimilation problem with a land surface model and then applied it to real data (Shi et al., 2015). ~~The Both~~ cases illustrate a way to use real world data for estimating several ~~illustrate that~~ parameters in hydrologic land models from different compartments can be updated successfully by multivariate data assimilation. (Kurtz et al., ~~2016~~) developed a particular CPU-efficient data 20 assimilation framework for the coupled land surface-subsurface model TerrSysMP (Shrestha et al., 2014). They successfully updated  $2 \times 10^7$  states and parameters in a synthetic experiment. Whereas these studies were made with land surface models, also in soil hydrological applications recently data assimilation was used to estimate 25 soil hydraulic parameters. Early work was by Wu and Margulis (2011, 2013) in the context of real-time control of waste water reuse in irrigation and showed the potential of EnKF also in soil hydrology. Montzka et al. (2013;2011) explored the role of the particle filter for handling non-Gaussianity in soil hydrology data assimilation. ~~They showed that the nonlinear character of the soil moisture retention characteristic is critical for joint state-parameter estimation in data assimilation systems and showed that the Particle Filter is an interesting alternative for soil hydraulic parameter estimation for 1D problems.~~ Erdal et al. (2014) investigated the role of bias in the conceptual soil model and explored bias aware EnKF as a way to deal with it. ~~Erdal et al. (2015)~~They

Field Code Changed

argued that often the exact location of soil layers is not known and that this can severely deteriorate the performance of EnKF. Song et al. (2014) worked on a modified iterative EnKF-based filter to handle the non-linearity and non-Gaussianity of data assimilation for the vadose zone. They proposed a modified procedure which avoids the high CPU-need of a fully iterative method, but which still gives stable results. Also Erdal et al. (2015) focused on handling of strong non-Gaussianity of the state variable in EnKF under very dry conditions. They showed that classical EnKF fails under such conditions and proposed two alternative strategies, both involving transformation of state variables, which performed favourably also under very dry conditions with strongly skewed pressure distributions. All these studies on joint state-parameter estimation showed in general that estimation of soil hydraulic or land surface parameters improves model predictions (strongly), but can be unstable for strongly non-Gaussian distributions and non-linear problems. ~~Montzka et al. (2013;2011) explored the role of the particle filter for handling non Gaussianity in soil hydrology data assimilation. They showed that the ability of a data assimilation system to correct the soil moisture state and estimate hydraulic parameters strongly depends on the nonlinear character of the soil moisture retention characteristic. Song et al. (2014) worked on a modified iterative filter to handle the non-linearity and non-Gaussianity of data assimilation for the vadose zone.~~ For a further literature review on data assimilation in the context of hydrological and land surface models we refer to Reichle (2008) and Montzka et al. (2012).

Field Code Changed

Shuttleworth et al. (2013) developed the Cosmic Ray Soil Moisture Interaction Code (COSMIC), which is a forward operator to be applied for assimilating neutron intensity observations from ~~CRP~~CRNS. The COSMIC code was evaluated for several sites (Baatz et al., 2014;Rosolem et al., 2014). ~~Its capability to propagate surface soil moisture information into the deeper soil column was analyzed by Rosolem et al. (2014).~~ The COSMIC operator was successfully implemented in the Data Assimilation Research Testbed (Rosolem et al., 2014) to allow for state updating by the Ensemble Adjustment Kalman Filter (Anderson, 2001). ~~The surface soil moisture information was propagated into greater soil depth than only the measurement depth using COSMIC in combination with data assimilation (Rosolem et al., 2014).~~ The COSMIC operator was implemented in a python interface that couples the land surface model CLM and the LETKF for joint state parameter updating (Han et al., 2015). Neutron counts measured by ~~CRP~~CRNS have been used in data assimilation studies to update model states (Han et al., 2015;Rosolem et al., 2014). Soil hydraulic parameters were also updated by assimilation of neutron counts ~~in one synthetic study (Han et al., 2016), but only for a synthetic study which showed~~showing its feasibility. ~~CRP~~CRNS were also used for inverse estimation of soil hydraulic parameters of the Hydrus-1D model (Villarreyes et al., 2014).

This work further explores the value of measured neutron intensity by ~~CRPs~~CRNS to improve modelling of terrestrial systems at the catchment scale (Simmer et al., 2015) using a land surface model. ~~Compared to existing work the~~The main novelties are:

(i) Data from a network of nine ~~CRPs~~CRNS were assimilated in the Community Land Model version 4.5 (CLM) with an evaluation of the information gain by this assimilation at the ~~larger~~ catchment scale. Until now evaluations with ~~CRPs~~CRNS were made for a single location, but not for a complete network of ~~CRPs~~CRNS. It is a very important question whether ~~CRPs~~CRNS can also improve the soil moisture characterization at the ~~larger~~ catchment scale ~~and how dense the CRP network should be.~~ The high variability of soil moisture at a short distance could potentially limit the ~~CRPs~~CRNS measurement value and make updating of soil moisture contents further away from the sensor meaningless. On the other hand, soil moisture, soil maps and atmospheric forcings show spatial correlations over larger distances (Kirkpatrick et al., 2014; Korres et al., 2015) which suggests that ~~CRPs~~CRNS measurements potentially carry important information to update soil moisture contents for larger regions: (e.g. Han et al., 2012). If it is found that ~~CRPs~~CRNS networks with a density like in this study (nine stations per 2354 km<sup>2</sup>) can improve soil moisture content characterization at the ~~larger~~ catchment scale, this is of high relevance and importance for agricultural applications, flood prediction and protection, and regional weather prediction (Whan et al., 2015; Koster et al., 2004; Seneviratne et al., 2010). The main research question addressed in this paper is therefore whether a ~~CRPs~~CRNS network of the density as in this study can improve large scale soil moisture characterization ~~by state and parameter updates.~~

(ii) Soil hydraulic parameters ~~were~~are updated in this study together with the soil moisture states in a real-world case study ~~at the larger catchment scale.~~ The study in this paper also allows some evaluation of the feasibility of the updated large scale soil hydraulic parameters.

~~In the following paragraphs are presented the model site and the measurements (2.1), the Community land Model and its parameterization (2.2), the COMIC forward model (2.3) and the data assimilation procedure (2.4).~~

## 2 Materials and methods

### 2.1 Site description and measurements

The model domain, the Rur catchment (2354 km<sup>2</sup>), is situated in western Germany and illustrated in Fig. 1. ~~Most prominent vegetation types are agricultural land use (mainly in the North), grassland, and coniferous and deciduous forest.~~ The altitude varies between 15 m a.s.l. in the flat northern part and 690 m a.s.l. in the hilly southern part. Precipitation, evapotranspiration and land use follow the topography. The dominant land use types are agriculture (mainly in the North), grassland, and coniferous and deciduous forest. Annual precipitation

ranges between less than 600 mm in the North ~~to~~and 1200 mm in the hilly South (Montzka et al., 2008). Annual potential evapotranspiration varies between 500 mm in the South and 700 mm in the North (Bogena et al., 2005). The Rur catchment ~~CRP~~CRNS network comprises nine ~~CRP~~CRNS (CRS1000, HydroInnova LLC, 2009) which were installed in 2011 and 2012 (Baatz et al., 2014). Climate and soil texture of the ~~CRP~~CRNS sites can be found in Table 1.

The ~~CRP~~CRNS were calibrated in the field using gravimetric soil samples. At each site, 18 soil samples were taken along three circles with distances of 25, 75 and 175 meters from the ~~CRP~~CRNS, six samples evenly distributed along each circle. Each sample was extracted with a 50.8 x 300 mm round HUMAX soil corer (Martin Burch AG, Switzerland). The samples were split into 6 sub-samples with 5 cm length each and oven dried at 105 °C for 48 hours to measure dry soil bulk density and soil moisture. ~~Lattice water was determined for each site using a heat conductivity detector. Lattice water, hydrogen from organic and an-organic sources, was determined for each site using a heat conductivity detector (Ray, 1954).~~ Soil bulk density, soil moisture, lattice water and 12 hour averaged measured neutron intensity were used to determine calibration parameters specific for each ~~CRP and the COSMIC operator.~~CRNS and the COSMIC operator. ~~This represents a compromise between the measurement noise (which follows a Poisson distribution) and the assumed variation of environmental variables over the averaging time window (Iwema et al., 2015).~~

## 2.2 Community land model and parameterization

The Community Land Model version 4.5 (CLM) was the land surface model of choice for simulating water and energy exchange between the land surface and the atmosphere (Oleson et al., 2013). Some of the key processes which are ~~solved~~modelled by CLM are radiative transfer in the canopy space, interception of precipitation by the vegetation and evaporation from intercepted water, water uptake by vegetation and transpiration, soil evaporation, photosynthesis, as well as water and energy flow in the subsurface. SWC in CLM is influenced by precipitation, infiltration into the soil, water uptake by vegetation, surface evaporation and surface and subsurface runoff. ~~Oleson et al. (2013) provide further details on CLM4.5. To limit the scope and complexity of this study, CLM was run using satellite phenology, e.g. prescribed leaf area index data and the biogeochemical module turned off.~~To limit the scope and complexity of this study, CLM was run using satellite phenology e.g. prescribed leaf area index data and the biogeochemical module turned off. ~~The biogeochemical module allows CLM to model the vegetation development dynamically, but it requires a large spin-up of 1000 years and little additional gain is expected for this study from these additionally modelled processes.~~

The spatial domain is discretized by rectangular grid cells by CLM. Each grid cell may have several types of land cover: Lake, urban, vegetated, wetland, and glacier. The vegetated part of the grid cell can be covered by several plant functional types which are all linked to a single soil column. The soil column is vertically discretized by ten soil layers and five bedrock layers. Layer thickness increases exponentially from 0.007 m at the surface to 2.86 m for layer 10. Vertical water flow in soils is modelled by the 1D Richards equation. Soil hydraulic parameters are determined from sand and clay content using pedotransfer functions for the mineral soil fraction (Clapp and Hornberger, 1978; Cosby et al., 1984), and organic matter content for the organic soil fraction (Lawrence and Slater, 2008).

The joint state-parameter estimation used in this study updates soil texture and organic matter in CLM. Hence, parameter estimates directly determine soil hydraulic properties in CLM. The following equations describe how soil texture and organic matter define the soil hydraulic properties in CLM such as porosity, hydraulic conductivity, the empirical exponent  $B$  and soil matric potential. Hydraulic conductivity ( $k(z)$  in mm/s) at the depth  $z$  between two layers ( $i$  and  $i+1$ ) is a function of soil moisture ( $\theta$  in  $\text{m}^3/\text{m}^3$  in layers  $i$  and  $i+1$ ), saturated hydraulic conductivity ( $k_{sat}$  in mm/s at  $z$ ), saturated soil moisture ( $\theta_{sat}$  in  $\text{m}^3/\text{m}^3$ ) and the empirical exponent  $B$ : ( $z_i$  in mm/s), saturated soil moisture ( $\theta_{sat}$  in  $\text{m}^3/\text{m}^3$ ) and the empirical exponent  $B$  (Oleson et al., 2013):

$$k(z) = \begin{cases} \phi_{ice} k_{sat,z} \left[ \frac{\theta_i(\theta_i + \theta_{i+1})}{0.5(\theta_{sat,i} + \theta_{sat,i+1})} \right]^{2B_i+3} & 1 \leq i \leq N_{levsoi} - 1 \\ \phi_{ice} k_{sat,z} \left( \frac{\theta_i}{\theta_{sat,i}} \right)^{2B_i+3} & i = N_{levsoi} \end{cases} \quad \text{--- } k(z_i) =$$

$$\begin{cases} \phi_{ice} k_{sat}(z_i) \left[ \frac{(\theta_i + \theta_{i+1})}{(\theta_{sat,i} + \theta_{sat,i+1})} \right]^{2B_i+3}, & 1 \leq i \leq N_{levsoi} - 1 \\ \phi_{ice} k_{sat}(z_i) \left( \frac{\theta_i}{\theta_{sat,i}} \right)^{2B_i+3}, & i = N_{levsoi} \end{cases}$$

where  $\phi_{ice}$  is the ice impedance factor. The ice impedance factor was implemented to simplify an increased tortuosity of water flow in a partly frozen pore space. It is calculated with  $\phi_{ice} = 10^{-\Omega F_{ice}}$  using the resistance factor  $\Omega = 6$  and the frozen fraction of soil porosity  $F_{ice} = \theta_{ice} / \theta_{sat,i}$ . Soil hydraulic properties are calculated separately for the mineral (*min*) and organic matter (*om*) soil components. Total porosity  $\theta_{sat,i}$  is calculated using the fraction of organic matter ( $f_{om,i}$ ) with:

$$\theta_{sat,i} = (1 - f_{om,i})\theta_{sat,min,i} + f_{om,i}\theta_{sat,om}$$

Formatted: Font: Italic

1

2

where the organic matter porosity is  $\theta_{sat,om} = 0.9$  and sand content in % determines the mineral soil porosity  $\theta_{sat,min}$  as:

$$\theta_{sat,min} = 0.489 - 0.00126 \times \%sand \quad 3$$

Analogous, the exponent  $B$  is calculated with

$$B_i = (1 - f_{om,i})B_{min,i} + f_{om,i}B_{om} \quad 4$$

Where  $B_{om} = 2.7$  is the organic exponent and the mineral exponent  $B_{min,i}$  is determined by clay content in % with:

$$B_{min,i} = 2.91 + 0.159 \times \%clay \quad 5$$

Saturated hydraulic conductivity is calculated for a connected and an unconnected fraction of the grid cell with:

$$k_{sat}[z_i](z_i) = (1 - f_{perc})k_{sat,uncon}[z_i](z_i) + f_{perc,i}k_{sat,om}[z_i](z_i) \quad 6$$

where  $f_{perc,i}$  is the fraction of a grid cell where water flows with saturated hydraulic conductivity of the organic matter ( $k_{sat,om}[z_i](z_i)$  in mm/s) through the organic material only, the so called connected flow pathway; whereas the saturated hydraulic conductivity of the unconnected part ( $k_{sat,uncon}[z_i](z_i)$  in mm/s) depends on organic and mineral saturated soil hydraulic conductivity:

$$k_{sat,uncon} = (1 - f_{perc}) \left( \frac{1 - f_{om}}{k_{sat,min}} + \frac{f_{om} - f_{perc}}{k_{sat,om}} \right)^{-1} \quad 7$$

where saturated hydraulic conductivity for mineral soil is calculated from the grid cell sand content as:

$$k_{sat,min}[z_i] = 0.0070556 \times 10^{-0.884+0.0153 \times \%sand} 10^{-0.884+0.0153 \times \%sand} \quad 8$$

The fraction  $f_{perc}$  is calculated with:

$$f_{perc} = \begin{cases} 0.908 \times (f_{om} - 0.5)^{0.139}, & f_{om} \geq 0.5 \\ 0, & f_{om} < 0.5 \end{cases} \quad 9$$

$$f_{perc} = 0 \quad f_{om} < 0.5 \quad 10$$

Soil matric potential (mm) is defined as function of saturated soil matric potential (mm) with:

$$\psi_i = \psi_{sat,i} \left( \frac{\theta_i}{\theta_{sat,i}} \right)^{-B_i} = [(1 - f_{om,i})\psi_{sat,min,i} + f_{om,i}\psi_{sat,om}] \left( \frac{\theta_i}{\theta_{sat,i}} \right)^{-B_i} \quad 10$$

where saturated organic matter matric potential is  $\psi_{sat,om} = -10.3$  ~~mm~~ and saturated mineral soil matric potential is calculated from sand content as:

$$\psi_{sat,min,i} = -10.0 \times 10^{1.88 - 0.0131 \times \%sand} 10^{1.88 - 0.0131 \times \%sand} \quad 11$$

### 2.3 Cosmic-ray forward model

SWC retrievals were calculated from neutron intensity observations with the ~~Cosmic~~Cosmic-ray Soil Moisture Interaction Code (COSMIC) (Shuttleworth et al., 2013) following calibration results and the procedure of Baatz et al. (2014). COSMIC parameterizes ~~interactions between neutrons and atoms in~~neutron transport within the ~~soil~~ subsurface, ~~relevant for soil moisture estimation. COSMIC and~~ was calibrated against the more complex Monte Carlo Neutron Particle model MCNPx (Pelowitz, 2005) ~~and, COSMIC~~ needs considerably less CPU-time than the MCNPx model. ~~The reduced CPU time need and the physically based parameterization make COSMIC a suitable data assimilation operator.~~ The code was tested at multiple sites for soil moisture determination (Baatz et al., 2014; Rosolem et al., 2014) and analyzed in detail by Rosolem et al. (2014).

COSMIC assumes that a number of high energy neutrons enter the soil. In the soil, ~~the number of~~ high energy neutrons ~~are~~ reduced by ~~interaction with~~interactions within the soil leading to ~~isotropic~~ generation of fast neutrons ~~with less energy~~ in each soil layer. Before resurfacing, ~~the number of~~ fast neutrons ~~are~~ reduced again by ~~their interaction with nuclei of elements within~~ soil ~~interaction~~ (Shuttleworth et al., 2013). The number of neutrons  $N_{CRP}$  that reaches the ~~CRPCRNS~~ can be summarized in a single integral as

$$N_{CRP} = N_{COSMIC} \int_0^{\infty} \left\{ A(z) [\alpha \rho_s(z) + \rho_w(z)] \exp \left( - \left[ \frac{m_s(z)}{L_1} + \frac{m_w(z)}{L_2} \right] \right) \right\} \cdot dz \quad 12$$

where  $N_{COSMIC}$  is an empirical coefficient that is ~~CRPCRNS~~ specific and needs to be estimated by calibration,  $A(z)$  is the integrated average attenuation of fast neutrons,  $\alpha = 0.404 - 0.101 \times \rho_s$  is the site specific empirical coefficient for the creation of fast neutrons by soil,  $\rho_s$  is the dry soil bulk density in  $g/cm^3$ ,  $\rho_w$  is the total soil water density in  $g/cm^3$ ,  $m_s$  and  $m_w$  are the mass of soil and water, respectively, per area in  $g/cm^2$ .  $L_1 = 162.0$   $g/cm^2$  and  $L_2 = 129.1$   $g/cm^2$  are ~~empirical coefficients~~scattering lengths for fast neutrons in solids and water, ~~respectively~~, that were estimated using the MCNPx code (Shuttleworth et al., 2013). The integrated average attenuation of fast neutrons  $A(z)$  can be found numerically by solving

$$A(z) = \left( \frac{2}{\pi} \right) \int_0^{\pi/2} \exp \left( \frac{-1}{\cos(\theta) \left[ \frac{m_s(z)}{L_3} + \frac{m_w(z)}{L_4} \right]} \right) \int_0^{\pi/2} \exp \left( \frac{-1}{\cos(\gamma) \left[ \frac{m_s(z)}{L_3} + \frac{m_w(z)}{L_4} \right]} \right) \cdot d\theta d\gamma \quad 13$$

where  $\theta$  is the angle along a vertical line below the ~~CRPCRNS~~ detector to the element that contributes to the attenuation of fast neutrons,  $L_3 = -31.65 + 99.29 \times \rho_s$  ~~is determined from soil bulk density~~ and  $L_4 = 3.16 \text{ g cm}^{-2}$  ~~is another empirical coefficient estimated~~ are the scattering length for fast neutrons in soil and water, respectively, determined using the MCNPx code (Shuttleworth et al., 2013). The COSMIC operator is discretized into 300 ~~vertical~~ layers of one cm thickness up to a depth of three meters. For each CLM grid cell in the model domain, simulated SWC in all CLM layers is used to generate a weighted SWC retrieval using the COSMIC code. Simulated SWC is handed from the CLM simulation history files to the COSMIC operator. Given the vertical SWC distribution of the individual CLM ~~soil column~~ grid cell, COSMIC internally calculates the contribution of each layer to the simulated neutron intensity signal at the ~~COSMIC~~ soil surface in COSMIC. In this study, the contribution of each CLM soil layer was used to calculate the weighted CLM SWC retrieval corresponding to the vertical distribution of simulated SWC in each grid cell.

Measured neutron intensity of ~~CRPCRNS~~ was used to inversely determine a ~~CRPCRNS~~ SWC retrieval as by Baatz et al. (2014) assuming a homogeneous vertical SWC distribution. Then, the weighted CLM SWC retrieval is used in the data assimilation scheme to relate the ~~CRP SWC retrieval to the model state~~ CRNS SWC retrieval to the model state. Alternatively, neutron flux data could be assimilated directly within the catchment. This would require calibration data throughout the catchment which is only feasible using spatially distributed data sets (e.g. Avery et al., 2016). However, high stands of biomass are a major factor for calibration in the Rur catchment (Baatz et al., 2015) and estimates of biomass come along with high uncertainties. To circumvent introducing these additional uncertainties, SWC retrievals are assimilated in this study. Changes in on-site biomass were assumed negligible.

#### 2.4 Data assimilation

~~This~~ To further expand the work of Han et al. (2016), this study uses the local ensemble transform Kalman filter (LETKF) (Hunt et al., 2007) to assimilate SWC retrievals by ~~CRPCRNS~~ into the land surface model CLM. ~~Besides other Ensemble Kalman Filter variants, the LETKF is applied in atmospheric sciences (Liu et al., 2012; Miyoshi and Kunii, 2012), ocean science (Penny et al., 2013) and also in land surface hydrology (Han et al., 2014a; Han et al., 2015).~~ Updates were calculated either for SWC states or jointly for SWC states and soil parameters depending on the experiment setup. For state updates only, the LETKF was used as proposed by Hunt et al. (2007). Calculations were made for an ensemble of model simulations which differed related to variations in model forcings and input parameters. The states of the different ensemble members are indicated by

$\mathbf{x}_i^f$  where  $i=1, \dots, N$  and  $N$  is the number of ensemble members.  $f$  marks the model prediction or forecast before the update. The individual state vectors  $\mathbf{x}_i^f$  contain the CLM-simulated SWC of the ten soil layers and the vertically weighted SWC retrieval obtained with the COSMIC operator. For each grid cell, a ~~vector~~matrix  $\mathbf{X}^f$  can be constructed which contains the deviations of the simulated states with respect to the ensemble mean  $\bar{\mathbf{x}}^f$ :

$$\mathbf{X}^f = [\mathbf{x}_1^f - \bar{\mathbf{x}}^f, \dots, \mathbf{x}_N^f - \bar{\mathbf{x}}^f] \quad 14$$

5 In case of joint state-parameter updates, a state augmentation approach was followed (Hendricks Franssen and Kinzelbach, 2008; Han et al., ~~2014b~~2014). In this case, the augmented model state ~~vector~~matrix  $\mathbf{X}^f$  is constructed from the simulated SWC of the ten soil layers, weighted SWC, and the grid cell's sand, clay and organic matter content.

10 In order to relate the measured neutron intensity with the simulated SWC of CLM, the observation operator  $\mathbf{H}$  (COSMIC) is applied on the measured neutron intensity in order to obtain the expected weighted SWC retrieval at each of the observation locations for each of the stochastic realizations:

$$\mathbf{y}_i^f = \mathbf{H}(\mathbf{x}_i^f) \quad 15$$

The ensemble realizations of the modelled SWC ~~retrieval~~retrievals at the measurement locations  $\mathbf{y}_1^f$  to  $\mathbf{y}_N^f$  with respect to the ensemble mean  $\bar{\mathbf{y}}^f$  are stored in the ~~vector~~matrix  $\mathbf{Y}^f$ :

$$\mathbf{Y}^f = [\mathbf{y}_1^f - \bar{\mathbf{y}}^f, \dots, \mathbf{y}_N^f - \bar{\mathbf{y}}^f] \quad 16$$

15 The observation error correlation was reduced in space by the factor  $f_{red}$  using the spherical model:

$$f_{red} = 1 - (1.5 \times d/d_{max}) + (0.5 \times [d/d_{max}]^3) \quad 17$$

where  $d$  is the distance to the observation and  $d_{max} = 40km$  is the maximum observation correlation length, about half the size of the catchment. Only SWC retrievals within the maximum observation correlation length were used for assimilation. This leads to a 'localized' size of  $\mathbf{Y}^f$  and the observation error covariance matrix  $\mathbf{R}$ . The intermediate covariance matrix  $\mathbf{P}^a$  (also called analysis error covariance matrix) is calculated according to:

$$\mathbf{P}^a = [(N - 1)\mathbf{I} + \mathbf{Y}^{fT} \mathbf{R}^{-1} \mathbf{Y}^f] \quad 18$$

20 In addition, the mean weight vector  $\bar{\mathbf{w}}^a$  is obtained as follows:

$$\bar{\mathbf{w}}^a = \mathbf{P}^a \mathbf{Y}^{fT} \mathbf{R}^{-1} (\mathbf{y}^0 - \bar{\mathbf{y}}^f) \quad 19$$

where  $\mathbf{y}^0$  ~~is CRP~~ contains the CRNS SWC retrieval retrievals at the measurement locations. In the ensemble space, a perturbation matrix  $\mathbf{W}^a$  is calculated from the symmetric square root of  $\mathbf{P}^a$ :

$$\mathbf{W}^a = [(\mathbf{N} - 1)\mathbf{P}^a]^{1/2} \quad 20$$

The final analysis  $\mathbf{X}^a$  is obtained from:

$$\mathbf{X}^a = \bar{\mathbf{x}}^f + \mathbf{X}^f [\bar{\mathbf{w}}^a + \mathbf{W}^a] \quad 21$$

A more detailed description of the LETKF can be found in (Hunt et al., 2007) and details on the implementation of the LETKF in combination with CLM are given by (Han et al., 2015) Han et al. (2015).

### 3 Model and Experiment Setup

#### 3.1 Model Setup

In this study, discretization and parameterization of the hydrological catchment was done on the basis of high resolution data. The ~~model of the~~ Rur catchment ~~domain is~~ was spatially discretized by rectangular grid cells of 0.008 degree size (~750 m). The model time step was set to hourly. Land cover was assumed to consist of vegetated land units only, and a single plant functional type (PFT) for each grid cell was defined. The plant functional types were derived from a remotely sensed land use map using RapidEye and ASTER data with 15 m resolution (Waldhoff, 2012). ~~Sand content~~ Contents of sand, clay ~~content~~ and organic matter ~~content~~ were derived from the high resolution regional soil map BK50 (Geologischer Dienst Nordrhein-Westfalen, 2009). ~~The BK50 soil map provides the high resolution soil texture for the catchment and is the most detailed soil map available for the defined region. As an alternative, simulations were also performed for a biased soil texture distribution with a fixed sand content of 80 % and clay content of 10 % (S80 soil map). This represents a large error with respect to the expected true soil properties. It allows~~ Alternative simulations were also performed with the FAO soil map of the global Harmonized World Soil Database (FAO, 2012) and with a biased soil texture with a fixed sand content of 80 % and clay content of 10 % (S80 soil map). Average sand and clay content are 22.5% and 21.4% for the BK50 soil map and 39% and 22% for the FAO soil map. The FAO soil map and the biased soil map represent large error with respect to the soil properties of the BK50 soil map. The FAO soil map and S80 soil map simulations allow evaluating the joint state-parameter estimation approach because given the expected bias, we can evaluate ~~whether and~~ to what ~~extent~~ the soil properties are modified by the data assimilation ~~to be closer to the available high resolution soil map. In addition,~~ This is important because in many regions across the Earth a high resolution soil map is not available ~~and land~~ Land surface models ~~which~~ are

applied for those regions, for example in the context of global simulations, and hence might be strongly affected by the error in soil properties. ~~It was tested how this impacted the simulation results.~~

Maximum saturated fraction, a surface parameter which is used for runoff generation, was calculated from a 10 meter digital elevation model (scilands GmbH, 2010). Leaf area index data were derived from monthly averaged Moderate Resolution Imaging Spectrometer data (MODIS). CLM was ~~supplied~~forced with hourly atmospheric ~~forcing~~ data from ~~the~~ COSMO DE reanalysis data set for the years 2010 to 2013 from the German Weather Service (DWD). The data was downscaled from a resolution of 2.8 km<sup>2</sup> to the CLM resolution using linear interpolation based on Delaunay triangulation. Forcing data include precipitation ~~in mm/s~~, incident solar and longwave radiation ~~in W/m<sup>2</sup>~~, air temperature ~~in K~~, air pressure ~~in hPa~~, wind speed ~~in m/s~~ and relative humidity ~~in kg/kg~~ at the lowest atmospheric level.

### 3.2 Model ensemble

Uncertainty was introduced into the regional CLM model by perturbed soil parameters and external model forcings. Contents of sand, clay and organic matter were perturbed with spatially correlated noise from a uniform sampling distribution with mean zero and standard ~~deviation 10 % or 30 % (Han et al., 2015)~~deviations 10 % and 30 % (Han et al., 2015). Soil texture perturbation considers that in CLM a single set of pedotransfer functions is assumed to be valid throughout the globe while usually pedotransfer functions are specific for regions (e.g. Patil and Singh, 2016). In other words, the perturbation of soil texture also covers the uncertainty in the pedotransfer function itself. By perturbing texture, soil parameters are also perturbed through the pedotransfer functions used in CLM as specified in Sect. 2.2. Precipitation ( $\sigma = 0.5$  or 1.0; lognormal distribution) and shortwave radiation ( $\sigma = 0.3$ ; lognormal distribution) were perturbed with multiplicative noise with mean equal to one. Longwave radiation ( $\sigma = 20 \text{ W m}^{-2}$ ) and air temperature ( $\sigma = 1\text{K}$ ) were perturbed with additive noise. The forcing perturbations were imposed with correlations in space (5 km) using a fast Fourier transform. Correlation in time was introduced with an AR(1)-model with autoregressive parameter ~~=~~0.33. These correlations and standard deviations were chosen based on previous data assimilation experiments (Reichle et al., 2010; Kumar et al., 2012; De Lannoy et al., 2012; Han et al., 2015). In this work, only results for precipitation perturbation with  $\sigma = 0.5$  will be shown as results for  $\sigma = 1.0$  were ~~very~~ similar. An ensemble size of 95 realizations was used in the simulations. ~~Based on previous work (Baatz et al., 2015),~~ the SWC retrieval uncertainty for CRP<sub>s</sub>CRNS<sub>s</sub> was estimated to be 0.03 cm<sup>3</sup>/cm<sup>3</sup> while fluctuations in the measurement standard deviation, related to the non-linear relation between observed neutron intensity and SWC, were assumed negligible.

Formatted: Font: Times New Roman

### 3.3 Experiment set-up

All simulation experiments in this study used initial conditions from a single five year spin-up run. ~~For the five year spin-up run, in which~~ a single forcing data set of the year 2010 was repeatedly used as atmospheric input. The soil moisture regime became stable after the five years spin-up period, and additional spin-up simulations would not affect soil moisture in the consecutive years. After this five year spin-up, soil parameters and forcing data of the consecutive years were perturbed. From 1<sup>st</sup> Jan. 2011 onwards, CLM was propagated forward with an ensemble of 95 realizations. On 20<sup>th</sup> Mar. 2011, the first SWC retrieval was assimilated and assimilation of SWC retrievals continued until 31<sup>st</sup> Dec. 2012. ~~From 1<sup>st</sup> January 2013 to 31<sup>st</sup> December 2013~~In the data assimilation period soil properties were estimated at every time step when observations were made available. For the year 2013, the model was propagated forward without data assimilation but with an ensemble of 95 realizations. The year 2013 was used exclusively as evaluation period for data assimilation experiments.

In total, 2631 simulation experiments were carried out using different setups (Table 2). ~~Two~~The present setups are intended to cover three different initial soil maps, three different sizes of a CRNS network and two different parameter perturbations. Three open loop simulations were run ~~for the BK50 soil map (OL-BK50) and the S80 soil map (OL-S80), respectively,~~ without data assimilation and soil parameter perturbation of 30 % ~~for the BK50 soil map (OL-BK50), the FAO soil map (OL-FAO) and the S80 soil map (OL-S80).~~ These simulations are referred to as reference runs for the respective soil map. Simulation results of data assimilation runs were compared to the reference runs for quantification of data assimilation benefits. Simulations were done with joint state-parameter estimation (PAR-), ~~two for the S80 soil map (PAR-S80-) and~~\*, two for the BK50 soil map (PAR-BK50-), ~~for which soil-~~\*, one for the FAO soil map (PAR-FAO-30), and two for the S80 soil map (PAR-S80-\*). Soil texture was perturbed by 10 % ~~and 30 % or 30 % as indicated by the experiment name (Table 2).~~ Two simulations were done with state updates only for the BK50 soil map (Stt-BK50) and the S80 soil map (Stt-BK50), ~~where soil texture was perturbed by 30 %.~~ These eight). These ten simulations form the basic set of experiments.

Besides the data assimilation experiments also a larger number of jackknifing simulations ~~was run~~were conducted to evaluate the impact of the CRNS data assimilation performance. ~~These simulations allow evaluating the impact of the CRP network to improve on SWC characterization at other unobserved locations, without CRP, in the model domain. In~~ nine jackknife ~~experiment~~ experiments, data from eight ~~CRP~~CRNS locations ~~were~~was assimilated (jk8-\* simulations) and data of the one CRP remaining CRNS was ~~excluded from~~

the assimilation not assimilated but kept for evaluation purpose. In addition, three simulations were conducted where data of four CRNS were assimilated (jk4-\* simulations) and data of the five remaining CRNS was used for evaluation. These three simulations represent a CRNS network with much less than the existing nine CRNS. At the evaluation location/locations, simulated SWC (which is affected by the assimilation of the other eight probes) was compared to CRPCRNS SWC retrievals. For jackknife simulations, the perturbation of soil texture was set to 30 % and precipitation perturbation was done with  $\sigma = 0.5\%$ . States and parameters at these sites were jointly updated, and simulations were made using either the BK50 and/or the S80 soil maps as input/initial parameterization. Therefore, a total of 4821 jackknife simulations (jk-S80-\* and jk-BK50-\*) was/were performed (two soil maps times nine different simulations leaving away one CRP at a time).

Simulation results were evaluated with the root mean square error ( $E_{RMS}$ ):

$$RMSE = \sqrt{\frac{\sum_{t=1}^n (SWC_{t,CLM} - SWC_{t,CRNS})^2}{n}} \quad E_{RMS} = \sqrt{\frac{\sum_{t=1}^n (\theta_{t,CLM} - \theta_{t,CRNS})^2}{n}} \quad 22$$

where  $n$  is the total number of time steps,  $SWC_{t,CLM}$  is the SWC simulated by CLM SWC retrieval at time step  $t$  and  $SWC_{t,CRNS}$  is the CRPCRNS SWC retrieval at time step  $t$ . In case SWC was assimilated at the corresponding time step,  $SWC_{t,CLM}$  is SWC prior to assimilation. In the case the  $E_{RMS}$  is estimated at a single point in time over all CRNs available, the number of time steps  $n$  can be replaced by the number of CRNs available. The second evaluation measurement in this study is the bias which is, in contrast to the  $E_{RMS}$ , a measure for systematic deviation:

$$bias = \frac{\sum_{t=1}^n (SWC_{t,CLM} - SWC_{t,CRNS})}{n} \quad \sum_{t=1}^n (\theta_{t,CLM} - \theta_{t,CRNS}) \quad 23$$

## 4 Results and Discussion

### 4.1 General Results

Table 3 summarizes the performance statistics in terms of  $E_{RMS}$  and bias for the assimilation period (2011 and 2012) and evaluation period (2013). Presented are results for the open loop scenarios with the BK50, FAO and S80, and data assimilation scenarios. Errors of open loop simulations are higher were highest for the S80-simulation than for (0.11  $\text{cm}^3/\text{cm}^3$ ), followed by the BK50-FAO simulation at all sites but Merzenhausen. At Merzenhausen  $E_{RMS}$  was 0.054  $\text{cm}^3/\text{cm}^3$  for the S80 soil map and (0.06707  $\text{cm}^3/\text{cm}^3$  for) and the BK50 soil map. Open loop simulations with the S80 soil map resulted in  $E_{RMS}$  values above 0.10  $\text{cm}^3/\text{cm}^3$  at five of nine sites. At all sites data assimilation results with the S80 soil map improved SWC compared to the

Formatted: Font: Italic, Subscript

open-loop simulations. This was also the case simulation ( $0.04 \text{ cm}^3/\text{cm}^3$ ). Mean absolute bias was highest for the S80 soil map ( $0.11 \text{ cm}^3/\text{cm}^3$ ), now as high for the FAO soil map ( $0.06 \text{ cm}^3/\text{cm}^3$ ) and lowest for the BK50 soil map simulations at all sites but Aachen where  $E_{\text{RMS}}$  was larger than for the open loop run. In general, data ( $0.02 \text{ cm}^3/\text{cm}^3$ ). Data assimilation improved simulations more for the S80 soil map ( $E_{\text{RMS}}$  reduced by  $0.07908 \text{ cm}^3/\text{cm}^3$ ) than for the FAO soil map ( $E_{\text{RMS}}$  reduced by  $0.04 \text{ cm}^3/\text{cm}^3$ ) or the BK50 soil map ( $E_{\text{RMS}}$  reduced by  $0.01 \text{ cm}^3/\text{cm}^3$ ). Room for improvement with the BK50 soil map runs was more limited because of the smaller open loop errors. Nevertheless, after state updating alone the BK50 soil map still gave smaller errors than the S80 soil map. However, joint state-parameter estimation further improved simulation results by reducing  $E_{\text{RMS}}$  values and the parameter. The BK50 soil map led to  $E_{\text{RMS}}$  values in open loop simulations lower than  $0.05 \text{ cm}^3/\text{cm}^3$  which left little room for error reduction considering a measurement error of  $0.03 \text{ cm}^3/\text{cm}^3$ . However, slight improvements by  $0.01 \text{ cm}^3/\text{cm}^3$  were possible at monitored locations in the data assimilation period but not in the evaluation period. Joint state-parameter estimation improved simulation results as shown by the reduced  $E_{\text{RMS}}$  and bias for the S80 and the FAO soil maps. The verification period (2013) with the updated soil hydraulic parameters for the FAO soil map resulted in an  $E_{\text{RMS}}$  value of  $0.05 \text{ cm}^3/\text{cm}^3$ , also clearly an improvement compared to the open loop run with an  $E_{\text{RMS}}$  of  $0.07 \text{ cm}^3/\text{cm}^3$  (Table 3). Joint state-parameter updating resulted in similar  $E_{\text{RMS}}$  values for the BK50 ( $0.028 \text{ cm}^3/\text{cm}^3$ ) and S80 all three initial soil map ( $0.03 \text{ cm}^3/\text{cm}^3$ ). The  $E_{\text{RMS}}$  maps the BK50, FAO and S80 soil map (each  $0.03 \text{ cm}^3/\text{cm}^3$ ). State updates (Stt-S80) improved  $E_{\text{RMS}}$  and bias for the S80 soil map ( $E_{\text{RMS}} = 0.06 \text{ cm}^3/\text{cm}^3$  for assimilation period) but much less compared to the joint state-parameter updates (PAR-S80-30). The  $E_{\text{RMS}}$  and bias for simulations with 10 % and 30 % perturbation of soil texture values did not show very different results, only showed very small differences (smaller than  $0.01 \text{ cm}^3/\text{cm}^3$ ).

The temporal course of simulated soil moisture in 2011 at the two sites Merzenhausen and Gevenich and Merzenhausen is shown in Fig. 2. The figure illustrates that simulated SWC at both sites was lowest with the S80 soil map than (OL-S80), highest with the BK50 soil map. In Gevenich and Merzenhausen, mean (OL-BK50) and the FAO soil map resulted in intermediate soil moisture (OL-FAO). Mean open loop SWC in 2011 was  $0.17 \text{ cm}^3/\text{cm}^3$  for the S80 soil map at both sites,  $0.24 \text{ cm}^3/\text{cm}^3$  for the FAO soil map and  $0.27 \text{ cm}^3/\text{cm}^3$  for the BK50 soil map at both sites. CRP measurements at Merzenhausen. Measurements with CRNS started in May 2011. In the data assimilation runs SWC was immediately affected at the Merzenhausen and Gevenich sites as soon as Merzenhausen CRP SWC retrievals were assimilated. The simulated SWC for the PAR-S80-30 data assimilation run increased as compared to the S80 open loop simulation. The at Merzenhausen. At Gevenich, the first observation at Gevenich was recorded on July 7<sup>th</sup>, 2011. In the data assimilation run shown (PAR-S80-

30) modelled SWC was immediately affected at both sites, Merzenhausen and Gevenich, as soon as data at Merzenhausen was assimilated. By that date, the July, simulated CLM-SWC retrieval with the biased soil map and data assimilation (PAR-S80-30) was already close to the CRP-CRNS SWC retrieval at the Gevenich site (Fig. 2) due to SWC updates which showed to have a). This demonstrates the beneficial impact of data availability for assimilation at one site and the information brought into space by the data assimilation scheme.

Fig. 2 also shows that the BK50 open loop run was close to the observed SWC at both sites, even without data assimilation.

Fig. 3 shows the temporal course of SWC from January 2011 to December 2013 at Heinsberg and Wildenrath.

Assimilation and evaluation results are shown for the ~~ease of open loop (OL-S80 and OL-FAO) simulations, only state updates (Stt-S80), joint state-parameter updates (PAR-S80-30), only state updates (Stt-S80), open loop (OL-S80) and CRP~~ and CRNS SWC retrievals. At Heinsberg, results show that ~~assimilated simulated SWC with assimilation~~ was closer to the ~~CRP-SWC retrieval~~ CRNS when both states and parameters were updated (PAR-S80-30) than if only states were updated (Stt-S80). This is the case ~~in for both periods~~ the assimilation ~~period~~ and ~~in~~ the evaluation period. At the beginning of the evaluation period, ~~(first few days of 2013), the Stt-S80 simulation shows an increase in bias between modeled CLM SWC retrievals and CRP SWC retrieval within the first few days of 2013. modeled SWC and CRNS.~~ The bias of Stt-S80 remained throughout the evaluation period. In contrast, ~~modeled SWC during the evaluation period was close to the CRP SWC retrieval~~ if parameters were previously updated (PAR-S80-30) modelled SWC was close to the CRNS during the evaluation period. Open loop SWC modelled with the FAO soil map is lower than the CRNS SWC retrievals at Heinsberg and higher than CRNS SWC retrievals at Wildenrath. At Wildenrath, results of the OL-S80 run suggest that the initial sand content of the biased soil map is closer to the optimal sand content than the sand content of the FAO soil map. Consequently, the OL-FAO bias was  $-0.05 \text{ cm}^3/\text{cm}^3$  and  $0.05 \text{ cm}^3/\text{cm}^3$  for Heinsberg and Wildenrath, respectively (Table 3 and 4 in Annex). At both sites, absolute bias was reduced with joint state-parameter updates to equal or less than  $0.01 \text{ cm}^3/\text{cm}^3$  (S80 and FAO soil map). The reduced bias is also well reflected in the temporal course of modelled SWC with joint state-parameter updates (PAR-S80-30).

It is interesting to notice that the error values for the verification period are very similar if soil hydraulic parameters were estimated in the assimilation period, independent of the initial soil map (Table 3).  $E_{RMS}$  values for the 2013 simulations with state updates only (Stt-BK50 and Stt-BK50) show that in the evaluation period the improvements by state updates (without parameter updates) were small (reduction by  $0.02 \text{ cm}^3/\text{cm}^3$  and  $0.00 \text{ cm}^3/\text{cm}^3$  for S80 and BK50, respectively) compared to the improvements obtained by joint state-parameter

updates (reduction by  $0.07 \text{ cm}^3/\text{cm}^3$  for S80). This illustrates the benefits of joint state-parameter updates compared to state updates only, and that soil moisture states are strongly determined by soil hydraulic parameters. The CRP at Wildenrath started operating on May 7<sup>th</sup>, 2012. SWC retrievals at other CRPs were assimilated already from May 2011 onwards and affected SWC at Wildenrath (Fig. 3). Until May 2012, The case of only state updates also illustrates that the improved characterization of soil moisture states in the assimilation period results in improved initial states for the verification period (Table 3) but in the verification period these improvements lose its influence quickly over time (Fig. 3 shows assimilated SWC (Stt S80 and PAR S80 30) was higher than open loop SWC. However, no SWC retrievals were available at the Wildenrath site for comparison during this period. When SWC retrievals from the CRP at Wildenrath became available and were assimilated into the model, assimilated (Stt S80 and PAR S80 30) and open loop (OL S80) SWC were close to CRP SWC retrievals. This was the case throughout the remaining assimilation and evaluation period. These results suggest that the high sand content of the biased soil map is not far from the optimal sand content at Wildenrath. Therefore, at Wildenrath, the high sand content of both soil maps (60 % and 80 %) resulted in good modeling results already for the open loop runs. This suggests that before May 2012, simulated SWC of the open loop runs with either soil map represented more realistic SWC than assimilated SWC during this period. This will be discussed further in the discussion section.

#### **4.2 — Verification period**

The year 2013 was the verification year without data assimilation.  $E_{\text{RMS}}$  values for the evaluation period 2013 are reported in Table 4. On the one hand, BK50 data assimilation runs with joint state parameter estimation resulted in improved SWC at three out of the nine sites compared to open loop BK50 runs. For the other six sites results worsened compared to the corresponding BK50 open loop run.  $E_{\text{RMS}}$  values increased from an average of  $0.041 \text{ cm}^3/\text{cm}^3$  (OL-BK50) over all sites to  $0.047 \text{ cm}^3/\text{cm}^3$  (PAR-BK50-30). On the other hand, for the S80 soil map, all sites except Wildenrath had significantly reduced  $E_{\text{RMS}}$  values for the case of data assimilation including parameter updating compared to the S80 open loop run. For the S80 simulations, average  $E_{\text{RMS}}$  over all sites for 2013 was on average  $0.12 \text{ cm}^3/\text{cm}^3$  for the open loop run and  $0.04 \text{ cm}^3/\text{cm}^3$  for the run including data assimilation. In case only states were updated (Stt S80 and Stt BK50),  $E_{\text{RMS}}$  was also slightly reduced (compared to open loop runs) for the majority of sites during the evaluation period in 2013. On average, this reduction was  $0.016 \text{ cm}^3/\text{cm}^3$  for the S80 soil map (Stt S80) and  $0.002 \text{ cm}^3/\text{cm}^3$  for the BK50 soil map (Stt BK50). At sites, where  $E_{\text{RMS}}$  was larger for data assimilation runs with state updating (compared to open loop runs), the increase was only  $0.001 \text{ cm}^3/\text{cm}^3$ .

Bias calculated on the basis of a comparison of hourly SWC measured by CRP and simulated for 2013 is reported in Table 5. The average bias for the S80 open loop run is  $0.11 \text{ cm}^3/\text{cm}^3$  while it is  $0.02 \text{ cm}^3/\text{cm}^3$  for the BK50 open loop run. Bias of the BK50 open loop run was positive at Merzenhausen, Gevenich, Heinsberg, and Aachen, and it was negative at Rollesbroich, Kall, RurAue, and Wuestebach. Bias was zero at Wildenrath for the BK50 open loop run. Bias of the S80 open loop run was negative at all sites indicating that modeled SWC was higher than measured SWC. Joint state parameter updates reduced the absolute bias on average to  $0.03 \text{ cm}^3/\text{cm}^3$  (PAR-S80-30) and  $0.02 \text{ cm}^3/\text{cm}^3$  (PAR-S80-10) for the S80 soil map. In case of the BK50 soil map, the bias in 2013 increased to  $0.03 \text{ cm}^3/\text{cm}^3$  by joint state parameter updates. State updates without parameter updates reduced the biases only marginally to  $0.01 \text{ cm}^3/\text{cm}^3$  for the BK50 soil map and to  $0.09 \text{ cm}^3/\text{cm}^3$  for the S80 soil map. This indicates that state updates also can slightly improve SWC characterization in the verification period due to improved initial conditions.

).

#### 4.34.2 Temporal evolution of mean $E_{\text{RMS}}$

Fig. 4 shows the temporal evolution of the hourly  $E_{\text{RMS}}$  calculated for all nine CRPs/CRNS.  $E_{\text{RMS}}$  was highest for the S80 open loop run and lowest for the PAR-S80-30 simulation. The FAO soil map resulted in errors mostly between  $0.05 \text{ cm}^3/\text{cm}^3$  and  $0.1 \text{ cm}^3/\text{cm}^3$  which is lower than the S80 soil map but not as good as simulation results with joint state-parameter updates (PAR-S80-30) or with the BK50 soil map (OL-BK50). State updates did not improve modeled SWC as much as joint state-parameter updates improved modeled SWC. The  $E_{\text{RMS}}$  in case of Stt-S80 also falls behind. For most of the time, the  $E_{\text{RMS}}$  of the BK50-Stt-S80 run is larger than the  $E_{\text{RMS}}$  of the OL-BK50 run. During the evaluation period, also the open loop run through most of with the time. Joint FAO soil map (OL-FAO) performs better than the Stt-S80 run. In contrast, joint state-parameter updates for the S80 soil map improved the  $E_{\text{RMS}}$  throughout most of the time compared to the open loop simulations based on the BK50 and S80 soil maps. During the assimilation period 2011-2012, (OL-BK50, OL-FAO and OL-S80). As shown in Fig. 4, the PAR-S80-30 simulation performed best out of the four simulations during the assimilation period 2011-2012. During the evaluation period 2013, OL-BK50 and PAR-S80-30 performed equally well except in summer 2013 when the PAR-S80-30 simulation yielded much higher  $E_{\text{RMS}}$  values than the BK50 open loop run.

#### 4.44.3 Jackknife simulations

The jackknife simulations investigated the impact of the network of CRPs/CRNS data for improving estimates of simulated SWC at locations between the CRPs, outside the network, beyond the CRNS stations. Spatial

improvements are possible by spatial correlation structures of atmospheric forcings, soil hydraulic parameters and soil moisture which are taken into account by the local ensemble transform Kalman filter. The errors and bias shown in Table 4 refer to the two open loop simulations (for the S80 soil map and the BK50 soil map) and the 18 jackknife simulations. All simulations with the BK50 and the S80 soil map. On average over the three runs where only data of four CRNS were assimilated (jk4-S80-\*), the  $E_{RMS}$  was  $0.07 \text{ m}^3/\text{m}^3$  which is much lower than the  $E_{RMS}$  for the open loop run ( $0.12 \text{ m}^3/\text{m}^3$ ), and only a bit higher than the case where eight CRNS were assimilated ( $E_{RMS}=0.06 \text{ m}^3/\text{m}^3$  for jk8-S80-\*). The improved simulation results were also due to the bias reduction from  $0.11 \text{ m}^3/\text{m}^3$  to  $0.05 \text{ m}^3/\text{m}^3$  in case of four and  $0.04 \text{ m}^3/\text{m}^3$  in case of eight assimilated CRNS. However, for the BK50 soil map where  $E_{RMS}$  ( $0.04 \text{ m}^3/\text{m}^3$ ) and bias ( $0.02 \text{ m}^3/\text{m}^3$ ) of the open loop run were already good, the jackknife simulations led to slightly higher  $E_{RMS}$  ( $0.05 \text{ m}^3/\text{m}^3$ ) and bias ( $0.04 \text{ m}^3/\text{m}^3$ ). More detailed site statistics (Tables 1 to 4 of the Annex) demonstrate that all jackknife simulations with the S80 soil map resulted in an improved  $E_{RMS}$  at the jackknife simulation locations compared to the open loop simulation, except for Wildenrath. In all cases the  $E_{RMS}$  was smaller than  $0.10 \text{ m}^3/\text{m}^3$ . Error reduction was smaller at sites where the open loop error was smaller. At sites with large open loop  $E_{RMS}$ , the assimilation could reduce the  $E_{RMS}$  by 50 % or more. In case of the BK50 soil map, the jackknife simulations resulted in  $E_{RMS}$  values below  $0.10 \text{ m}^3/\text{m}^3$  at all sites. However, in this case only at Merzenhausen the  $E_{RMS}$  was reduced during the data assimilation period. At Wildenrath, the  $E_{RMS}$  was highest for jk-BK50 ( $0.091 \text{ m}^3/\text{m}^3$ ) and jk-S80 ( $0.095 \text{ m}^3/\text{m}^3$ ). The average absolute bias for the

The jackknife simulations illustrate that a network of CRNS can improve modelled SWC if the soil map information is not sufficient. This suggests that assimilation of CRNS data is particularly useful for regions with little information on subsurface parameters. A trade-off can be expected between the initial uncertainty on soil moisture and parameters, and the density of a CRNS network. In case of a large uncertainty, like in regions with limited information about soils or a strongly biased soil map (e.g. FAO or S80 soil map) and a low density of meteorological stations, a sparse network of probes can already be helpful for improving soil moisture characterization. The results of the real world jackknife experiments was  $0.04 \text{ cm}^3/\text{cm}^3$  for both soil maps, BK50 and S80, in the evaluation period 2013 (Table 5). Hence, bias in the jk-S80-\* simulations improved compared to the open loop run but not demonstrated that already four CRNS are beneficial but it is desirable to have more CRNS for improved parameter estimates. The results also suggest that the additional information gain for an extra CRNS reduces for a denser network, because the soil moisture characterization did not improve so much more if eight instead of four CRNS were used for assimilation. However, in regions with a high density of meteorological stations and a high resolution soil map it can be expected that a denser CRNS network is needed

than in this study to further lower the error of soil moisture characterization. Further potentially synthetic experiments in the jk-BK50-\* simulations, where bias was already small other regions with networks of CRNS are needed to get more quantitative information about this.

#### 4.5.4.4 Temporal evolution of ~~parameters~~ parameter estimates and parameter uncertainty

The temporal evolution of ~~the percentage~~ sand content estimates during the assimilation period for the nine CRP sites with CRNS is shown in Fig. 5 for PAR-S80-30, PAR-S80-10, PAR-BK50-30, PAR-BK50-10, jk8-S80-30\* and jk8-BK50-30\*-.\*. Time series start on March 20<sup>th</sup>, 2011, the date of the first assimilated CRPCRNS SWC retrieval at Wuestebach. At Wuestebach and sites within the influence sphere of Wuestebach (Aachen, Kall and Rollesbroich) ~~show also a change in~~, sand content estimates were updated from this date March 20<sup>th</sup>, 2011 onwards. ~~Because of the localization, all~~ other sites show a ~~change~~ first update in sand content in May 2012 when Rollesbroich and Merzenhausen start operating, and their data ~~is~~ was assimilated. ~~All~~ During the data assimilation period with joint state-parameter updates, all sites show variability in sand content over time. ~~estimates over time with differences in magnitude. Values and spread in sand content amongst the experiments is smaller at the sites Merzenhausen, Gevenich, RurAue, Heinsberg and Wildenrath, compared to the sites Wuestebach, Kall, Aachen and RurAue, Rollesbroich and Heinsberg show some peaks in the time series, were spread is considerably larger. At the sites Merzenhausen, Aachen, Gevenich, and Wildenrath show a smoother course compared to the other sites. Sand levels approach a constant site specific value for the sites Merzenhausen (45 %), Kall (30 %), Kall, Gevenich (41 %), RurAue (30 %), and Heinsberg (42 %) and Wildenrath (62 %) with a reasonable spread amongst the experiments. The spread in estimated sand content for the sites Wuestebach, Aachen and Rollesbroich is larger, and it seems not to have stabilized at the end of the assimilation. Sand content estimates, sand content estimates of the jackknife simulations was/were close to the sand content of the other data assimilation experiments with joint state-parameter estimation. A comparison of parameter estimates at the end of the assimilation period indicates that initial soil parameterization has a limited effect on the resulting parameter estimates. -at the sites Merzenhausen, Gevenich, RurAue and Heinsberg. Evolution of the sand content for the jackknife simulations showed larger deviations from the sand content estimated by other data assimilation experiments for the sites Wuestebach, Kall, Aachen, Rollesbroich and Wildenrath. Parameter estimates of jk8-BK50-\* and jk8-S80-\* are close together at the end of the assimilation period.~~

~~The~~ Estimates of the soil hydraulic parameter B and saturated hydraulic conductivity are shown in Fig. 6 and Fig. 7 for PAR-S80-30, PAR-S80-10, PAR-BK50-30, PAR-BK50-10, jk8-S80-30\* and jk8-BK50-30\*-.\*.

Formatted: Font: 9 pt, Font color: Black, English (U.S.)

Updates of soil hydraulic parameters start in March and May 2011 with the assimilation of CRNS\_SWC retrievals depending on the location. The B parameter increases estimates increase for all simulations. Throughout the whole assimilation period the empirical B parameter varies considerably within short time intervals. The total range of the B parameter estimates is between 2.7 and 14 at all sites. At the sites 5 Merzenhausen, Kall, Aachen, Gevenich and Rollesbroich, B generally ranges between 6 and 10. At Wuestebach, Heinsberg and RurAue, B ranges estimates of B range most of the time between 8 and 12, and at Wildenrath, B is below 8. Initial saturated hydraulic conductivity  $k_{sat}$  is rather high ( $k_{sat} > 0.015$  mm/s) in case of high sand content i.e. for the S80 soil map, and rather low ( $k_{sat} < 0.005$  mm/s) in case of low sand content i.e. for the BK50 soil map. In case of the S80 soil map, at all sites except Wildenrath, high initial saturated hydraulic 10 conductivity decreases,  $k_{sat}$  estimates decrease quickly by through joint state-parameter updates to values below 0.01 mm/s. The initial spread in  $k_{sat}$  values estimates amongst the simulation scenarios decreases at most sites. At Wuestebach, Merzenhausen, Aachen, Gevenich, RurAue and Heinsberg, the spread is rather small particularly at the end of the assimilation period, while at Wildenrath  $k_{sat}$  ranges from 0.005 to 0.015 for individual experiments at the end of the assimilation period. The discussion section will elaborate more on this.

15 Temporally not stable parameter estimates imply that there may be multiple or seasonal optimal parameter values. This is also supported by the findings of the temporal behaviour of site average  $E_{RMS}$  (Fig. 4) e.g. during the evaluation period when in the dry summer 2013 the  $E_{RMS}$  peaks for the PAR-S80-30 simulation. In this context, it is important to mention that many possible error sources were not subject to calibration in this study but could be crucial for an even better modelled soil moisture and more reliable soil parameter estimation. In this study we only considered uncertainty of soil parameters, but also vegetation parameters are uncertain. Also a number of other CLM-specific hydrologic parameters (e.g. decay factor for subsurface runoff and maximum subsurface drainage) strongly influence state variables in CLM and hence show potential for optimization (Sun et al., 2013). Considering this uncertainty from multiple parameters could give a better parameter uncertainty characterization (Shi et al., 2014). Precipitation is also an important forcing for hydrologic modelling. For this study, precipitation data from the COSMO DE re-analysis were used. A product which optimally combines precipitation estimates from radar and gauge measurements is expected to give better precipitation estimates than the reanalysis. This could improve the soil moisture characterization and also potentially lead to better parameter estimates. Further improvements and constraining of parameter uncertainty is also possible using multivariate data assimilation with observations such as latent heat flux (e.g. Shi et al., 2014). Also other error sources related to the model structure play a significant role. These options should be subject of future investigations.

Formatted: Don't add space between paragraphs of the same style

#### 4.6.4.5 Latent heat and sensible heat flux

Latent heat flux or evapotranspiration (ET) is another important diagnostic variable of ~~the CLM model and~~ surface models (e.g. Best et al., 2015) and of importance for atmospheric models. Results of the data assimilation experiments showed that soil texture updates altered soil moisture states significantly. In Fig. 8 it is shown that joint state-parameter estimation also altered ET ~~during the evaluation period~~. Fig. 8 shows ET within the evaluation period 2013 across the whole catchment for four ~~simulations~~ simulation experiments. On the one hand, ET was similar for both open loop simulations (OL-S80 and OL-BK50) in the South of the catchment. On the other hand, ET in the North was up to 80 mm per year lower for the S80 open loop run compared to the BK50 open loop run. ~~Regarding open loop runs, the~~ The differences can be linked to the drier soil conditions ~~in~~ ease for OL-S80 compared to OL-BK50 simulation results. The differences in ET between the runs with and without parameter updates were larger for the S80 soil map than for the BK50 soil map. For PAR-S80-10, ET increased by up to 40 mm per year in the ~~Northern~~ northern part of the catchment through data assimilation. ~~The differences between open loop ET and data assimilation ET were larger for the S80 soil map than for the BK50 soil map. This could be related to while the change in ET from OL-BK50 to PAR-BK50-10 is rather small. This is linked to the comparatively larger update in SWC in case of the S80 scenario compared to the BK50 scenario.~~ updates made to soil hydraulic parameters.

## 5 Discussion

~~The applied data assimilation scheme improved soil moisture characterization in the majority of simulation experiments with the regional Community Land Model (CLM). During 2011 and 2012, the biased S80 soil map gave a  $E_{RMS}$  up to  $0.17 \text{ cm}^3/\text{cm}^3$  (at Rollesbroich) in the open loop simulation which left plenty of room for improvements. The soil map BK50 led to  $E_{RMS}$ -values in open loop simulations below  $0.05 \text{ cm}^3/\text{cm}^3$  which left little room for error reduction considering the measurement error of  $0.03 \text{ cm}^3/\text{cm}^3$ . For the simulations starting with 80 % sand content, sand content was closer to the values of the BK50 soil map after joint state parameter estimation. However, the temporal evolution of the updated soil texture and the soil hydraulic parameters was not stable. Temporal fluctuations imply that there may be multiple or seasonal optimal parameter values. This is also supported by the findings of the temporal behavior of  $E_{RMS}$  during the evaluation period e.g. when in the dry summer 2013 the  $E_{RMS}$  peaked in the PAR S80 30 simulation. Many possible error sources were not subject to calibration in this study but they could be crucial for an even better soil moisture and more stable soil parameter estimation. In this study we only considered uncertainty of soil parameters, but also vegetation parameters are uncertain. Also a number of other CLM specific hydrologic parameters (e.g. decay factor for subsurface runoff and maximum subsurface drainage) strongly influence state variables in CLM and hence show also potential for~~

5 optimization. Considering this uncertainty could give a better uncertainty characterization. Precipitation is an important forcing for the model calculations and its estimate could be improved. ~~For this study, precipitation data from the COSMO-DE re-analysis were used. A product which optimally combines gauge measurements and precipitation estimates from radar could give better precipitation estimates. This could improve the soil moisture characterization and also potentially lead to better parameter estimates. Also other error sources like the ones related to the model structure play a significant role. This should be subject of future investigation.~~

10 Evaluation simulations for 2013 led to partly improved and partly deteriorated  $E_{RMS}$  values when the BK50 soil map was used as prior information on the soil hydraulic properties. The simulations with the S80 soil map on the contrary showed an improved soil moisture characterization in all simulation scenarios and the updated soil hydraulic parameter estimates for those simulations approached the values of the BK50 soil map. These results indicate that the soil hydraulic parameters derived from the BK50 soil map were already well suited for soil moisture predictions and updating soil texture and soil parameters could not improve further the results.  $E_{RMS}$  values for simulations with state updates only (Stt-BK50 and Stt-S80) in 2013 imply the beneficial role of state updates only. However, the improvements in the evaluation period by state updates (without parameter values) are small compared to the improvements obtained by joint state parameter estimation. ~~This illustrates the benefits of joint state parameter updates compared to state updates only, and that soil moisture states are strongly determined by soil hydraulic parameters. It also illustrates that the improved characterization of soil moisture states in the assimilation period which results in improved initial states for the verification period loses its influence in the verification period fast over time.~~

25 The jackknife simulations illustrated that a network of CRPs can improve modeled SWC if the soil map information is not sufficient. Temporal evolution of subsurface parameters of the jackknife simulations (e.g. jk-S80\*) was close to the evolution of parameter estimates by other simulations (e.g. PAR-S80-10). Parameter estimates at jackknife test sites were inferred from multiple surrounding CRP sites, while updates at sites with CRP information were strongly inferred from single site information. Additionally, the impact of soil parameter estimates on ET is different in the North of the catchment compared to the South. While ET in the North of the catchment was impacted by the estimated soil properties during the evaluation period 2013 for PAR-S80-10, ET in the South was not as much impacted by estimated soil properties. This is related to the fact that in the North ET is moisture limited in summer, whereas in the South this is not moisture limited but energy limited. Therefore, ET in the North is sensitive to variations in soil hydraulic parameter values, whereas in the South this is not the case. In the South, ET is sensitive to model forcings like incoming shortwave radiation. Nearing et al.

(2016) came to the conclusion that soil parameter uncertainty dominates soil moisture uncertainty and forcing uncertainty dominates ET uncertainty. Our findings in the southern part of the catchment support their conclusion, but in the northern part of the catchment soil parameter uncertainty strongly affect ET. Hence particularly in the northern part of the catchment, further observations such as ET measurements are desirable for further improving the land surface model. These additional observations could be used for future land surface model benchmarking (Best et al., 2015) or for more constrained parameter estimates. ~~A comparison of parameter estimates at the end of the assimilation period indicates that initial soil parameterization has a limited effect on the resulting parameter estimates. Parameter estimates of jk-BK50-30\* and jk-S80-30\* are close together at the end of the assimilation period. The CRP network led to improved results for the jackknife evaluation simulations in case of the biased soil map. This suggests that assimilation of CRP data is particularly useful for regions with little information on subsurface parameters. We expect a tradeoff between the initial uncertainty on soil moisture content (related to the quality of the soil map and meteorological data) and the density of a CRP network. In case of a large uncertainty, like in regions with limited information about soils and a low density of meteorological stations, a sparse network of probes can already be helpful for improving soil moisture characterization. On the other hand, in regions with a high density of meteorological stations and a high resolution soil map it can be expected that a high resolution CRP network is needed to further lower the error of soil moisture characterization. Further experiments in other regions with networks of CRPs are needed to get more quantitative information about this.~~

~~A question that remains to be answered is whether it is more beneficial to assimilate neutron counts measured by CRPs directly or to assimilate CRP-SWC retrievals derived from the neutron counts, as done in this study. Fast neutron intensity measured by CRPs is also affected by vegetation. Neutron count rate decreases with increasing biomass because of the hydrogen content in vegetation (Baatz et al., 2015). Seasonal biomass changes at a single site have a rather small impact on neutron intensity compared to differences between grass land site and a forest site (Baatz et al., 2015). Therefore, using measured neutron flux directly in a data assimilation framework in a catchment with different vegetation types would require to account for the effects of vegetation types on neutron intensity. Hence, vegetation estimates for each grid cell would be necessary. At present, there are two methods that include biomass in the CRP calibration process (BaatzShi et al., 2015; Franz et al., 2013b) but both methods naturally require accurate biomass estimates, which are typically not available. Besides the uncertainty associated with CRP methods using biomass in the calibration process, biomass estimates also come along with high uncertainties. Therefore, in the case of a catchment with different vegetation types, it is desirable to circumvent the use of biomass estimates, and assimilate directly SWC retrievals obtained at the observation sites~~

instead of assimilating neutron intensity. Therefore, this study uses CRP SWC retrievals in the data assimilation scheme assuming that seasonal changes of biomass can be neglected.

.

## 65 Conclusions and Outlook

This real-world case study demonstrates the benefits of assimilating data from a network of nine cosmic-ray probes (CRP) neutron sensors (CRNS) soil water content (SWC) retrievals into a land surface model shows the potential of CRNS networks to improve subsurface parameterization in regional land surface models, especially if prior information on soil properties is limited. CRNS SWC retrievals were assimilated into the land surface model CLM version 4.5. Although information on neutron flux intensity was only available at few locations in the catchment, using the local ensemble transform Kalman filter (LETKF) allows updating of soil water content (SWC). SWC and subsurface parameters were updated with the LETKF at unmonitored locations in the catchment considering model and observation uncertainties. Joint state-parameter estimates improved soil moisture estimates during the assimilation and during the evaluation period. The  $E_{\text{RMS-Error}}$  and bias for the soil moisture characterization reduced strongly for simulations initialized with a biased soil map and similarly well if initialized with the FAO soil map. Simulations initialized with a biased or global soil map approached values similar to error statistics with joint state-parameter updates as the ones obtained when the regional soil map was used as input to the simulations.  $E_{\text{RMS-Error}}$  values in simulations with the regional soil map were not improved during the evaluation period, because open loop simulation results were already close to the observations. The beneficial results of joint state-parameter updates were confirmed by additional jackknife experiments. This real-world case study on assimilating CRP SWC retrievals into a land surface model shows the potential of CRP networks to improve subsurface parameterization in regional land surface models, especially if prior information on soil properties is limited, with eight and four CRNS for assimilation. In many areas of the world, less detailed only global soil maps (e.g. the FAO soil map) are available than the but no detailed high resolution regional soil map applied in this study. In has shown that in these areas, a more advanced sub-surface characterization is possible using CRPCRNS measurements and the data assimilation framework presented in this study.

For now, CRP neutron intensity observations by CRNS were not assimilated directly. In future studies it would be desirable to use the COSMIC operator for assimilating neutron intensity observations directly. However, in this case the impact of biomass on the CRPCRNS measurement signal would have to be taken into account. Therefore, it is desirable to further develop the COSMIC operator to include the impact of biomass on neutron intensities. Using the biogeochemical module of CLM would then allow to characterize model local vegetation

states as input for the measurement operator. Remotely sensed vegetation states are another option to characterize vegetation states as input for the measurement operator. Both methods require additional field measurements for the verification of vegetation state estimates. The further extension of the data assimilation framework would also enable the estimation of additional sub-land surface parameters. ~~The~~In addition, the impact of other sub-surface parameters such as subsurface drainage parameters and the surface drainage decay factor on SWC states and radiative surface fluxes has already been shown (Sun et al., 2013). Estimation of these parameters is desirable because of the inherent uncertainty of these globally tuned parameters. However, estimation of soil texture and organic matter content was demonstrated to be already beneficial for improved SWC ~~modeling~~modelling. Hence, this study represents a way forward towards the integration of ~~CRPCRNS~~ information in the calibration or real-time updating of ~~large scale weather prediction~~land surface models.

#### Data Availability

Most data presented in this study are freely available via the TERENO data portal TEODOOR (<http://teodoor.icg.kfa-juelich.de/>). Atmospheric data were licensed by the German Weather Service (DWD), and the BK50 soil map was licensed by the Geologischer Dienst Nordrhein-Westfalen.

#### 15 Acknowledgements

~~We~~The authors gratefully acknowledge the support by the SFB-TR32 "Pattern in Soil-Vegetation-Atmosphere Systems: Monitoring, Modelling and Data Assimilation" funded by the Deutsche Forschungsgemeinschaft (DFG) and TERENO (Terrestrial Environmental Observatories) funded by the Helmholtz-Gemeinschaft. The authors also gratefully acknowledge the computing time granted by the John von Neumann Institute for Computing (NIC) and provided on the supercomputer JURECA at Jülich Supercomputing Centre (JSC). Finally, the authors acknowledge and thank four anonymous referees for providing constructive comments and the Editor, Nunzio Romano, for guiding the revision process.

#### 7 References

Ajami, H., McCabe, M. F., Evans, J. P., and Stisen, S.: Assessing the impact of model spin-up on surface water-groundwater interactions using an integrated hydrologic model, *Water Resour Res*, 50, 2636-2656, 10.1002/2013wr014258, 2014.  
Anderson, J. L.: An ensemble adjustment Kalman filter for data assimilation, *Mon Weather Rev*, 129, 2884-2903, Doi 10.1175/1520-0493(2001)129<2884: Aeakff>2.0.Co;2, 2001.

Formatted: No bullets or numbering

- Avery, W. A., Finkenbiner, C., Franz, T. E., Wang, T. J., Nguy-Robertson, A. L., Suyker, A., Arkebauer, T., and Munoz-Arriola, F.: [Incorporation of globally available datasets into the roving cosmic-ray neutron probe method for estimating field-scale soil water content](#), *Hydrol Earth Syst Sc*, 20, 3859-3872, [10.5194/hess-20-3859-2016](#), 2016.
- 5 Baatz, R., Bogen, H. R., Hendricks Franssen, H. J., Huisman, J. A., Qu, W., Montzka, C., and Vereecken, H.: Calibration of a catchment scale cosmic-ray probe network: A comparison of three parameterization methods, *J Hydrol*, 516, 231-244, [http://dx.doi.org/10.1016/j.jhydrol.2014.02.026](#), [http://dx.doi.org/10.1016/j.jhydrol.2014.02.026](#), 2014.
- Baatz, R., Bogen, H. R., Hendricks Franssen, H. J., Huisman, J. A., Montzka, C., and Vereecken, H.: An empirical vegetation correction for soil water content quantification using cosmic ray probes, *Water Resour Res*, 51, 2030-2046, [10.1002/2014WR016443](#), 2015.
- 10 Bateni, S. M., and Entekhabi, D.: Surface heat flux estimation with the ensemble Kalman smoother: Joint estimation of state and parameters, *Water Resour Res*, 48, Artn W08521 [10.1029/2011wr011542](#), 2012.
- Bell, J. E., Leeper, R. D., Palecki, M. A., Coopersmith, E., Wilson, T., Bilotta, R., and Embler, S.: [Evaluation of the 2012 Drought with a Newly Established National Soil Monitoring Network](#), *Vadose Zone J*, 14, [10.2136/vzj2015.02.0023](#), 2015.
- 15 Best, M. J., Abramowitz, G., Johnson, H. R., Pitman, A. J., Balsamo, G., Boone, A., Cuntz, M., Decharme, B., Dirmeyer, P. A., Dong, J., Ek, M., Guo, Z., Haverd, V., Van den Hurk, B. J. J., Nearing, G. S., Pak, B., Peters-Lidard, C., Santanello, J. A., Stevens, L., and Vuichard, N.: [The Plumbing of Land Surface Models: Benchmarking Model Performance](#), *J Hydrometeorol*, [16](#), [1425-1442](#), [10.1175/JHM-D-14-0158.1](#), 2015.
- 20 Bogen, H. R., Herbst, M., Hake, J. F., Kunkel, R., Montzka, C., Pütz, T., Vereecken, H., and Wendland, F.: MOSYRUR - Water balance analysis in the Rur basin., in: *Schriften des Forschungszentrums Jülich. Reihe Umwelt/Environment*, Jülich, 2005.
- Bogen, H. R., Huisman, J. A., Baatz, R., Hendricks-Franssen, H. J., and Vereecken, H.: Accuracy of the cosmic-ray soil water content probe in humid forest ecosystems: The worst case scenario, *Water Resour Res*, 49, [5778-5791](#), [Doi 10.1002/WATERWRCR.20463](#), 2013.
- 25 Bonan, G. B., Levis, S., Kergoat, L., and Oleson, K. W.: [Landscapes as patches of plant functional types: An integrating concept for climate and ecosystem models](#), *Global Biogeochem Cy*, [16](#), [10.1029/2000GB001360](#), 2002.
- Brutsaert, W.: [Hydrology : an introduction](#), Cambridge University Press, Cambridge : New York, xi, 605 p. pp., 2005.
- Burgers, G., van Leeuwen, P. J., and Evensen, G.: Analysis scheme in the ensemble Kalman filter, *Mon Weather Rev*, 126, 1719-1724, [Doi 10.1175/1520-0493\(1998\)126<1719:Asitek>2.0.Co;2](#), 1998.
- 30 Chen, F., Manning, K. W., LeMone, M. A., Trier, S. B., Alfieri, J. G., Roberts, R., Tewari, M., Niyogi, D., Horst, T. W., Oncley, S. P., Basara, J. B., and Blanken, P. D.: Description and evaluation of the characteristics of the NCAR high-resolution land data assimilation system, *J Appl Meteorol Clim*, 46, 694-713, [10.1175/Jam2463.1](#), 2007.
- Chen, Y., and Zhang, D. X.: Data assimilation for transient flow in geologic formations via ensemble Kalman filter, *Adv Water Resour*, 29, 1107-1122, [10.1016/j.advwatres.2005.09.007](#), 2006.
- 35 Clapp, R. B., and Hornberger, G. M.: Empirical Equations for Some Soil Hydraulic-Properties, *Water Resour Res*, 14, 601-604, [Doi 10.1029/Wr014i004p00601](#), 1978.
- Cosby, B. J., Hornberger, G. M., Clapp, R. B., and Ginn, T. R.: A Statistical Exploration of the Relationships of Soil-Moisture Characteristics to the Physical-Properties of Soils, *Water Resour Res*, 20, 682-690, [Doi 10.1029/Wr020i006p00682](#), 1984.
- 40 Cosh, M. H., Ochsner, T. E., McKee, L., Dong, J. N., Basara, J. B., Evett, S. R., Hatch, C. E., Small, E. E., Steele-Dunne, S. C., Zreda, M., and Sayde, C.: [The Soil Moisture Active Passive Marena, Oklahoma, In Situ Sensor Testbed \(SMAP-MOISST\): Testbed Design and Evaluation of In Situ Sensors](#), *Vadose Zone J*, [15](#), [10.2136/vzj2015.09.0122](#), 2016.
- Crow, W. T.: Correcting land surface model predictions for the impact of temporally sparse rainfall rate measurements using an ensemble Kalman filter and surface brightness temperature observations, *J Hydrometeorol*, 4, 960-973, 2003.
- 45 Crow, W. T., Berg, A. A., Cosh, M. H., Loew, A., Mohanty, B. P., Panciera, R., de Rosnay, P., Ryu, D., and Walker, J. P.: Upscaling Sparse Ground-Based Soil Moisture Observations for the Validation of Coarse-Resolution Satellite Soil Moisture Products, *Rev Geophys*, 50, Artn Rg2002 [Doi 10.1029/2011rg000372](#), 2012.
- De Lannoy, G. J. M., Reichle, R. H., Arsenault, K. R., Houser, P. R., Kumar, S., Verhoest, N. E. C., and Pauwels, V. R. N.: Multiscale assimilation of Advanced Microwave Scanning Radiometer-EOS snow water equivalent and Moderate Resolution Imaging Spectroradiometer snow cover fraction observations in northern Colorado, *Water Resour Res*, 48, Artn W01522 [Doi 10.1029/2011wr010588](#), 2012.

- Desilets, D., Zreda, M., and Ferre, T. P. A.: Nature's neutron probe: Land surface hydrology at an elusive scale with cosmic rays, *Water Resour Res*, 46, 10.1029/2009WR008726, 2010.
- Desilets, D., and Zreda, M.: Footprint diameter for a cosmic ray soil moisture probe: Theory and Monte Carlo simulations, *Water Resour Res*, 49, 3566-3575, Doi 10.1002/Wrcr.20187, 2013.
- 5 | De Lannoy, G. J. M., and Reichle, R. H.: Assimilation of SMOS brightness temperatures or soil moisture retrievals into a land surface model, *Hydrol Earth Syst Sc*, 20, 4895-4911, 10.5194/hess-20-4895-2016, 2016.
- Draper, C. S., Mahfouf, J. F., and Walker, J. P.: An EKF assimilation of AMSR-E soil moisture into the ISBA land surface scheme, *J Geophys Res-Atmos*, 114, 10.1029/2008JD011650, 2009.
- Dunne, S., and Entekhabi, D.: An ensemble-based reanalysis approach to land data assimilation, *Water Resour Res*, 41, Artn W02013  
10.1029/2004wr003449, 2005.
- Eltahir, E. A. B.: A soil moisture rainfall feedback mechanism I. Theory and observations, *Water Resour Res*, 34, 765-776, Doi 10.1029/97wr03499, 1998.
- Erdal, D., Neuweiler, I., and Wollschlager, U.: Using a bias aware EnKF to account for unresolved structure in an unsaturated zone model, *Water Resour Res*, 50, 132-147, 10.1002/2012wr013443, 2014.
- 15 | Erdal, D., Rahman, M. A., and Neuweiler, I.: The importance of state transformations when using the ensemble Kalman filter for unsaturated flow modeling: Dealing with strong nonlinearities, *Adv Water Resour*, 86, 354-365, 10.1016/j.advwatres.2015.09.008, 2015.
- 20 | Evans, J. G., Ward, H. C., Blake, J. R., Hewitt, E. J., Morrison, R., Fry, M., Ball, L. A., Doughty, L. C., Libre, J. W., Hitt, O. E., Rylett, D., Ellis, R. J., Warwick, A. C., Brooks, M., Parkes, M. A., Wright, G. M. H., Singer, A. C., Boorman, D. B., and Jenkins, A.: Soil water content in southern England derived from a cosmic-ray soil moisture observing system – COSMOS-UK, *Hydrol Process*, 30, 4987-4999, 10.1002/hyp.10929, 2016.
- Evensen, G.: Sequential Data Assimilation with a Nonlinear Quasi-Geostrophic Model Using Monte-Carlo Methods to Forecast Error Statistics, *J Geophys Res-Oceans*, 99, 10143-10162, Doi 10.1029/94jc00572, 1994.
- 25 | FAO, I., ISRIC, ISSCAS, J. Harmonized World Soil Database v1.2, Rome, Italy, 2012.
- Franz, T. E., Zreda, M., Ferre, T. P. A., Rosolem, R., Zweck, C., Stillman, S., Zeng, X., and Shuttleworth, W. J.: Measurement depth of the cosmic ray soil moisture probe affected by hydrogen from various sources, *Water Resour Res*, 48, Artn W08515  
Doi 10.1029/2012wr011871, 2012.
- 30 | Franz, T. E., Zreda, M., Ferre, T. P. A., and Rosolem, R.: An assessment of the effect of horizontal soil moisture heterogeneity on the area-average measurement of cosmic-ray neutrons, *Water Resour Res*, 49, 6450-6458, Doi 10.1002/Wrcr.20530, 2013a2013.
- Franz, T. E., Zreda, M., Rosolem, R., and Ferre, T. P. A.: A universal calibration function for determination of soil moisture with cosmic ray neutrons, *Hydrol Earth Syst Sc*, 17, 453-460, DOI 10.5194/hess-17-453-2013, 2013b.
- 35 | GmbH, s.: Digital Elevation Model 10 without anthropogenic landforms, *landforms*, 2010.
- Han, X., Li, X., Franssen, H. J. H., Montzka, C., and Vereecken, H.: Soil moisture and soil properties estimation, and Montzka, C.: Spatial horizontal correlation characteristics in the Community Land Model with synthetic brightness temperature observations, *Water Resour Res*, 50, 6081-6105, 10.1002/2013WR014586, 2014a  
land data assimilation of soil moisture, *Hydrol Earth Syst Sc*, 16, 1349-1363, 10.5194/hess-16-1349-2012, 2012.
- 40 | Han, X., Franssen, H. J. H., Rosolem, R., Jin, R., Li, X., and Vereecken, H.: Correction of systematic model forcing bias of CLM using assimilation of cosmic-ray Neutrons and land surface temperature: a study in the Heihe Catchment, China, *Hydrol. Earth Syst. Sci.*, 19, 615-629, 10.5194/hess-19-615-2015, 2015.
- Han, X., Franssen, H.-J. H., Bello, M. Á. J., Rosolem, R., Bogena, H., Alzamora, F. M., Chanzy, A., and Vereecken, H.: Simultaneous Soil Moisture and Properties Estimation for a Drip Irrigated Field by Assimilating Cosmic-ray Neutron Intensity, *J Hydrol*, <http://dx.doi.org/10.1016/j.jhydrol.2016.05.050>, <http://dx.doi.org/10.1016/j.jhydrol.2016.05.050>, 2016.
- 45 | Han, X. J., Franssen, H. J. H., Li, X., Zhang, Y. L., Montzka, C., and Vereecken, H.: Joint Assimilation of Surface Temperature and L-Band Microwave Brightness Temperature in Land Data Assimilation, *Vadose Zone J*, 12, Doi 10.2136/vzj2012.vzj2012.0072, 2013.
- Han, X. J., Franssen, H. J. H., Montzka, C., and Vereecken, H.: Soil moisture and soil properties estimation in the Community Land Model with synthetic brightness temperature observations, *Water Resour Res*, 50, 6081-6105, 10.1002/2013WR014586, 2014b2014.
- 50 | Hawdon, A., McJannet, D., and Wallace, J.: Calibration and correction procedures for cosmic-ray neutron soil moisture probes located across Australia, *Water Resour Res*, 50, 5029-5043, 10.1002/2013WR015138, 2014.

- Hendricks Franssen, H. J., and Kinzelbach, W.: Real-time groundwater flow modeling with the Ensemble Kalman Filter: Joint estimation of states and parameters and the filter inbreeding problem, *Water Resour Res*, 44, Artn W09408 Doi 10.1029/2007wr006505, 2008.
- 5 ~~Houser, P. R., Shuttleworth, W. J., Famiglietti, J. S., Gupta, H. V., Syed, K. H., and Goodrich, D. C.: Integration of soil moisture remote sensing and hydrologic modeling using data assimilation, *Water Resour Res*, 34, 3405-3420, Doi 10.1029/1998wr900001, 1998.~~
- Hunt, B. R., Kostelich, E. J., and Szunyogh, I.: Efficient data assimilation for spatiotemporal chaos: A local ensemble transform Kalman filter, *Physica D*, 230, 112-126, DOI 10.1016/j.physd.2006.11.008, 2007.
- 10 ~~Hurkmans, R., Paniconi, C., and Troch, P. A.: Numerical assessment of a dynamical relaxation data assimilation scheme for a catchment hydrological model, *Hydrol Process*, 20, 549-563, 10.1002/hyp.5921, 2006.~~
- ~~Iwema, J., Rosolem, R., Baatz, R., Wagener, T., and Bogaen, H. R.: Investigating temporal field sampling strategies for site-specific calibration of three soil moisture-neutron intensity parameterisation methods, *Hydrol Earth Syst Sc.* 19, 3203-3216, 10.5194/hess-19-3203-2015, 2015.~~
- 15 Jackson, T. J., Le Vine, D. M., Hsu, A. Y., Oldak, A., Starks, P. J., Swift, C. T., Isham, J. D., and Haken, M.: Soil moisture mapping at regional scales using microwave radiometry: The Southern Great Plains Hydrology Experiment, *Ieee T Geosci Remote*, 37, 2136-2151, Doi 10.1109/36.789610, 1999.
- ~~Kerr, Y. H., Waldteufel, P., Richaume, P., Wigneron, J. P., Ferrazzoli, P., Mahmoodi, A., Al Bitar, A., Cabot, F., Gruhier, C., Juglea, S. E., Leroux, D., Mialon, A., and Delwart, S.: The SMOS Soil Moisture Retrieval Algorithm, *Ieee T Geosci Remote*, 50, 1384-1403, Doi 10.1109/Tgrs.2012.2184548, 2012.~~
- 20 ~~Kirkpatrick, J. B., Green, K., Bridle, K. L., and Venn, S. E.: Patterns of variation in Australian alpine soils and their relationships to parent material, vegetation formation, climate and topography, *Catena*, 121, 186-194, 10.1016/j.catena.2014.05.005, 2014.~~
- Kohli, M., Schron, M., Zreda, M., Schmidt, U., Dietrich, P., and Zacharias, S.: Footprint characteristics revised for field-scale soil moisture monitoring with cosmic-ray neutrons, *Water Resour Res*, 51, 5772-5790, 10.1002/2015WR017169, 2015.
- 25 ~~Korres, W., Reichenau, T. G., Fiener, P., Kovama, C. N., Bogaen, H. R., Comelissen, T., Baatz, R., Herbst, M., Diekkruger, B., Vereecken, H., and Schneider, K.: Spatio-temporal soil moisture patterns - A meta-analysis using plot to catchment scale data, *J Hydrol*, 520, 326-341, 10.1016/j.jhydrol.2014.11.042, 2015.~~
- Koster, R. D., Dirmeyer, P. A., Guo, Z. C., Bonan, G., Chan, E., Cox, P., Gordon, C. T., Kanae, S., Kowalczyk, E., Lawrence, D., Liu, P., Lu, C. H., Malyshev, S., McAvaney, B., Mitchell, K., Mocko, D., Oki, T., Oleson, K., Pitman, A., Sud, Y. C., Taylor, C. M., Versegny, D., Vasic, R., Xue, Y. K., Yamada, T., and Team, G.: Regions of strong coupling between soil moisture and precipitation, *Science*, 305, 1138-1140, DOI 10.1126/science.1100217, 2004.
- 30 Kumar, S. V., Reichle, R. H., Harrison, K. W., Peters-Lidard, C. D., Yatheendradas, S., and Santanello, J. A.: A comparison of methods for a priori bias correction in soil moisture data assimilation, *Water Resour Res*, 48, Artn W03515 Doi 10.1029/2010wr010261, 2012.
- 35 Kurtz, W., He, G. W., Kollet, S. J., Maxwell, R. M., Vereecken, H., and Franssen, H. J. H.: TerrSysMP-PDAF version 1.0): a modular high-performance data assimilation framework for an integrated land surface-subsurface model, *Geosci Model Dev*, 9, 1341-1360, 10.5194/gmd-9-1341-2016, 2016.
- Lawrence, D. M., and Slater, A. G.: Incorporating organic soil into a global climate model, *Clim Dynam*, 30, 145-160, 10.1007/s00382-007-0278-1, 2008.
- 40 Lee, J. H.: Spatial-Scale Prediction of the SVAT Soil Hydraulic Variables Characterizing Stratified Soils on the Tibetan Plateau from an EnKF Analysis of SAR Soil Moisture, *Vadose Zone J*, 13, 10.2136/vzj2014.06.0060, 2014.
- ~~Liu, J. J., Fung, I., Kalnay, E., Kang, J. S., Olsen, E. T., and Chen, L.: Simultaneous assimilation of AIRS Xco(2) and meteorological observations in a carbon-climate model with an ensemble Kalman filter, *J Geophys Res Atmos*, 117, Artn D05309 Doi 10.1029/2011jd016642, 2012.~~
- 45 ~~Lv, L., Franz, T. E., Robinson, D. A., and Jones, S. B.: Measured and Modeled Soil Moisture Compared with Cosmic Ray Neutron Probe Estimates in a Mixed Forest, *Vadose Zone J*, 13, 10.2136/vzj2014.06.0077, 2014.~~
- ~~Miyoshi, T., and Kuniti, M.: The Local Ensemble Transform Kalman Filter with the Weather Research and Forecasting Model: Experiments with Real Observations, *Pure Appl Geophys*, 169, 321-333, 10.1007/s00024-011-0373-4, 2012.~~
- 50 Montzka, C., Canty, M., Kunkel, R., Menz, G., Vereecken, H., and Wendland, F.: Modelling the water balance of a mesoscale catchment basin using remotely sensed land cover data, *J Hydrol*, 353, 322-334, DOI 10.1016/j.jhydrol.2008.02.018, 2008.

- Montzka, C., Moradkhani, H., Weihermuller, L., Franssen, H. J. H., Canty, M., and Vereecken, H.: Hydraulic parameter estimation by remotely-sensed top soil moisture observations with the particle filter, *J Hydrol*, 399, 410-421, [DOI 10.1016/j.jhydrol.2011.01.020](https://doi.org/10.1016/j.jhydrol.2011.01.020), 2011.
- 5 Montzka, C., Pauwels, V. R. N., Franssen, H. J. H., Han, X. J., and Vereecken, H.: Multivariate and Multiscale Data Assimilation in Terrestrial Systems: A Review, *Sensors-Basel*, 12, 16291-16333, [10.3390/s121216291](https://doi.org/10.3390/s121216291), 2012.
- Montzka, C., Grant, J. P., Moradkhani, H., Franssen, H. J. H., Weihermuller, L., Drusch, M., and Vereecken, H.: Estimation of Radiative Transfer Parameters from L-Band Passive Microwave Brightness Temperatures Using Advanced Data Assimilation, *Vadose Zone J*, 12, 10.2136/vzj2012.0040, 2013.
- 10 Moradkhani, H., Sorooshian, S., Gupta, H. V., and Houser, P. R.: Dual state-parameter estimation of hydrological models using ensemble Kalman filter, *Adv Water Resour*, 28, 135-147, [10.1016/j.advwatres.2004.09.002](https://doi.org/10.1016/j.advwatres.2004.09.002), 2005.
- [Nearing, G. S., Mocko, D. M., Peters-Lidard, C. D., Kumar, S. V., and Xia, Y. L.: Benchmarking NLDAS-2 Soil Moisture and Evapotranspiration to Separate Uncertainty Contributions. \*J Hydrometeorol\*, 17, 745-759, 10.1175/Jhm-D-15-0063.1, 2016.](https://doi.org/10.1175/JHM-D-15-0063.1)
- Nordrhein-Westfalen, G. D.: Informationssystem Bodenkarte 50, 1:50000, 2009.
- 15 Oglesby, R. J., and Erickson, D. J.: Soil-Moisture and the Persistence of North-American Drought, *J Climate*, 2, 1362-1380, [Doi 10.1175/1520-0442\(1989\)002<1362:Smato>2.0.Co;2](https://doi.org/10.1175/1520-0442(1989)002<1362:Smato>2.0.Co;2), 1989.
- Oleson, K., Lawrence, D. M., Bonan, G. B., Drewniak, B., Huang, M., Koven, C. D., Levis, S., Li, F., Riley, J. M., Subin, Z. M., Swenson, S., Thornton, P. E., Bozbiyik, A., Fisher, R., Heald, C. L., Kluzek, E., Lamarque, J.-F., Lawrence, P. J., Leung, L. R., Lipscomb, W., Muszala, S. P., Ricciuto, D. M., Sacks, W. J., Sun, Y., Tang, J., and Yang, Z.-L.: Technical description of version 4.5 of the Community Land Model (CLM), NCAR Technical Note NCAR/TN-503+STR, 420, [10.5065/D6RR1W7M](https://doi.org/10.5065/D6RR1W7M), 2013.
- [Patil, N. G., and Singh, S. K.: Pedotransfer Functions for Estimating Soil Hydraulic Properties: A Review. \*Pedosphere\*, 26, 417-430, 10.1016/S1002-0160\(15\)60054-6, 2016.](https://doi.org/10.1016/S1002-0160(15)60054-6)
- 25 Pauwels, V. R. N., Balenzano, A., Satalino, G., Skriver, H., Verhoest, N. E. C., and Mattia, F.: Optimization of Soil Hydraulic Model Parameters Using Synthetic Aperture Radar Data: An Integrated Multidisciplinary Approach, *Ieee T Geosci Remote*, 47, 455-467, [10.1109/Tgrs.2008.2007849](https://doi.org/10.1109/Tgrs.2008.2007849), 2009.
- Pelowitz, D. B.: MCNPX user's manual, version 5, Rep. LA-CP-05-0369, Los Alamos National Laboratory, Los AlamosLA-CP-05-0369, 2005.
- 30 [Penny, S. G., Kalnay, E., Carton, J. A., Hunt, B. R., Ide, K., Miyoshi, T., and Chepurin, G. A.: The local ensemble transform Kalman filter and the running in place algorithm applied to a global ocean general circulation model, \*Nonlinear Proc Geoph\*, 20, 1031-1046, 10.5194/npg-20-1031-2013, 2013.](https://doi.org/10.1029/2013GL018313)
- [Ray, N. H.: Gas Chromatography .I. The Separation and Estimation of Volatile Organic Compounds by Gas-Liquid Partition Chromatography. \*J Appl Chem\*, 4, 21-25, 1954.](https://doi.org/10.1002/jlch.10001)
- 35 Reichle, R. H., McLaughlin, D. B., and Entekhabi, D.: Hydrologic data assimilation with the ensemble Kalman filter, *Mon Weather Rev*, 130, 103-114, [Doi 10.1175/1520-0493\(2002\)130<0103:Hdawte>2.0.Co;2](https://doi.org/10.1175/1520-0493(2002)130<0103:Hdawte>2.0.Co;2), 2002a.
- Reichle, R. H., Walker, J. P., Koster, R. D., and Houser, P. R.: Extended versus ensemble Kalman filtering for land data assimilation, *J Hydrometeorol*, 3, 728-740, [Doi 10.1175/1525-7541\(2002\)003<0728:Evekff>2.0.Co;2](https://doi.org/10.1175/1525-7541(2002)003<0728:Evekff>2.0.Co;2), 2002b.
- Reichle, R. H.: Data assimilation methods in the Earth sciences, *Adv Water Resour*, 31, 1411-1418, [10.1016/j.advwatres.2008.01.001](https://doi.org/10.1016/j.advwatres.2008.01.001), 2008.
- 40 Reichle, R. H., Kumar, S. V., Mahanama, S. P. P., Koster, R. D., and Liu, Q.: Assimilation of Satellite-Derived Skin Temperature Observations into Land Surface Models, *J Hydrometeorol*, 11, 1103-1122, [Doi 10.1175/2010jhm1262.1](https://doi.org/10.1175/2010jhm1262.1), 2010.
- [Rhodin, A., Kucharski, F., Callies, U., Eppel, D. P., and Wergen, W.: Variational analysis of effective soil moisture from screen level atmospheric parameters: Application to a short range weather forecast model, \*Q J Roy Meteor Soc\*, 125, 2427-2448, Doi 10.1256/Smsqj.55904, 1999.](https://doi.org/10.1029/1999JD000199)
- 45 Robinson, D. A., Campbell, C. S., Hopmans, J. W., Hornbuckle, B. K., Jones, S. B., Knight, R., Ogden, F., Selker, J., and Wendroth, O.: Soil moisture measurement for ecological and hydrological watershed-scale observatories: A review, *Vadose Zone J*, 7, 358-389, [Doi 10.2136/Vzj2007.0143](https://doi.org/10.2136/Vzj2007.0143), 2008.
- Rosolem, R., Hoar, T., Arellano, A., Anderson, J. L., Shuttleworth, W. J., Zeng, X., and Franz, T. E.: Translating aboveground cosmic-ray neutron intensity to high-frequency soil moisture profiles at sub-kilometer scale, *Hydrol. Earth Syst. Sci.*, 18, 4363-4379, [10.5194/hess-18-4363-2014](https://doi.org/10.5194/hess-18-4363-2014), 2014.
- 50 Seneviratne, S. I., Luthi, D., Litschi, M., and Schar, C.: Land-atmosphere coupling and climate change in Europe, *Nature*, 443, 205-209, [Doi 10.1038/Nature05095](https://doi.org/10.1038/Nature05095), 2006.

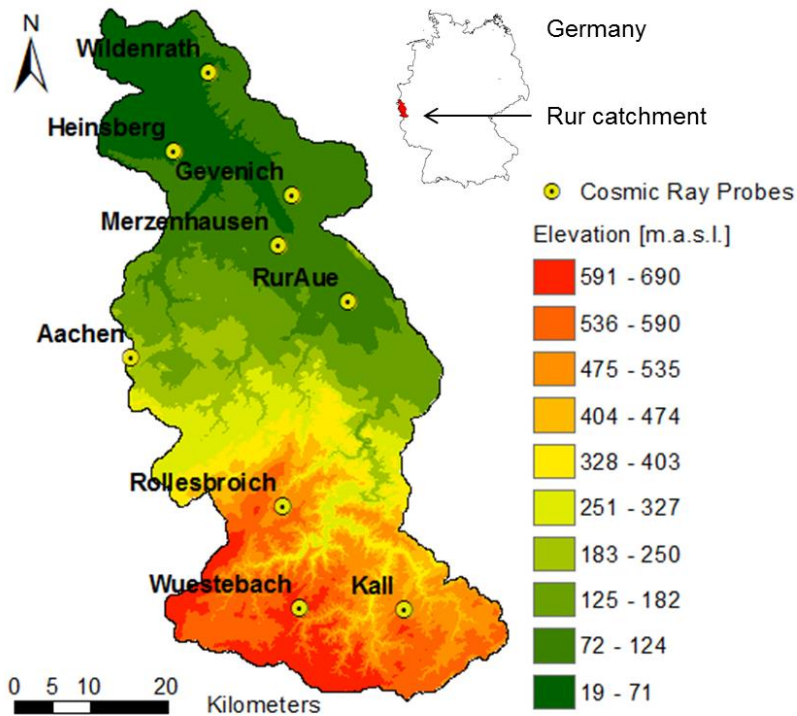
- Seneviratne, S. I., Corti, T., Davin, E. L., Hirschi, M., Jaeger, E. B., Lehner, I., Orlowsky, B., and Teuling, A. J.: Investigating soil moisture–climate interactions in a changing climate: A review, *Earth-Science Reviews*, 99, 125-161, <http://dx.doi.org/10.1016/j.earscirev.2010.02.004>, <http://dx.doi.org/10.1016/j.earscirev.2010.02.004>, 2010.
- 5 | ~~Sheffield, J., and Wood, E. F.: Global trends and variability in soil moisture and drought characteristics, 1950–2000, from observation driven Simulations of the terrestrial hydrologic cycle, *J Climate*, 21, 432–458, 10.1175/2007JCLI1822.1, 2008.~~
- Shi, Y. N., Davis, K. J., Zhang, F. Q., Duffy, C. J., and Yu, X.: Parameter estimation of a physically based land surface hydrologic model using the ensemble Kalman filter : A synthetic experiment, *Water Resour Res*, 50, 706-724, 10.1002/2013wr014070, 2014.
- 10 | Shi, Y. N., Davis, K. J., Zhang, F. Q., Duffy, C. J., and Yu, X.: Parameter estimation of a physically-based land surface hydrologic model using an ensemble Kalman filter: A multivariate real-data experiment, *Adv Water Resour*, 83, 421-427, 10.1016/j.advwatres.2015.06.009, 2015.
- Shrestha, P., Sulis, M., Masbou, M., Kollet, S., and Simmer, C.: A Scale-Consistent Terrestrial Systems Modeling Platform Based on COSMO, CLM, and ParFlow, *Mon Weather Rev*, 142, 3466-3483, 10.1175/Mwr-D-14-00029.1, 2014.
- 15 | Shuttleworth, J., Rosolem, R., Zreda, M., and Franz, T.: The COSmic-ray Soil Moisture Interaction Code (COSMIC) for use in data assimilation, *Hydrol Earth Syst Sc*, 17, 3205-3217, DOI 10.5194/hess-17-3205-2013, 2013.
- Simmer, C., Thiele-Eich, I., Masbou, M., Amelung, W., Bogen, H., Crewell, S., Diekkruger, B., Ewert, F., Franssen, H. J. H., Huisman, J. A., Kemna, A., Klitzsch, N., Kollet, S., Langensiepen, M., Lohnert, U., Rahman, A. S. M. M., Rascher, U., Schneider, K., Schween, J., Shao, Y. P., Shrestha, P., Stiebler, M., Sulis, M., Vanderborcht, J., Vereecken, H., van der Kruk, J., Waldhoff, G., and Zerenner, T.: MONITORING AND MODELING THE TERRESTRIAL SYSTEM FROM PORES TO
- 20 | CATCHMENTS The Transregional Collaborative Research Center on Patterns in the Soil-Vegetation-Atmosphere System, *B Am Meteorol Soc*, 96, 1765-1787, 10.1175/Bams-D-13-00134.1, 2015.
- Song, X. H., Shi, L. S., Ye, M., Yang, J. Z., and Navon, I. M.: Numerical Comparison of Iterative Ensemble Kalman Filters for Unsaturated Flow Inverse Modeling, *Vadose Zone J*, 13, 10.2136/vzj2013.05.0083, 2014.
- 25 | Sun, Y., Hou, Z., Huang, M., Tian, F., and Leung, L. R.: Inverse modeling of hydrologic parameters using surface flux and runoff observations in the Community Land Model, *Hydrol Earth Syst Sc*, 17, 4995-5011, 10.5194/hess-17-4995-2013, 2013.
- Temimi, M., Lakhankar, T., Zhan, X. W., Cosh, M. H., Krakauer, N., Fares, A., Kelly, V., Khanbilvardi, R., and Kumassi, L.: Soil Moisture Retrieval Using Ground-Based L-Band Passive Microwave Observations in Northeastern USA, *Vadose Zone J*, 13, 10.2136/vzj2013.06.0101, 2014.
- 30 | Vereecken, H., Huisman, J. A., Bogen, H., Vanderborcht, J., Vrugt, J. A., and Hopmans, J. W.: On the value of soil moisture measurements in vadose zone hydrology: A review, *Water Resour Res*, 44, Artn W00d06  
Doi 10.1029/2008wr006829, 2008.
- Vereecken, H., Schnepf, A., Hopmans, J. W., Javaux, M., Or, D., Roose, D. O. T., Vanderborcht, J., Young, M. H., Amelung, W., Aitkenhead, M., Allison, S. D., Assouline, S., Baveye, P., Berli, M., Bruggemann, N., Finke, P., Flury, M., Gaiser, T., Govers, G., Ghezzehei, T., Hallett, P., Franssen, H. J. H., Heppell, J., Horn, R., Huisman, J. A., Jacques, D.,
- 35 | Jonard, F., Kollet, S., Lafolie, F., Lamorski, K., Leitner, D., McBratney, A., Minasny, B., Montzka, C., Nowak, W., Pachepsky, Y., Padian, J., Romano, N., Roth, K., Rothfuss, Y., Rowe, E. C., Schwen, A., Simunek, J., Tiktak, A., Van Dam, J., van der Zee, S. E. A. T. M., Vogel, H. J., Vrugt, J. A., Wohling, T., and Young, I. M.: Modeling Soil Processes: Review, Key Challenges, and New Perspectives, *Vadose Zone J*, 15, 10.2136/vzj2015.09.0131, 2016.
- Villareyes, C. A. R., Baroni, G., and Oswald, S. E.: Inverse modelling of cosmic-ray soil moisture for field-scale soil hydraulic parameters, *Eur J Soil Sci*, 65, 876-886, 10.1111/ejss.12162, 2014.
- 40 | Vrugt, J. A., Diks, C. G. H., Gupta, H. V., Bouten, W., and Verstraten, J. M.: Improved treatment of uncertainty in hydrologic modeling: Combining the strengths of global optimization and data assimilation, *Water Resour Res*, 41, Artn W01017  
10.1029/2004wr003059, 2005.
- 45 | Waldhoff, G.: Enhanced land use classification of 2009 for the Rur catchment, in, TR32DB, 2012.
- Whan, K., Zscheischler, J., Orth, R., Shongwe, M., Rahimi, M., Asare, E. O., and Seneviratne, S. I.: Impact of soil moisture on extreme maximum temperatures in Europe, *Weather and Climate Extremes*, 9, 57-67, <http://dx.doi.org/10.1016/j.wace.2015.05.001>, <http://dx.doi.org/10.1016/j.wace.2015.05.001>, 2015.
- 50 | Wu, C. C., and Margulis, S. A.: Feasibility of real-time soil state and flux characterization for wastewater reuse using an embedded sensor network data assimilation approach, *J Hydrol*, 399, 313-325, 10.1016/j.jhydrol.2011.01.011, 2011.
- Wu, C. C., and Margulis, S. A.: Real-Time Soil Moisture and Salinity Profile Estimation Using Assimilation of Embedded Sensor Datastreams, *Vadose Zone J*, 12, 10.2136/vzj2011.0176, 2013.

- Zacharias, S., Bogen, H., Samaniego, L., Mauder, M., Fuss, R., Putz, T., Frenzel, M., Schwank, M., Baessler, C., Butterbach-Bahl, K., Bens, O., Borg, E., Brauer, A., Dietrich, P., Hajnsek, I., Helle, G., Kiese, R., Kunstmann, H., Klotz, S., Munch, J. C., Papen, H., Priesack, E., Schmid, H. P., Steinbrecher, R., Rosenbaum, U., Teutsch, G., and Vereecken, H.: A Network of Terrestrial Environmental Observatories in Germany, *Vadose Zone J*, 10, 955-973, Doi 10.2136/Vzj2010.0139, 2011.
- 5 Zreda, M., Desilets, D., Ferre, T. P. A., and Scott, R. L.: Measuring soil moisture content non-invasively at intermediate spatial scale using cosmic-ray neutrons, *Geophys Res Lett*, 35, 10.1029/2008GL035655, 2008.
- Zreda, M., Shuttleworth, W. J., Zeng, X., Zweck, C., Desilets, D., Franz, T., and Rosolem, R.: COSMOS: the COsmic-ray Soil Moisture Observing System (vol 16, pg 4079, 2012), *Hydrol Earth Syst Sc*, 17, 1065-1066, DOI 10.5194/hess-17-1065-2013, 2012.
- 10

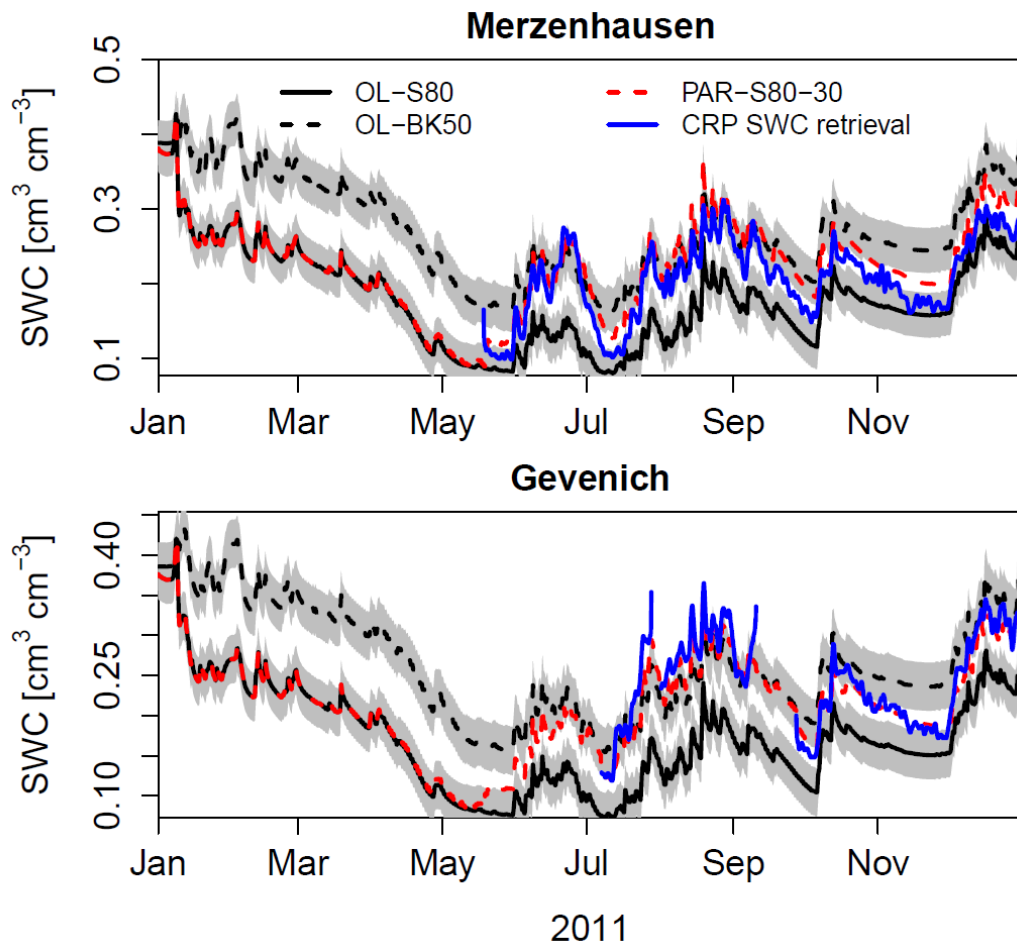
Figures

Formatted: Heading 1

Formatted: Font: Not Bold



5 | Fig. 1. Map of the Rur catchment and locations of the nine cosmic-ray probes-neutron sensors. The hilly South of the catchment is prone to more rainfall, lower average temperatures and less potential evapotranspiration than the North of the catchment.



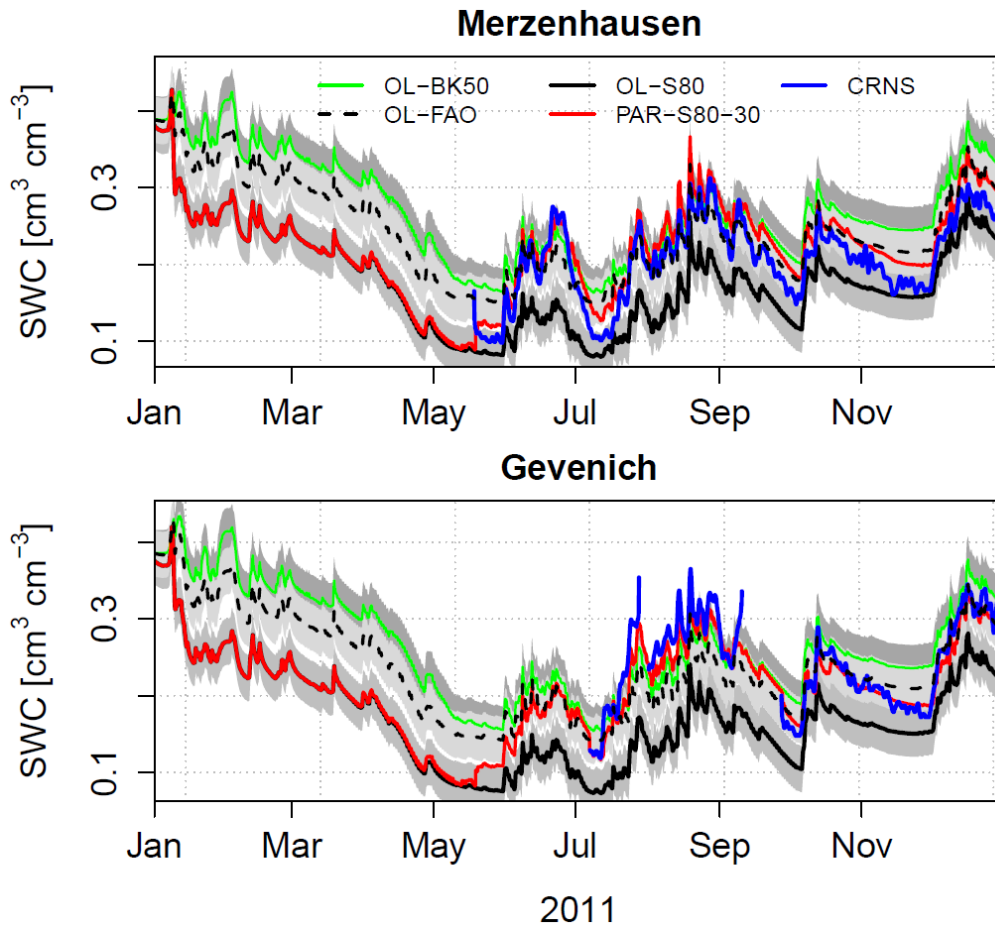
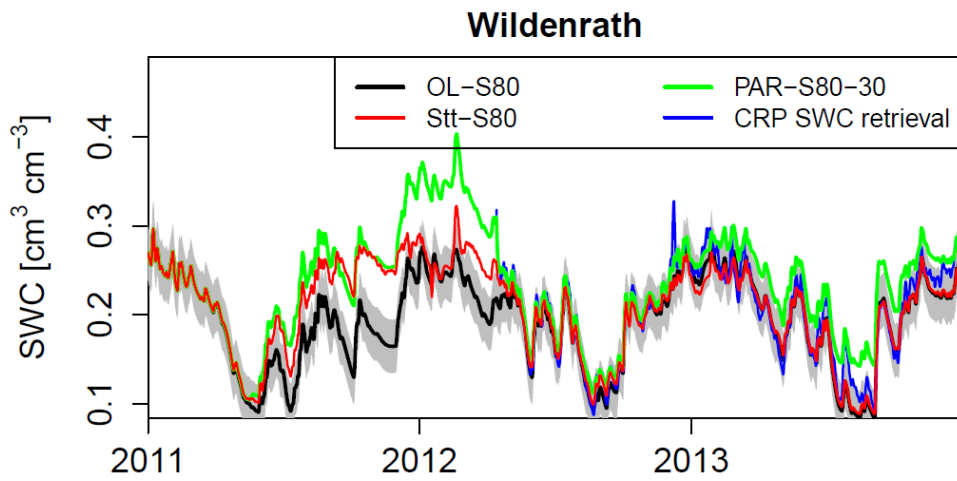
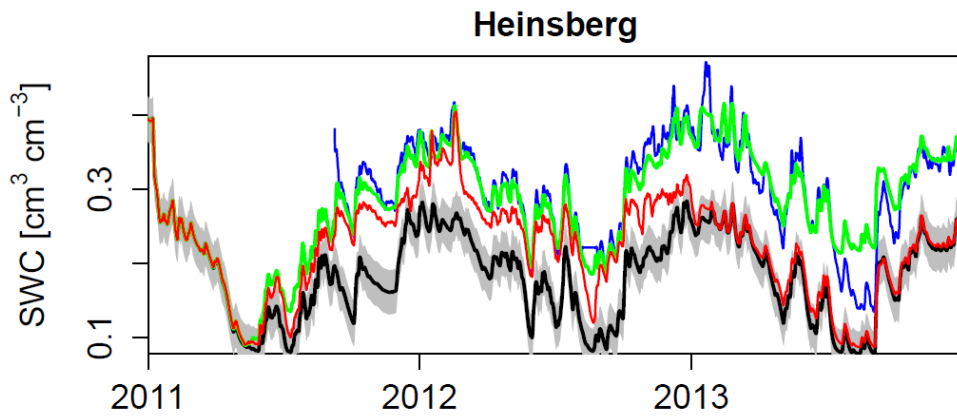


Fig. 2. Temporal evolution of simulated soil water content (SWC) retrievals, calculated with open loop (OL-\*) simulations and data assimilation including parameter updating (PAR-S80-30), together with the CRP-soil-water-content:CRNS SWC retrieval-(SWC) during the first year of simulation at the sites Merzenhausen and Gevenich. Simulated SWC was vertically weighted using the COSMIC operator to obtain the appropriate SWC corresponding to the CRP:CRNS SWC retrieval.



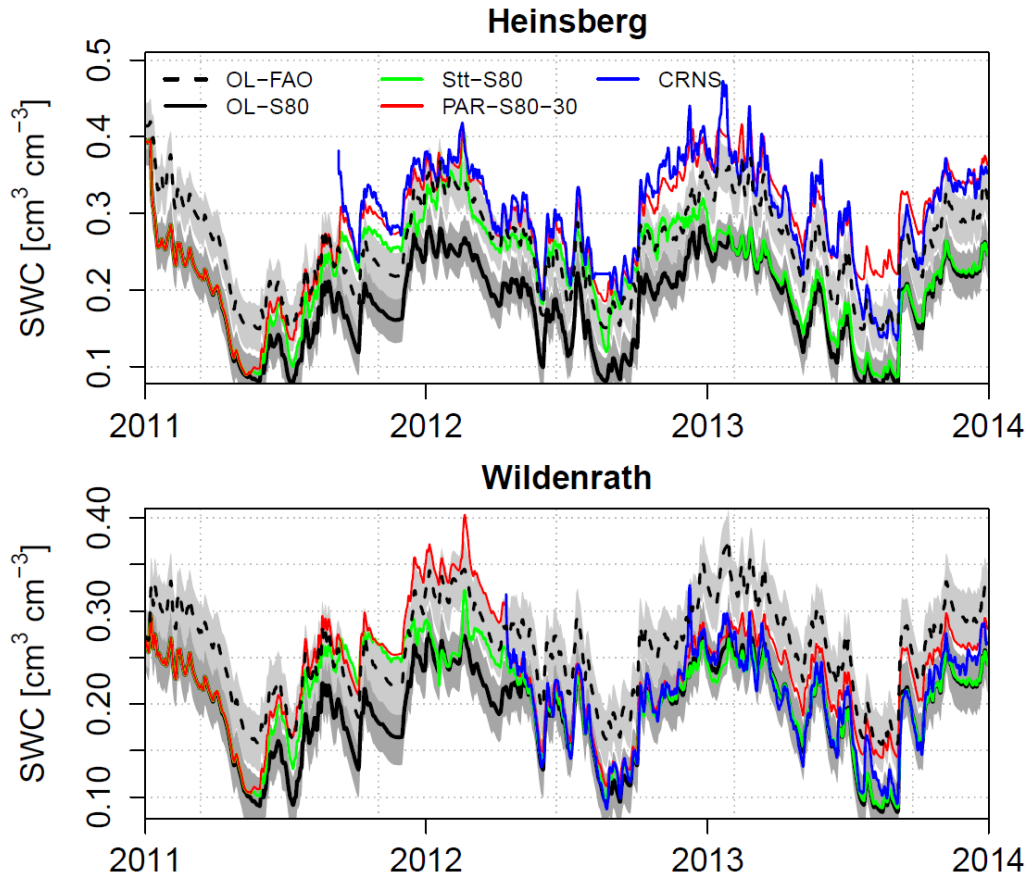


Fig. 3. Temporal evolution of simulated soil water content (SWC) retrievals, calculated with open loop (OL-S80,\*), data assimilation with state update only (Stt-BK50S80), and data assimilation including parameter updating (PAR-S80-30), together with the CRP-soil water content (SWC)CRNS SWC

5 retrieval at the sites Heinsberg and Wildenrath for the data assimilation period 2011 and 2012, and the evaluation period 2013. Simulated SWC was vertically weighted to obtain the appropriate SWC corresponding to the CRPCRNS SWC retrieval.

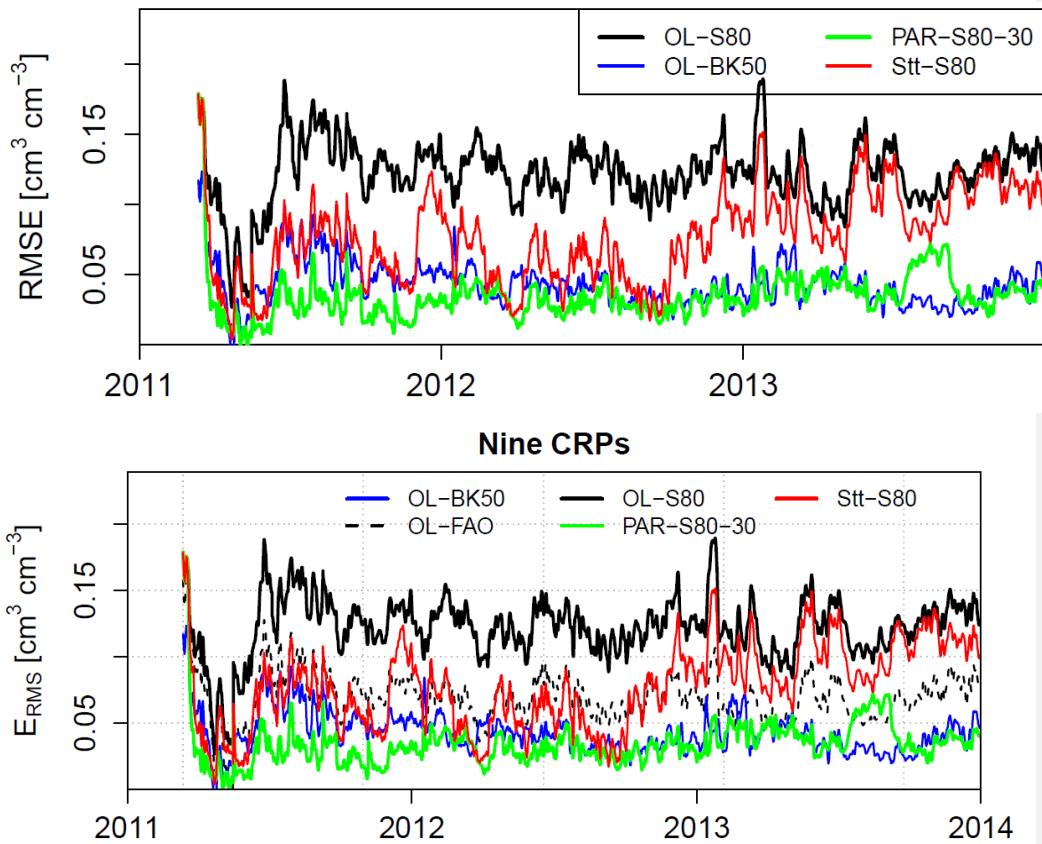
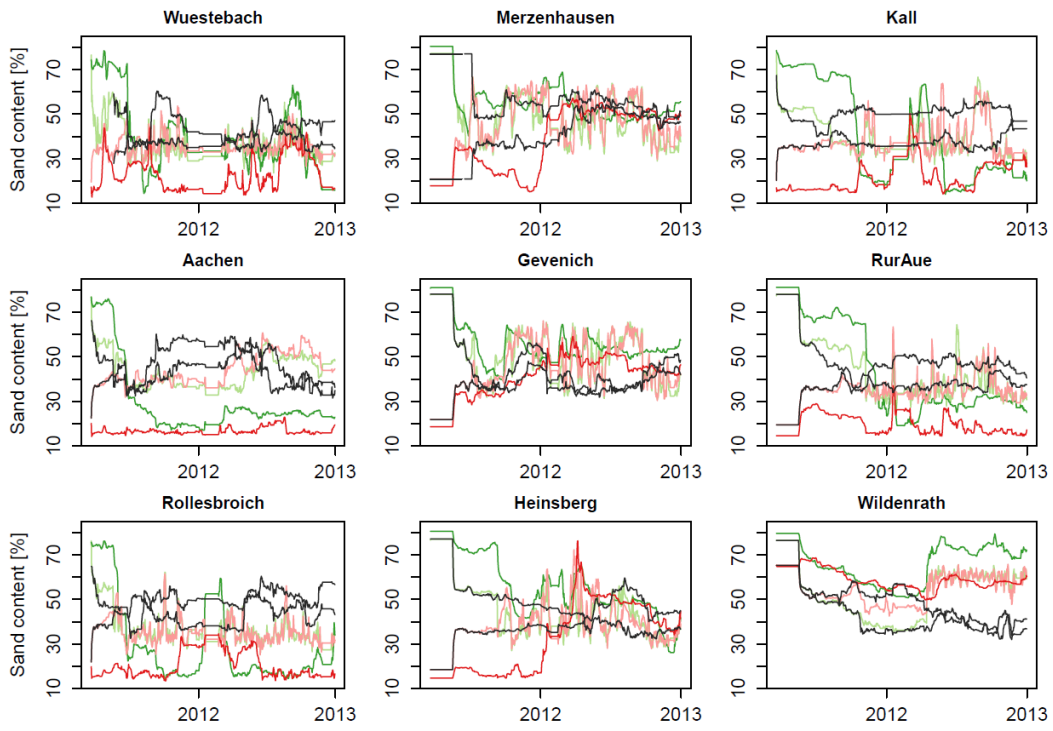


Fig. 4. Temporal evolution of root mean square error ( $E_{\text{RMS}}$ ) for hourly SWC retrievals.  $E_{\text{RMS}}$  is calculated hourly for all nine CRP's-CRNS for open loop (OL-\*) runs for soil maps S80, BK50 and BK50FAO, joint state-parameter updates (PAR-S80-30) and state updates only (Stt-S80) during the assimilation period with joint state-parameter updates (2011 and 2012) and verification period (2013).



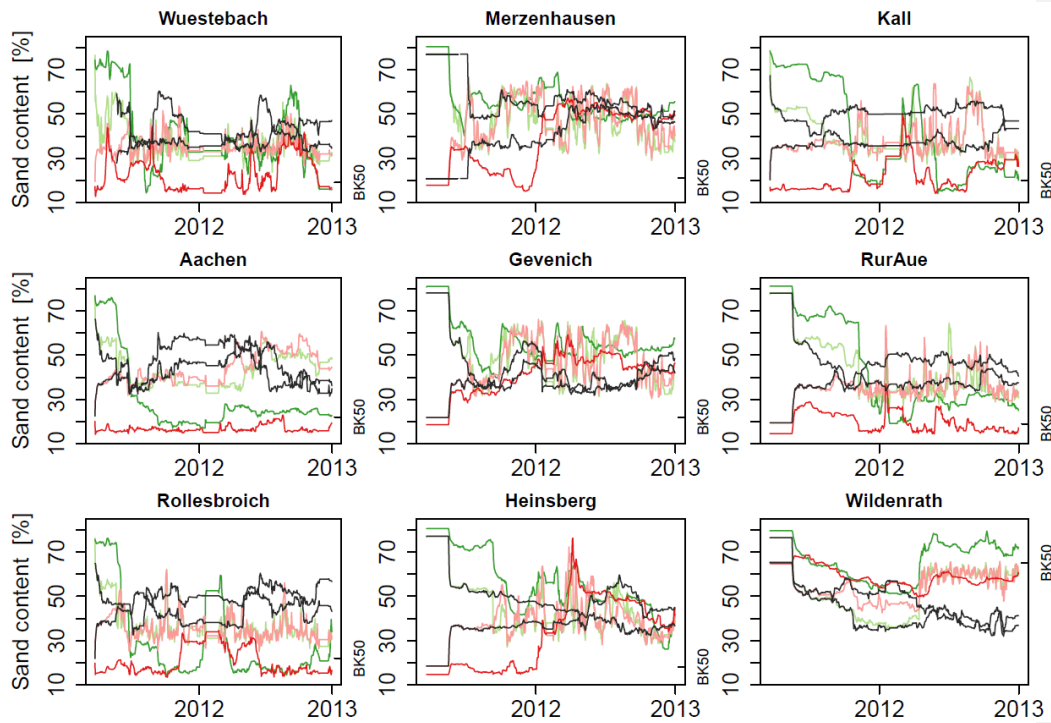
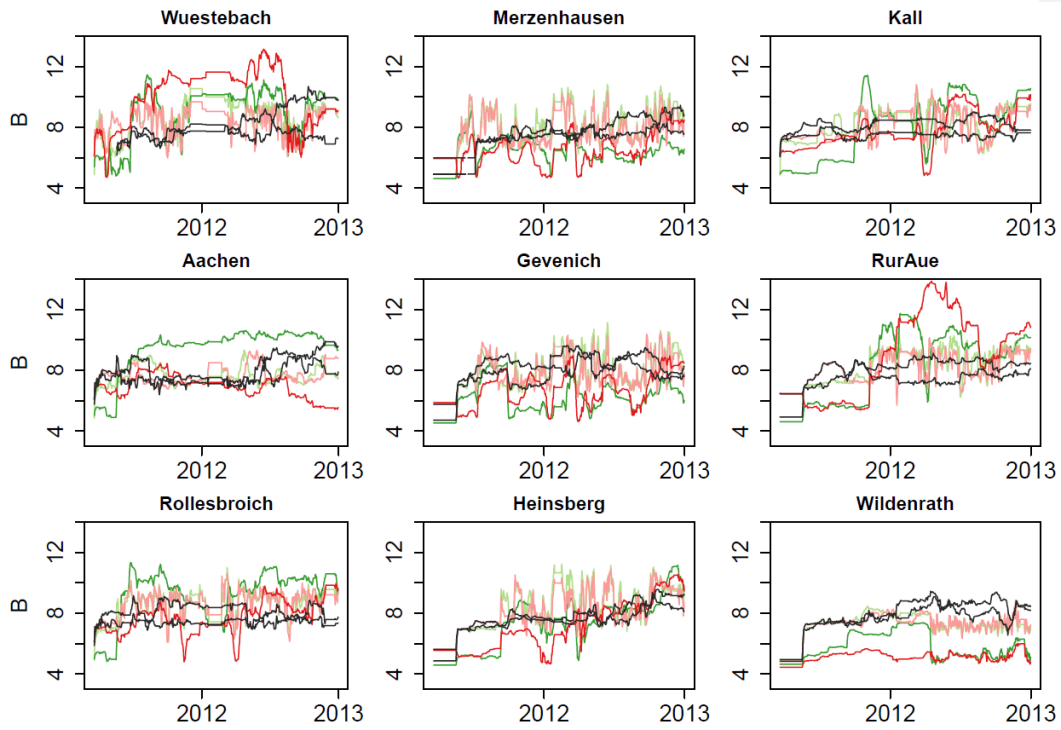


Fig. 5. Temporal evolutionAt nine sites, estimates of the percentage sand content are shown for simulations with parameter update: PAR-S80-30 (green), PAR-S80-10 (light green), PAR-BK50-30 (red), PAR-BK50-10 (light red), ~~jkjk8-S80-30\*~~ (black) and ~~jkjk8-BK50-30\*~~ (black). The value of the  
 5 BK50 soil map is marked at the second y-axis.



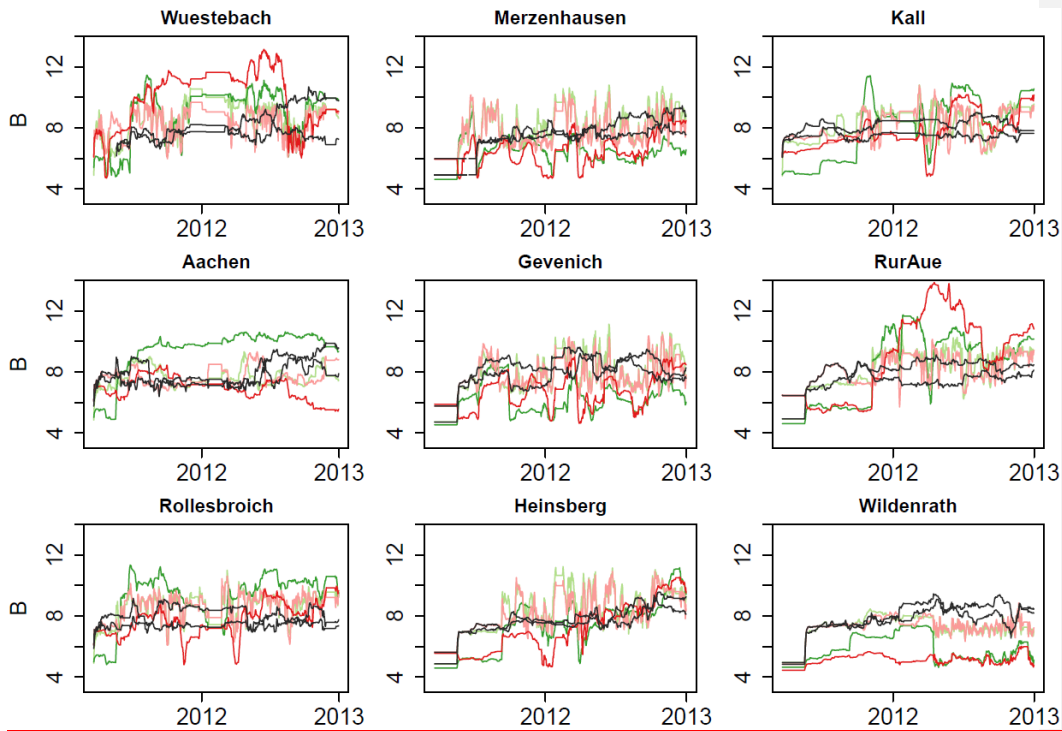
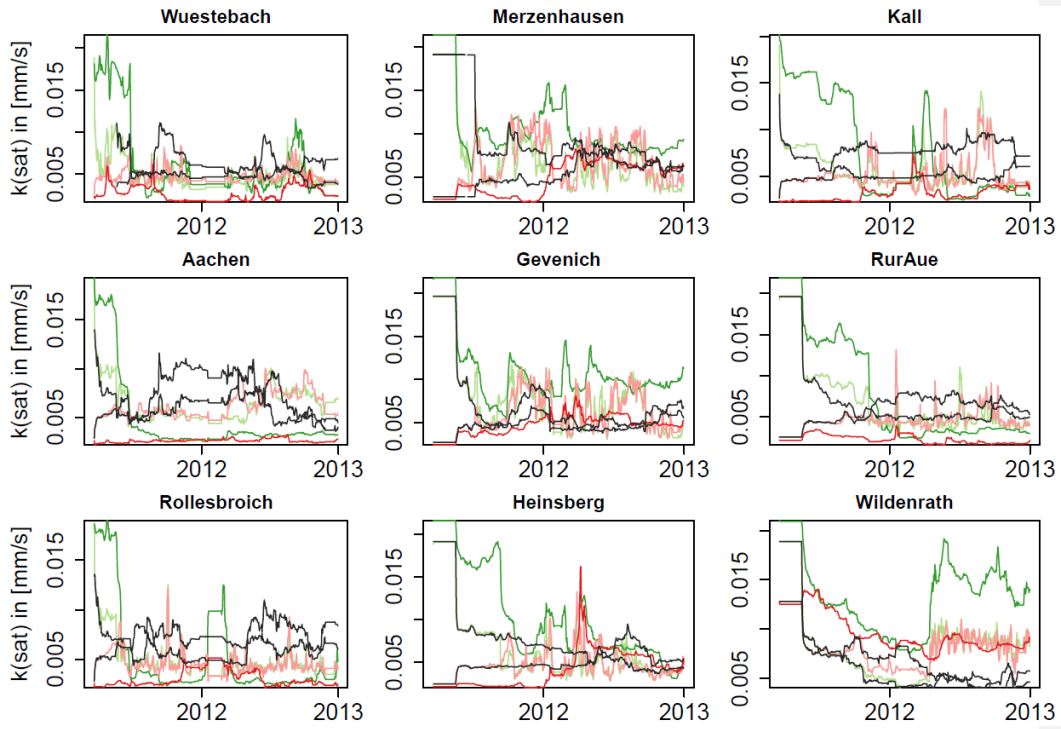


Fig. 6. Temporal evolution At nine sites, estimates of the B parameter (top 15cm) are shown for simulations with parameter update: PAR-S80-30 (green), PAR-S80-10 (light green), PAR-BK50-30 (red), PAR-BK50-10 (light red),  $\mu_{jk}k8-S80-30^{*-*}$  (black) and  $\mu_{jk}k8-BK50-30^{*-*}$  (black).



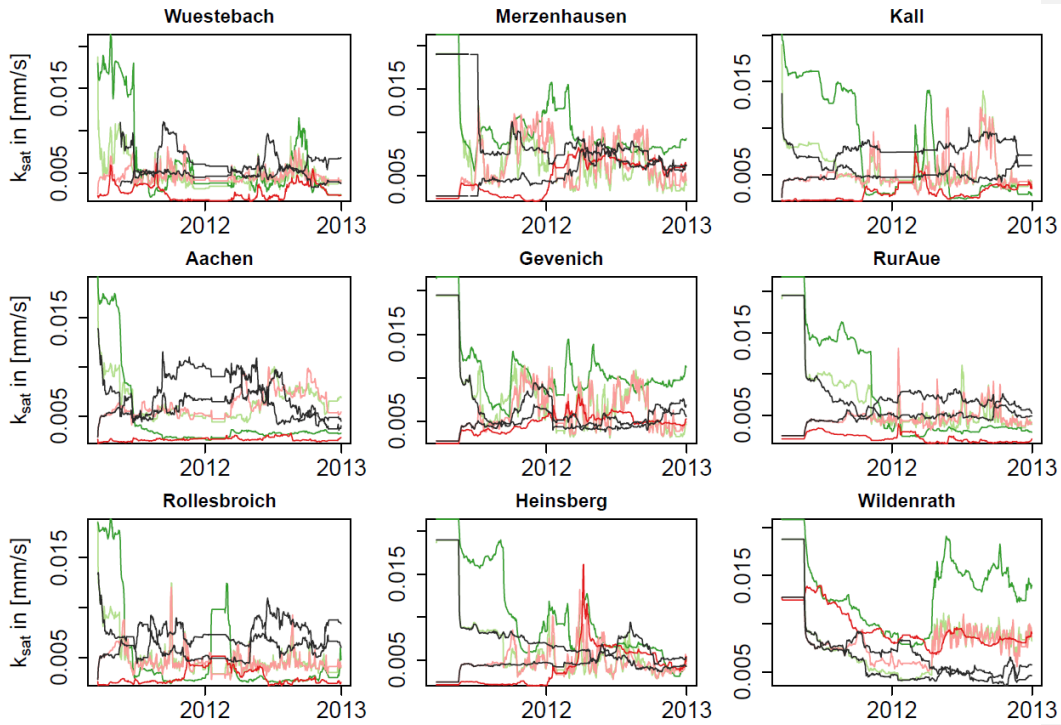
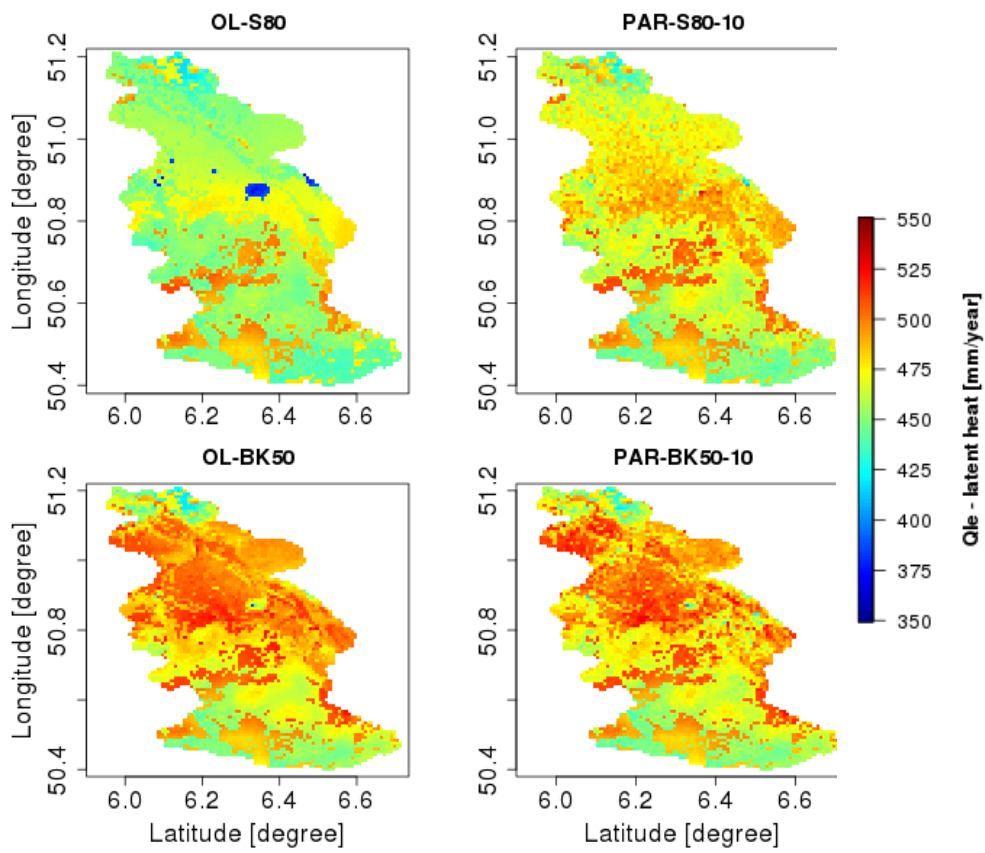


Fig. 7. Temporal evolutionAt nine sites, estimates of saturated hydraulic conductivity (top 15cm) are shown for simulations with parameter update: PAR-S80-30 (green), PAR-S80-10 (light green), PAR-BK50-30 (red), PAR-BK50-10 (light red), ~~j\_k8-S80-30\*~~ (black) and ~~j\_k8-BK50-30\*~~ (black).



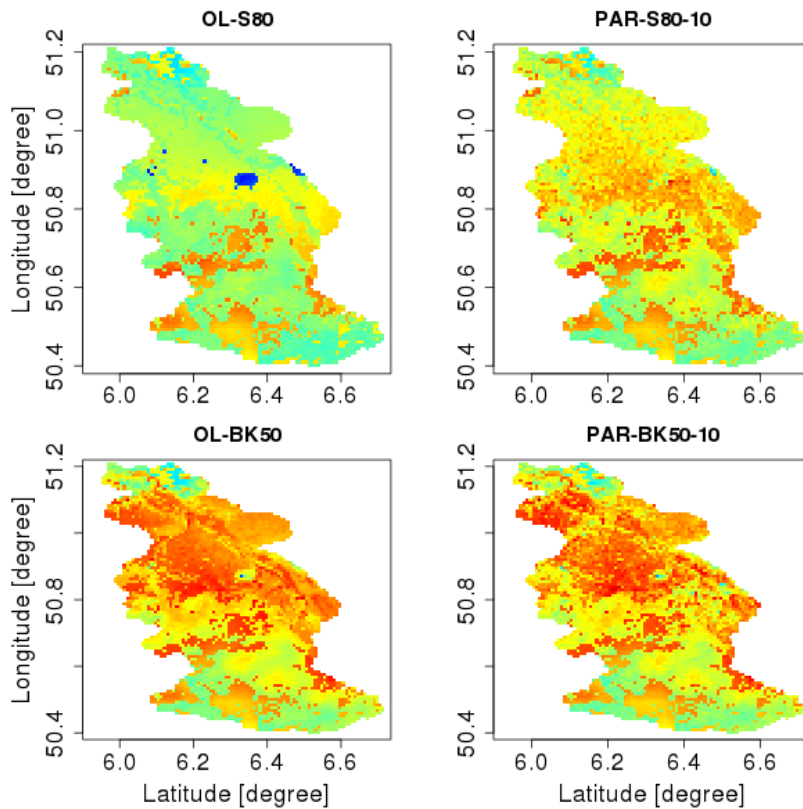


Fig. 8. Annual evapotranspiration (ET) is shown in the year 2013 (evaluation period ~~(year 2013)~~ for simulations OL-S80, OL-BK50, ~~, no assimilation~~). This figure demonstrates the impact of parameter updates (PAR-S80-10 and PAR-BK50-10) in comparison to open loop (OL-S80) and reference soil map (OL-BK50). ET changes in the North but not as much in the South.

## Tables

Table 1: Site information on elevation (m.a.s.l.), average annual precipitation (mm/year), CLM plant functional type, [\(Bonan et al., 2002\)](#), sand content (%), clay content (%), and the date of the first SWC retrieval assimilated.

Name	m.a.s.l.	Precip.	Plant functional type	Sand	Clay	Date of first assimilation
Aachen	232	952	Crops	22	23	13.01.2012
Gevenich	108	884	Crops	22	20	07.07.2011
Heinsberg	57	814	Crops	18	19	09.09.2011
Kall	504	935	C3 <del>non-arctic</del> -grass	20	22	15.09.2011
Merzenhausen	94	825	Crops	21	22	19.05.2011
Rollsbroich	515	1307	C3 <del>non-arctic</del> -grass	22	23	19.05.2011
RurAue	102	743	C3 <del>non-arctic</del> -grass	19	26	08.11.2011
Wildenrath	76	856	Broadleaf deciduous temperate tree	65	12	07.05.2012
Wuestebach	605	1401	Needleleaf evergreen temperate tree	19	23	20.03.2011

5



5

Table 3--: Root mean square error ( $E_{RMS}$  in  $cm^3/cm^3$ ) and mean absolute bias ( $cm^3/cm^3$ ) for open loop simulations (OL-\*), data assimilation with state updates (Stt-\*) and joint state-parameter updates (PAR-\*) for the assimilation period (2011 and 2012) and the evaluation period (2013). Error and bias was averaged over all sites with observations. Site specific errors and biases are provided in the Annex 1 to 4.

<u>Soil map</u>	<u>Simulation</u>	<u>Site average</u>			
		<u>Data assimilation 2011 &amp; 2012</u>		<u>Evaluation period 2013</u>	
		<u><math>E_{RMS}</math></u>	<u>Absolute bias</u>	<u><math>E_{RMS}</math></u>	<u>Absolute bias</u>
<u>BK50</u>	<u>OL-BK50</u>	<u>0.04</u>	<u>0.02</u>	<u>0.04</u>	<u>0.02</u>
	<b><u>Stt-BK50</u></b>	<b><u>0.03</u></b>	<b><u>0.01</u></b>	<b><u>0.04</u></b>	<b><u>0.01</u></b>
	<u>PAR-BK50-10</u>	<u>0.03</u>	<u>0.01</u>	<u>0.05</u>	<u>0.03</u>
	<u>PAR-BK50-30</u>	<u>0.03</u>	<u>0.01</u>	<u>0.05</u>	<u>0.03</u>
<u>FAO</u>	<u>OL-FAO</u>	<u>0.07</u>	<u>0.06</u>	<u>0.07</u>	<u>0.06</u>
	<b><u>PAR-FAO-30</u></b>	<b><u>0.03</u></b>	<b><u>0.02</u></b>	<b><u>0.05</u></b>	<b><u>0.03</u></b>
<u>Biased (S80)</u>	<u>OL-S80</u>	<u>0.12</u>	<u>0.11</u>	<u>0.12</u>	<u>0.11</u>
	<u>Stt-S80</u>	<u>0.06</u>	<u>0.05</u>	<u>0.10</u>	<u>0.09</u>
	<b><u>PAR-S80-10</u></b>	<b><u>0.03</u></b>	<b><u>0.01</u></b>	<b><u>0.05</u></b>	<b><u>0.03</u></b>
	<b><u>PAR-S80-30</u></b>	<b><u>0.03</u></b>	<b><u>0.02</u></b>	<b><u>0.04</u></b>	<b><u>0.02</u></b>

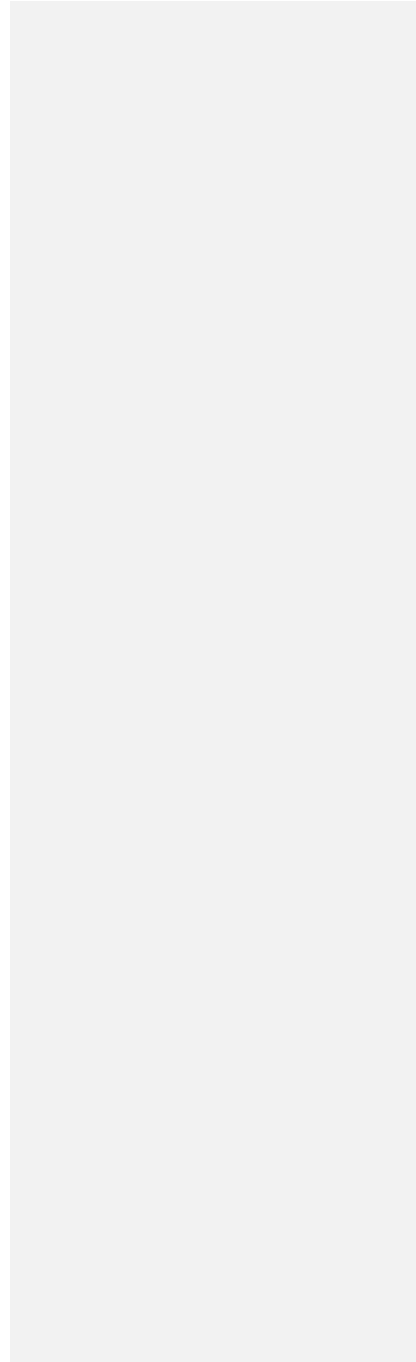
5

Table 4: Root mean square error ( $E_{RMS}$  in  $cm^3/cm^3$ ) and mean absolute bias ( $cm^3/cm^3$ ) for open loop (OL-\*), jackknife simulations with eight CRNS (simulations jk8-S80-1 to 9 were averaged) and with four CRNS (simulations jk4-S80-A to C). Results were averaged over the omitted sites only. Data at omitted sites was not assimilated while at the other sites data was assimilated. At sites where data was assimilated  $E_{RMS}$  and bias was equal to the values found in simulation PAR-S80-30. Site specific errors and biases are provided in the Annex 1 to 4.

<u>Soil map</u>	<u>Simulation</u>	<u>Site average</u>			
		<u>Data assimilation</u>		<u>Evaluation period</u>	
		<u>2011 &amp; 2012</u>		<u>2013</u>	
		<u><math>E_{RMS}</math></u>	<u>Absolute bias</u>	<u><math>E_{RMS}</math></u>	<u>Absolute bias</u>
<u>BK50</u>	<b><u>OL-BK50</u></b>	<b><u>0.04</u></b>	<b><u>0.02</u></b>	<b><u>0.04</u></b>	<b><u>0.02</u></b>
-	<u>jk8-BK50-1 to 9</u>	<u>0.06</u>	<u>0.04</u>	<u>0.05</u>	<u>0.04</u>
<u>Biased (S80)</u>	<u>OL-S80</u>	<u>0.12</u>	<u>0.11</u>	<u>0.12</u>	<u>0.11</u>
-	<b><u>jk8-S80-1 to 9</u></b>	<b><u>0.06</u></b>	<b><u>0.05</u></b>	<b><u>0.06</u></b>	<b><u>0.04</u></b>
-	<u>jk4-S80-A</u>	<u>0.08</u>	<u>0.06</u>	<u>0.06</u>	<u>0.04</u>
-	<u>jk4-S80-B</u>	<u>0.06</u>	<u>0.05</u>	<u>0.06</u>	<u>0.05</u>
-	<u>jk4-S80-C</u>	<u>0.07</u>	<u>0.05</u>	<u>0.07</u>	<u>0.06</u>



|



Table

Annex 4:  $E_{RMS}$  ( $cm^3/cm^3$ ) at CRPCRNS-sites for open loop, data assimilation and jackknife simulations on the basis of a comparison with CRPCRNS SWC retrievals during for the verification period (2013). For each jackknife simulation experiments (21 in total) only one  $E_{RMS}$  the error of the omitted sites is reported. The  $E_{RMS}$  of the location that is meant for evaluation best cases are marked bold.

Soil map	Year 2013	Rollebroich	Merzenhausen	Gevenich	Heinsberg	Kall	RurAue	Wuestebach	Aachen	Wildenrath	Average $E_{RMS}$
BK50	OL-BK50	<b>0.04404</b>	<b>0.06507</b>	<b>0.03604</b>	<b>0.02703</b>	<b>0.04805</b>	<b>0.03804</b>	<b>0.04805</b>	<b>0.04204</b>	<b>0.01702</b>	<b>0.04404</b>
-	Stt-BK50	<b>0.04104</b>	<b>0.05405</b>	<b>0.03403</b>	<b>0.02703</b>	<b>0.04905</b>	<b>0.03804</b>	<b>0.04805</b>	<b>0.04104</b>	<b>0.01802</b>	<b>0.039</b>
-	PAR-BK50-10	<b>0.06807</b>	<b>0.06206</b>	<b>0.03604</b>	<b>0.03804</b>	<b>0.05606</b>	<b>0.05606</b>	<b>0.04304</b>	<b>0.05806</b>	<b>0.01702</b>	<b>0.048</b>
-	PAR-BK50-30	<b>0.05205</b>	<b>0.06106</b>	<b>0.03504</b>	<b>0.03303</b>	<b>0.06807</b>	<b>0.04805</b>	<b>0.04304</b>	<b>0.04805</b>	<b>0.03504</b>	<b>0.047</b>
-	jk8-BK50*-1 to 9	<b>0.03604</b>	<b>0.04705</b>	<b>0.02804</b>	<b>0.02503</b>	<b>0.04205</b>	<b>0.03104</b>	<b>0.04005</b>	<b>0.05406</b>	<b>0.10611</b>	<b>0.04505</b>
FAO	OL-FAO	<b>0.08</b>	<b>0.04</b>	<b>0.04</b>	<b>0.05</b>	<b>0.09</b>	<b>0.09</b>	<b>0.07</b>	<b>0.09</b>	<b>0.07</b>	<b>0.068</b>
-	PAR-FAO-30	<b>0.06</b>	<b>0.06</b>	<b>0.04</b>	<b>0.04</b>	<b>0.06</b>	<b>0.03</b>	<b>0.05</b>	<b>0.07</b>	<b>0.04</b>	<b>0.049</b>
Biased (S80)	OL-S80	<b>0.15716</b>	<b>0.06206</b>	<b>0.10611</b>	<b>0.11512</b>	<b>0.16016</b>	<b>0.15415</b>	<b>0.09910</b>	<b>0.16717</b>	<b>0.01902</b>	<b>0.115</b>
-	Stt-S80	<b>0.10010</b>	<b>0.06306</b>	<b>0.10711</b>	<b>0.10611</b>	<b>0.09910</b>	<b>0.14615</b>	<b>0.09710</b>	<b>0.15816</b>	<b>0.02002</b>	<b>0.100</b>
-	PAR-S80-10	<b>0.06006</b>	<b>0.03904</b>	<b>0.04304</b>	<b>0.04004</b>	<b>0.06406</b>	<b>0.04304</b>	<b>0.05205</b>	<b>0.06006</b>	<b>0.01902</b>	<b>0.047</b>
-	PAR-S80-30	<b>0.04905</b>	<b>0.05906</b>	<b>0.03704</b>	<b>0.03604</b>	<b>0.05305</b>	<b>0.03203</b>	<b>0.04605</b>	<b>0.04705</b>	<b>0.03504</b>	<b>0.044</b>
-	jk8-S80*-1 to 9	<b>0.07908</b>	<b>0.04605</b>	<b>0.04204</b>	<b>0.03604</b>	<b>0.059</b>	<b>0.03804</b>	<b>0.06306</b>	<b>0.04404</b>	<b>0.10511</b>	<b>0.057</b>
-	jk4-S80-A	<b>0.05</b>	<b>0.03</b>	<b>0.05</b>	<b>0.04</b>	<b>-</b>	<b>0.16</b>	<b>-</b>	<b>-</b>	<b>-</b>	<b>0.065</b>
-	jk4-S80-B	<b>0.05</b>	<b>0.07</b>	<b>-</b>	<b>0.04</b>	<b>0.07</b>	<b>0.07</b>	<b>-</b>	<b>-</b>	<b>-</b>	<b>0.061</b>
-	jk4-S80-C	<b>-</b>	<b>0.05</b>	<b>0.04</b>	<b>-</b>	<b>0.07</b>	<b>-</b>	<b>-</b>	<b>0.06</b>	<b>0.13</b>	<b>0.069</b>

5

Table



<u>jk4-S80-A</u>	<u>-0.05</u>	<u>-0.02</u>	<u>-0.03</u>	<u>-0.06</u>	=	<u>-0.16</u>	=
<u>jk4-S80-B</u>	<u>-0.07</u>	<u>0.02</u>	=	<u>-0.04</u>	<u>-0.05</u>	<u>-0.07</u>	=
<u>jk4-S80-C</u>	<u>-0.07</u>	<u>0.03</u>	<u>0.04</u>	<u>0.02</u>	<u>0.02</u>	<u>0.04</u>	<u>-0.02</u>

**Deleted Cells**

**Formatted:** Font: 10 pt, Font color: Auto

**Inserted Cells**

**Formatted:** English (U.S.)

**Formatted:** Left, Line spacing: single

**Formatted:** English (U.S.)

Annex 4: Bias (cm<sup>3</sup>/cm<sup>3</sup>) at CRNS-sites for open loop, data assimilation and jackknife simulations compared to CRNS SWC retrievals for the data assimilation period (2011 and 2012). For jackknife experiments (21 in total) only the bias of the omitted sites is reported. The best cases are marked bold.

<u>- Soil map</u>	<u>2013</u>	<u>Rollebroich</u>	<u>Merzenhausen</u>	<u>Geve-nich</u>	<u>Heins-berg</u>	<u>Kall</u>	<u>RurAue</u>	<u>Wueste-bach</u>	<u>Aachen</u>	<u>Wilden-rath</u>	<u>Mean absolute bias</u>
<u>BK50</u>	<u>OL-BK50</u>	<u>-0.03</u>	<u>0.06</u>	<u>0.01</u>	<u>0.00</u>	<u>-0.02</u>	<u>0.00</u>	<u>-0.02</u>	<u>0.01</u>	<u>0.00</u>	<u><b>0.02</b></u>
-	<u>Stt-BK50</u>	<u>-0.01</u>	<u>0.04</u>	<u>0.00</u>	<u>0.00</u>	<u>-0.01</u>	<u>-0.01</u>	<u>-0.02</u>	<u>0.00</u>	<u>-0.01</u>	<u><b>0.01</b></u>
-	<u>PAR-BK50-10</u>	<u>0.06</u>	<u>0.05</u>	<u>0.01</u>	<u>0.02</u>	<u>0.04</u>	<u>0.04</u>	<u>0.02</u>	<u>-0.04</u>	<u>0.00</u>	<u>0.03</u>
-	<u>PAR-BK50-30</u>	<u>0.03</u>	<u>0.05</u>	<u>0.00</u>	<u>0.02</u>	<u>0.04</u>	<u>0.03</u>	<u>-0.01</u>	<u>-0.03</u>	<u>0.03</u>	<u>0.03</u>
-	<u>jk8-BK50-1 to 9</u>	<u>-0.02</u>	<u>0.04</u>	<u>0.01</u>	<u>-0.01</u>	<u>-0.03</u>	<u>-0.02</u>	<u>-0.04</u>	<u>-0.05</u>	<u>0.11</u>	<u>0.04</u>
<u>FAO</u>	<u>OL-FAO</u>	<u>-0.08</u>	<u>0.02</u>	<u>-0.02</u>	<u>-0.04</u>	<u>-0.08</u>	<u>-0.08</u>	<u>-0.05</u>	<u>-0.08</u>	<u>0.06</u>	<u>0.06</u>
-	<u>PAR-FAO-30</u>	<u>0.04</u>	<u>0.05</u>	<u>0.00</u>	<u>0.02</u>	<u>0.03</u>	<u>0.00</u>	<u>-0.02</u>	<u>-0.06</u>	<u>0.03</u>	<u><b>0.03</b></u>
<u>Biased (S80)</u>	<u>OL-S80</u>	<u>-0.15</u>	<u>-0.05</u>	<u>-0.10</u>	<u>-0.11</u>	<u>-0.16</u>	<u>-0.15</u>	<u>-0.09</u>	<u>-0.16</u>	<u>-0.01</u>	<u>0.11</u>
-	<u>Stt-S80</u>	<u>-0.09</u>	<u>-0.05</u>	<u>-0.10</u>	<u>-0.10</u>	<u>-0.08</u>	<u>-0.14</u>	<u>-0.09</u>	<u>-0.15</u>	<u>-0.01</u>	<u>0.09</u>
-	<u>PAR-S80-10</u>	<u>0.04</u>	<u>0.03</u>	<u>-0.03</u>	<u>0.03</u>	<u>0.05</u>	<u>0.03</u>	<u>0.03</u>	<u>-0.04</u>	<u>-0.01</u>	<u><b>0.03</b></u>
-	<u>PAR-S80-30</u>	<u>0.03</u>	<u>0.05</u>	<u>-0.01</u>	<u>0.02</u>	<u>0.03</u>	<u>0.01</u>	<u>-0.01</u>	<u>-0.03</u>	<u>0.03</u>	<u><b>0.02</b></u>
-	<u>jk8-S80-1 to 9</u>	<u>-0.07</u>	<u>0.03</u>	<u>0.02</u>	<u>0.02</u>	<u>-0.05</u>	<u>-0.02</u>	<u>-0.04</u>	<u>-0.03</u>	<u>0.10</u>	<u>0.04</u>
-	<u>jk4-S80-A</u>	<u>0.00</u>	<u>0.01</u>	<u>0.03</u>	<u>-0.03</u>	<u>=</u>	<u>-0.15</u>	<u>=</u>	<u>=</u>	<u>=</u>	<u>0.04</u>
-	<u>jk4-S80-B</u>	<u>-0.03</u>	<u>0.06</u>	<u>=</u>	<u>-0.03</u>	<u>-0.06</u>	<u>-0.06</u>	<u>=</u>	<u>=</u>	<u>=</u>	<u>0.05</u>
-	<u>jk4-S80-C</u>	<u>=</u>	<u>0.04</u>	<u>0.02</u>	<u>=</u>	<u>-0.05</u>	<u>=</u>	<u>=</u>	<u>-0.05</u>	<u>0.13</u>	<u>0.06</u>

5

Formatted: Justified, Space After: 0 pt



## Evaluating the value of a network of cosmic-ray probes for improving land surface modelling

Roland Baatz<sup>1,2</sup>, Harrie-Jan Hendricks Franssen<sup>1,2</sup>, Xujun Han<sup>1,2</sup>, Tim Hoar<sup>3</sup>, Heye R. Bogaen<sup>1</sup> and Harry Vereecken<sup>1,2</sup>

5 <sup>1</sup>Agrosphere (IBG-3), Forschungszentrum Jülich GmbH, 52425 Jülich, Germany.

<sup>2</sup>HPSC-TerrSys , 52425 Jülich, Germany.

<sup>3</sup>NCAR Data Assimilation Research Section, Boulder, CO, USA.

*Correspondence to:* Roland Baatz (r.baatz@fz-juelich.de)



**Abstract:** Land surface models can model matter and energy fluxes between the land surface and atmosphere, and provide a lower boundary condition to atmospheric circulation models. For these applications, accurate soil moisture quantification is highly desirable but not always possible given limited observations and limited subsurface data accuracy. Cosmic-ray probes (CRPs) offer an interesting alternative to indirectly measure soil moisture and provide an observation that can be assimilated into land surface models for improved soil moisture prediction. Synthetic studies have shown the potential to estimate subsurface parameters of land surface models with the assimilation of CRP observations. In this study, the potential of a network of CRPs for estimating subsurface parameters and improved soil moisture states is tested in a real-world case scenario using the local ensemble transform Kalman filter with the Community Land Model. The potential of the CRP network was tested by assimilating CRP-data for the years 2011 and 2012 (with or without soil hydraulic parameter estimation), followed by the verification year 2013. This was done using (i) the regional soil map as input information for the simulations, and (ii) an erroneous, biased soil map. For the regional soil map, soil moisture characterization was only improved in the assimilation period but not in the verification period. For the biased soil map, soil moisture characterization improved in both periods strongly from a bias of  $0.11 \text{ cm}^3/\text{cm}^3$  to  $0.03 \text{ cm}^3/\text{cm}^3$  (assimilation period) and from  $0.12 \text{ cm}^3/\text{cm}^3$  to  $0.05 \text{ cm}^3/\text{cm}^3$  (verification period) and the estimated soil hydraulic parameters were after assimilation closer to the ones of the regional soil map. Finally, the value of the CRP network was also evaluated with jackknifing data assimilation experiments. It was found that the CRP network is able to improve soil moisture estimates at locations between the assimilation sites from a  $E_{\text{RMS}}$  of  $0.12 \text{ cm}^3/\text{cm}^3$  to  $0.06 \text{ cm}^3/\text{cm}^3$  (verification period), but again only if the initial soil map was biased.

## 20 1 Introduction

Soil water content (SWC) is a key variable of land surface hydrology and has a strong control on the partitioning of net radiation between latent and sensible heat flux. Knowledge of SWC is relevant for the assessment of plant water stress and agricultural production, as well as runoff generation as a response to precipitation events (Vereecken et al., 2008; Robinson et al., 2008). In atmospheric circulation models, SWC is important as a lower boundary condition and is calculated as a state variable in land surface models. Coupling of atmospheric circulation models and land surface models allows quantifying the role of soil moisture on atmospheric processes such as soil moisture-precipitation feedbacks (Koster et al., 2004; Eltahir, 1998) and summer climate variability and drought (Oglesby and Erickson, 1989; Sheffield and Wood, 2008; Seneviratne et al., 2006; Bell et al., 2015). It is therefore important to improve the modelling and prediction of SWC, but this is hampered by model deficiencies and lack of high quality data (Vereecken et al., 2016). Soil moisture measured by ground-born remote sensing technologies provides information over large areas (e.g. Ajami et al., 2014). However, space-born remote sensing supplies only information on the upper few centimeters, and data are not reliable for areas with dense vegetation. Therefore, in this paper an alternative source for soil moisture information is explored. Cosmic-ray probes (CRPs) measure fast neutron intensity which allows estimating SWC at an intermediate scale (Zreda et al., 2008; Desilets et al., 2010; Cosh et al., 2016; Lv et al., 2014) which is closer to the desired application scale of land surface models (Ajami et al., 2014; Chen et al.,



7;Shrestha et al., 2014). **Fast neutrons originate from moderation of secondary cosmic particles from outer space by**  
**terrestrial atoms.** These particles are mainly fast neutrons, which are moderated most effectively by hydrogen **because of the**  
**similar atomic mass.** Therefore, the corresponding neutron intensity measured by CRPs strongly depends on the amount of  
hydrogen within the CRP footprint, allowing for a continuous non-invasive soil moisture estimate over an area of ~15 ha  
5 (Kohli et al., 2015). The spatial **extend** of this measurement is desirable as it matches with the desired grid cell size of a land  
surface model (Crow et al., 2012) and **small** scale heterogeneities are averaged over a larger area (Franz et al., 2013a; Desilets  
and Zreda, 2013). Vertical measurement depth ranges from a maximum of ~70 cm under completely dry conditions and  
decreases to roughly ~12 cm under wet conditions (e.g. 40 vol. % soil moisture) (Bogena et al., 2013). Worldwide several  
CRP networks exist, like the North American **COSMOS network (Zreda et al., 2012), the German CRP network (Baatz et**  
10 **al., 2014) installed in the context of the TERENO infrastructure measure (Zacharias et al., 2011) and the Australian**  
**COSMoZ network (Hawdon et al., 2014).**

**moisture data assimilation** provides a way to improve imperfect land surface model predictions with measured soil  
moisture data by merging model predictions and data, and can consider the uncertainty of initial conditions, model  
15 parameters and model forcings. Ensemble Kalman Filtering (EnKF) is one of the most commonly applied data assimilation  
methods (Evensen, 1994; Burgers et al., 1998). ~~Soil moisture data assimilation has been the subject of intensive study for  
more than a decade now. An early contribution was provided by Houser et al. (1998) who assimilated remotely sensed soil  
moisture observations from a microwave radiometer into a land atmosphere transfer scheme using four-dimensional  
variational data assimilation. Rhodin et al. (1999) assimilated soil moisture data for a four day period in order to obtain an  
20 improved characterization of the lower boundary condition for an atmospheric circulation model. They also used a  
variational data assimilation approach.~~ More recently, the Ensemble Kalman Filter (Reichle et al., 2002a; Dunne and  
Entekhabi, 2005; Crow, 2003), the Extended Kalman Filter (Draper et al., 2009; Reichle et al., 2002b), four-dimensional  
variational methods (Hurkmans et al., 2006) and the Local Ensemble Transform Kalman Filter (Han et al., 2015; Han et al.,  
2013) were applied for updating soil moisture states in land surface models. Reichle et al. (2002a) performed a synthetic  
25 experiment using L-band microwave observations of the Southern Great Plains Hydrology Experiment (Jackson et al., 1999)  
to analyze the effect of ensemble size and prediction error. Dunne and Entekhabi (2005) showed that an Ensemble Kalman  
Smoother approach, where data from multiple time steps was assimilated to update current and past states, can yield a  
reduced prediction error compared to a pure filtering approach.

30 More recent work addressed joint state-parameter estimation in hydrologic land surface models with data assimilation  
methods. **It state-parameter estimation with EnKF is possible** by an augmented state vector approach (Chen and Zhang,  
2006), a dual approach (Moradkhani et al., 2005) or an approach with an additional external optimization loop (Vrugt et al.,  
2005). Pauwels et al. (2009) optimized soil hydraulic parameters of a land surface model with synthetic aperture radar data.  
Lee (2014) used Synthetic Aperture Radar soil moisture data to estimate soil hydraulic properties at the Tibetan plateau



using the EnKF and a Soil Vegetation Atmosphere Transfer model. Bateni and Entekhabi (2012) assimilated land surface temperature with an Ensemble Kalman Smoother and achieved a better estimate of the partitioning of energy between sensible and latent heat fluxes. Han et al. (2014b) updated soil hydraulic parameters of the Community Land Model (CLM) by assimilation of synthetic brightness temperature data with the Local Ensemble Transform Kalman Filter (LETKF) (Hunt et al., 2007). Shi et al. (2014) used the Ensemble Kalman Filter for a synthetic multivariate data assimilation problem with a land surface model and then applied it to real data (Shi et al., 2015). The cases illustrated a way to use real world data for estimating several parameters in hydrologic land models. (Kurtz et al., 2016) developed a particular CPU-efficient data assimilation framework for the coupled land surface-subsurface model TerrSysMP (Shrestha et al., 2014). They successfully updated  $2 \times 10^7$  states and parameters in a synthetic experiment. Whereas these studies were made with land surface models, also in soil hydrological applications recently data assimilation was used to estimate soil hydraulic parameters. Early work was by Wu and Margulis (2011, 2013) in the context of real-time control of waste water reuse in irrigation. Erdal et al. (2014) investigated the role of bias in the conceptual soil model and explored bias aware EnKF as a way to deal with it. Erdal et al. (2015) focused on handling of strong -Gaussianity of the state variable in EnKF under very dry conditions. Montzka et al. (2013;2011) explored the role of the particle filter for handling non-Gaussianity in soil hydrology data assimilation. They showed that the ability of a data assimilation system to correct the soil moisture state and estimate hydraulic parameters strongly depends on the nonlinear character of the soil moisture retention characteristic. Song et al. (2014) worked on a modified iterative filter to handle the non-linearity and non-Gaussianity of data assimilation for the vadose zone. For a further literature review on data assimilation in the context of hydrological and land surface models we refer to Reichle (2008) and Montzka et al. (2012).

20

Shuttleworth et al. (2013) developed the Cosmic Ray Soil Moisture Interaction Code (COSMIC), which is a forward operator to be applied for assimilating neutron intensity observations from CRPs. The COSMIC code was evaluated for several sites (Baatz et al., 2014;Rosolem et al., 2014). Its capability to propagate surface soil moisture information into the deeper soil column was analyzed by Rosolem et al. (2014). The COSMIC operator was successfully implemented in the Data Assimilation Research Testbed (Rosolem et al., 2014) to allow for state updating by the Ensemble Adjustment Kalman Filter (Anderson, 2001). The COSMIC operator was implemented in a python interface that couples the land surface model CLM and the LETKF for joint state parameter updating (Han et al., 2015). Neutron counts measured by CRP have been used in data assimilation studies to update model states (Han et al., 2015;Rosolem et al., 2014). Soil hydraulic parameters were also updated by assimilation of neutron counts (Han et al., 2016), but only for a synthetic study which showed its feasibility. CRPs were also used for inverse estimation of soil hydraulic parameters of the Hydrus-1D model (Villarreyes et al., 2014).

30

This work further explores the value of measured neutron intensity by CRPs to improve modelling of terrestrial systems at the catchment scale (Simmer et al., 2015) using a land surface model.  ~~compared to existing work~~ the main novelties are:



(i) Data from a network of nine CRPs were assimilated in the Community Land Model version 4.5 (CLM) with an evaluation of the information gain by this assimilation at the larger catchment scale. Until now evaluations with CRPs were made for a single location, but not for a complete network of CRPs. It is a very important question whether CRPs can also improve the soil moisture characterization at the larger catchment scale and how dense the CRP network should be. The high variability of soil moisture at a short distance could potentially limit the CRP measurement value and make updating of soil moisture contents further away from the sensor meaningless. On the other hand, soil maps and atmospheric forcings show spatial correlations over larger distances which suggests that CRP measurements potentially carry important information to update soil moisture contents for larger regions. If it is found that CRP networks with a density like in this study (10 stations per 2354 km<sup>2</sup>) can improve soil moisture content characterization at the larger catchment scale, this is of high relevance and importance for agricultural applications, flood prediction and protection, and regional weather prediction (Whan et al., 2015;Koster et al., 2004;Seneviratne et al., 2010). The main research question addressed in this paper is therefore whether a CRP network of the density in this study can improve large scale soil moisture characterization by state and parameter updates.

(ii) Soil hydraulic parameters were updated together with the soil moisture states in a real-world case study at the larger catchment scale. The study in this paper also allows some evaluation of the feasibility of the updated large scale soil hydraulic parameters.

In the following paragraphs are presented the model site and the measurements (2.1), the Community land Model and its parameterization (2.2), the MIC forward model (2.3) and the data assimilation procedure (2.4).

## 2 Materials and methods

### 2.1 Site description and measurements

model domain, the Rur catchment (2354 km<sup>2</sup>), is situated in western Germany and illustrated in Fig. 1. Most prominent vegetation types are agricultural land use (mainly in the North), grassland, and coniferous and deciduous forest. The altitude varies between 15 m a.s.l. in the flat northern part and 690 m a.s.l. in the hilly southern part. Precipitation, evapotranspiration and land use follow the topography. Annual precipitation ranges between less than 600 mm in the North 200 mm in the hilly South (Montzka et al., 2008). Annual potential evapotranspiration varies between 500 mm in the South and 700 mm in the North (Bogena et al., 2005). The Rur catchment CRP network comprises nine CRPs (CRS1000, HydroInnova LLC, 2009) which were installed in 2011 and 2012 (Baatz et al., 2014). Climate and soil texture of the CRP sites can be found in Table 1. The CRPs were calibrated in the field using gravimetric soil samples. At each site, 18 soil samples were taken along three circles with distances of 25, 75 and 175 meters from the CRP, six samples evenly distributed along each circle. Each sample was extracted with a 50.8 x 300 mm round HUMAX soil corer (Martin Burch AG, Switzerland). The samples were split into 6 sub-samples with 5 cm length each and oven dried at 105 °C for 48 hours to measure dry soil bulk density and soil moisture. Ice water was determined for each site using a heat conductivity detector. Soil bulk density, soil moisture,



Ice water and hour averaged measured neutron intensity were used to determine poration parameters specific for each CRP and the COSMIC operator.

## 2.2 Community land model and parameterization

5 The Community Land Model version 4.5 (CLM) was the land surface model of choice for simulating water and energy exchange between the land surface and the atmosphere (Oleson et al., 2013). Some of the key processes which are solved by CLM are radiative transfer in the canopy space, interception of precipitation by the vegetation and evaporation from intercepted water, water uptake by vegetation and transpiration, soil evaporation, photosynthesis, as well as water and energy flow in the subsurface. SWC in CLM is influenced by precipitation, infiltration into the soil, water uptake by vegetation, surface evaporation and surface and subsurface runoff. Oleson et al. (2013) provide further details on CLM4.5. To limit the scope and complexity of this study, CLM was run using satellite phenology, e.g. prescribed leaf area index data and the biogeochemical module turned off.

15 The spatial domain is discretized by rectangular grid cells by CLM. Each grid cell may have several types of land cover: Lake, urban, vegetated, wetland, and glacier. The vegetated part of the grid cell can be covered by several plant functional types which are all linked to a single soil column. The soil column is vertically discretized by ten soil layers and five bedrock layers. Layer thickness increases exponentially from 0.007 m at the surface to 2.86 m for layer 10. Vertical water flow in is modelled by the 1D Richards equation. Soil hydraulic parameters are determined from sand and clay content using pedotransfer functions for the mineral soil fraction (Clapp and Hornberger, 1978; Cosby et al., 1984), and organic matter content for the organic soil fraction (Lawrence and Slater, 2008).

25 The following equations describe how soil texture and organic matter define the soil hydraulic properties in CLM such as porosity, hydraulic conductivity, the empirical exponent  $B$  and soil matric potential. Hydraulic conductivity ( $k[z]$  in mm/s) at the depth  $z$  between two layers ( $i$  and  $i+1$ ) is a function of soil moisture ( $\theta$  in  $\text{m}^3/\text{m}^3$  in layers  $i$  and  $i+1$ ), saturated hydraulic conductivity ( $k_{sat}$  in mm/s at  $z$ ), saturated soil moisture ( $\theta_{sat}$  in  $\text{m}^3/\text{m}^3$ ) and the empirical exponent  $B$ :

$$= \begin{cases} \phi_{ice} k_{sat,z} \left[ \frac{0.5(\theta_i + \theta_{i+1})}{0.5(\theta_{sat,i} + \theta_{sat,i+1})} \right]^{2B_i+3} & 1 \leq i \leq N_{levsoi} - 1 \\ \phi_{ice} k_{sat,z} \left( \frac{\theta_i}{\theta_{sat,i}} \right)^{2B_i+3} & i = N_{levsoi} \end{cases} \quad 1$$

where  $\phi_{ice}$  is the ice impedance factor. The ice impedance factor was implemented to simplify an increased tortuosity of water flow in a partly frozen pore space. It is calculated with  $\phi_{ice} = 10^{-\Omega F_{ice}}$  using the resistance factor  $\Omega = 6$  and the frozen fraction of soil porosity  $F_{ice} = \theta_{ice}/\theta_{sat,i}$ . Soil hydraulic properties are calculated separately for the mineral (*min*) and organic matter (*om*) soil components. Total porosity  $\theta_{sat,i}$  is calculated using the fraction of organic matter ( $f_{om,i}$ ) with:



$$\theta_{sat,i} = (1 - f_{om,i})\theta_{sat,min,i} + f_{om,i}\theta_{sat,om} \quad 2$$

where the organic matter porosity is  $\theta_{sat,om} = 0.9$  and sand content in % determines the mineral soil porosity  $\theta_{sat,min}$  as:

$$\theta_{sat,min} = 0.489 - 0.00126 \times \%sand \quad 3$$

Analogous, the exponent  $B$  is calculated with

$$B_i = (1 - f_{om,i})B_{min,i} + f_{om,i}B_{om} \quad 4$$

Where  $B_{om} = 2.7$  is the organic exponent and the mineral exponent  $B_{min,i}$  is determined by clay content in % with:

$$B_{min,i} = 2.91 + 0.159 \times \%clay \quad 5$$

Saturated hydraulic conductivity is calculated for a connected and an unconnected fraction of the grid cell with:

$$k_{sat}[z_i] = (1 - f_{perc})k_{sat,uncon}[z_i] + f_{perc,i}k_{sat,om}[z_i] \quad 6$$

- 5 where  $f_{perc,i}$  is the fraction of a grid cell where water flows with saturated hydraulic conductivity of the organic matter ( $k_{sat,om}[z_i]$  in mm/s) through the organic material only, the so called connected flow pathway, whereas the saturated hydraulic conductivity of the unconnected part ( $k_{sat,uncon}[z_i]$  in mm/s) depends on organic and mineral saturated soil hydraulic conductivity:

$$k_{sat,uncon} = (1 - f_{perc}) \left( \frac{1 - f_{om}}{k_{sat,min}} + \frac{f_{om} - f_{perc}}{k_{sat,om}} \right)^{-1} \quad 7$$

where saturated hydraulic conductivity for mineral soil is calculated from the grid cell sand content as:

$$k_{sat,min}[z_i] = 0.0070556 \times 10^{-0.884 + 0.0153 \times \%sand} \quad 8$$

- 10 The fraction  $f_{perc}$  is calculated with:

$$f_{perc} = 0.908 \times (f_{om} - 0.5)^{0.139} \quad f_{om} \geq 0.5 \quad 9$$

$$f_{perc} = 0 \quad f_{om} < 0.5 \quad 10$$

Soil matric potential (mm) is defined as function of saturated soil matric potential (mm) with:

$$\psi_i = \psi_{sat,i} \left( \frac{\theta_i}{\theta_{sat,i}} \right)^{-B_i} = [(1 - f_{om,i})\psi_{sat,min,i} + f_{om,i}\psi_{sat,om}] \left( \frac{\theta_i}{\theta_{sat,i}} \right)^{-B_i} \quad 11$$

where saturated organic matter matric potential is  $\psi_{sat,om} = -10.3 \text{ mm}$  and saturated mineral soil matric potential is calculated from sand content as:

$$\psi_{sat,min,i} = -10.0 \times 10^{1.88 - 0.0131 \times \%sand} \quad 12$$



### 2.3 Cosmic-ray forward model

SWC retrievals were calculated from neutron intensity observations with the Cosmic-ray Soil Moisture Interaction Code COSMIC (Shuttleworth et al., 2013) following calibration results and the procedure of Baatz et al. (2014). COSMIC parameterizes interactions between neutrons and atoms in the subsurface, relevant for soil moisture estimation. COSMIC was calibrated against the more complex Monte Carlo Neutron Particle model MCNPx (Pelowitz, 2005) and needs considerably less CPU-time than the MCNPx model. The reduced CPU-time need and the physically based parameterization make COSMIC a suitable data assimilation operator. The code was tested at multiple sites for soil moisture determination (Baatz et al., 2014; Rosolem et al., 2014) and analyzed in detail by Rosolem et al. (2014).

COSMIC assumes that a number of high energy neutrons enter the soil. In the soil, high energy neutrons are reduced by interaction with the soil leading to the production of fast neutrons with less energy in each soil layer. Before surfacing, fast neutrons are produced again by interaction (Shuttleworth et al., 2013). The number of neutrons  $N_{CRP}$  that reaches the CRP can be summarized in a single integral as

$$N_{CRP} = N_{COSMIC} \int_0^{\infty} \left\{ A(z) [\alpha \rho_s(z) + \rho_w(z)] \exp \left( - \left[ \frac{m_s(z)}{L_1} + \frac{m_w(z)}{L_2} \right] \right) \right\} \cdot dz \quad 13$$

where  $N_{COSMIC}$  is an empirical coefficient that is CRP specific and needs to be estimated by calibration,  $A(z)$  is the integrated average attenuation of fast neutrons,  $\alpha = 0.404 - 0.101 \times \rho_s$  is the site specific empirical coefficient for the creation of fast neutrons by soil,  $\rho_s$  is the dry soil bulk density in  $\text{g/cm}^3$ ,  $\rho_w$  is the total soil water density in  $\text{g/cm}^3$ ,  $m_s$  and  $m_w$  are the mass of soil and water, respectively, per area in  $\text{g/cm}^2$ .  $L_1 = 162.0 \text{ g cm}^{-2}$  and  $L_2 = 129.1 \text{ g cm}^{-2}$  are empirical coefficients that were estimated using the MCNPx code (Shuttleworth et al., 2013). The integrated average attenuation of fast neutrons  $A(z)$  can be found numerically by solving

$$A(z) = \left( \frac{2}{\pi} \right) \int_0^{\pi/2} \exp \left( \frac{-1}{\cos(\theta)} \left[ \frac{m_s(z)}{L_3} + \frac{m_w(z)}{L_4} \right] \right) \cdot d\theta \quad 14$$

where  $\theta$  is the angle along a vertical line below the CRP detector to the element that contributes to the attenuation of fast neutrons,  $L_3 = -31.65 + 99.29 \times \rho_s$  is determined from soil bulk density and  $L_4 = 3.16 \text{ g cm}^{-2}$  is another empirical coefficient estimated using the MCNPx code (Shuttleworth et al., 2013). The COSMIC operator is discretized into 300 vertical layers of one cm thickness up to a depth of three meters. For each CLM grid cell in the model domain, simulated SWC is used to generate a SWC retrieval using the COSMIC code. Simulated SWC is handed from the CLM simulation history files to the COSMIC operator. Given the vertical SWC distribution of the individual CLM soil column, COSMIC internally calculates the contribution of each layer to the simulated neutron intensity signal at the COSMIC soil surface. In this study, the contribution of each layer was used to calculate the weighted CLM SWC retrieval corresponding to the vertical distribution of simulated SWC in each grid cell. Measured neutron intensity of CRPs was used to inversely



determine a CRP SWC retrieval as by Baatz et al. (2014) assuming a homogeneous vertical SWC distribution. Then, the weighted CLM SWC retrieval is used in the data assimilation scheme to relate the CRP SWC retrieval to the model state.

## 2.4 Data assimilation

5 This study uses the local ensemble transform Kalman filter (LETKF) (Hunt et al., 2007) to assimilate SWC retrievals by CRPs into the land surface model CLM. Besides other Ensemble Kalman Filter variants, the LETKF is applied in atmospheric sciences (Liu et al., 2012; Miyoshi and Kunii, 2012), ocean science (Penny et al., 2013) and also in land surface hydrology (Han et al., 2014a; Han et al., 2015). Updates were calculated either for states or jointly for states and parameters. For state updates only, the LETKF was used as proposed by Hunt et al. (2007). Calculations were made for an ensemble of  
 10 model simulations which differed related to variations in model forcings and input parameters. The states of the different ensemble members are indicated by  $\mathbf{x}_i^f$  where  $i=1, \dots, N$  and  $N$  is the number of ensemble members. The individual state vectors  $\mathbf{x}_i^f$  contain the CLM-simulated SWC of the ten soil layers and the vertically weighted SWC retrieval obtained with the COSMIC operator. For each grid cell, a vector  $\mathbf{X}^f$  can be constructed which contains the deviations of the simulated states with respect to the ensemble mean  $\bar{\mathbf{x}}^f$  :

$$\mathbf{X}^f = [\mathbf{x}_1^f - \bar{\mathbf{x}}^f, \dots, \mathbf{x}_N^f - \bar{\mathbf{x}}^f] \quad 15$$

15 In case of joint state-parameter updates, a state augmentation approach was followed (Hendricks Franssen and Kinzelbach, 2008; Han et al., 2014b). In this case, the augmented model state vector  $\mathbf{X}^f$  is constructed from the weighted SWC, and the grid cell's sand, clay and organic matter content.

In order to relate the measured neutron intensity with the simulated SWC of CLM, the observation operator  $\mathbf{H}$  (COSMIC) is  
 20 applied on the measured neutron intensity in order to obtain the expected weighted SWC retrieval for each of the stochastic realizations:

$$\mathbf{y}_i^f = \mathbf{H}(\mathbf{x}_i^f) \quad 16$$

The ensemble realizations of the modelled SWC retrieval  $\mathbf{y}_1^f$  to  $\mathbf{y}_N^f$  with respect to the ensemble mean  $\bar{\mathbf{y}}^f$  are stored in the vector  $\mathbf{Y}^f$ :

$$\mathbf{Y}^f = [\mathbf{y}_1^f - \bar{\mathbf{y}}^f, \dots, \mathbf{y}_N^f - \bar{\mathbf{y}}^f] \quad 17$$

The observation error correlation was reduced in space by the factor  $f_{red}$  using the spherical model:

$$f_{red} = 1 - (1.5 \times d/d_{max}) + (0.5 \times [d/d_{max}]^3) \quad 18$$

25 where  $d$  is the distance to the observation and  $d_{max} = 40km$  is the maximum observation correlation length, about half the size of the catchment. Only SWC retrievals within the maximum observation correlation length were used for assimilation.



This leads to a ‘localized’ size of  $\mathbf{Y}^f$  and the observation error covariance matrix  $\mathbf{R}$ . The intermediate covariance matrix  $\mathbf{P}^a$  (also called analysis error covariance matrix) is calculated according to:

$$\mathbf{P}^a = [(\mathbf{N} - 1)\mathbf{I} + \mathbf{Y}^{fT}\mathbf{R}^{-1}\mathbf{Y}^f] \quad 19$$

In addition, the mean weight vector  $\bar{\mathbf{w}}^a$  is obtained as follows:

$$\bar{\mathbf{w}}^a = \mathbf{P}^a \mathbf{Y}^{fT} \mathbf{R}^{-1} (\mathbf{y}^0 - \bar{\mathbf{y}}^f) \quad 20$$

where  $\mathbf{y}^0$  is CRP SWC retrieval. In the ensemble space, a perturbation matrix  $\mathbf{W}^a$  is calculated from the symmetric square root of  $\mathbf{P}^a$ :

$$\mathbf{W}^a = [(\mathbf{N} - 1)\mathbf{P}^a]^{1/2} \quad 21$$

The final analysis  $\mathbf{X}^a$  is obtained from:

$$\mathbf{X}^a = \bar{\mathbf{x}}^f + \mathbf{X}^f [\bar{\mathbf{w}}^a + \mathbf{W}^a] \quad 22$$

A more detailed description of the LETKF can be found in (Hunt et al., 2007) and details on the implementation of the LETKF in combination with CLM are given by (Han et al., 2015).

## 10 3 Model and Experiment Setup

### 3.1 Model Setup

In this study, discretization and parameterization of the hydrological catchment was done on the basis of high resolution data. The Rur catchment domain is spatially discretized by rectangular grid cells of 0.008 degree size (~750 m). The model time step was set to hourly. Land cover was assumed to consist of vegetated land units only, and a single plant functional type (PFT) for each grid cell was defined. The plant functional types were derived from a remotely sensed land use map using RapidEye and ASTER data with 15 m resolution (Waldhoff, 2012). Sand content, clay content and organic matter content were derived from the high resolution regional soil map BK50 (Geologischer Dienst Nordrhein-Westfalen, 2009). The BK50 soil map provides the high resolution soil texture for the catchment and is the most detailed soil map available for the defined region. As an alternative, simulations were also performed for a biased soil texture distribution with a fixed sand content of 80 % and clay content of 10 % (S80 soil map). This represents a large error with respect to the expected true soil properties. It allows evaluating the joint state-parameter estimation approach because given the expected bias, we can evaluate whether and to what extent the soil properties are modified by the data assimilation to be closer to the available high resolution soil map. In addition, in many regions across the Earth a high resolution soil map is not available and land surface models which are applied for those regions, for example in the context of global simulations, might be strongly affected by the error in soil properties. As tested how this impacted the simulation results. Maximum saturated fraction, a surface parameter which is used for runoff generation, was calculated from a 10 meter digital elevation model (GmbH, 2010). Leaf area index data were derived from monthly averaged Moderate Resolution Imaging Spectrometer data



(MODIS). CLM was supplied with hourly atmospheric forcing data from a reanalysis data set for the years 2010 to 2013 from the German Weather Service (DWD). The data was downscaled from a resolution of 2.8 km<sup>2</sup> to the CLM resolution using linear interpolation based on Delaunay triangulation. Forcing data include precipitation in mm/s, incident solar and longwave radiation in W/m<sup>2</sup>, air temperature in K, air pressure in hPa, wind speed in m/s and relative humidity in kg/kg at the lowest atmospheric level.

### 3.2 Model ensemble

Uncertainty was introduced into the regional CLM model by perturbed soil parameters and forcings. Contents of sand, clay and organic matter were perturbed with spatially correlated noise from a uniform sampling distribution with mean zero and standard deviation 10 % or 30 % (Han et al., 2015). By perturbing texture, soil parameters are also perturbed through the pedotransfer functions used in CLM as specified in Sect. 2.2. Precipitation ( $\sigma = 1.0$ ; lognormal distribution) and shortwave radiation ( $\sigma = 0.3$ ; lognormal distribution) were perturbed with multiplicative noise with mean equal to one. Longwave radiation ( $\sigma = 20 \text{ W m}^{-2}$ ) and air temperature ( $\sigma = 1\text{K}$ ) were perturbed with additive noise. The forcing perturbations were imposed with correlations in space (5 km) using a fast Fourier transform. Correlation in time was introduced with an AR(1)-model with autoregressive parameter=0.33. These correlations and standard deviations were chosen based on previous data assimilation experiments (Reichle et al., 2010; Kumar et al., 2012; De Lannoy et al., 2012; Han et al., 2015). In this work, only results for precipitation perturbation with  $\sigma = 0.5$  will be shown as results for  $\sigma = 1.0$  were similar. An ensemble size of 95 realizations was used in the simulations. Based on previous work (Baatz et al., 2015), the SWC retrieval uncertainty for CRPs was estimated to be 0.03 cm<sup>3</sup>/cm<sup>3</sup>.

### 3.3 Experiment set-up

All simulation experiments in this study used initial conditions from a single five year spin-up run. For the five year spin-up run, a single forcing data set of the year 2010 was repeatedly used as atmospheric input. The soil moisture regime became stable after five years spin-up period, and additional spin-up simulations would not affect soil moisture in the consecutive years. After this five year spin-up, soil parameters and forcing data of the consecutive years were perturbed. From 1<sup>st</sup> Jan. 2011 onwards, CLM was propagated forward with an ensemble of 95 realizations. On 20<sup>th</sup> Mar. 2011, the first SWC retrieval was assimilated and assimilation of SWC retrievals continued until 31<sup>st</sup> Dec. 2012. From 1<sup>st</sup> January 2013 to 31<sup>st</sup> December 2013 the model was propagated forward without data assimilation but with an ensemble of 95 realizations. The year 2013 was used exclusively as evaluation period for data assimilation experiments.

In total, 26 simulation experiments were carried out using different setups (Table 2). Two open loop simulations were run for the BK50 soil map (OL-BK50) and the S80 soil map (OL-S80), respectively, without data assimilation and soil parameter perturbation of 30 %. These simulations are referred to as reference runs for the respective soil map. Simulation results of data assimilation runs were compared to the reference runs for quantification of data assimilation benefits. Simulations were



done with joint state-parameter estimation (PAR-), two for the S80 soil map (PAR-S80-) and two for the BK50 soil map (PAR-BK50-), for which soil texture was perturbed by 10 % and 30 %. Two simulations were done with state updates only for the BK50 soil map (Stt-BK50) and the S80 soil map (Stt-S80), where soil texture was perturbed by 30 %. These eight simulations form the basic set of experiments.

5

Besides the data assimilation experiments also a larger number of jackknifing simulations was run to evaluate the data assimilation performance. These simulations allow evaluating the impact of the CRP network to improve SWC characterization at other locations, without CRP. In a jackknife experiment, data from eight CRP locations were assimilated and one CRP was excluded from the assimilation for evaluation purpose. At the evaluation location, simulated SWC (which is affected by the assimilation of the other eight probes) was compared to CRP SWC retrievals. For jackknife simulations, the perturbation of soil texture was set to 30 % and precipitation perturbation was done with  $\sigma = 0.5$ . States and parameters at these sites were jointly updated, and simulations were made using the BK50 and the S80 soil maps as input. Therefore, a total of 18 jackknife simulations (jk-S80-\* and jk-BK50-\*) was performed (two soil maps times nine different simulations leaving away one CRP at a time).

15

Simulation results were evaluated with the root mean square error (CRP)s:

$$RMSE = \sqrt{\frac{\sum_{t=1}^n (SWC_{t,CLM} - SWC_{t,CRP})^2}{n}} \quad 23$$

where  $n$  is the total number of time steps,  $SWC_{t,CLM}$  is the CLM SWC retrieval at time step  $t$  and  $SWC_{t,CRP}$  is the CRP SWC retrieval at time step  $t$ . In case SWC was assimilated at the corresponding time step,  $SWC_{t,CLM}$  is SWC prior to assimilation.

In the case the  $E_{RMS}$  is estimated at a single point in time over all CRPs available, the number of time steps  $n$  can be replaced by the number of CRPs available. The second evaluation measurement in this study (CRP)s: **the bias:**

$$bias = \frac{\sum_{t=1}^n (SWC_{t,CLM} - SWC_{t,CRP})}{n} \quad 24$$

## 4 Results

### 4.1 General Results

Table 3 summarizes the performance statistics in terms of  $E_{RMS}$  for the assimilation period (2011 and 2012). Presented are results for the open loop scenario and six data assimilation scenarios. Errors of open loop simulations are higher for the S80-simulation than for the BK50-simulation at all sites but Merzenhausen. At Merzenhausen  $E_{RMS}$  was  $0.054 \text{ cm}^3/\text{cm}^3$  for the S80 soil map and  $0.067 \text{ cm}^3/\text{cm}^3$  for the BK50 soil map. Open loop simulations with the S80 soil map resulted in  $E_{RMS}$ -values above  $0.10 \text{ cm}^3/\text{cm}^3$  at five of nine sites. At all sites data assimilation results with the S80 soil map improved SWC compared to the open loop simulations. This was also the case for the BK50 soil map simulations at all sites but Aachen



where  $E_{RMS}$  was larger than for the open loop run. In general, data assimilation improved simulations more for the S80 soil map ( $E_{RMS}$  reduced by  $0.079 \text{ cm}^3/\text{cm}^3$ ) than for the BK50 soil map ( $E_{RMS}$  reduced by  $0.01 \text{ cm}^3/\text{cm}^3$ ). Room for improvement with the BK50 soil map runs was more limited because of the smaller open loop errors. Nevertheless, after state updating alone the BK50 soil map still gave smaller errors than the S80 soil map. However, joint state-parameter estimation further improved simulation results by reducing  $E_{RMS}$ -values and the parameter updating resulted in similar  $E_{RMS}$ -values for the BK50 ( $0.028 \text{ cm}^3/\text{cm}^3$ ) and S80 soil map ( $0.03 \text{ cm}^3/\text{cm}^3$ ). The  $E_{RMS}$  for simulations with 10 % and 30 % perturbation of soil texture values  not show very different results.

The temporal course of soil moisture in 2011 at the two sites Gevenich and Merzenhausen is shown in Fig. 2. The figure  illustrates that SWC at both sites was lower with the S80 soil map than with the BK50 soil map. ~~In Gevenich and Merzenhausen,~~  mean open loop SWC in 2011 was  $0.17 \text{ cm}^3/\text{cm}^3$  for the S80 soil map at both sites and  $0.27 \text{ cm}^3/\text{cm}^3$  for the BK50 soil map at both sites. CRP measurements at Merzenhausen started in May 2011. In the data assimilation runs SWC was immediately affected at the Merzenhausen and Gevenich sites as soon as Merzenhausen CRP SWC retrievals were assimilated. The simulated SWC for the PAR-S80-30 data assimilation run increased as compared to the S80 open loop simulation. The first observation at Gevenich was recorded on July 7<sup>th</sup>, 2011. By that date, the simulated CLM SWC retrieval was already close to the CRP SWC retrieval at the Gevenich site (Fig. 2) due to SWC updates which showed to have a beneficial impact. Fig. 2 also shows that the  50 open loop run was close to the observed SWC at both sites, even without data assimilation.

Fig. 3 shows the temporal course of SWC from January 2011 to December 2013 at Heinsberg and Wildenrath. Assimilation and evaluation results are shown for the case of joint state-parameter updates (PAR-S80-30), only state updates (Stt-S80), open loop (OL-S80) and CRP SWC retrievals. At Heinsberg, results show that assimilated SWC was closer to the CRP SWC retrieval when both states and parameters were updated (PAR-S80-30) than if only states were updated (Stt-S80). This is the case in the assimilation period and in the evaluation period. At the beginning of the evaluation period, the Stt-S80 simulation shows an increase in bias between modeled CLM SWC retrievals and CRP SWC retrieval within the first few days of 2013. The bias of Stt-S80 remained throughout the evaluation period. In contrast, modeled SWC during the evaluation period was close to the CRP SWC retrieval if parameters were previously updated (PAR-S80-30).

The CRP at Wildenrath started operating on May 7<sup>th</sup>, 2012. SWC retrievals at other CRPs were assimilated already from May 2011 onwards and affected SWC at Wildenrath (Fig. 3). Until May 2012, Fig. 3 shows assimilated SWC (Stt-S80 and PAR-S80-30) was higher than open loop SWC. However, no SWC retrievals were available at the Wildenrath site for comparison during this period. When SWC retrievals from the CRP at Wildenrath became available and were assimilated into the model, assimilated (Stt-S80 and PAR-S80-30) and open loop (OL-S80) SWC were close to CRP SWC retrievals. This was the case throughout the remaining assimilation and evaluation period. These results suggest that the high sand



content of the biased soil map is not far from the optimal sand content at Wildenrath. Therefore, at Wildenrath, the high sand content of both soil maps (60 % and 80 %) resulted in good modeling results already for the open loop runs. This suggests that before May 2012, simulated SWC of the open loop runs with either soil map represented more realistic SWC than assimilated SWC during this period. This will be discussed further in the discussion section.

5

## 4.2 Verification period

The year 2013 was the verification year without data assimilation.  $E_{RMS}$  values for the evaluation period 2013 are reported in Table 4. On the one hand, BK50 data assimilation runs with joint state-parameter estimation resulted in improved SWC at three out of the nine sites compared to open loop BK50-runs. For the other six sites results worsened compared to the corresponding BK50 open loop run.  $E_{RMS}$  values increased from an average of  $0.041 \text{ cm}^3/\text{cm}^3$  (OL-BK50) over all sites to  $0.047 \text{ cm}^3/\text{cm}^3$  (PAR-BK50-30). On the other hand, for the S80 soil map, all sites except Wildenrath had significantly reduced  $E_{RMS}$  values for the case of data assimilation including parameter updating compared to the S80 open loop run. For the S80 simulations, average  $E_{RMS}$  over all sites for 2013 was on average  $0.12 \text{ cm}^3/\text{cm}^3$  for the open loop run and  $0.04 \text{ cm}^3/\text{cm}^3$  for the run including data assimilation. In case only states were updated (Stt-S80 and Stt-BK50),  $E_{RMS}$  was also slightly reduced (compared to open loop runs) for the majority of sites during the evaluation period in 2013. On average, this reduction was  $0.016 \text{ cm}^3/\text{cm}^3$  for the S80 soil map (Stt-S80) and  $0.002 \text{ cm}^3/\text{cm}^3$  for the BK50 soil map (Stt-BK50). At sites, where  $E_{RMS}$  was larger for data assimilation runs with state updating (compared to open loop runs), the increase was only  $0.001 \text{ cm}^3/\text{cm}^3$ .

Bias calculated on the basis of a comparison of hourly SWC measured by CRP and simulated for 2013 is reported in Table 5. The average bias for the S80 open loop run is  $0.11 \text{ cm}^3/\text{cm}^3$  while it is  $0.02 \text{ cm}^3/\text{cm}^3$  for the BK50 open loop run. Bias of the BK50 open loop run was positive at Merzenhausen, Gevenich, Heinsberg, and Aachen, and it was negative at Rollesbroich, Kall, RurAue, and Wuestebach. Bias was zero at Wildenrath for the BK50 open loop run. Bias of the S80 open loop run was negative at all sites indicating that modeled SWC was higher than measured SWC. Joint state-parameter updates reduced the absolute bias on average to  $0.03 \text{ cm}^3/\text{cm}^3$  (PAR-S80-30) and  $0.02 \text{ cm}^3/\text{cm}^3$  (PAR-S80-10) for the S80 soil map. In case of the BK50 soil map, the bias in 2013 increased to  $0.03 \text{ cm}^3/\text{cm}^3$  by joint state-parameter updates. State updates without parameter updates reduced the biases only marginally to  $0.01 \text{ cm}^3/\text{cm}^3$  for the BK50 soil map and to  $0.09 \text{ cm}^3/\text{cm}^3$  for the S80 soil map. This indicates that state updates also can slightly improve SWC-characterization in the verification period due to improved initial conditions.

30

## 4.3 Temporal evolution of mean $E_{RMS}$

Fig. 4 shows the temporal evolution of the hourly  $E_{RMS}$  calculated for all nine CRPs.  $E_{RMS}$  was highest for the S80 open loop run and lowest for the PAR-S80-30 simulation. State updates did not improve modeled SWC as much as joint state-parameter updates improved modeled SWC. The  $E_{RMS}$  in case of Stt-S80 also falls behind the  $E_{RMS}$  of the BK50 open loop



run through most of the time. Joint state-parameter updates for the S80 soil map improved the  $E_{RMS}$  throughout most of the time compared to the open loop simulations based on the BK50 and S80 soil maps. During the assimilation period 2011-2012, the PAR-S80-30 simulation performed best out of the four simulations. During the evaluation period 2013, OL-BK50 and PAR-S80-30 performed equally well except in summer 2013 when the PAR-S80-30 simulation yielded much higher  $E_{RMS}$ -values than the BK50 open loop run.

#### 4.4 Jackknife simulations

The jackknife simulations investigated the impact of the network of CRPs for improving estimates of SWC at locations between the CRPs, outside the network. The errors shown in Table 4 refers to the two open loop simulations (for the S80 soil map and the BK50 soil map) and the 18 jackknife simulations. All simulations with the S80 soil map resulted in an improved  $E_{RMS}$  in the jackknife simulations compared to the open loop simulation, except for Wildenrath. In all cases the  $E_{RMS}$  was smaller than  $0.10 \text{ m}^3/\text{m}^3$ . Error reduction was smaller at sites where the open loop error was smaller. At sites with large open loop  $E_{RMS}$ , the assimilation could reduce the  $E_{RMS}$  by 50 % or more. In case of the BK50 soil map, the jackknife simulations resulted in  $E_{RMS}$ -values below  $0.10 \text{ m}^3/\text{m}^3$  at all sites. However, in this case only at Merzenhausen the  $E_{RMS}$  was reduced during the data assimilation period. At Wildenrath, the  $E_{RMS}$  was highest for jk-BK50 ( $0.091 \text{ m}^3/\text{m}^3$ ) and jk-S80 ( $0.095 \text{ m}^3/\text{m}^3$ ). The average absolute bias for the jackknife experiments was  $0.04 \text{ cm}^3/\text{cm}^3$  for both soil maps, BK50 and S80, in the evaluation period 2013 (Table 5). Hence, bias in the jk-S80-\* simulations improved compared to the open loop run but not in the jk-BK50-\* simulations, where bias was already small.

#### 4.5 Temporal evolution of parameters

The temporal evolution of the percentage sand content during the assimilation period for the nine CRP sites is shown in Fig. 5 for PAR-S80-30, PAR-S80-10, PAR-BK50-30, PAR-BK50-10, jk-S80-30\* and jk-BK50-30\*. Time series start on March 20<sup>th</sup>, 2011, the date of the first assimilated CRP SWC retrieval at Wuestebach. Wuestebach and sites within the influence sphere of Wuestebach (Aachen, Kall and Rollesbroich) show also a change in sand content from this date onwards. All other sites show a change in sand content in May 2012 when Rollesbroich and Merzenhausen start operating and their data is assimilated.  sites show variability in sand content over time. Wuestebach, Kall, RurAue, Rollesbroich and Heinsberg show some peaks in the time series. Merzenhausen, Aachen, Gevenich, and Wildenrath show a smoother course compared to  other sites. Sand levels approach a constant site-specific value for the sites Merzenhausen (45 %), Kall (30 %), Gevenich (41 %), RurAue (30 %), Heinsberg (42 %) and Wildenrath (62 %) with a reasonable spread amongst the experiments. The spread in estimated sand content for the sites Wuestebach, Aachen and Rollesbroich is larger, and it seems not to have stabilized at the end of the assimilation. Sand content estimates of the jackknife simulations was close to the sand content of the other data assimilation experiments with joint state-parameter estimation at the sites Merzenhausen, Gevenich, RurAue and Heinsberg. Evolution of the sand content for the jackknife simulations showed larger deviations from the sand content estimated by other data assimilation experiments for the sites Wuestebach, Kall, Aachen, Rollesbroich and Wildenrath.



The soil hydraulic parameter  $B$  and saturated hydraulic conductivity are shown in Fig. 6 and Fig. 7 for PAR-S80-30, PAR-S80-10, PAR-BK50-30, PAR-BK50-10, jk-S80-30\* and jk-BK50-30\*. Updates of soil hydraulic parameters start in March and May 2011 with the assimilation of SWC retrievals depending on the location. The  $B$  parameter increases for all simulations. Throughout the whole assimilation period  $B$  varies considerably within short time intervals. The total range of the  $B$  parameter is between 2.7 and 14 at all sites. At the sites Merzenhausen, Kall, Aachen, Gevenich and Rollesbroich, it generally ranges between 6 and 10. At Wuestebach, Heinsberg and RurAue,  $B$  ranges most of the time between 8 and 12, and at Wildenrath,  $B$  is below 8. Initial saturated hydraulic conductivity is rather high ( $k_{sat} > 0.015$  mm/s) in case of high sand content i.e. for the S80 soil map, and rather low ( $k_{sat} < 0.005$  mm/s) in case of low sand content i.e. for the BK50 soil map. In case of the S80 soil map, at all sites except Wildenrath, high initial saturated hydraulic conductivity decreases quickly by parameter updates to values below 0.01 mm/s. The initial spread in  $k_{sat}$  values amongst the simulation scenarios decreases at most sites. At Wuestebach, Merzenhausen, Aachen, Gevenich, RurAue and Heinsberg, the spread is rather small particularly at the end of the assimilation period, while at Wildenrath  $k_{sat}$  ranges from 0.005 to 0.015 for individual experiments at the end of the assimilation period. The discussion section will elaborate more on this.

15

#### 4.6 Latent heat and sensible heat

Latent heat flux or evapotranspiration (ET) is another important diagnostic variable of the CLM model and of importance for atmospheric models. Results of the data assimilation experiments showed that soil texture updates altered soil moisture states significantly. In Fig. 8 it is shown that joint state-parameter estimation also altered ET. Fig. 8 shows ET within the evaluation period 2013 across the whole catchment for four simulations. On the one hand, ET was similar for both open loop simulations in the South of the catchment. On the other hand, ET in the North was up to 80 mm per year lower for the S80 open loop run compared to the BK50 open loop run. Regarding open loop runs, the differences can be linked to the drier soil conditions in case OL-S80 compared OL-BK50 simulation results. For PAR-S80-10, ET increased by up to 40 mm per year in the Northern part of the catchment through data assimilation. The differences between open loop ET and data assimilation ET were larger for the S80 soil map than for the BK50 soil map. This could be related to the larger update in SWC in case of the S80 scenario compared to the BK50 scenario.

25

## 5 Discussion

The applied data assimilation scheme improved soil moisture characterization in the majority of simulation experiments with the regional Community Land Model (CLM). During 2011 and 2012, the biased S80 soil map gave a  $E_{RMS}$  up to  $0.17 \text{ cm}^3/\text{cm}^3$  (at Rollesbroich) in the open loop simulation which left plenty of room for improvements. The soil map BK50 led to  $E_{RMS}$ -values in open loop simulations below  $0.05 \text{ cm}^3/\text{cm}^3$  which left little room for error reduction considering the measurement error of  $0.03 \text{ cm}^3/\text{cm}^3$ . For the simulations starting with 80 % sand content, sand content was closer to the values of the BK50 soil map after joint state-parameter estimation. However, the temporal evolution of the updated soil

30



texture and the soil hydraulic parameters was not stable. Temporal fluctuations imply that there may be multiple or seasonal optimal parameter values. This is also supported by the findings of the temporal behavior of  $E_{RMS}$  during the evaluation period e.g. when in the dry summer 2013 the  $E_{RMS}$  peaked in the PAR-S80-30 simulation. Many possible error sources were not subject to calibration in this study but they could be crucial for an even better soil moisture and more stable soil parameter estimation. In this study we only considered uncertainty of soil parameters, but also vegetation parameters are uncertain. Also a number of other CLM-specific hydrologic parameters (e.g. decay factor for subsurface runoff and maximum subsurface drainage) strongly influence state variables in CLM and hence show also potential for optimization. Considering this uncertainty could give a better uncertainty characterization. Precipitation is an important forcing for the model calculations and its estimate could be improved. For this study, precipitation data from the COSMO\_DE re-analysis were used. A product which optimally combines gauge measurements and precipitation estimates from radar could give better precipitation estimates. This could improve the soil moisture characterization and also potentially lead to better parameter estimates. Also other error sources like the ones related to the model structure play a significant role. This should be subject of future investigation.

Evaluation simulations for 2013 led to partly improved and partly deteriorated  $E_{RMS}$  values when the BK50 soil map was used as prior information on the soil hydraulic properties. The simulations with the S80 soil map on the contrary showed an improved soil moisture characterization in all simulation scenarios and the updated soil hydraulic parameter estimates for those simulations approached the values of the BK50 soil map. These results indicate that the soil hydraulic parameters derived from the BK50 soil map were already well suited for soil moisture predictions and updating soil texture and soil parameters could not improve further the results.  $E_{RMS}$  values for simulations with state updates only (Stt-BK50 and Stt-BK50) in 2013 imply the beneficial role of state updates only. However, the improvements in the evaluation period by state updates (without parameter values) are small compared to the improvements obtained by joint state-parameter estimation. This illustrates the benefits of joint state-parameter updates compared to state updates only, and that soil moisture states are strongly determined by soil hydraulic parameters. It also illustrates that the improved characterization of soil moisture states in the assimilation period which results in improved initial states for the verification period loses its influence in the verification period fast over time.

The jackknife simulations illustrated that a network of CRPs can improve modeled SWC if the soil map information is not sufficient. Temporal evolution of subsurface parameters of the jackknife simulations (e.g. jk-S80-\*) was close to the evolution of parameter estimates by other simulations (e.g. PAR-S80-10). Parameter estimates at jackknife test sites were inferred from multiple surrounding CRP sites, while updates at sites with CRP information were strongly inferred from single site information. A comparison of parameter estimates at the end of the assimilation period indicates that initial soil parameterization has a limited effect on the resulting parameter estimates. Parameter estimates of jk-BK50-30\* and jk-S80-30\* are close together at the end of the assimilation period. The CRP network led to improved results for the jackknife



evaluation simulations in case of the biased soil map. This suggests that assimilation of CRP data is particularly useful for regions with little information on subsurface parameters. We expect a tradeoff between the initial uncertainty on soil moisture content (related to the quality of the soil map and meteorological data) and the density of a CRP network. In case of a large uncertainty, like in regions with limited information about soils and a low density of meteorological stations, a sparse network of probes can already be helpful for improving soil moisture characterization. On the other hand, in regions with a high density of meteorological stations and a high resolution soil map it can be expected that a high resolution CRP network is needed to further lower the error of soil moisture characterization. Further experiments in other regions with networks of CRPs are needed to get more quantitative information about this.

A question that remains to be answered is whether it is more beneficial to assimilate neutron counts measured by CRPs directly or to assimilate CRP SWC retrievals derived from the neutron counts, as done in this study. Fast neutron intensity measured by CRPs is also affected by vegetation. Neutron count rate decreases with increasing biomass because of the hydrogen content in vegetation (Baatz et al., 2015). Seasonal biomass changes at a single site have a rather small impact on neutron intensity compared to differences between grass land site and a forest site (Baatz et al., 2015). Therefore, using measured neutron flux directly in a data assimilation framework in a catchment with different vegetation types would require to account for the effects of vegetation types on neutron intensity. Hence, vegetation estimates for each grid cell would be necessary. At present, there are two methods that include biomass in the CRP calibration process (Baatz et al., 2015; Franz et al., 2013b) but both methods naturally require accurate biomass estimates, which are typically not available. Besides the uncertainty associated with CRP methods using biomass in the calibration process, biomass estimates also come along with high uncertainties. Therefore, in the case of a catchment with different vegetation types, it is desirable to circumvent the use of biomass estimates, and assimilate directly SWC retrievals obtained at the observation sites instead of assimilating neutron intensity. Therefore, this study uses CRP SWC retrievals in the data assimilation scheme assuming that seasonal changes of biomass can be neglected.

## 6 Conclusions and Outlook

This study demonstrates the benefits of assimilating data from a network of nine cosmic-ray probes (CRP) in the land surface model CLM version 4.5. Although information on neutron flux intensity was only available at few locations in the catchment, the local ensemble transform Kalman filter (LETKF) allows updating of soil water content (SWC) at unmonitored locations in the catchment considering model and observation uncertainties. Joint state-parameter estimates improved soil moisture estimates during the assimilation and during the evaluation period. The  $E_{RMS}$  and bias for the soil moisture characterization reduced strongly for simulations initialized with a biased soil map and approached values similar to the ones obtained when the regional soil map was used as input to the simulations.  $E_{RMS}$ -values in simulations with a regional soil map were not improved, because open loop simulation results were already close to the observations. The beneficial results of joint state-parameter updates were confirmed by additional jackknife experiments. This real-world case



5 study on assimilating CRP SWC retrievals into a land surface model shows the potential of CRP networks to improve subsurface parameterization in regional land surface models, especially if prior information on soil properties is limited. In many areas of the world, less detailed soil maps are available than the high resolution regional soil map applied in this study. In these areas, more advanced sub-surface characterization is possible using CRP measurements and the data assimilation framework presented in this study.

For now, CRP neutron intensity observations were not assimilated directly. In future studies it would be desirable to use the COSMIC operator for assimilating neutron intensity observations directly. However, in this case the impact of biomass on the CRP measurement signal would have to be taken into account. Therefore, it is desirable to further develop the COSMIC  
10 operator to include the impact of biomass on neutron intensities. Using the biogeochemical module of CLM would then allow to characterize local vegetation states as input for the measurement operator. Remotely sensed vegetation states are another option to characterize vegetation states as input for the measurement operator. Both methods require additional field measurements for the verification of vegetation state estimates. The further extension of the data assimilation framework would also enable the estimation of additional sub-surface parameters. The impact of other sub-surface parameters such as  
15 subsurface drainage parameters and the surface drainage decay factor on SWC states and radiative surface fluxes has already been shown (Sun et al., 2013). Estimation of these parameters is desirable because of the inherent uncertainty of these globally tuned parameters. However, estimation of soil texture and organic matter content was demonstrated to be already beneficial for improved SWC modeling. Hence, this study represents a way forward towards the integration of CRP information in the calibration of large scale weather prediction models.

## 20 **Data Availability**

Most data presented in this study are freely available via the TERENO data portal TEODOOR (<http://teodoor.icg.kfa-juelich.de/>). Atmospheric data were licensed by the German Weather Service (DWD), and the BK50 soil map was licensed by the Geologischer Dienst Nordrhein-Westfalen.

## **Acknowledgements**

25 We gratefully acknowledge the support by the SFB-TR32 "Pattern in Soil-Vegetation-Atmosphere Systems: Monitoring, Modelling and Data Assimilation" funded by the Deutsche Forschungsgemeinschaft (DFG) and TERENO (Terrestrial Environmental Observatories) funded by the Helmholtz-Gemeinschaft. The authors also gratefully acknowledge the computing time granted by the John von Neumann Institute for Computing (NIC) and provided on the supercomputer JURECA at Jülich Supercomputing Centre (JSC).

30



## 7 References

- Ajami, H., McCabe, M. F., Evans, J. P., and Stisen, S.: Assessing the impact of model spin-up on surface water-groundwater interactions using an integrated hydrologic model, *Water Resour Res*, 50, 2636-2656, 10.1002/2013wr014258, 2014.
- Anderson, J. L.: An ensemble adjustment Kalman filter for data assimilation, *Mon Weather Rev*, 129, 2884-2903, Doi 10.1175/1520-0493(2001)129<2884:Aeakff>2.0.Co;2, 2001.
- 5 Baatz, R., Bogena, H. R., Hendricks Franssen, H. J., Huisman, J. A., Qu, W., Montzka, C., and Vereecken, H.: Calibration of a catchment scale cosmic-ray probe network: A comparison of three parameterization methods, *J Hydrol*, 516, 231-244, <http://dx.doi.org/10.1016/j.jhydrol.2014.02.026>, 2014.
- Baatz, R., Bogena, H. R., Hendricks Franssen, H. J., Huisman, J. A., Montzka, C., and Vereecken, H.: An empirical vegetation correction for soil water content quantification using cosmic ray probes, *Water Resour Res*, 51, 2030-2046, 10.1002/2014WR016443, 2015.
- 10 Bateni, S. M., and Entekhabi, D.: Surface heat flux estimation with the ensemble Kalman smoother: Joint estimation of state and parameters, *Water Resour Res*, 48, Artn W08521 10.1029/2011wr011542, 2012.
- Bell, J. E., Leeper, R. D., Palecki, M. A., Coopersmith, E., Wilson, T., Bilotta, R., and Embler, S.: Evaluation of the 2012 Drought with a Newly Established National Soil Monitoring Network, *Vadose Zone J*, 14, 10.2136/vzj2015.02.0023, 2015.
- 15 Bogena, H. R., Herbst, M., Hake, J. F., Kunkel, R., Montzka, C., Pütz, T., Vereecken, H., and Wendland, F.: MOSYRUR - Water balance analysis in the Rur basin., in: *Schriften des Forschungszentrums Jülich. Reihe Umwelt/Environment*, Jülich, 2005.
- Bogena, H. R., Huisman, J. A., Baatz, R., Franssen, H. J. H., and Vereecken, H.: Accuracy of the cosmic-ray soil water content probe in humid forest ecosystems: The worst case scenario, *Water Resour Res*, 49, 5778-5791, Doi 10.1002/Wrcr.20463, 2013.
- 20 Burgers, G., van Leeuwen, P. J., and Evensen, G.: Analysis scheme in the ensemble Kalman filter, *Mon Weather Rev*, 126, 1719-1724, Doi 10.1175/1520-0493(1998)126<1719:Asitek>2.0.Co;2, 1998.
- Chen, F., Manning, K. W., LeMone, M. A., Trier, S. B., Alfieri, J. G., Roberts, R., Tewari, M., Niyogi, D., Horst, T. W., Oncley, S. P., Basara, J. B., and Blanken, P. D.: Description and evaluation of the characteristics of the NCAR high-resolution land data assimilation system, *J Appl Meteorol Clim*, 46, 694-713, 10.1175/Jam2463.1, 2007.
- 25 Chen, Y., and Zhang, D. X.: Data assimilation for transient flow in geologic formations via ensemble Kalman filter, *Adv Water Resour*, 29, 1107-1122, 10.1016/j.advwatres.2005.09.007, 2006.
- Clapp, R. B., and Hornberger, G. M.: Empirical Equations for Some Soil Hydraulic-Properties, *Water Resour Res*, 14, 601-604, Doi 10.1029/Wr014i004p00601, 1978.
- Cosby, B. J., Hornberger, G. M., Clapp, R. B., and Ginn, T. R.: A Statistical Exploration of the Relationships of Soil-Moisture Characteristics to the Physical-Properties of Soils, *Water Resour Res*, 20, 682-690, Doi 10.1029/Wr020i006p00682, 1984.
- 30 Cosh, M. H., Ochsner, T. E., McKee, L., Dong, J. N., Basara, J. B., Evett, S. R., Hatch, C. E., Small, E. E., Steele-Dunne, S. C., Zreda, M., and Sayde, C.: The Soil Moisture Active Passive Marena, Oklahoma, In Situ Sensor Testbed (SMAP-MOISST): Testbed Design and Evaluation of In Situ Sensors, *Vadose Zone J*, 15, 10.2136/vzj2015.09.0122, 2016.
- Crow, W. T.: Correcting land surface model predictions for the impact of temporally sparse rainfall rate measurements using an ensemble Kalman filter and surface brightness temperature observations, *J Hydrometeorol*, 4, 960-973, 2003.
- 35 Crow, W. T., Berg, A. A., Cosh, M. H., Loew, A., Mohanty, B. P., Panciera, R., de Rosnay, P., Ryu, D., and Walker, J. P.: Upscaling Sparse Ground-Based Soil Moisture Observations for the Validation of Coarse-Resolution Satellite Soil Moisture Products, *Rev Geophys*, 50, Artn Rg2002 Doi 10.1029/2011rg000372, 2012.
- 40 De Lannoy, G. J. M., Reichle, R. H., Arsenault, K. R., Houser, P. R., Kumar, S., Verhoest, N. E. C., and Pauwels, V. R. N.: Multiscale assimilation of Advanced Microwave Scanning Radiometer-EOS snow water equivalent and Moderate Resolution Imaging Spectroradiometer snow cover fraction observations in northern Colorado, *Water Resour Res*, 48, Artn W01522 Doi 10.1029/2011wr010588, 2012.
- Desilets, D., Zreda, M., and Ferre, T. P. A.: Nature's neutron probe: Land surface hydrology at an elusive scale with cosmic rays, *Water Resour Res*, 46, 10.1029/2009WR008726, 2010.
- 45 Desilets, D., and Zreda, M.: Footprint diameter for a cosmic-ray soil moisture probe: Theory and Monte Carlo simulations, *Water Resour Res*, 49, 3566-3575, Doi 10.1002/Wrcr.20187, 2013.
- Draper, C. S., Mahfouf, J. F., and Walker, J. P.: An EKF assimilation of AMSR-E soil moisture into the ISBA land surface scheme, *J Geophys Res-Atmos*, 114, 10.1029/2008JD011650, 2009.
- 50 Dunne, S., and Entekhabi, D.: An ensemble-based reanalysis approach to land data assimilation, *Water Resour Res*, 41, Artn W02013 10.1029/2004wr003449, 2005.
- Eltahir, E. A. B.: A soil moisture rainfall feedback mechanism 1. Theory and observations, *Water Resour Res*, 34, 765-776, Doi 10.1029/97wr03499, 1998.
- Erdal, D., Neuweiler, I., and Wollschlager, U.: Using a bias aware EnKF to account for unresolved structure in an unsaturated zone model, *Water Resour Res*, 50, 132-147, 10.1002/2012wr013443, 2014.



- Erdal, D., Rahman, M. A., and Neuweiler, I.: The importance of state transformations when using the ensemble Kalman filter for unsaturated flow modeling: Dealing with strong nonlinearities, *Adv Water Resour*, 86, 354-365, 10.1016/j.advwatres.2015.09.008, 2015.
- Evensen, G.: Sequential Data Assimilation with a Nonlinear Quasi-Geostrophic Model Using Monte-Carlo Methods to Forecast Error Statistics, *J Geophys Res-Oceans*, 99, 10143-10162, Doi 10.1029/94jc00572, 1994.
- 5 Franz, T. E., Zreda, M., Ferre, T. P. A., and Rosolem, R.: An assessment of the effect of horizontal soil moisture heterogeneity on the area-average measurement of cosmic-ray neutrons, *Water Resour Res*, 49, 6450-6458, Doi 10.1002/Wrcr.20530, 2013a.
- Franz, T. E., Zreda, M., Rosolem, R., and Ferre, T. P. A.: A universal calibration function for determination of soil moisture with cosmic-ray neutrons, *Hydrol Earth Syst Sc*, 17, 453-460, DOI 10.5194/hess-17-453-2013, 2013b.
- GmbH, s.: Digital Elevation Model 10 without anthropogenic landfo<sub>RMS</sub>, 2010.
- 10 Han, X., Franssen, H. J. H., Montzka, C., and Vereecken, H.: Soil moisture and soil properties estimation in the Community Land Model with synthetic brightness temperature observations, *Water Resour Res*, 50, 6081-6105, 10.1002/2013WR014586, 2014a.
- Han, X., Franssen, H. J. H., Rosolem, R., Jin, R., Li, X., and Vereecken, H.: Correction of systematic model forcing bias of CLM using assimilation of cosmic-ray Neutrons and land surface temperature: a study in the Heihe Catchment, China, *Hydrol. Earth Syst. Sci.*, 19, 615-629, 10.5194/hess-19-615-2015, 2015.
- 15 Han, X., Franssen, H.-J. H., Bello, M. Á. J., Rosolem, R., Bogena, H., Alzamora, F. M., Chanzy, A., and Vereecken, H.: Simultaneous Soil Moisture and Properties Estimation for a Drip Irrigated Field by Assimilating Cosmic-ray Neutron Intensity, *J Hydrol*, <http://dx.doi.org/10.1016/j.jhydrol.2016.05.050>, 2016.
- Han, X. J., Franssen, H. J. H., Li, X., Zhang, Y. L., Montzka, C., and Vereecken, H.: Joint Assimilation of Surface Temperature and L-Band Microwave Brightness Temperature in Land Data Assimilation, *Vadose Zone J*, 12, Doi 10.2136/Vzj2012.0072, 2013.
- 20 Han, X. J., Franssen, H. J. H., Montzka, C., and Vereecken, H.: Soil moisture and soil properties estimation in the Community Land Model with synthetic brightness temperature observations, *Water Resour Res*, 50, 6081-6105, 10.1002/2013WR014586, 2014b.
- Hawdon, A., McJannet, D., and Wallace, J.: Calibration and correction procedures for cosmic-ray neutron soil moisture probes located across Australia, *Water Resour Res*, 50, 5029-5043, 10.1002/2013WR015138, 2014.
- Hendricks Franssen, H. J., and Kinzelbach, W.: Real-time groundwater flow modeling with the Ensemble Kalman Filter: Joint estimation of states and parameters and the filter inbreeding problem, *Water Resour Res*, 44, Artn W09408  
 25 Doi 10.1029/2007wr006505, 2008.
- Houser, P. R., Shuttleworth, W. J., Famiglietti, J. S., Gupta, H. V., Syed, K. H., and Goodrich, D. C.: Integration of soil moisture remote sensing and hydrologic modeling using data assimilation, *Water Resour Res*, 34, 3405-3420, Doi 10.1029/1998wr900001, 1998.
- Hunt, B. R., Kostelich, E. J., and Szunyogh, I.: Efficient data assimilation for spatiotemporal chaos: A local ensemble transform Kalman filter, *Physica D*, 230, 112-126, Doi 10.1016/j.physd.2006.11.008, 2007.
- 30 Hurkmans, R., Paniconi, C., and Troch, P. A.: Numerical assessment of a dynamical relaxation data assimilation scheme for a catchment hydrological model, *Hydrol Process*, 20, 549-563, 10.1002/hyp.5921, 2006.
- Jackson, T. J., Le Vine, D. M., Hsu, A. Y., Oldak, A., Starks, P. J., Swift, C. T., Isham, J. D., and Haken, M.: Soil moisture mapping at regional scales using microwave radiometry: The Southern Great Plains Hydrology Experiment, *Ieee T Geosci Remote*, 37, 2136-2151,  
 35 Doi 10.1109/36.789610, 1999.
- Kohli, M., Schron, M., Zreda, M., Schmidt, U., Dietrich, P., and Zacharias, S.: Footprint characteristics revised for field-scale soil moisture monitoring with cosmic-ray neutrons, *Water Resour Res*, 51, 5772-5790, 10.1002/2015WR017169, 2015.
- Koster, R. D., Dirmeyer, P. A., Guo, Z. C., Bonan, G., Chan, E., Cox, P., Gordon, C. T., Kanae, S., Kowalczyk, E., Lawrence, D., Liu, P., Lu, C. H., Malyshev, S., McAvaney, B., Mitchell, K., Mocko, D., Oki, T., Oleson, K., Pitman, A., Sud, Y. C., Taylor, C. M., Versegny, D.,  
 40 Vasic, R., Xue, Y. K., Yamada, T., and Team, G.: Regions of strong coupling between soil moisture and precipitation, *Science*, 305, 1138-1140, DOI 10.1126/science.1100217, 2004.
- Kumar, S. V., Reichle, R. H., Harrison, K. W., Peters-Lidard, C. D., Yatheendradas, S., and Santanello, J. A.: A comparison of methods for a priori bias correction in soil moisture data assimilation, *Water Resour Res*, 48, Artn W03515  
 Doi 10.1029/2010wr010261, 2012.
- 45 Kurtz, W., He, G. W., Kollet, S. J., Maxwell, R. M., Vereecken, H., and Franssen, H. J. H.: TerrSysMP-PDAF version 1.0): a modular high-performance data assimilation framework for an integrated land surface-subsurface model, *Geosci Model Dev*, 9, 1341-1360, 10.5194/gmd-9-1341-2016, 2016.
- Lawrence, D. M., and Slater, A. G.: Incorporating organic soil into a global climate model, *Clim Dynam*, 30, 145-160, 10.1007/s00382-007-0278-1, 2008.
- 50 Lee, J. H.: Spatial-Scale Prediction of the SVAT Soil Hydraulic Variables Characterizing Stratified Soils on the Tibetan Plateau from an EnKF Analysis of SAR Soil Moisture, *Vadose Zone J*, 13, 10.2136/vzj2014.06.0060, 2014.
- Liu, J. J., Fung, I., Kalnay, E., Kang, J. S., Olsen, E. T., and Chen, L.: Simultaneous assimilation of AIRS Xco(2) and meteorological observations in a carbon climate model with an ensemble Kalman filter, *J Geophys Res-Atmos*, 117, Artn D05309  
 10.1029/2011jd016642, 2012.
- 55 Ly, L., Franz, T. E., Robinson, D. A., and Jones, S. B.: Measured and Modeled Soil Moisture Compared with Cosmic-Ray Neutron Probe Estimates in a Mixed Forest, *Vadose Zone J*, 13, 10.2136/vzj2014.06.0077, 2014.



- Miyoshi, T., and Kunii, M.: The Local Ensemble Transform Kalman Filter with the Weather Research and Forecasting Model: Experiments with Real Observations, *Pure Appl Geophys*, 169, 321-333, 10.1007/s00024-011-0373-4, 2012.
- Montzka, C., Canty, M., Kunkel, R., Menz, G., Vereecken, H., and Wendland, F.: Modelling the water balance of a mesoscale catchment basin using remotely sensed land cover data, *J Hydrol*, 353, 322-334, DOI 10.1016/j.jhydrol.2008.02.018, 2008.
- 5 Montzka, C., Moradkhani, H., Weihermuller, L., Franssen, H. J. H., Canty, M., and Vereecken, H.: Hydraulic parameter estimation by remotely-sensed top soil moisture observations with the particle filter, *J Hydrol*, 399, 410-421, 10.1016/j.jhydrol.2011.01.020, 2011.
- Montzka, C., Pauwels, V. R. N., Franssen, H. J. H., Han, X. J., and Vereecken, H.: Multivariate and Multiscale Data Assimilation in Terrestrial Systems: A Review, *Sensors-Basel*, 12, 16291-16333, 10.3390/s121216291, 2012.
- Montzka, C., Grant, J. P., Moradkhani, H., Franssen, H. J. H., Weihermuller, L., Drusch, M., and Vereecken, H.: Estimation of Radiative  
 10 Transfer Parameters from L-Band Passive Microwave Brightness Temperatures Using Advanced Data Assimilation, *Vadose Zone J*, 12, 10.2136/vzj2012.0040, 2013.
- Moradkhani, H., Sorooshian, S., Gupta, H. V., and Houser, P. R.: Dual state-parameter estimation of hydrological models using ensemble Kalman filter, *Adv Water Resour*, 28, 135-147, 10.1016/j.advwatres.2004.09.002, 2005.
- Nordrhein-Westfalen, G. D.: Informationssystem Bodenkarte 50, 1:50000, 2009.
- 15 Oglesby, R. J., and Erickson, D. J.: Soil-Moisture and the Persistence of North-American Drought, *J Climate*, 2, 1362-1380, Doi 10.1175/1520-0442(1989)002<1362:Smatpo>2.0.Co;2, 1989.
- Oleson, K., Lawrence, D. M., Bonan, G. B., Drewniak, B., Huang, M., Koven, C. D., Levis, S., Li, F., Riley, J. M., Subin, Z. M., Swenson, S., Thornton, P. E., Bozbiyik, A., Fisher, R., Heald, C. L., Kluzek, E., Lamarque, J.-F., Lawrence, P. J., Leung, L. R., Lipscomb, W., Muszala, S. P., Ricciuto, D. M., Sacks, W. J., Sun, Y., Tang, J., and Yang, Z.-L.: Technical description of version 4.5 of the Community  
 20 Land Model (CLM), NCAR Technical Note NCAR/TN-503+STR, 420, 10.5065/D6RR1W7M, 2013.
- Pauwels, V. R. N., Balenzano, A., Satalino, G., Skriver, H., Verhoest, N. E. C., and Mattia, F.: Optimization of Soil Hydraulic Model Parameters Using Synthetic Aperture Radar Data: An Integrated Multidisciplinary Approach, *Ieee T Geosci Remote*, 47, 455-467, 10.1109/Tgrs.2008.2007849, 2009.
- Pelowitz, D. B.: MCNPX user's manual, version 5, Rep. LA-CP-05-0369, Los Alamos National Laboratory, Los Alamos LA-CP-05-0369,  
 25 2005.
- Penny, S. G., Kalnay, E., Carton, J. A., Hunt, B. R., Ide, K., Miyoshi, T., and Chepurin, G. A.: The local ensemble transform Kalman filter and the running-in-place algorithm applied to a global ocean general circulation model, *Nonlinear Proc Geoph*, 20, 1031-1046, 10.5194/npg-20-1031-2013, 2013.
- Reichle, R. H., McLaughlin, D. B., and Entekhabi, D.: Hydrologic data assimilation with the ensemble Kalman filter, *Mon Weather Rev*,  
 30 130, 103-114, Doi 10.1175/1520-0493(2002)130<0103:Hdawte>2.0.Co;2, 2002a.
- Reichle, R. H., Walker, J. P., Koster, R. D., and Houser, P. R.: Extended versus ensemble Kalman filtering for land data assimilation, *J Hydrometeorol*, 3, 728-740, Doi 10.1175/1525-7541(2002)003<0728:Evekkf>2.0.Co;2, 2002b.
- Reichle, R. H.: Data assimilation methods in the Earth sciences, *Adv Water Resour*, 31, 1411-1418, 10.1016/j.advwatres.2008.01.001, 2008.
- 35 Reichle, R. H., Kumar, S. V., Mahanama, S. P. P., Koster, R. D., and Liu, Q.: Assimilation of Satellite-Derived Skin Temperature Observations into Land Surface Models, *J Hydrometeorol*, 11, 1103-1122, Doi 10.1175/2010jhm1262.1, 2010.
- Rhodin, A., Kucharski, F., Callies, U., Eppel, D. P., and Wergen, W.: Variational analysis of effective soil moisture from screen-level atmospheric parameters: Application to a short-range weather forecast model, *Q J Roy Meteor Soc*, 125, 2427-2448, Doi 10.1256/Smsqj.55904, 1999.
- 40 Robinson, D. A., Campbell, C. S., Hopmans, J. W., Hornbuckle, B. K., Jones, S. B., Knight, R., Ogden, F., Selker, J., and Wendroth, O.: Soil moisture measurement for ecological and hydrological watershed-scale observatories: A review, *Vadose Zone J*, 7, 358-389, Doi 10.2136/Vzj2007.0143, 2008.
- Rosolem, R., Hoar, T., Arellano, A., Anderson, J. L., Shuttleworth, W. J., Zeng, X., and Franz, T. E.: Translating aboveground cosmic-ray neutron intensity to high-frequency soil moisture profiles at sub-kilometer scale, *Hydrol. Earth Syst. Sci.*, 18, 4363-4379, 10.5194/hess-18-  
 45 4363-2014, 2014.
- Seneviratne, S. I., Luthi, D., Litschi, M., and Schar, C.: Land-atmosphere coupling and climate change in Europe, *Nature*, 443, 205-209, Doi 10.1038/Nature05095, 2006.
- Seneviratne, S. I., Corti, T., Davin, E. L., Hirschi, M., Jaeger, E. B., Lehner, I., Orlowsky, B., and Teuling, A. J.: Investigating soil moisture-climate interactions in a changing climate: A review, *Earth-Science Reviews*, 99, 125-161, <http://dx.doi.org/10.1016/j.earscirev.2010.02.004>, 2010.
- 50 Sheffield, J., and Wood, E. F.: Global trends and variability in soil moisture and drought characteristics, 1950-2000, from observation-driven Simulations of the terrestrial hydrologic cycle, *J Climate*, 21, 432-458, 10.1175/2007JCLI1822.1, 2008.
- Shi, Y. N., Davis, K. J., Zhang, F. Q., Duffy, C. J., and Yu, X.: Parameter estimation of a physically based land surface hydrologic model using the ensemble Kalman filter : A synthetic experiment, *Water Resour Res*, 50, 706-724, 10.1002/2013wr014070, 2014.



- Shi, Y. N., Davis, K. J., Zhang, F. Q., Duffy, C. J., and Yu, X.: Parameter estimation of a physically-based land surface hydrologic model using an ensemble Kalman filter: A multivariate real-data experiment, *Adv Water Resour*, 83, 421-427, 10.1016/j.advwatres.2015.06.009, 2015.
- 5 Shrestha, P., Sulis, M., Masbou, M., Kollet, S., and Simmer, C.: A Scale-Consistent Terrestrial Systems Modeling Platform Based on COSMO, CLM, and ParFlow, *Mon Weather Rev*, 142, 3466-3483, 10.1175/Mwr-D-14-00029.1, 2014.
- Shuttleworth, J., Rosolem, R., Zreda, M., and Franz, T.: The COsmic-ray Soil Moisture Interaction Code (COSMIC) for use in data assimilation, *Hydrol Earth Syst Sc*, 17, 3205-3217, DOI 10.5194/hess-17-3205-2013, 2013.
- Simmer, C., Thiele-Eich, I., Masbou, M., Amelung, W., Bogena, H., Crewell, S., Diekkruger, B., Ewert, F., Franssen, H. J. H., Huisman, J. A., Kemna, A., Klitzsch, N., Kollet, S., Langensiepen, M., Lohnert, U., Rahman, A. S. M. M., Rascher, U., Schneider, K., Schween, J., Shao, Y. P., Shrestha, P., Stiebler, M., Sulis, M., Vanderborght, J., Vereecken, H., van der Kruk, J., Waldhoff, G., and Zerenner, T.: MONITORING AND MODELING THE TERRESTRIAL SYSTEM FROM PORES TO CATCHMENTS The Transregional Collaborative Research Center on Patterns in the Soil-Vegetation-Atmosphere System, *B Am Meteorol Soc*, 96, 1765-1787, 10.1175/Bams-D-13-00134.1, 2015.
- 10 Song, X. H., Shi, L. S., Ye, M., Yang, J. Z., and Navon, I. M.: Numerical Comparison of Iterative Ensemble Kalman Filters for Unsaturated Flow Inverse Modeling, *Vadose Zone J*, 13, 10.2136/vzj2013.05.0083, 2014.
- 15 Sun, Y., Hou, Z., Huang, M., Tian, F., and Leung, L. R.: Inverse modeling of hydrologic parameters using surface flux and runoff observations in the Community Land Model, *Hydrol Earth Syst Sc*, 17, 4995-5011, 10.5194/hess-17-4995-2013, 2013.
- Temimi, M., Lakhankar, T., Zhan, X. W., Cosh, M. H., Krakauer, N., Fares, A., Kelly, V., Khanbilvardi, R., and Kumassi, L.: Soil Moisture Retrieval Using Ground-Based L-Band Passive Microwave Observations in Northeastern USA, *Vadose Zone J*, 13, 10.2136/vzj2013.06.0101, 2014.
- 20 Vereecken, H., Huisman, J. A., Bogena, H., Vanderborght, J., Vrugt, J. A., and Hopmans, J. W.: On the value of soil moisture measurements in vadose zone hydrology: A review, *Water Resour Res*, 44, Artn W00d06  
Doi 10.1029/2008wr006829, 2008.
- Vereecken, H., Schnepf, A., Hopmans, J. W., Javaux, M., Or, D., Roose, D. O. T., Vanderborght, J., Young, M. H., Amelung, W., Aitkenhead, M., Allison, S. D., Assouline, S., Baveye, P., Berli, M., Bruggemann, N., Finke, P., Flury, M., Gaiser, T., Govers, G., Ghezzehei, T., Hallett, P., Franssen, H. J. H., Heppell, J., Horn, R., Huisman, J. A., Jacques, D., Jonard, F., Kollet, S., Lafolie, F., Lamorski, K., Leitner, D., McBratney, A., Minasny, B., Montzka, C., Nowak, W., Pachepsky, Y., Padarian, J., Romano, N., Roth, K., Rothfuss, Y., Rowe, E. C., Schwen, A., Simunek, J., Tiktak, A., Van Dam, J., van der Zee, S. E. A. T. M., Vogel, H. J., Vrugt, J. A., Wohling, T., and Young, I. M.: Modeling Soil Processes: Review, Key Challenges, and New Perspectives, *Vadose Zone J*, 15, 10.2136/vzj2015.09.0131, 2016.
- 25 Villarreyes, C. A. R., Baroni, G., and Oswald, S. E.: Inverse modelling of cosmic-ray soil moisture for field-scale soil hydraulic parameters, *Eur J Soil Sci*, 65, 876-886, 10.1111/ejss.12162, 2014.
- Vrugt, J. A., Diks, C. G. H., Gupta, H. V., Bouten, W., and Verstraten, J. M.: Improved treatment of uncertainty in hydrologic modeling: Combining the strengths of global optimization and data assimilation, *Water Resour Res*, 41, Artn W01017  
10.1029/2004wr003059, 2005.
- 30 Waldhoff, G.: Enhanced land use classification of 2009 for the Rur catchment, in, TR32DB, 2012.
- Whan, K., Zscheischler, J., Orth, R., Shongwe, M., Rahimi, M., Asare, E. O., and Seneviratne, S. I.: Impact of soil moisture on extreme maximum temperatures in Europe, *Weather and Climate Extremes*, 9, 57-67, <http://dx.doi.org/10.1016/j.wace.2015.05.001>, 2015.
- Wu, C. C., and Margulis, S. A.: Feasibility of real-time soil state and flux characterization for wastewater reuse using an embedded sensor network data assimilation approach, *J Hydrol*, 399, 313-325, 10.1016/j.jhydrol.2011.01.011, 2011.
- 40 Wu, C. C., and Margulis, S. A.: Real-Time Soil Moisture and Salinity Profile Estimation Using Assimilation of Embedded Sensor Datastreams, *Vadose Zone J*, 12, 10.2136/vzj2011.0176, 2013.
- Zacharias, S., Bogena, H., Samaniego, L., Mauder, M., Fuss, R., Putz, T., Frenzel, M., Schwank, M., Baessler, C., Butterbach-Bahl, K., Bens, O., Borg, E., Brauer, A., Dietrich, P., Hajnsek, I., Helle, G., Kiese, R., Kunstmann, H., Klotz, S., Munch, J. C., Papen, H., Priesack, E., Schmid, H. P., Steinbrecher, R., Rosenbaum, U., Teutsch, G., and Vereecken, H.: A Network of Terrestrial Environmental Observatories in Germany, *Vadose Zone J*, 10, 955-973, Doi 10.2136/Vzj2010.0139, 2011.
- Zreda, M., Desilets, D., Ferre, T. P. A., and Scott, R. L.: Measuring soil moisture content non-invasively at intermediate spatial scale using cosmic-ray neutrons, *Geophys Res Lett*, 35, 10.1029/2008GL035655, 2008.
- 45 Zreda, M., Shuttleworth, W. J., Zeng, X., Zweck, C., Desilets, D., Franz, T., and Rosolem, R.: COSMOS: the COsmic-ray Soil Moisture Observing System (vol 16, pg 4079, 2012), *Hydrol Earth Syst Sc*, 17, 1065-1066, DOI 10.5194/hess-17-1065-2013, 2012.
- 50



## Figures

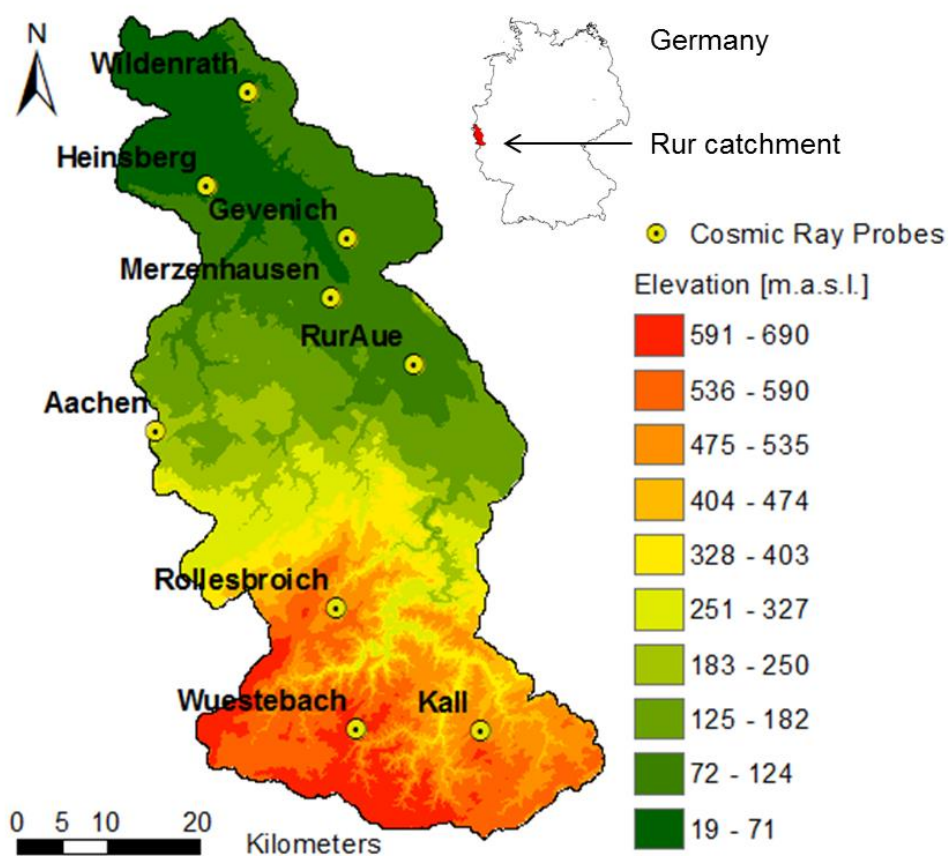


Fig. 1. Map of the Rur catchment and locations of the nine cosmic-ray probes. The hilly South of the catchment is prone to more rainfall,  
5 lower average temperatures and less potential evapotranspiration than the North of the catchment.

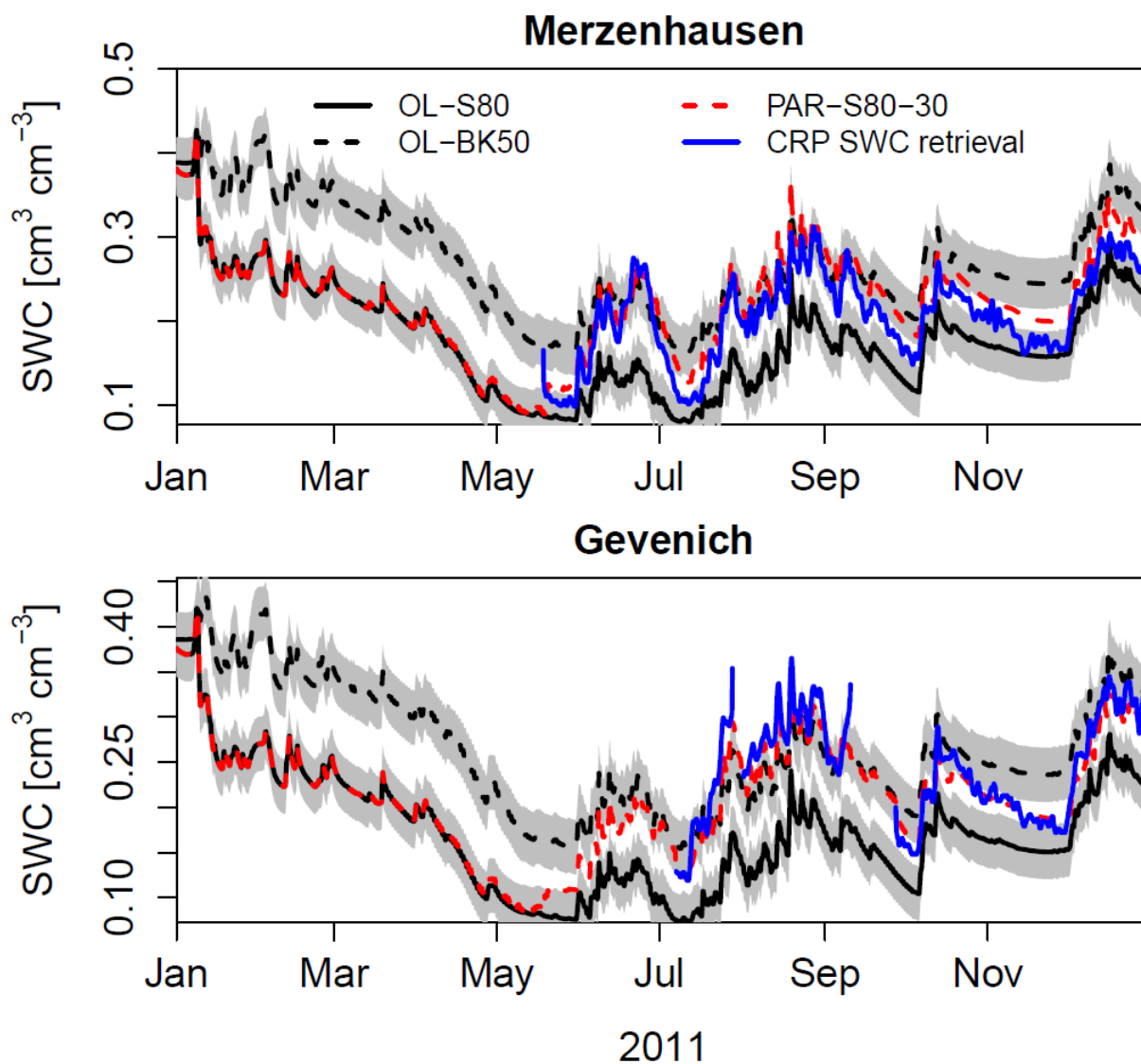


Fig. 2. Temporal evolution of simulated SWC, calculated with open loop (OL-\*) simulations and data assimilation including parameter updating (PAR-S80-30), together with the CRP soil water content retrieval (SWC) during the first year of simulation at the sites Merzenhausen and Gevenich. Simulated SWC was vertically weighted using the COSMIC operator to obtain the appropriate SWC corresponding to the CRP SWC retrieval.

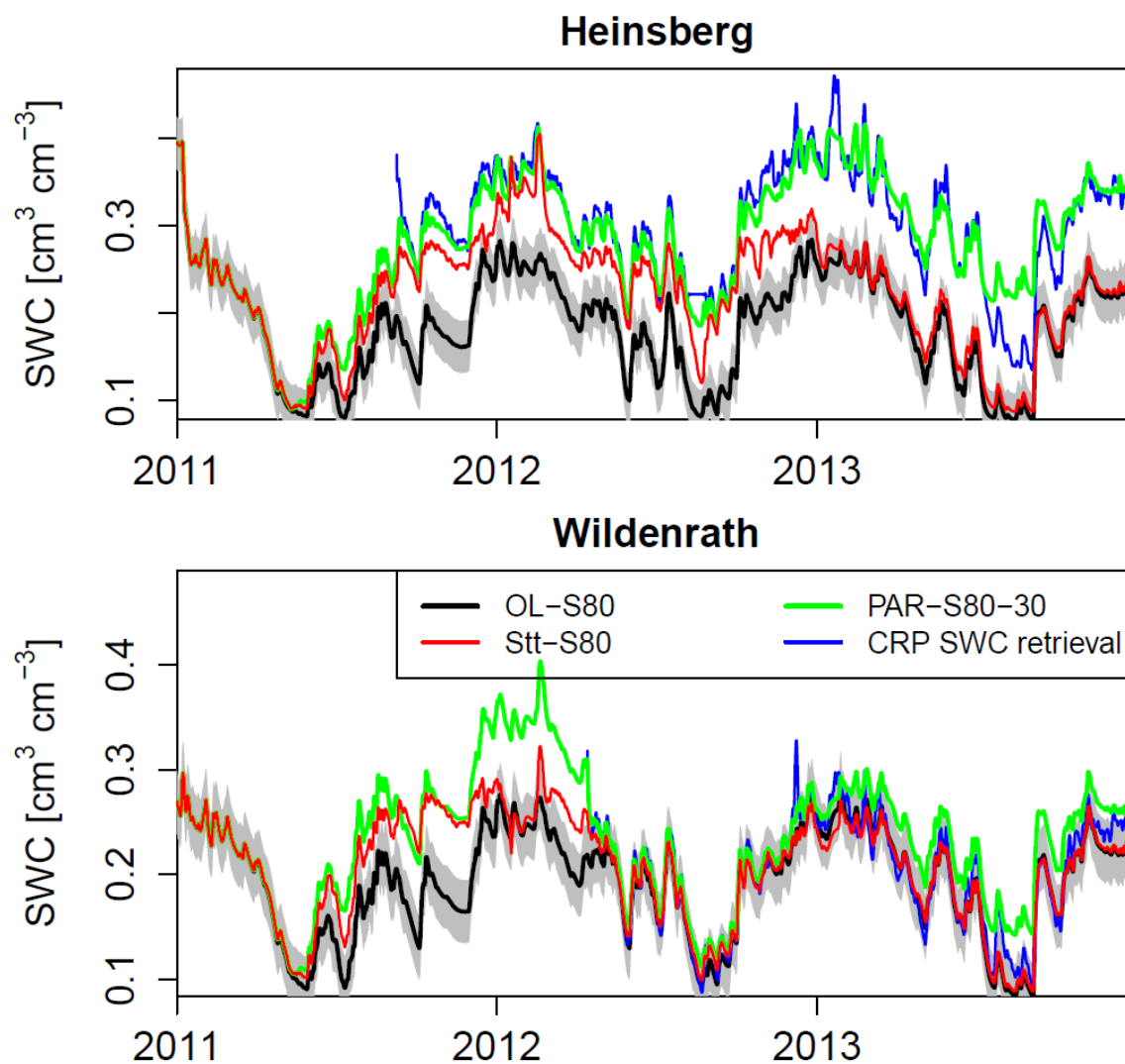


Fig. 3. Temporal evolution of simulated SWC retrievals, calculated with open loop (OL-S80), data assimilation with state update only (Stt-BK50), and data assimilation including parameter updating (PAR-S80-30), together with the CRP soil water content (SWC) retrieval at the sites Heinsberg and Wildenrath for the data assimilation period 2011 and 2012, and the evaluation period 2013. Simulated SWC was vertically weighted to obtain the appropriate SWC corresponding to the CRP SWC retrieval.

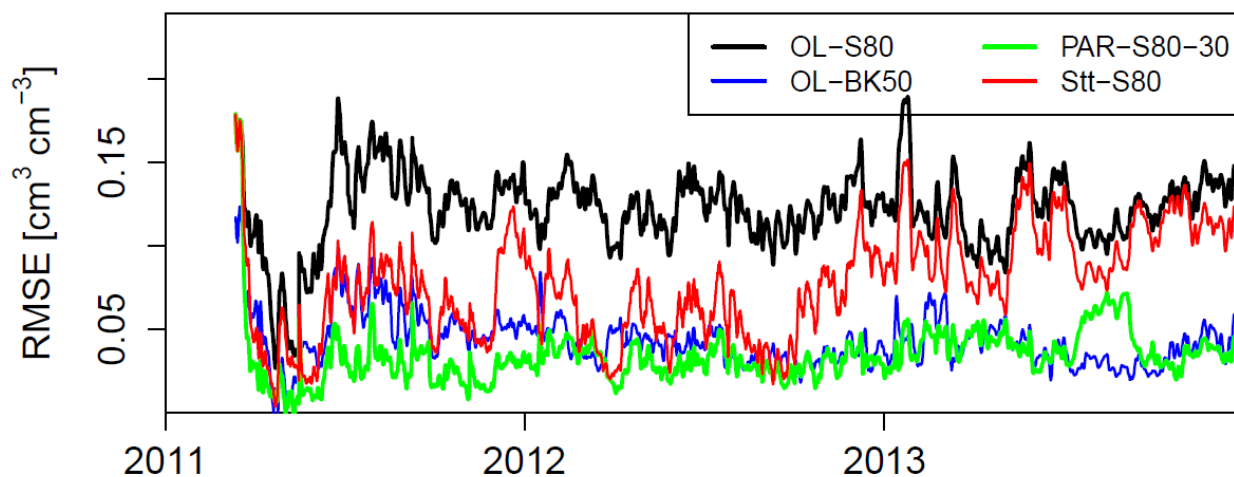


Fig. 4. Temporal evolution of root mean square error ( $E_{RMS}$ ) for hourly SWC retrievals.  $E_{RMS}$  is calculated hourly for nine CRP's for open loop runs for soil maps S80 and BK50, joint state-parameter updates (PAR-S80-30) and state updates only (Stt-S80) during the assimilation period (2011 and 2012) and verification period (2013).

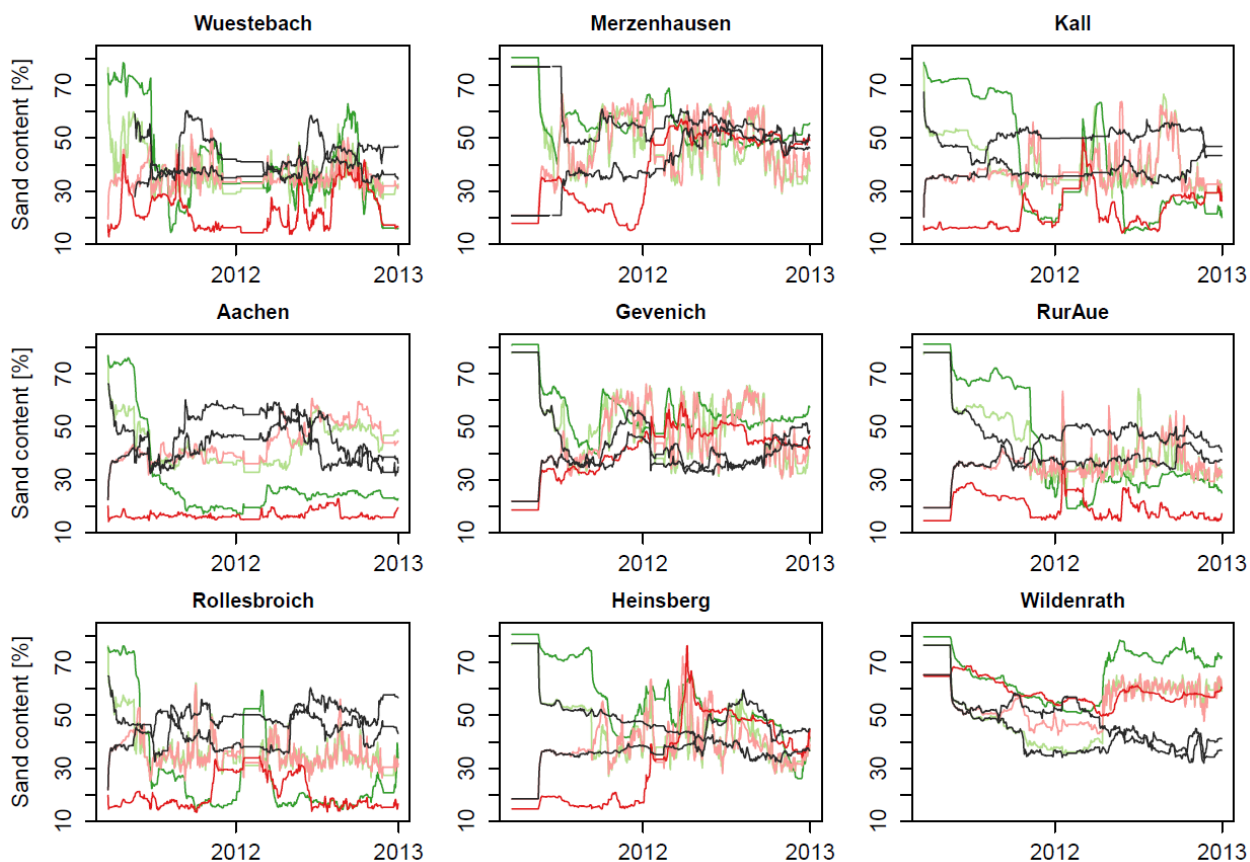


Fig. 5. Temporal evolution of the percentage sand content for simulations with parameter update: PAR-S80-30 (green), PAR-S80-10 (light green), PAR-BK50-30 (red), PAR-BK50-10 (light red), jk-S80-30\* (black) and jk-BK50-30\* (black).

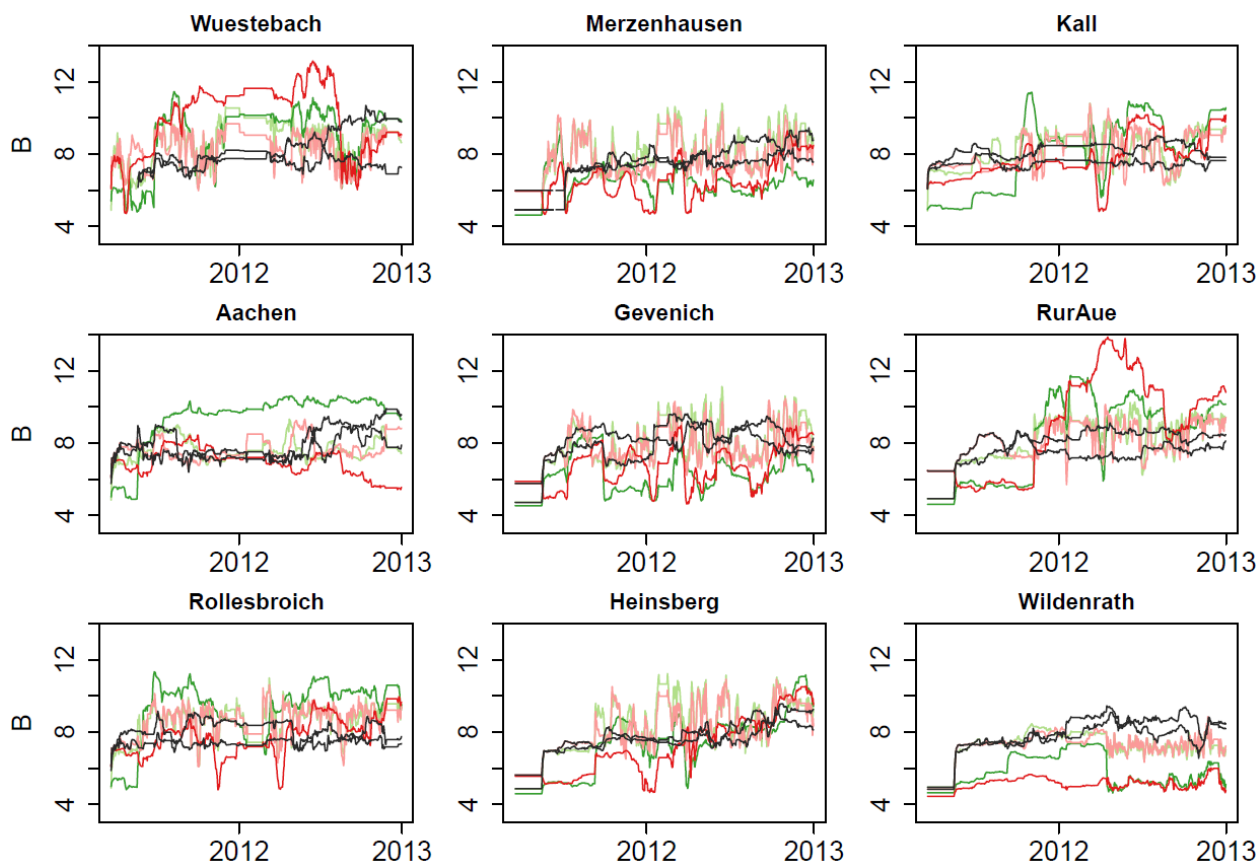


Fig. 6. Temporal evolution of the B parameter (top 15cm) for simulations with parameter update: PAR-S80-30 (green), PAR-S80-10 (light green), PAR-BK50-30 (red), PAR-BK50-10 (light red), jk-S80-30\* (black) and jk-BK50-30\* (black).

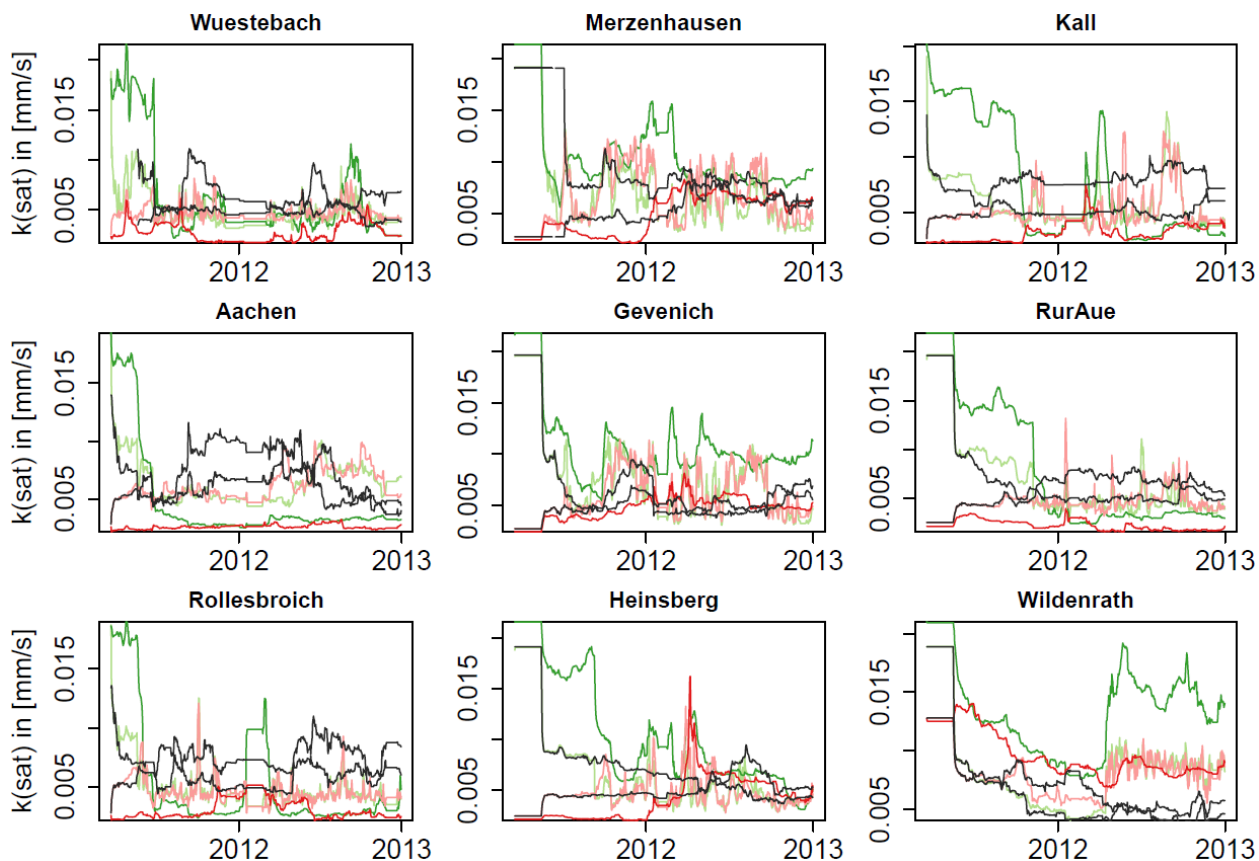


Fig. 7. Temporal evolution of saturated hydraulic conductivity (top 15cm) for simulations with parameter update: PAR-S80-30 (green), PAR-S80-10 (light green), PAR-BK50-30 (red), PAR-BK50-10 (light red), jk-S80-30\* (black) and jk-BK50-30\* (black).

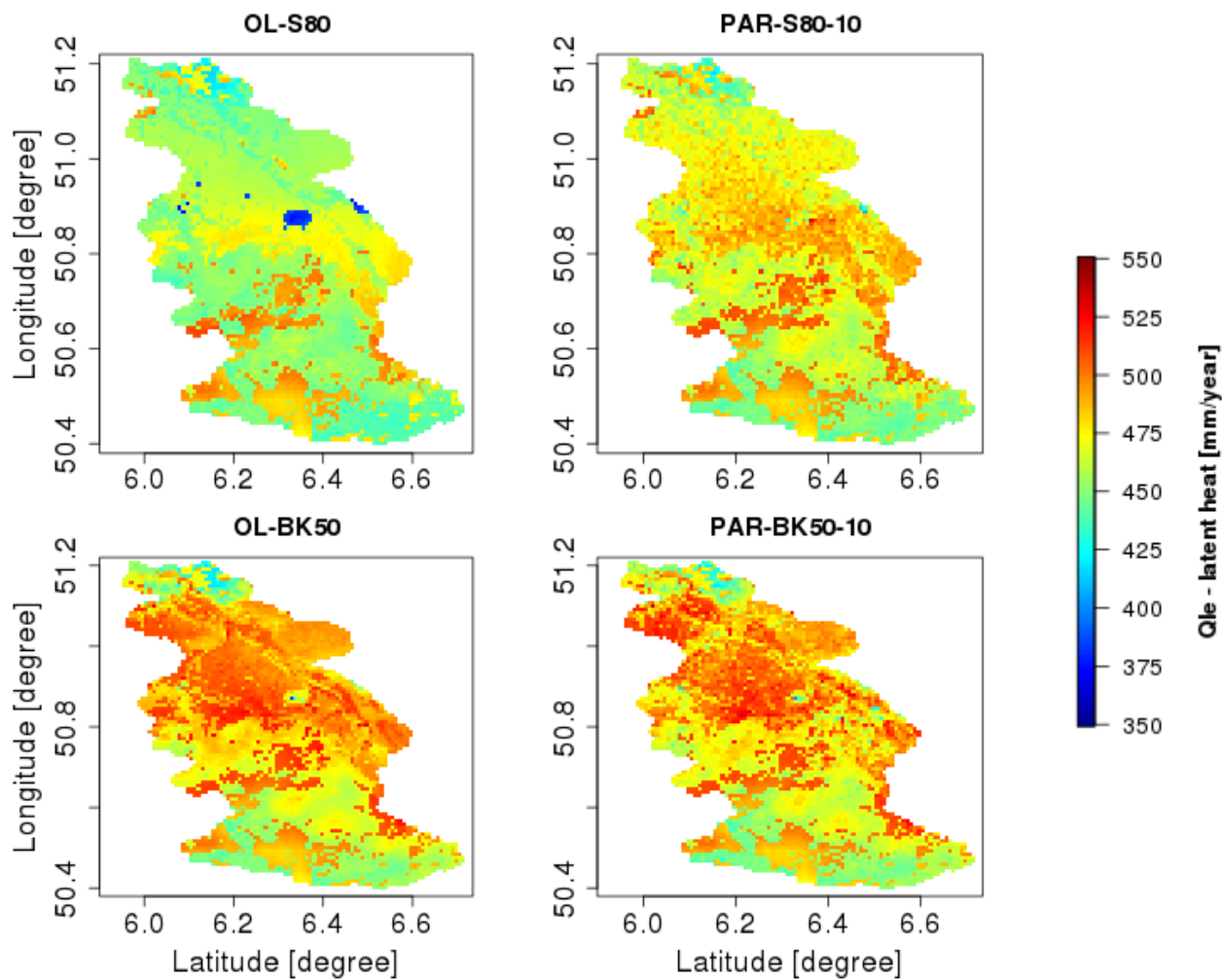


Fig. 8. Annual evapotranspiration in the evaluation period (year 2013) for simulations OL-S80, OL-BK50, PAR-S80-10 and PAR-BK50-10.



## Tables

Table 1: Site information on elevation (m.a.s.l.), average annual precipitation (mm/year), CLM plant functional type, sand content (%), clay content (%), and the date of the first SWC retrieval assimilated.

Name	m.a.s.l.	Precip.	Plant functional type	Sand	Clay	Date of first assimilation
Aachen	232	952	Crops	22	23	13.01.2012
Gevenich	108	884	Crops	22	20	07.07.2011
Heinsberg	57	814	Crops	18	19	09.09.2011
Kall	504	935	C3 non arctic grass	20	22	15.09.2011
Merzenhausen	94	825	Crops	21	22	19.05.2011
Rollesbroich	515	1307	C3 non arctic grass	22	23	19.05.2011
RurAue	102	743	C3 non arctic grass	19	26	08.11.2011
Wildenrath	76	856	Broadleaf deciduous temperate tree	65	12	07.05.2012
Wuestebach	605	1401	Needleleaf evergreen temperate tree	19	23	20.03.2011



Table 2: Overview of simulation scenarios: Open loop (OL-\*) with variation in the soil map BK50 or S80, data assimilation run with state update (Stt) or joint state- and parameter update (PAR) with variation in the soil map perturbation (-10 or -30), and jackknife evaluation runs (jk-S80-1 to 9, and jk-BK50-1 to 9).

Simulation Code	Soil Perturbation		Sand Content		Update	
	10	30	BK50	80 % fix	State	Parameter
OL-BK50		+	+			
OL-S80		+		+		
Stt-BK50		+	+		+	
Stt-S80		+		+	+	
PAR-BK50-30		+	+		+	+
PAR-BK50-10	+		+		+	+
PAR-S80-30		+		+	+	+
PAR-S80-10	+			+	+	+
jk-BK50-1 to 9		+	+		+	+
jk-S80-1 to 9		+		+	+	+



Table 3:  $E_{\text{RMS}}$  ( $\text{cm}^3/\text{cm}^3$ ) at CRP sites for open loop runs and different data assimilation scenarios, for the assimilation period (2011 and 2012).

2011 & 2012	Rollesbroich	Merzenhausen	Gevenich	Heinsberg	Kall	RurAue	Wuestebach	Aachen	Wildenrath	Average $E_{\text{RMS}}$
OL-BK50	0.054	0.067	0.039	0.035	0.042	0.027	0.041	0.032	0.017	0.039
Stt-BK50	0.033	0.041	0.021	0.022	0.030	0.024	0.038	0.023	0.017	0.028
PAR-BK50-10	0.036	0.036	0.019	0.021	0.033	0.025	0.035	0.045	0.015	0.029
PAR-BK50-30	0.031	0.034	0.018	0.019	0.027	0.023	0.040	0.044	0.016	0.028
jk-BK50-*	0.070	0.058	0.073	0.035	0.048	0.050	0.053	0.050	0.091	0.059
OL-S80	0.170	0.053	0.081	0.117	0.149	0.158	0.065	0.169	0.020	0.109
Stt-S80	0.104	0.020	0.037	0.051	0.083	0.056	0.060	0.086	0.018	0.057
PAR-S80-10	0.032	0.038	0.024	0.023	0.033	0.023	0.036	0.048	0.015	0.030
PAR-S80-30	0.029	0.035	0.018	0.019	0.027	0.023	0.039	0.068	0.016	0.030
jk-S80-*	0.082	0.038	0.063	0.026	0.062	0.034	0.038	0.073	0.095	0.057



Table 4:  $E_{RMS}$  ( $\text{cm}^3/\text{cm}^3$ ) at CRP-sites for open loop, data assimilation and jackknife simulations on the basis of a comparison with CRP SWC retrievals during the verification period (2013). For each jackknife simulation only one  $E_{RMS}$  is reported: The  $E_{RMS}$  of the location that is meant for evaluation.

Year 2013	Rollesbroich	Merzenhausen	Gevenich	Heinsberg	Kall	RurAue	Wuestebach	Aachen	Wildenrath	Average $E_{RMS}$
OL-BK50	0.044	0.065	0.036	0.027	0.048	0.038	0.048	0.042	0.017	0.041
Stt-BK50	0.041	0.054	0.034	0.027	0.049	0.038	0.048	0.041	0.018	0.039
PAR-BK50-10	0.068	0.062	0.036	0.038	0.056	0.056	0.043	0.058	0.017	0.048
PAR-BK50-30	0.052	0.061	0.035	0.033	0.068	0.048	0.043	0.048	0.035	0.047
jk-BK50-*	0.036	0.047	0.028	0.025	0.042	0.031	0.040	0.054	0.106	0.045
OL-S80	0.157	0.062	0.106	0.115	0.160	0.154	0.099	0.167	0.019	0.115
Stt-S80	0.100	0.063	0.107	0.106	0.099	0.146	0.097	0.158	0.020	0.100
PAR-S80-10	0.060	0.039	0.043	0.040	0.064	0.043	0.052	0.060	0.019	0.047
PAR-S80-30	0.049	0.059	0.037	0.036	0.053	0.032	0.046	0.047	0.035	0.044
jk-S80-*	0.079	0.046	0.042	0.036	0.059	0.038	0.063	0.044	0.105	0.057



Table 5: Bias ( $\text{cm}^3/\text{cm}^3$ ) at CRP-sites for open loop, data assimilation and jackknife simulations compared to CRP SWC retrievals during the verification period (2013). For each jackknife simulation only one bias is reported: The bias of the location that is meant for evaluation.

Year 2013	Rollesbroich	Merzenhausen	Gevenich	Heinsberg	Kall	Rur-Aue	Wuestebach	Aachen	Wildenrath	Mean absolute bias
OL-BK50	-0.03	0.06	0.01	0.00	-0.02	0.00	-0.02	0.01	0.00	0.02
Stt-BK50	-0.01	0.04	0.00	0.00	-0.01	-0.01	-0.02	0.00	0.00	0.01
PAR-BK50-10	0.06	0.05	0.01	0.02	0.04	0.04	0.02	-0.04	0.00	0.03
PAR-BK50-30	0.03	0.05	0.00	0.02	0.04	0.03	-0.01	-0.03	0.03	0.03
jk-BK50-*	-0.02	0.04	0.01	-0.01	-0.03	-0.02	-0.03	-0.05	0.11	0.04
OL-S80	-0.17	-0.05	-0.08	-0.12	-0.15	-0.16	-0.09	-0.17	-0.01	0.11
Stt-S80	-0.09	-0.05	-0.10	-0.10	-0.08	-0.14	-0.09	-0.15	-0.01	0.09
PAR-S80-10	0.03	0.05	-0.01	0.02	0.03	0.01	-0.01	-0.03	0.03	0.02
PAR-S80-30	0.04	0.02	-0.03	0.02	0.05	0.03	0.03	-0.04	-0.01	0.03
jk-S80-*	-0.07	0.03	0.02	0.02	-0.04	-0.02	-0.04	-0.03	0.10	0.04

5

**Evaluating the valueEvaluation of a network of cosmic-ray  
probes neutron sensor network for improvingimproved land  
surface modellingmodel prediction**

5 Roland Baatz<sup>1,2</sup>, Harrie-Jan Hendricks Franssen<sup>1,2</sup>, Xujun Han<sup>1,2</sup>, Tim Hoar<sup>3</sup>, Heye ~~R.~~Reemt  
Bogena<sup>1</sup> and Harry Vereecken<sup>1,2</sup>

<sup>1</sup>Agrosphere (IBG-3), Forschungszentrum Jülich GmbH, 52425 Jülich, Germany.

<sup>2</sup>HPSC-TerrSys , 52425 Jülich, Germany.

<sup>3</sup>NCAR Data Assimilation Research Section, Boulder, CO, USA.

10 *Correspondence to:* Roland Baatz (r.baatz@fz-juelich.de)

**Abstract:** ~~Land surface models can model matter and energy fluxes between the land surface and atmosphere, and provide a lower boundary condition to atmospheric circulation models. For these applications, accurate In-situ soil moisture quantification is sensors provide highly desirable accurate but not always possible given limited observations and limited subsurface data accuracy. Cosmic ray probes (CRPs) offer an interesting alternative to indirectly measure very local soil moisture and provide an observation that can be assimilated into land surface models for improved measurements while remotely sensed soil moisture prediction. Synthetic studies have shown the potential to estimate subsurface parameters of land surface models with the assimilation of CRP observations is strongly affected by vegetation and surface roughness. In contrast, Cosmic-Ray Neutron Sensors (CRNS) allow highly accurate soil moisture estimation at the field scale which could be valuable to improve land surface model predictions. In this study, the potential of a network of CRPs/CRNS installed in the 2354 km<sup>2</sup> Rur catchment (Germany) for estimating subsurface soil hydraulic parameters and improved/improving soil moisture states is/was tested in a real world case scenario using. Data measured by the CRNS were assimilated with the local ensemble transform Kalman filter within the Community Land Model. The potential of the CRP network was tested by assimilating CRP data v. 4.5. Data of four, eight and nine CRNS were assimilated for the years 2011 and 2012 (with ~~or~~ and without soil hydraulic parameter estimation), followed by the verification year 2013, without data assimilation. This was done using (i) the regional soil map/high resolution soil map, (ii) the FAO soil map and (iii) an erroneous, biased soil map as input information for the simulations, and (ii) an erroneous, biased soil map. For the regional soil map, soil moisture characterization was only improved in the assimilation period but not in the verification period. For the FAO soil map and the biased soil map, soil moisture characterization/predictions improved in both periods strongly from/to a  $E_{RMS}$  root mean square error of  $0.11 \text{ cm}^3/\text{cm}^3$  to  $0.03 \text{ cm}^3/\text{cm}^3$  (for the assimilation period) and from  $0.12 \text{ cm}^3/\text{cm}^3$  to  $0.05 \text{ cm}^3/\text{cm}^3$  (verification/for the evaluation period) and the estimated soil hydraulic parameters were after. Improvements were limited by the measurement error of CRNS ( $0.03 \text{ cm}^3/\text{cm}^3$ ). The positive results obtained with data assimilation closer to the ones of of nine CRNS were confirmed by the regional soil map. Finally, the value of the CRP network was also evaluated with jackknifing data-jackknife experiments with four and eight CRNS used for assimilation experiments. It was found that the CRP network is able to improve soil moisture estimates at locations between the assimilation sites from-. The results demonstrate that assimilated data of a  $E_{RMS}$ -CRNS network can improve the characterization of soil moisture content at the catchment scale by updating spatially distributed soil hydraulic parameters of  $0.12 \text{ cm}^3/\text{cm}^3$  to  $0.06 \text{ cm}^3/\text{cm}^3$  (verification period), but again only if the initial soil map was biased a land surface model.~~

## 1 Introduction

Soil water content (SWC) is a key variable of land surface hydrology and has a strong control on the partitioning of net radiation between latent and sensible heat flux- (Brutsaert, 2005). Knowledge of SWC is relevant for the assessment of plant water stress and agricultural production, as well as runoff generation as a response to precipitation events (Vereecken et al., 2008;Robinson et al., 2008). In atmospheric circulation models, SWC is important as a lower boundary condition ~~and while it~~ is calculated as a state variable in land surface models. Coupling of atmospheric circulation models and land surface models allows quantifying the role of soil moisture on atmospheric processes such as soil moisture-precipitation feedbacks (Koster et al., 2004;Eltahir, 1998) and summer climate variability and drought (Seneviratne et al., 2006;Oglesby and Erickson, 1989;~~Sheffield and Wood, 2008~~;~~Seneviratne et al., 2006~~;~~Bell et al., 2015~~). It is therefore important to improve the modelling and prediction of SWC,~~but this is hampered by~~. Data assimilation of soil moisture provides a way to improve imperfect land surface model deficiencies and predictions. Here, soil moisture measurements are used to update model predictions by optimally considering the uncertainty of model initial conditions, model parameters and model forcings. However, there is a lack of high quality soil moisture data (Vereecken et al., 2016). Soil moisture measured by space-~~borne~~ remote sensing technologies provides information over large areas (~~e.g. Temimi et al., 2014~~). ~~However, space born remote sensing supplies only information on the upper few centimeters, but is strongly affected by vegetation and data are not reliable for areas with dense vegetation-surface roughness (e.g. Temimi et al., 2014)~~. Therefore, in this paper an alternative source for soil moisture information is explored- which can measure soil moisture more accurately under dense vegetation (Bogena et al., 2013). Cosmic-ray ~~probes (CRPs)~~ neutron sensors (CRNS) measure fast neutron intensity ~~which allows estimating SWC at an intermediate scale of ~15 ha (Kohli et al., 2015;Zreda et al., 2008;Desilets et al., 2010;Cosh et al., 2016;Lv et al., 2014)~~ which is ~~closer to~~ the desired application scale of land surface models (Ajami et al., 2014;Chen et al., 2007;Shrestha et al., 2014). Fast neutrons originate from ~~moderation collisions~~ of secondary cosmic particles from outer space ~~by with~~ terrestrial atoms. ~~These particles are mainly fast~~ Fast neutrons, ~~which in turn~~ are moderated most effectively by hydrogen because ~~of the mass of a neutron is similar atomic mass to that of a nucleus of the hydrogen atom~~. Therefore, the corresponding fast neutron intensity measured by ~~CRPs~~ CRNS strongly depends on the amount of hydrogen within the ~~CRP~~ CRNS footprint, allowing for a continuous non-invasive soil moisture estimate ~~over an area of ~15 ha (Kohli et al., 2015)~~ at the field scale. The spatial ~~extent~~ extent of this measurement is desirable as it matches with the desired grid cell size of a high resolution land surface model (Crow et al., 2012) and small scale heterogeneities are averaged over a larger area (Franz et al., ~~2013a;Desilets and Zreda, 2013~~;Kohli et al., 2015). Vertical measurement depth ranges from a maximum of ~70 cm under completely dry conditions and decreases to roughly ~12 cm under wet conditions

(e.g. 40 vol. % soil moisture) (~~Bogena et al., 2013~~). ~~Worldwide several CRP~~(Kohli et al., 2015; Franz et al., 2012). ~~Worldwide several CRNS~~ networks exist, like the North American COSMOS network (Zreda et al., 2012), the German ~~CRP~~CRNS network (Baatz et al., 2014) installed in the context of the TERENO infrastructure measure (Zacharias et al., 2011) ~~and~~, the Australian COSMoZ network (~~Hawdon et al., 2014~~)(Hawdon et al., 2014) and the British COSMOS-UK (Evans et al., 2016).

~~Soil moisture~~In this work, fast neutron intensity data ~~assimilation provides~~measured by CRNS are assimilated in a ~~wayland surface model, to evaluate the impact those data can have to improve imperfect soil moisture characterization and~~ land surface model predictions ~~with measured soil moisture data by merging model predictions and data, and can consider the uncertainty of initial conditions, model parameters and model forcings.~~ The Ensemble Kalman Filtering (EnKF) is one of the most commonly applied data assimilation methods (Evensen, 1994; Burgers et al., 1998). ~~Soil moisture data assimilation has been the subject of intensive study for more than a decade now. An early contribution was provided by Houser et al. (1998) who assimilated remotely sensed soil moisture observations from a microwave radiometer into a land atmosphere transfer scheme using four dimensional variational data assimilation. Rhodin et al. (1999) assimilated soil moisture data for a four day period in order to obtain an improved characterization of the lower boundary condition for an atmospheric circulation model. They also used a variational data assimilation approach. More recently, the~~The EnKF is much less CPU intensive compared to alternative methods such as the particle filter (e.g. Montzka et al., 2011) because for high dimensional problems the EnKF requires a much smaller ensemble size to achieve ~~reasonable good predictions.~~ The Ensemble Kalman Filter (Reichle et al., 2002a; Dunne and Entekhabi, 2005; Crow, 2003; ~~De Lannoy and Reichle, 2016~~), ~~and variants like~~ the Extended Kalman Filter (Draper et al., 2009; Reichle et al., 2002b), ~~four dimensional variational methods (Hulkmans et al., 2006)~~ and the Local Ensemble Transform Kalman Filter (Han et al., 2015; Han et al., 2013) were applied for updating soil moisture states in land surface models. Reichle et al. (2002a) performed a synthetic experiment using L-band microwave observations of the Southern Great Plains Hydrology Experiment (Jackson et al., 1999) to ~~analyze~~analyse the effect of ensemble size and ~~prediction error~~forecast errors. Dunne and Entekhabi (2005) showed that an Ensemble Kalman Smoother approach, where data from multiple time steps was assimilated to update current and past states, can yield a reduced prediction error compared to a pure filtering approach. More recently, state updates with the EnKF were tested for the Soil Moisture Ocean Salinity (SMOS, Kerr et al., 2012) mission. De Lannoy and Reichle (2016) assimilated SMOS temperature brightness and soil moisture retrievals into a land surface model with large improvements in surface soil moisture. However, localized error patterns were not captured well enough and locally optimized EnKF error parameters would improve prediction results further.

More recent work addressed joint ~~state-parameter estimation~~updating of model states and parameters in hydrologic and land surface models with data assimilation methods. Joint state-parameter estimation with EnKF is possible by an augmented state vector approach (Chen and Zhang, 2006), a dual approach (Moradkhani et al., 5 2005) or an approach with an additional external optimization loop (Vrugt et al., 2005). In the augmented state vector approach, parameters are included in the state vector and are updated via cross-covariances between states and parameters. The cross-covariances are estimated from the ensemble. In the dual approach, first parameters are updated by data assimilation, and the assimilation step is repeated with the updated parameters to update also the states by data assimilation. In the approach with an external optimization loop the parameters are not updated by EnKF, but in an external optimization loop. Pauwels et al. (2009) ~~optimized~~were one of the first to optimize soil hydraulic parameters of a land surface model ~~with~~by data assimilation, assimilating synthetic aperture radar data. Lee (2014) used Synthetic Aperture Radar soil moisture data to estimate soil hydraulic properties at the Tibetan plateau using the EnKF and a Soil Vegetation Atmosphere Transfer model. Bateni and Entekhabi (2012) assimilated land surface temperature with an Ensemble Kalman Smoother and achieved a better estimate of the 10 partitioning of energy between sensible and latent heat fluxes. Han et al. (~~2014b~~2014) updated soil hydraulic parameters of the Community Land Model (CLM) by assimilation of synthetic brightness temperature data with the Local Ensemble Transform Kalman Filter (LETKF) (Hunt et al., 2007)~~- and showed the potential of this approach for improving land surface states and fluxes like evapotranspiration.~~ Shi et al. (2014) used the Ensemble Kalman Filter for a synthetic multivariate data assimilation problem with a land surface model and then applied it to real data (Shi et al., 2015). ~~The Both~~ cases illustrate a way to use real world data for estimating severalillustrate that parameters ~~in hydrologic land models from different compartments can be updated successfully by multivariate data assimilation.~~ (Kurtz et al., ~~2016~~) developed a particular CPU-efficient data assimilation framework for the coupled land surface-subsurface model TerrSysMP (Shrestha et al., 2014). They 15 successfully updated  $2 \times 10^7$  states and parameters in a synthetic experiment. Whereas these studies were made with land surface models, also in soil hydrological applications recently data assimilation was used to estimate soil hydraulic parameters. Early work was by Wu and Margulis (2011, 2013) in the context of real-time control of waste water reuse in irrigation and showed the potential of EnKF also in soil hydrology. Montzka et al. (2013;2011) explored the role of the particle filter for handling non-Gaussianity in soil hydrology data assimilation. They showed that the nonlinear character of the soil moisture retention characteristic is critical for joint state-parameter estimation in data assimilation systems and showed that the Particle Filter is an interesting alternative for soil hydraulic parameter estimation for 1D problems. Erdal et al. (2014) investigated the role of 20 bias in the conceptual soil model and explored bias aware EnKF as a way to deal with it. ~~Erdal et al. (2015)~~They

argued that often the exact location of soil layers is not known and that this can severely deteriorate the performance of EnKF. Song et al. (2014) worked on a modified iterative EnKF-based filter to handle the non-linearity and non-Gaussianity of data assimilation for the vadose zone. They proposed a modified procedure which avoids the high CPU-need of a fully iterative method, but which still gives stable results. Also Erdal et al. (2015) focused on handling of strong non-Gaussianity of the state variable in EnKF under very dry conditions. They showed that classical EnKF fails under such conditions and proposed two alternative strategies, both involving transformation of state variables, which performed favourably also under very dry conditions with strongly skewed pressure distributions. All these studies on joint state-parameter estimation showed in general that estimation of soil hydraulic or land surface parameters improves model predictions (strongly), but can be unstable for strongly non-Gaussian distributions and non-linear problems. ~~Montzka et al. (2013;2011) explored the role of the particle filter for handling non Gaussianity in soil hydrology data assimilation. They showed that the ability of a data assimilation system to correct the soil moisture state and estimate hydraulic parameters strongly depends on the nonlinear character of the soil moisture retention characteristic. Song et al. (2014) worked on a modified iterative filter to handle the non-linearity and non-Gaussianity of data assimilation for the vadose zone.~~ For a further literature review on data assimilation in the context of hydrological and land surface models we refer to Reichle (2008) and Montzka et al. (2012).

Shuttleworth et al. (2013) developed the Cosmic Ray Soil Moisture Interaction Code (COSMIC), which is a forward operator to be applied for assimilating neutron intensity observations from ~~CRPs~~CRNS. The COSMIC code was evaluated for several sites (Baatz et al., 2014;Rosolem et al., 2014). ~~Its capability to propagate surface soil moisture information into the deeper soil column was analyzed by Rosolem et al. (2014).~~ The COSMIC operator was successfully implemented in the Data Assimilation Research Testbed (Rosolem et al., 2014) to allow for state updating by the Ensemble Adjustment Kalman Filter (Anderson, 2001). ~~The surface soil moisture information was propagated into greater soil depth than only the measurement depth using COSMIC in combination with data assimilation (Rosolem et al., 2014).~~ The COSMIC operator was implemented in a python interface that couples the land surface model CLM and the LETKF for joint state parameter updating (Han et al., 2015). Neutron counts measured by ~~CRPs~~CRNS have been used in data assimilation studies to update model states (Han et al., 2015;Rosolem et al., 2014). Soil hydraulic parameters were also updated by assimilation of neutron counts ~~in one synthetic study (Han et al., 2016), but only for a synthetic study which showed~~showing its feasibility. ~~CRPs~~CRNS were also used for inverse estimation of soil hydraulic parameters of the Hydrus-1D model (Villarreyes et al., 2014).

This work further explores the value of measured neutron intensity by ~~CRPs~~CRNS to improve modelling of terrestrial systems at the catchment scale (Simmer et al., 2015) using a land surface model. ~~Compared to existing work the~~The main novelties are:

(i) Data from a network of nine ~~CRPs~~CRNS were assimilated in the Community Land Model version 4.5 (CLM) with an evaluation of the information gain by this assimilation at the ~~larger~~ catchment scale. Until now evaluations with ~~CRPs~~CRNS were made for a single location, but not for a complete network of ~~CRPs~~CRNS. It is a very important question whether ~~CRPs~~CRNS can also improve the soil moisture characterization at the ~~larger~~ catchment scale ~~and how dense the CRP network should be.~~ The high variability of soil moisture at a short distance could potentially limit the ~~CRPs~~CRNS measurement value and make updating of soil moisture contents further away from the sensor meaningless. On the other hand, soil moisture, soil maps and atmospheric forcings show spatial correlations over larger distances (Kirkpatrick et al., 2014; Korres et al., 2015) which suggests that ~~CRPs~~CRNS measurements potentially carry important information to update soil moisture contents for larger regions: (e.g. Han et al., 2012). If it is found that ~~CRPs~~CRNS networks with a density like in this study (nine stations per 2354 km<sup>2</sup>) can improve soil moisture content characterization at the ~~larger~~ catchment scale, this is of high relevance and importance for agricultural applications, flood prediction and protection, and regional weather prediction (Whan et al., 2015; Koster et al., 2004; Seneviratne et al., 2010). The main research question addressed in this paper is therefore whether a ~~CRPs~~CRNS network of the density as in this study can improve large scale soil moisture characterization ~~by state and parameter updates.~~

(ii) Soil hydraulic parameters ~~were~~are updated in this study together with the soil moisture states in a real-world case study ~~at the larger catchment scale.~~ The study in this paper also allows some evaluation of the feasibility of the updated large scale soil hydraulic parameters.

~~In the following paragraphs are presented the model site and the measurements (2.1), the Community land Model and its parameterization (2.2), the COMIC forward model (2.3) and the data assimilation procedure (2.4).~~

## 2 Materials and methods

### 2.1 Site description and measurements

The model domain, the Rur catchment (2354 km<sup>2</sup>), is situated in western Germany and illustrated in Fig. 1. ~~Most prominent vegetation types are agricultural land use (mainly in the North), grassland, and coniferous and deciduous forest.~~ The altitude varies between 15 m a.s.l. in the flat northern part and 690 m a.s.l. in the hilly southern part. Precipitation, evapotranspiration and land use follow the topography. The dominant land use types are agriculture (mainly in the North), grassland, and coniferous and deciduous forest. Annual precipitation

ranges between less than 600 mm in the North ~~to~~and 1200 mm in the hilly South (Montzka et al., 2008). Annual potential evapotranspiration varies between 500 mm in the South and 700 mm in the North (Bogena et al., 2005). The Rur catchment ~~CRP~~CRNS network comprises nine ~~CRP~~CRNS (CRS1000, HydroInnova LLC, 2009) which were installed in 2011 and 2012 (Baatz et al., 2014). Climate and soil texture of the ~~CRP~~CRNS sites can be found in Table 1.

The ~~CRP~~CRNS were calibrated in the field using gravimetric soil samples. At each site, 18 soil samples were taken along three circles with distances of 25, 75 and 175 meters from the ~~CRP~~CRNS, six samples evenly distributed along each circle. Each sample was extracted with a 50.8 x 300 mm round HUMAX soil corer (Martin Burch AG, Switzerland). The samples were split into 6 sub-samples with 5 cm length each and oven dried at 105 °C for 48 hours to measure dry soil bulk density and soil moisture. ~~Lattice water was determined for each site using a heat conductivity detector. Lattice water, hydrogen from organic and an-organic sources, was determined for each site using a heat conductivity detector (Ray, 1954).~~ Soil bulk density, soil moisture, lattice water and 12 hour averaged measured neutron intensity were used to determine calibration parameters specific for each ~~CRP and the COSMIC operator.~~CRNS and the COSMIC operator. ~~This represents a compromise between the measurement noise (which follows a Poisson distribution) and the assumed variation of environmental variables over the averaging time window (Iwema et al., 2015).~~

## 2.2 Community land model and parameterization

The Community Land Model version 4.5 (CLM) was the land surface model of choice for simulating water and energy exchange between the land surface and the atmosphere (Oleson et al., 2013). Some of the key processes which are ~~solved~~modelled by CLM are radiative transfer in the canopy space, interception of precipitation by the vegetation and evaporation from intercepted water, water uptake by vegetation and transpiration, soil evaporation, photosynthesis, as well as water and energy flow in the subsurface. SWC in CLM is influenced by precipitation, infiltration into the soil, water uptake by vegetation, surface evaporation and surface and subsurface runoff. ~~Oleson et al. (2013) provide further details on CLM4.5. To limit the scope and complexity of this study, CLM was run using satellite phenology, e.g. prescribed leaf area index data and the biogeochemical module turned off.~~To limit the scope and complexity of this study, CLM was run using satellite phenology e.g. prescribed leaf area index data and the biogeochemical module turned off. ~~The biogeochemical module allows CLM to model the vegetation development dynamically, but it requires a large spin-up of 1000 years and little additional gain is expected for this study from these additionally modelled processes.~~

The spatial domain is discretized by rectangular grid cells by CLM. Each grid cell may have several types of land cover: Lake, urban, vegetated, wetland, and glacier. The vegetated part of the grid cell can be covered by several plant functional types which are all linked to a single soil column. The soil column is vertically discretized by ten soil layers and five bedrock layers. Layer thickness increases exponentially from 0.007 m at the surface to 2.86 m for layer 10. Vertical water flow in soils is modelled by the 1D Richards equation. Soil hydraulic parameters are determined from sand and clay content using pedotransfer functions for the mineral soil fraction (Clapp and Hornberger, 1978; Cosby et al., 1984), and organic matter content for the organic soil fraction (Lawrence and Slater, 2008).

The joint state-parameter estimation used in this study updates soil texture and organic matter in CLM. Hence, parameter estimates directly determine soil hydraulic properties in CLM. The following equations describe how soil texture and organic matter define the soil hydraulic properties in CLM such as porosity, hydraulic conductivity, the empirical exponent  $B$  and soil matric potential. Hydraulic conductivity ( $k(z)$  in mm/s) at the depth  $z$  between two layers ( $i$  and  $i+1$ ) is a function of soil moisture ( $\theta$  in  $\text{m}^3/\text{m}^3$  in layers  $i$  and  $i+1$ ), saturated hydraulic conductivity ( $k_{sat}$  in mm/s at  $z$ ), saturated soil moisture ( $\theta_{sat}$  in  $\text{m}^3/\text{m}^3$ ) and the empirical exponent  $B$  ( $B(z_i)$  in mm/s), saturated soil moisture ( $\theta_{sat}$  in  $\text{m}^3/\text{m}^3$ ) and the empirical exponent  $B$  (Oleson et al., 2013):

$$k(z) = \left\{ \begin{array}{l} \phi_{ice} k_{sat,z} \left[ \frac{\theta_i(\theta_i + \theta_{i+1})}{0.5(\theta_{sat,i} + \theta_{sat,i+1})} \right]^{2B_i+3} \quad 1 \leq i \leq N_{levsoi} - 1 \\ \phi_{ice} k_{sat,z} \left( \frac{\theta_i}{\theta_{sat,i}} \right)^{2B_i+3} \quad i = N_{levsoi} \end{array} \right\} \quad \text{---} k(z_i) =$$

$$\left\{ \begin{array}{l} \phi_{ice} k_{sat}(z_i) \left[ \frac{(\theta_i + \theta_{i+1})}{(\theta_{sat,i} + \theta_{sat,i+1})} \right]^{2B_i+3}, \quad 1 \leq i \leq N_{levsoi} - 1 \\ \phi_{ice} k_{sat}(z_i) \left( \frac{\theta_i}{\theta_{sat,i}} \right)^{2B_i+3}, \quad i = N_{levsoi} \end{array} \right.$$

where  $\phi_{ice}$  is the ice impedance factor. The ice impedance factor was implemented to simplify an increased tortuosity of water flow in a partly frozen pore space. It is calculated with  $\phi_{ice} = 10^{-\Omega F_{ice}}$  using the resistance factor  $\Omega = 6$  and the frozen fraction of soil porosity  $F_{ice} = \theta_{ice}/\theta_{sat,i}$ . Soil hydraulic properties are calculated separately for the mineral (*min*) and organic matter (*om*) soil components. Total porosity  $\theta_{sat,i}$  is calculated using the fraction of organic matter ( $f_{om,i}$ ) with:

$$\theta_{sat,i} = (1 - f_{om,i})\theta_{sat,min,i} + f_{om,i}\theta_{sat,om}$$

where the organic matter porosity is  $\theta_{sat,om} = 0.9$  and sand content in % determines the mineral soil porosity  $\theta_{sat,min}$  as:

$$\theta_{sat,min} = 0.489 - 0.00126 \times \%sand \quad 3$$

Analogous, the exponent  $B$  is calculated with

$$B_i = (1 - f_{om,i})B_{min,i} + f_{om,i}B_{om} \quad 4$$

Where  $B_{om} = 2.7$  is the organic exponent and the mineral exponent  $B_{min,i}$  is determined by clay content in % with:

$$B_{min,i} = 2.91 + 0.159 \times \%clay \quad 5$$

Saturated hydraulic conductivity is calculated for a connected and an unconnected fraction of the grid cell with:

$$k_{sat}[z_i](z_i) = (1 - f_{perc})k_{sat,uncon}[z_i](z_i) + f_{perc,i}k_{sat,om}[z_i](z_i) \quad 6$$

where  $f_{perc,i}$  is the fraction of a grid cell where water flows with saturated hydraulic conductivity of the organic matter ( $k_{sat,om}[z_i](z_i)$  in mm/s) through the organic material only, the so called connected flow pathway; whereas the saturated hydraulic conductivity of the unconnected part ( $k_{sat,uncon}[z_i](z_i)$  in mm/s) depends on organic and mineral saturated soil hydraulic conductivity:

$$k_{sat,uncon} = (1 - f_{perc}) \left( \frac{1 - f_{om}}{k_{sat,min}} + \frac{f_{om} - f_{perc}}{k_{sat,om}} \right)^{-1} \quad 7$$

where saturated hydraulic conductivity for mineral soil is calculated from the grid cell sand content as:

$$k_{sat,min}[z_i] = 0.0070556 \times 10^{-0.884+0.0153 \times \%sand} \quad 8$$

The fraction  $f_{perc}$  is calculated with:

$$f_{perc} = \begin{cases} 0.908 \times (f_{om} - 0.5)^{0.139}, & f_{om} \geq 0.5 \\ 0, & f_{om} < 0.5 \end{cases} \quad 9$$

$$f_{perc} = 0 \quad f_{om} < 0.5 \quad 10$$

Soil matric potential (mm) is defined as function of saturated soil matric potential (mm) with:

$$\psi_i = \psi_{sat,i} \left( \frac{\theta_i}{\theta_{sat,i}} \right)^{-B_i} = [(1 - f_{om,i})\psi_{sat,min,i} + f_{om,i}\psi_{sat,om}] \left( \frac{\theta_i}{\theta_{sat,i}} \right)^{-B_i} \quad 10$$

where saturated organic matter matric potential is  $\psi_{sat,om} = -10.3$  ~~mm~~ and saturated mineral soil matric potential is calculated from sand content as:

$$\psi_{sat,min,i} = -10.0 \times 10^{1.88 - 0.0131 \times \%sand} 10^{1.88 - 0.0131 \times \%sand} \quad 11$$

### 2.3 Cosmic-ray forward model

SWC retrievals were calculated from neutron intensity observations with the ~~Cosmic~~Cosmic-ray Soil Moisture Interaction Code (COSMIC) (Shuttleworth et al., 2013) following calibration results and the procedure of Baatz et al. (2014). COSMIC parameterizes ~~interactions between neutrons and atoms in~~neutron transport within the soil subsurface, ~~relevant for soil moisture estimation. COSMIC and~~ was calibrated against the more complex Monte Carlo Neutron Particle model MCNPx (Pelowitz, 2005) ~~and, COSMIC~~ needs considerably less CPU-time than the MCNPx model. ~~The reduced CPU time need and the physically based parameterization make COSMIC a suitable data assimilation operator.~~ The code was tested at multiple sites for soil moisture determination (Baatz et al., 2014; Rosolem et al., 2014) and analyzed in detail by Rosolem et al. (2014).

COSMIC assumes that a number of high energy neutrons enter the soil. In the soil, ~~the number of~~ high energy neutrons ~~are~~ reduced by ~~interaction with~~interactions within the soil leading to ~~isotropic~~ generation of fast neutrons ~~with less energy~~ in each soil layer. Before resurfacing, ~~the number of~~ fast neutrons ~~are~~ reduced again by ~~their interaction with nuclei of elements within~~soil ~~interaction~~ (Shuttleworth et al., 2013). The number of neutrons  $N_{CRP}$  that reaches the ~~CRPCRN~~ can be summarized in a single integral as

$$N_{CRP} = N_{COSMIC} \int_0^{\infty} \left\{ A(z) [\alpha \rho_s(z) + \rho_w(z)] \exp \left( - \left[ \frac{m_s(z)}{L_1} + \frac{m_w(z)}{L_2} \right] \right) \right\} \cdot dz \quad 12$$

where  $N_{COSMIC}$  is an empirical coefficient that is ~~CRPCRN~~ specific and needs to be estimated by calibration,  $A(z)$  is the integrated average attenuation of fast neutrons,  $\alpha = 0.404 - 0.101 \times \rho_s$  is the site specific empirical coefficient for the creation of fast neutrons by soil,  $\rho_s$  is the dry soil bulk density in  $\text{g/cm}^3$ ,  $\rho_w$  is the total soil water density in  $\text{g/cm}^3$ ,  $m_s$  and  $m_w$  are the mass of soil and water, respectively, per area in  $\text{g/cm}^2$ .  $L_1 = 162.0 \text{ g cm}^2$  and  $L_2 = 129.1 \text{ g cm}^2$  are ~~empirical coefficients~~scattering lengths for fast neutrons in solids and water, ~~respectively~~, that were estimated using the MCNPx code (Shuttleworth et al., 2013). The integrated average attenuation of fast neutrons  $A(z)$  can be found numerically by solving

$$A(z) = \left( \frac{2}{\pi} \right) \int_0^{\pi/2} \exp \left( \frac{-1}{\cos(\theta) \left[ \frac{m_s(z)}{L_3} + \frac{m_w(z)}{L_4} \right]} \right) \int_0^{\pi/2} \exp \left( \frac{-1}{\cos(\gamma) \left[ \frac{m_s(z)}{L_3} + \frac{m_w(z)}{L_4} \right]} \right) \cdot d\theta d\gamma \quad 13$$

where  $\theta$  is the angle along a vertical line below the ~~CRPCRNS~~ detector to the element that contributes to the attenuation of fast neutrons,  $L_3 = -31.65 + 99.29 \times \rho_s$  ~~is determined from soil bulk density~~ and  $L_4 = 3.16 \text{ g cm}^{-2}$  ~~is another empirical coefficient estimated~~ are the scattering length for fast neutrons in soil and water, respectively, determined using the MCNPx code (Shuttleworth et al., 2013). The COSMIC operator is discretized into 300 ~~vertical~~ layers of one cm thickness up to a depth of three meters. For each CLM grid cell in the model domain, simulated SWC in all CLM layers is used to generate a weighted SWC retrieval using the COSMIC code. Simulated SWC is handed from the CLM simulation history files to the COSMIC operator. Given the vertical SWC distribution of the individual CLM ~~soil column~~ grid cell, COSMIC internally calculates the contribution of each layer to the simulated neutron intensity signal at the ~~COSMIC~~ soil surface in COSMIC. In this study, the contribution of each CLM soil layer was used to calculate the weighted CLM SWC retrieval corresponding to the vertical distribution of simulated SWC in each grid cell.

Measured neutron intensity of ~~CRPsCRNS~~ was used to inversely determine a ~~CRPCRNS~~ SWC retrieval as by Baatz et al. (2014) assuming a homogeneous vertical SWC distribution. Then, the weighted CLM SWC retrieval is used in the data assimilation scheme to relate the ~~CRP SWC retrieval to the model state~~ CRNS SWC retrieval to the model state. Alternatively, neutron flux data could be assimilated directly within the catchment. This would require calibration data throughout the catchment which is only feasible using spatially distributed data sets (e.g. Avery et al., 2016). However, high stands of biomass are a major factor for calibration in the Rur catchment (Baatz et al., 2015) and estimates of biomass come along with high uncertainties. To circumvent introducing these additional uncertainties, SWC retrievals are assimilated in this study. Changes in on-site biomass were assumed negligible.

#### 2.4 Data assimilation

~~This~~ To further expand the work of Han et al. (2016), this study uses the local ensemble transform Kalman filter (LETKF) (Hunt et al., 2007) to assimilate SWC retrievals by ~~CRPsCRNS~~ into the land surface model CLM. ~~Besides other Ensemble Kalman Filter variants, the LETKF is applied in atmospheric sciences (Liu et al., 2012; Miyoshi and Kunii, 2012), ocean science (Penny et al., 2013) and also in land surface hydrology (Han et al., 2014a; Han et al., 2015).~~ Updates were calculated either for SWC states or jointly for SWC states and soil parameters depending on the experiment setup. For state updates only, the LETKF was used as proposed by Hunt et al. (2007). Calculations were made for an ensemble of model simulations which differed related to variations in model forcings and input parameters. The states of the different ensemble members are indicated by

$\mathbf{x}_i^f$  where  $i=1, \dots, N$  and  $N$  is the number of ensemble members.  $f$  marks the model prediction or forecast before the update. The individual state vectors  $\mathbf{x}_i^f$  contain the CLM-simulated SWC of the ten soil layers and the vertically weighted SWC retrieval obtained with the COSMIC operator. For each grid cell, a ~~vector~~matrix  $\mathbf{X}^f$  can be constructed which contains the deviations of the simulated states with respect to the ensemble mean  $\bar{\mathbf{x}}^f$ :

$$\mathbf{X}^f = [\mathbf{x}_1^f - \bar{\mathbf{x}}^f, \dots, \mathbf{x}_N^f - \bar{\mathbf{x}}^f] \quad 14$$

5 In case of joint state-parameter updates, a state augmentation approach was followed (Hendricks Franssen and Kinzelbach, 2008; Han et al., ~~2014b~~2014). In this case, the augmented model state ~~vector~~matrix  $\mathbf{X}^f$  is constructed from the simulated SWC of the ten soil layers, weighted SWC, and the grid cell's sand, clay and organic matter content.

10 In order to relate the measured neutron intensity with the simulated SWC of CLM, the observation operator  $\mathbf{H}$  (COSMIC) is applied on the measured neutron intensity in order to obtain the expected weighted SWC retrieval at each of the observation locations for each of the stochastic realizations:

$$\mathbf{y}_i^f = \mathbf{H}(\mathbf{x}_i^f) \quad 15$$

The ensemble realizations of the modelled SWC ~~retrieval~~retrievals at the measurement locations  $\mathbf{y}_1^f$  to  $\mathbf{y}_N^f$  with respect to the ensemble mean  $\bar{\mathbf{y}}^f$  are stored in the ~~vector~~matrix  $\mathbf{Y}^f$ :

$$\mathbf{Y}^f = [\mathbf{y}_1^f - \bar{\mathbf{y}}^f, \dots, \mathbf{y}_N^f - \bar{\mathbf{y}}^f] \quad 16$$

15 The observation error correlation was reduced in space by the factor  $f_{red}$  using the spherical model:

$$f_{red} = 1 - (1.5 \times d/d_{max}) + (0.5 \times [d/d_{max}]^3) \quad 17$$

where  $d$  is the distance to the observation and  $d_{max} = 40km$  is the maximum observation correlation length, about half the size of the catchment. Only SWC retrievals within the maximum observation correlation length were used for assimilation. This leads to a 'localized' size of  $\mathbf{Y}^f$  and the observation error covariance matrix  $\mathbf{R}$ . The intermediate covariance matrix  $\mathbf{P}^a$  (also called analysis error covariance matrix) is calculated according to:

$$\mathbf{P}^a = [(N-1)\mathbf{I} + \mathbf{Y}^{fT}\mathbf{R}^{-1}\mathbf{Y}^f] \quad 18$$

20 In addition, the mean weight vector  $\bar{\mathbf{w}}^a$  is obtained as follows:

$$\bar{\mathbf{w}}^a = \mathbf{P}^a \mathbf{Y}^{fT} \mathbf{R}^{-1} (\mathbf{y}^0 - \bar{\mathbf{y}}^f) \quad 19$$

where  $\mathbf{y}^0$  ~~is CRP~~ contains the CRNS SWC retrieval retrievals at the measurement locations. In the ensemble space, a perturbation matrix  $\mathbf{W}^a$  is calculated from the symmetric square root of  $\mathbf{P}^a$ :

$$\mathbf{W}^a = [(\mathbf{N} - 1)\mathbf{P}^a]^{1/2} \quad 20$$

The final analysis  $\mathbf{X}^a$  is obtained from:

$$\mathbf{X}^a = \bar{\mathbf{x}}^f + \mathbf{X}^f [\bar{\mathbf{w}}^a + \mathbf{W}^a] \quad 21$$

A more detailed description of the LETKF can be found in (Hunt et al., 2007) and details on the implementation of the LETKF in combination with CLM are given by (Han et al., 2015) Han et al. (2015).

### 3 Model and Experiment Setup

#### 3.1 Model Setup

In this study, discretization and parameterization of the hydrological catchment was done on the basis of high resolution data. The ~~model of the~~ Rur catchment ~~domain is~~ was spatially discretized by rectangular grid cells of 0.008 degree size (~750 m). The model time step was set to hourly. Land cover was assumed to consist of vegetated land units only, and a single plant functional type (PFT) for each grid cell was defined. The plant functional types were derived from a remotely sensed land use map using RapidEye and ASTER data with 15 m resolution (Waldhoff, 2012). ~~Sand content~~ Contents of sand, clay ~~content~~ and organic matter ~~content~~ were derived from the high resolution regional soil map BK50 (Geologischer Dienst Nordrhein-Westfalen, 2009). ~~The BK50 soil map provides the high resolution soil texture for the catchment and is the most detailed soil map available for the defined region. As an alternative, simulations were also performed for a biased soil texture distribution with a fixed sand content of 80 % and clay content of 10 % (S80 soil map). This represents a large error with respect to the expected true soil properties. It allows~~ Alternative simulations were also performed with the FAO soil map of the global Harmonized World Soil Database (FAO, 2012) and with a biased soil texture with a fixed sand content of 80 % and clay content of 10 % (S80 soil map). Average sand and clay content are 22.5% and 21.4% for the BK50 soil map and 39% and 22% for the FAO soil map. The FAO soil map and the biased soil map represent large error with respect to the soil properties of the BK50 soil map. The FAO soil map and S80 soil map simulations allow evaluating the joint state-parameter estimation approach because given the expected bias, we can evaluate ~~whether and~~ to what ~~extent~~ the soil properties are modified by the data assimilation ~~to be closer to the available high resolution soil map. In addition,~~ This is important because in many regions across the Earth a high resolution soil map is not available ~~and land~~ Land surface models ~~which~~ are

applied for those regions, for example in the context of global simulations, and hence might be strongly affected by the error in soil properties. ~~It was tested how this impacted the simulation results.~~

5 Maximum saturated fraction, a surface parameter which is used for runoff generation, was calculated from a 10 meter digital elevation model (scilands GmbH, 2010). Leaf area index data were derived from monthly averaged Moderate Resolution Imaging Spectrometer data (MODIS). CLM was ~~supplied~~forced with hourly atmospheric ~~forcing~~ data from ~~the~~ COSMO DE reanalysis data set for the years 2010 to 2013 from the German Weather Service (DWD). The data was downscaled from a resolution of 2.8 km<sup>2</sup> to the CLM resolution using linear interpolation based on Delaunay triangulation. Forcing data include precipitation ~~in mm/s~~, incident solar and 10 longwave radiation ~~in W/m<sup>2</sup>~~, air temperature ~~in K~~, air pressure ~~in hPa~~, wind speed ~~in m/s~~ and relative humidity ~~in kg/kg~~ at the lowest atmospheric level.

### 3.2 Model ensemble

15 Uncertainty was introduced into the regional CLM model by perturbed soil parameters and external model forcings. Contents of sand, clay and organic matter were perturbed with spatially correlated noise from a uniform sampling distribution with mean zero and standard ~~deviation 10 % or 30 % (Han et al., 2015)~~deviations 10 % and 30 % (Han et al., 2015). Soil texture perturbation considers that in CLM a single set of pedotransfer functions is assumed to be valid throughout the globe while usually pedotransfer functions are specific for regions (e.g. Patil and Singh, 2016). In other words, the perturbation of soil texture also covers the uncertainty in 20 the pedotransfer function itself. By perturbing texture, soil parameters are also perturbed through the pedotransfer functions used in CLM as specified in Sect. 2.2. Precipitation ( $\sigma = 0.5$  or 1.0; lognormal distribution) and shortwave radiation ( $\sigma = 0.3$ ; lognormal distribution) were perturbed with multiplicative noise with mean equal to one. Longwave radiation ( $\sigma = 20 \text{ W m}^{-2}$ ) and air temperature ( $\sigma = 1\text{K}$ ) were perturbed with additive noise. The forcing perturbations were imposed with correlations in space (5 km) using a fast Fourier 25 transform. Correlation in time was introduced with an AR(1)-model with autoregressive parameter ~~=~~0.33. These correlations and standard deviations were chosen based on previous data assimilation experiments (Reichle et al., 2010; Kumar et al., 2012; De Lannoy et al., 2012; Han et al., 2015). In this work, only results for precipitation perturbation with  $\sigma = 0.5$  will be shown as results for  $\sigma = 1.0$  were ~~very~~ similar. An ensemble size of 95 realizations was used in the simulations. Based on previous work (Baatz et al., 2015), the SWC retrieval 30 uncertainty for CRPs/CRNS was estimated to be  $0.03 \text{ cm}^3/\text{cm}^3$  while fluctuations in the measurement standard deviation, related to the non-linear relation between observed neutron intensity and SWC, were assumed negligible.

### 3.3 Experiment set-up

All simulation experiments in this study used initial conditions from a single five year spin-up run. ~~For the five year spin-up run, in which~~ a single forcing data set of the year 2010 was repeatedly used as atmospheric input. The soil moisture regime became stable after the five years spin-up period, and additional spin-up simulations would not affect soil moisture in the consecutive years. After this five year spin-up, soil parameters and forcing data of the consecutive years were perturbed. From 1<sup>st</sup> Jan. 2011 onwards, CLM was propagated forward with an ensemble of 95 realizations. On 20<sup>th</sup> Mar. 2011, the first SWC retrieval was assimilated and assimilation of SWC retrievals continued until 31<sup>st</sup> Dec. 2012. ~~From 1<sup>st</sup> January 2013 to 31<sup>st</sup> December 2013~~In the data assimilation period soil properties were estimated at every time step when observations were made available. For the year 2013, the model was propagated forward without data assimilation but with an ensemble of 95 realizations. The year 2013 was used exclusively as evaluation period for data assimilation experiments.

In total, 2631 simulation experiments were carried out using different setups (Table 2). ~~Two~~The present setups are intended to cover three different initial soil maps, three different sizes of a CRNS network and two different parameter perturbations. Three open loop simulations were run ~~for the BK50 soil map (OL-BK50) and the S80 soil map (OL-S80), respectively,~~ without data assimilation and soil parameter perturbation of 30 % ~~for the BK50 soil map (OL-BK50), the FAO soil map (OL-FAO) and the S80 soil map (OL-S80).~~ These simulations are referred to as reference runs for the respective soil map. Simulation results of data assimilation runs were compared to the reference runs for quantification of data assimilation benefits. Simulations were done with joint state-parameter estimation (PAR-), ~~two for the S80 soil map (PAR-S80-) and -\*),~~ two for the BK50 soil map (PAR-BK50-), ~~for which soil -\*),~~ one for the FAO soil map (PAR-FAO-30), and two for the S80 soil map (PAR-S80-\*). Soil texture was perturbed by 10 % ~~and 30 %-or 30 % as indicated by the experiment name (Table 2).~~ Two simulations were done with state updates only for the BK50 soil map (Stt-BK50) and the S80 soil map (Stt-BK50), ~~where soil texture was perturbed by 30 %. These eight).~~ These ten simulations form the basic set of experiments.

Besides the data assimilation experiments also a larger number of jackknifing simulations ~~was run~~were conducted to evaluate the impact of the CRNS data assimilation performance. These simulations allow evaluating the impact of the CRP network to improve on SWC characterization at ~~other unobserved~~ locations, ~~without CRP, in the model domain.~~ In ~~nine~~ jackknife ~~experiment~~ experiments, data from eight ~~CRP~~CRNS locations ~~were~~was assimilated (jk8-\* simulations) and data of the one CRP remaining CRNS was ~~excluded from~~

the assimilation not assimilated but kept for evaluation purpose. In addition, three simulations were conducted where data of four CRNS were assimilated (jk4-\* simulations) and data of the five remaining CRNS was used for evaluation. These three simulations represent a CRNS network with much less than the existing nine CRNS. At the evaluation location/locations, simulated SWC (which is affected by the assimilation of the other eight probes) was compared to CRPCRNS SWC retrievals. For jackknife simulations, the perturbation of soil texture was set to 30 % and precipitation perturbation was done with  $\sigma = 0.5\%$ . States and parameters at these sites were jointly updated, and simulations were made using either the BK50 and/or the S80 soil maps as input/initial parameterization. Therefore, a total of 4821 jackknife simulations (jk-S80-\* and jk-BK50-\*) was/were performed (two soil maps times nine different simulations leaving away one CRP at a time).

Simulation results were evaluated with the root mean square error ( $E_{RMS}$ ):

$$RMSE = \sqrt{\frac{\sum_{t=1}^n (SWC_{t,CLM} - SWC_{t,CRP})^2}{n}} \quad E_{RMS} = \sqrt{\frac{\sum_{t=1}^n (\theta_{t,CLM} - \theta_{t,CRNS})^2}{n}} \quad 22$$

where  $n$  is the total number of time steps,  $SWC_{t,CLM}$  is the SWC simulated by CLM SWC retrieval at time step  $t$  and  $SWC_{t,CRP}$  is the CRPCRNS SWC retrieval at time step  $t$ . In case SWC was assimilated at the corresponding time step,  $SWC_{t,CLM}$  is SWC prior to assimilation. In the case the  $E_{RMS}$  is estimated at a single point in time over all CRPs/CRNS available, the number of time steps  $n$  can be replaced by the number of CRPs/CRNS available. The second evaluation measurement in this study is the bias which is, in contrast to the  $E_{RMS}$ , a measure for systematic deviation:

$$bias = \frac{\sum_{t=1}^n (SWC_{t,CLM} - SWC_{t,CRP})}{n} \quad \frac{\sum_{t=1}^n (\theta_{t,CLM} - \theta_{t,CRNS})}{n} \quad 23$$

## 4 Results and Discussion

### 4.1 General Results

Table 3 summarizes the performance statistics in terms of  $E_{RMS}$  and bias for the assimilation period (2011 and 2012) and evaluation period (2013). Presented are results for the open loop scenarios/scenarios with the BK50, FAO and S80, and data assimilation scenarios. Errors of open loop simulations are higher/were highest for the S80-simulation than for (0.11 cm<sup>3</sup>/cm<sup>3</sup>), followed by the BK50-FAO simulation at all sites but Merzenhausen. At Merzenhausen  $E_{RMS}$  was 0.054 cm<sup>3</sup>/cm<sup>3</sup> for the S80 soil map and (0.06707 cm<sup>3</sup>/cm<sup>3</sup> for) and the BK50 soil map. Open loop simulations with the S80 soil map resulted in  $E_{RMS}$  values above 0.10 cm<sup>3</sup>/cm<sup>3</sup> at five of nine sites. At all sites data assimilation results with the S80 soil map improved SWC compared to the

open-loop simulations. This was also the case simulation ( $0.04 \text{ cm}^3/\text{cm}^3$ ). Mean absolute bias was highest for the S80 soil map ( $0.11 \text{ cm}^3/\text{cm}^3$ ), now as high for the FAO soil map ( $0.06 \text{ cm}^3/\text{cm}^3$ ) and lowest for the BK50 soil map simulations at all sites but Aachen where  $E_{\text{RMS}}$  was larger than for the open loop run. In general, data ( $0.02 \text{ cm}^3/\text{cm}^3$ ). Data assimilation improved simulations more for the S80 soil map ( $E_{\text{RMS}}$  reduced by  $0.07908 \text{ cm}^3/\text{cm}^3$ ) than for the FAO soil map ( $E_{\text{RMS}}$  reduced by  $0.04 \text{ cm}^3/\text{cm}^3$ ) or the BK50 soil map ( $E_{\text{RMS}}$  reduced by  $0.01 \text{ cm}^3/\text{cm}^3$ ). Room for improvement with the BK50 soil map runs was more limited because of the smaller open loop errors. Nevertheless, after state updating alone the BK50 soil map still gave smaller errors than the S80 soil map. However, joint state-parameter estimation further improved simulation results by reducing  $E_{\text{RMS}}$  values and the parameter. The BK50 soil map led to  $E_{\text{RMS}}$  values in open loop simulations lower than  $0.05 \text{ cm}^3/\text{cm}^3$  which left little room for error reduction considering a measurement error of  $0.03 \text{ cm}^3/\text{cm}^3$ . However, slight improvements by  $0.01 \text{ cm}^3/\text{cm}^3$  were possible at monitored locations in the data assimilation period but not in the evaluation period. Joint state-parameter estimation improved simulation results as shown by the reduced  $E_{\text{RMS}}$  and bias for the S80 and the FAO soil maps. The verification period (2013) with the updated soil hydraulic parameters for the FAO soil map resulted in an  $E_{\text{RMS}}$  value of  $0.05 \text{ cm}^3/\text{cm}^3$ , also clearly an improvement compared to the open loop run with an  $E_{\text{RMS}}$  of  $0.07 \text{ cm}^3/\text{cm}^3$  (Table 3). Joint state-parameter updating resulted in similar  $E_{\text{RMS}}$  values for the BK50 ( $0.028 \text{ cm}^3/\text{cm}^3$ ) and S80 all three initial soil map ( $0.03 \text{ cm}^3/\text{cm}^3$ ). The  $E_{\text{RMS}}$  maps the BK50, FAO and S80 soil map (each  $0.03 \text{ cm}^3/\text{cm}^3$ ). State updates (Stt-S80) improved  $E_{\text{RMS}}$  and bias for the S80 soil map ( $E_{\text{RMS}} = 0.06 \text{ cm}^3/\text{cm}^3$  for assimilation period) but much less compared to the joint state-parameter updates (PAR-S80-30). The  $E_{\text{RMS}}$  and bias for simulations with 10 % and 30 % perturbation of soil texture values did not show very different results, only showed very small differences (smaller than  $0.01 \text{ cm}^3/\text{cm}^3$ ).

The temporal course of simulated soil moisture in 2011 at the two sites Merzenhausen and Gevenich and Merzenhausen is shown in Fig. 2. The figure illustrates that simulated SWC at both sites was lowest with the S80 soil map than (OL-S80), highest with the BK50 soil map. In Gevenich and Merzenhausen, mean (OL-BK50) and the FAO soil map resulted in intermediate soil moisture (OL-FAO). Mean open loop SWC in 2011 was  $0.17 \text{ cm}^3/\text{cm}^3$  for the S80 soil map at both sites,  $0.24 \text{ cm}^3/\text{cm}^3$  for the FAO soil map and  $0.27 \text{ cm}^3/\text{cm}^3$  for the BK50 soil map at both sites. CRP measurements at Merzenhausen. Measurements with CRNS started in May 2011. In the data assimilation runs SWC was immediately affected at the Merzenhausen and Gevenich sites as soon as Merzenhausen CRP SWC retrievals were assimilated. The simulated SWC for the PAR-S80-30 data assimilation run increased as compared to the S80 open loop simulation. The at Merzenhausen. At Gevenich, the first observation at Gevenich was recorded on July 7<sup>th</sup>, 2011. In the data assimilation run shown (PAR-S80-

30) modelled SWC was immediately affected at both sites, Merzenhausen and Gevenich, as soon as data at Merzenhausen was assimilated. By ~~that date, the July,~~ simulated ~~CLM-SWC retrieval with the biased soil map~~ and data assimilation (PAR-S80-30) was already close to the ~~CRP~~CRNS SWC retrieval at the Gevenich site (Fig. 2) ~~due to SWC updates which showed to have a -). This demonstrates the~~ beneficial impact of data

5 availability for assimilation at one site and the information brought into space by the data assimilation scheme. Fig. 2 also shows that the BK50 open loop run was close to the observed SWC at both sites, even without data assimilation.

Fig. 3 shows the temporal course of SWC from January 2011 to December 2013 at Heinsberg and Wildenrath.

10 Assimilation and evaluation results are shown for the ~~ease of open loop (OL-S80 and OL-FAO) simulations,~~ only state updates (Stt-S80), joint state-parameter updates (PAR-S80-30), ~~only state updates (Stt-S80), open loop (OL-S80) and CRP~~ and CRNS SWC retrievals. At Heinsberg, results show that ~~assimilated simulated~~ SWC with assimilation was closer to the ~~CRP-SWC retrieval~~CRNS when both states and parameters were updated (PAR-S80-30) than if only states were updated (Stt-S80). This is the case ~~in for both periods~~ the assimilation period and ~~in~~ the evaluation period. At the beginning of the evaluation period, ~~(first few days of 2013),~~ the Stt-S80 simulation shows an increase in bias between ~~modeled CLM-SWC retrievals and CRP-SWC retrieval within the first few days of 2013.~~ modelled SWC and CRNS. The bias of Stt-S80 remained throughout the evaluation period. In contrast, ~~modeled SWC during the evaluation period was close to the CRP-SWC retrieval~~ if parameters were previously updated (PAR-S80-30) modelled SWC was close to the CRNS during the evaluation

15 period. Open loop SWC modelled with the FAO soil map is lower than the CRNS SWC retrievals at Heinsberg and higher than CRNS SWC retrievals at Wildenrath. At Wildenrath, results of the OL-S80 run suggest that the initial sand content of the biased soil map is closer to the optimal sand content than the sand content of the FAO soil map. Consequently, the OL-FAO bias was  $-0.05 \text{ cm}^3/\text{cm}^3$  and  $0.05 \text{ cm}^3/\text{cm}^3$  for Heinsberg and Wildenrath, respectively (Table 3 and 4 in Annex). At both sites, absolute bias was reduced with joint state-parameter

20 updates to equal or less than  $0.01 \text{ cm}^3/\text{cm}^3$  (S80 and FAO soil map). The reduced bias is also well reflected in the temporal course of modelled SWC with joint state-parameter updates (PAR-S80-30).

It is interesting to notice that the error values for the verification period are very similar if soil hydraulic parameters were estimated in the assimilation period, independent of the initial soil map (Table 3).  $E_{\text{RMS}}$  values

30 for the 2013 simulations with state updates only (Stt-BK50 and Stt-BK50) show that in the evaluation period the improvements by state updates (without parameter updates) were small (reduction by  $0.02 \text{ cm}^3/\text{cm}^3$  and  $0.00 \text{ cm}^3/\text{cm}^3$  for S80 and BK50, respectively) compared to the improvements obtained by joint state-parameter

updates (reduction by  $0.07 \text{ cm}^3/\text{cm}^3$  for S80). This illustrates the benefits of joint state-parameter updates compared to state updates only, and that soil moisture states are strongly determined by soil hydraulic parameters. The CRP at Wildenrath started operating on May 7<sup>th</sup>, 2012. SWC retrievals at other CRPs were assimilated already from May 2011 onwards and affected SWC at Wildenrath (Fig. 3). Until May 2012, The case of only state updates also illustrates that the improved characterization of soil moisture states in the assimilation period results in improved initial states for the verification period (Table 3) but in the verification period these improvements lose its influence quickly over time (Fig. 3 shows assimilated SWC (Stt S80 and PAR S80 30) was higher than open loop SWC. However, no SWC retrievals were available at the Wildenrath site for comparison during this period. When SWC retrievals from the CRP at Wildenrath became available and were assimilated into the model, assimilated (Stt S80 and PAR S80 30) and open loop (OL S80) SWC were close to CRP SWC retrievals. This was the case throughout the remaining assimilation and evaluation period. These results suggest that the high sand content of the biased soil map is not far from the optimal sand content at Wildenrath. Therefore, at Wildenrath, the high sand content of both soil maps (60 % and 80 %) resulted in good modeling results already for the open loop runs. This suggests that before May 2012, simulated SWC of the open loop runs with either soil map represented more realistic SWC than assimilated SWC during this period. This will be discussed further in the discussion section.

#### **4.2 — Verification period**

The year 2013 was the verification year without data assimilation.  $E_{\text{RMS}}$  values for the evaluation period 2013 are reported in Table 4. On the one hand, BK50 data assimilation runs with joint state-parameter estimation resulted in improved SWC at three out of the nine sites compared to open loop BK50 runs. For the other six sites results worsened compared to the corresponding BK50 open loop run.  $E_{\text{RMS}}$  values increased from an average of  $0.041 \text{ cm}^3/\text{cm}^3$  (OL-BK50) over all sites to  $0.047 \text{ cm}^3/\text{cm}^3$  (PAR-BK50-30). On the other hand, for the S80 soil map, all sites except Wildenrath had significantly reduced  $E_{\text{RMS}}$  values for the case of data assimilation including parameter updating compared to the S80 open loop run. For the S80 simulations, average  $E_{\text{RMS}}$  over all sites for 2013 was on average  $0.12 \text{ cm}^3/\text{cm}^3$  for the open loop run and  $0.04 \text{ cm}^3/\text{cm}^3$  for the run including data assimilation. In case only states were updated (Stt S80 and Stt BK50),  $E_{\text{RMS}}$  was also slightly reduced (compared to open loop runs) for the majority of sites during the evaluation period in 2013. On average, this reduction was  $0.016 \text{ cm}^3/\text{cm}^3$  for the S80 soil map (Stt S80) and  $0.002 \text{ cm}^3/\text{cm}^3$  for the BK50 soil map (Stt BK50). At sites, where  $E_{\text{RMS}}$  was larger for data assimilation runs with state updating (compared to open loop runs), the increase was only  $0.001 \text{ cm}^3/\text{cm}^3$ .

Bias calculated on the basis of a comparison of hourly SWC measured by CRP and simulated for 2013 is reported in Table 5. The average bias for the S80 open loop run is  $0.11 \text{ cm}^3/\text{cm}^3$  while it is  $0.02 \text{ cm}^3/\text{cm}^3$  for the BK50 open loop run. Bias of the BK50 open loop run was positive at Merzenhausen, Gevenich, Heinsberg, and Aachen, and it was negative at Rollesbroich, Kall, RurAue, and Wuestebach. Bias was zero at Wildenrath for the BK50 open loop run. Bias of the S80 open loop run was negative at all sites indicating that modeled SWC was higher than measured SWC. Joint state parameter updates reduced the absolute bias on average to  $0.03 \text{ cm}^3/\text{cm}^3$  (PAR-S80-30) and  $0.02 \text{ cm}^3/\text{cm}^3$  (PAR-S80-10) for the S80 soil map. In case of the BK50 soil map, the bias in 2013 increased to  $0.03 \text{ cm}^3/\text{cm}^3$  by joint state parameter updates. State updates without parameter updates reduced the biases only marginally to  $0.01 \text{ cm}^3/\text{cm}^3$  for the BK50 soil map and to  $0.09 \text{ cm}^3/\text{cm}^3$  for the S80 soil map. This indicates that state updates also can slightly improve SWC characterization in the verification period due to improved initial conditions.

).

#### 4.34.2 Temporal evolution of mean $E_{\text{RMS}}$

Fig. 4 shows the temporal evolution of the hourly  $E_{\text{RMS}}$  calculated for all nine CRPs/CRNS.  $E_{\text{RMS}}$  was highest for the S80 open loop run and lowest for the PAR-S80-30 simulation. The FAO soil map resulted in errors mostly between  $0.05 \text{ cm}^3/\text{cm}^3$  and  $0.1 \text{ cm}^3/\text{cm}^3$  which is lower than the S80 soil map but not as good as simulation results with joint state-parameter updates (PAR-S80-30) or with the BK50 soil map (OL-BK50). State updates did not improve modeled SWC as much as joint state-parameter updates improved modeled SWC. The  $E_{\text{RMS}}$  in case of Stt-S80 also falls behind. For most of the time, the  $E_{\text{RMS}}$  of the BK50-Stt-S80 run is larger than the  $E_{\text{RMS}}$  of the OL-BK50 run. During the evaluation period, also the open loop run through most of with the time. Joint FAO soil map (OL-FAO) performs better than the Stt-S80 run. In contrast, joint state-parameter updates for the S80 soil map improved the  $E_{\text{RMS}}$  throughout most of the time compared to the open loop simulations based on the BK50 and S80 soil maps. During the assimilation period 2011-2012, (OL-BK50, OL-FAO and OL-S80). As shown in Fig. 4, the PAR-S80-30 simulation performed best out of the four simulations during the assimilation period 2011-2012. During the evaluation period 2013, OL-BK50 and PAR-S80-30 performed equally well except in summer 2013 when the PAR-S80-30 simulation yielded much higher  $E_{\text{RMS}}$  values than the BK50 open loop run.

#### 4.44.3 Jackknife simulations

The jackknife simulations investigated the impact of the network of CRPs/CRNS data for improving estimates of simulated SWC at locations between the CRPs, outside the network, beyond the CRNS stations. Spatial

improvements are possible by spatial correlation structures of atmospheric forcings, soil hydraulic parameters and soil moisture which are taken into account by the local ensemble transform Kalman filter. The errors and bias shown in Table 4 refer to the two open loop simulations (for the S80 soil map and the BK50 soil map) and the 18 jackknife simulations. All simulations with the BK50 and the S80 soil map. On average over the three runs where only data of four CRNS were assimilated (jk4-S80-\*), the  $E_{RMS}$  was  $0.07 \text{ m}^3/\text{m}^3$  which is much lower than the  $E_{RMS}$  for the open loop run ( $0.12 \text{ m}^3/\text{m}^3$ ), and only a bit higher than the case where eight CRNS were assimilated ( $E_{RMS}=0.06 \text{ m}^3/\text{m}^3$  for jk8-S80-\*). The improved simulation results were also due to the bias reduction from  $0.11 \text{ m}^3/\text{m}^3$  to  $0.05 \text{ m}^3/\text{m}^3$  in case of four and  $0.04 \text{ m}^3/\text{m}^3$  in case of eight assimilated CRNS. However, for the BK50 soil map where  $E_{RMS}$  ( $0.04 \text{ m}^3/\text{m}^3$ ) and bias ( $0.02 \text{ m}^3/\text{m}^3$ ) of the open loop run were already good, the jackknife simulations led to slightly higher  $E_{RMS}$  ( $0.05 \text{ m}^3/\text{m}^3$ ) and bias ( $0.04 \text{ m}^3/\text{m}^3$ ). More detailed site statistics (Tables 1 to 4 of the Annex) demonstrate that all jackknife simulations with the S80 soil map resulted in an improved  $E_{RMS}$  at the jackknife simulation locations compared to the open loop simulation, except for Wildenrath. In all cases the  $E_{RMS}$  was smaller than  $0.10 \text{ m}^3/\text{m}^3$ . Error reduction was smaller at sites where the open loop error was smaller. At sites with large open loop  $E_{RMS}$ , the assimilation could reduce the  $E_{RMS}$  by 50 % or more. In case of the BK50 soil map, the jackknife simulations resulted in  $E_{RMS}$  values below  $0.10 \text{ m}^3/\text{m}^3$  at all sites. However, in this case only at Merzenhausen the  $E_{RMS}$  was reduced during the data assimilation period. At Wildenrath, the  $E_{RMS}$  was highest for jk-BK50 ( $0.091 \text{ m}^3/\text{m}^3$ ) and jk-S80 ( $0.095 \text{ m}^3/\text{m}^3$ ). The average absolute bias for the

The jackknife simulations illustrate that a network of CRNS can improve modelled SWC if the soil map information is not sufficient. This suggests that assimilation of CRNS data is particularly useful for regions with little information on subsurface parameters. A trade-off can be expected between the initial uncertainty on soil moisture and parameters, and the density of a CRNS network. In case of a large uncertainty, like in regions with limited information about soils or a strongly biased soil map (e.g. FAO or S80 soil map) and a low density of meteorological stations, a sparse network of probes can already be helpful for improving soil moisture characterization. The results of the real world jackknife experiments was  $0.04 \text{ cm}^3/\text{cm}^3$  for both soil maps, BK50 and S80, in the evaluation period 2013 (Table 5). Hence, bias in the jk-S80-\* simulations improved compared to the open loop run but not demonstrated that already four CRNS are beneficial but it is desirable to have more CRNS for improved parameter estimates. The results also suggest that the additional information gain for an extra CRNS reduces for a denser network, because the soil moisture characterization did not improve so much more if eight instead of four CRNS were used for assimilation. However, in regions with a high density of meteorological stations and a high resolution soil map it can be expected that a denser CRNS network is needed

than in this study to further lower the error of soil moisture characterization. Further potentially synthetic experiments in the jk-BK50-\* simulations, where bias was already small other regions with networks of CRNS are needed to get more quantitative information about this.

#### 4.5.4.4 Temporal evolution of ~~parameters~~ parameter estimates and parameter uncertainty

The temporal evolution of ~~the percentage~~ sand content estimates during the assimilation period for the nine CRP sites with CRNS is shown in Fig. 5 for PAR-S80-30, PAR-S80-10, PAR-BK50-30, PAR-BK50-10, ~~jk8-S80-30\* and jk8-BK50-30\*.~~ Time series start on March 20<sup>th</sup>, 2011, the date of the first assimilated ~~CRP~~CRNS SWC retrieval at Wuestebach. At Wuestebach and sites within the influence sphere of Wuestebach (Aachen, Kall and Rollesbroich) ~~show also a change in~~, sand content estimates were updated from ~~this date~~March 20<sup>th</sup>, 2011 onwards. ~~All~~Because of the localization, all other sites show a ~~change~~first update in sand content in May 2012 when Rollesbroich and Merzenhausen start operating, and their data ~~is~~was assimilated. ~~All~~During the data assimilation period with joint state-parameter updates, all sites show variability in sand content ~~over time.~~ estimates over time with differences in magnitude. Values and spread in sand content estimates amongst the experiments is smaller at the sites Merzenhausen, Gevenich, RurAue, Heinsberg and Wildenrath, compared to the sites Wuestebach, ~~Kall, Aachen and RurAue,~~ Rollesbroich and Heinsberg show some peaks in the time series; ~~were spread is considerably larger.~~ At the sites Merzenhausen, ~~Aachen, Gevenich, and Wildenrath show a smoother course compared to the other sites.~~ Sand levels approach a constant site specific value for the sites Merzenhausen (45 %), Kall (30 %), ~~Kall, Gevenich (41 %),~~ RurAue (30 %), ~~and~~ Heinsberg (42 %) and Wildenrath (62 %) with a reasonable spread amongst the experiments. The spread in estimated sand content for the sites Wuestebach, Aachen and Rollesbroich is larger, and it seems not to have stabilized at the end of the assimilation. ~~Sand content estimates, sand content estimates~~ of the jackknife simulations ~~was~~were close to the sand content of the other data assimilation experiments with joint state-parameter estimation. A comparison of parameter estimates at the end of the assimilation period indicates that initial soil parameterization has a limited effect on the resulting parameter estimates. ~~at the sites Merzenhausen, Gevenich, RurAue and Heinsberg.~~ Evolution of the sand content for the jackknife simulations showed larger deviations from the sand content estimated by other data assimilation experiments for the sites Wuestebach, Kall, Aachen, Rollesbroich and Wildenrath. Parameter estimates of jk8-BK50-\* and jk8-S80-\* are close together at the end of the assimilation period.

~~The~~Estimates of the soil hydraulic parameter B and saturated hydraulic conductivity are shown in Fig. 6 and Fig. 7 for PAR-S80-30, PAR-S80-10, PAR-BK50-30, PAR-BK50-10, ~~jk8-S80-30\* and jk8-BK50-30\*.~~

Updates of soil hydraulic parameters start in March and May 2011 with the assimilation of CRNS\_SWC retrievals depending on the location. The B parameter increases estimates increase for all simulations. Throughout the whole assimilation period the empirical B parameter varies considerably within short time intervals. The total range of the B parameter estimates is between 2.7 and 14 at all sites. At the sites  
5 Merzenhausen, Kall, Aachen, Gevenich and Rollesbroich, B generally ranges between 6 and 10. At Wuestebach, Heinsberg and RurAue, B ranges estimates of B range most of the time between 8 and 12, and at Wildenrath, B is below 8. Initial saturated hydraulic conductivity  $k_{sat}$  is rather high ( $k_{sat} > 0.015$  mm/s) in case of high sand content i.e. for the S80 soil map, and rather low ( $k_{sat} < 0.005$  mm/s) in case of low sand content i.e. for the BK50 soil map. In case of the S80 soil map, at all sites except Wildenrath, high initial saturated hydraulic  
10 conductivity decreases,  $k_{sat}$  estimates decrease quickly by through joint state-parameter updates to values below 0.01 mm/s. The initial spread in  $k_{sat}$  values estimates amongst the simulation scenarios decreases at most sites. At Wuestebach, Merzenhausen, Aachen, Gevenich, RurAue and Heinsberg, the spread is rather small particularly at the end of the assimilation period, while at Wildenrath  $k_{sat}$  ranges from 0.005 to 0.015 for individual experiments at the end of the assimilation period. The discussion section will elaborate more on this.

15  
Temporally not stable parameter estimates imply that there may be multiple or seasonal optimal parameter values. This is also supported by the findings of the temporal behaviour of site average  $E_{RMS}$  (Fig. 4) e.g. during the evaluation period when in the dry summer 2013 the  $E_{RMS}$  peaks for the PAR-S80-30 simulation. In this context, it is important to mention that many possible error sources were not subject to calibration in this study but could be crucial for an even better modelled soil moisture and more reliable soil parameter estimation. In this study we only considered uncertainty of soil parameters, but also vegetation parameters are uncertain. Also a number of other CLM-specific hydrologic parameters (e.g. decay factor for subsurface runoff and maximum subsurface drainage) strongly influence state variables in CLM and hence show potential for optimization (Sun et al., 2013). Considering this uncertainty from multiple parameters could give a better parameter uncertainty characterization (Shi et al., 2014). Precipitation is also an important forcing for hydrologic modelling. For this study, precipitation data from the COSMO DE re-analysis were used. A product which optimally combines precipitation estimates from radar and gauge measurements is expected to give better precipitation estimates than the reanalysis. This could improve the soil moisture characterization and also potentially lead to better parameter estimates. Further improvements and constraining of parameter uncertainty is also possible using multivariate data assimilation with observations such as latent heat flux (e.g. Shi et al., 2014). Also other error sources related to the model structure play a significant role. These options should be subject of future investigations.

#### 4.6.4.5 Latent heat and sensible heat flux

Latent heat flux or evapotranspiration (ET) is another important diagnostic variable of ~~the CLM model and~~ surface models (e.g. Best et al., 2015) and of importance for atmospheric models. Results of the data assimilation experiments showed that soil texture updates altered soil moisture states significantly. In Fig. 8 it is shown that joint state-parameter estimation also altered ET ~~during the evaluation period~~. Fig. 8 shows ET within the evaluation period 2013 across the whole catchment for four ~~simulations~~ simulation experiments. On the one hand, ET was similar for both open loop simulations (OL-S80 and OL-BK50) in the South of the catchment. On the other hand, ET in the North was up to 80 mm per year lower for the S80 open loop run compared to the BK50 open loop run. ~~Regarding open loop runs, the~~ The differences can be linked to the drier soil conditions ~~in~~ ease for OL-S80 compared to OL-BK50 simulation results. The differences in ET between the runs with and without parameter updates were larger for the S80 soil map than for the BK50 soil map. For PAR-S80-10, ET increased by up to 40 mm per year in the ~~Northern~~ northern part of the catchment through data assimilation. ~~The differences between open loop ET and data assimilation ET were larger for the S80 soil map than for the BK50 soil map. This could be related to while the change in ET from OL-BK50 to PAR-BK50-10 is rather small. This is linked to the comparatively larger update in SWC in case of the S80 scenario compared to the BK50 scenario.~~ updates made to soil hydraulic parameters.

## 5 Discussion

~~The applied data assimilation scheme improved soil moisture characterization in the majority of simulation experiments with the regional Community Land Model (CLM). During 2011 and 2012, the biased S80 soil map gave a  $E_{RMS}$  up to  $0.17 \text{ cm}^3/\text{cm}^3$  (at Rollesbroich) in the open loop simulation which left plenty of room for improvements. The soil map BK50 led to  $E_{RMS}$ -values in open loop simulations below  $0.05 \text{ cm}^3/\text{cm}^3$  which left little room for error reduction considering the measurement error of  $0.03 \text{ cm}^3/\text{cm}^3$ . For the simulations starting with 80 % sand content, sand content was closer to the values of the BK50 soil map after joint state parameter estimation. However, the temporal evolution of the updated soil texture and the soil hydraulic parameters was not stable. Temporal fluctuations imply that there may be multiple or seasonal optimal parameter values. This is also supported by the findings of the temporal behavior of  $E_{RMS}$  during the evaluation period e.g. when in the dry summer 2013 the  $E_{RMS}$  peaked in the PAR-S80-30 simulation. Many possible error sources were not subject to calibration in this study but they could be crucial for an even better soil moisture and more stable soil parameter estimation. In this study we only considered uncertainty of soil parameters, but also vegetation parameters are uncertain. Also a number of other CLM specific hydrologic parameters (e.g. decay factor for subsurface runoff and maximum subsurface drainage) strongly influence state variables in CLM and hence show also potential for~~

5 optimization. Considering this uncertainty could give a better uncertainty characterization. Precipitation is an important forcing for the model calculations and its estimate could be improved. ~~For this study, precipitation data from the COSMO-DE re-analysis were used. A product which optimally combines gauge measurements and precipitation estimates from radar could give better precipitation estimates. This could improve the soil moisture characterization and also potentially lead to better parameter estimates. Also other error sources like the ones related to the model structure play a significant role. This should be subject of future investigation.~~

10 Evaluation simulations for 2013 led to partly improved and partly deteriorated  $E_{RMS}$  values when the BK50 soil map was used as prior information on the soil hydraulic properties. The simulations with the S80 soil map on the contrary showed an improved soil moisture characterization in all simulation scenarios and the updated soil hydraulic parameter estimates for those simulations approached the values of the BK50 soil map. These results indicate that the soil hydraulic parameters derived from the BK50 soil map were already well suited for soil moisture predictions and updating soil texture and soil parameters could not improve further the results.  $E_{RMS}$  values for simulations with state updates only (Stt-BK50 and Stt-S80) in 2013 imply the beneficial role of state updates only. However, the improvements in the evaluation period by state updates (without parameter values) are small compared to the improvements obtained by joint state parameter estimation. ~~This illustrates the benefits of joint state parameter updates compared to state updates only, and that soil moisture states are strongly determined by soil hydraulic parameters. It also illustrates that the improved characterization of soil moisture states in the assimilation period which results in improved initial states for the verification period loses its influence in the verification period fast over time.~~

25 The jackknife simulations illustrated that a network of CRPs can improve modeled SWC if the soil map information is not sufficient. Temporal evolution of subsurface parameters of the jackknife simulations (e.g. jk-S80\*) was close to the evolution of parameter estimates by other simulations (e.g. PAR-S80-10). Parameter estimates at jackknife test sites were inferred from multiple surrounding CRP sites, while updates at sites with CRP information were strongly inferred from single site information. Additionally, the impact of soil parameter estimates on ET is different in the North of the catchment compared to the South. While ET in the North of the catchment was impacted by the estimated soil properties during the evaluation period 2013 for PAR-S80-10, ET in the South was not as much impacted by estimated soil properties. This is related to the fact that in the North ET is moisture limited in summer, whereas in the South this is not moisture limited but energy limited. Therefore, ET in the North is sensitive to variations in soil hydraulic parameter values, whereas in the South this is not the case. In the South, ET is sensitive to model forcings like incoming shortwave radiation. Nearing et al.

(2016) came to the conclusion that soil parameter uncertainty dominates soil moisture uncertainty and forcing uncertainty dominates ET uncertainty. Our findings in the southern part of the catchment support their conclusion, but in the northern part of the catchment soil parameter uncertainty strongly affect ET. Hence particularly in the northern part of the catchment, further observations such as ET measurements are desirable for further improving the land surface model. These additional observations could be used for future land surface model benchmarking (Best et al., 2015) or for more constrained parameter estimates. ~~A comparison of parameter estimates at the end of the assimilation period indicates that initial soil parameterization has a limited effect on the resulting parameter estimates. Parameter estimates of jk-BK50-30\* and jk-S80-30\* are close together at the end of the assimilation period. The CRP network led to improved results for the jackknife evaluation simulations in case of the biased soil map. This suggests that assimilation of CRP data is particularly useful for regions with little information on subsurface parameters. We expect a tradeoff between the initial uncertainty on soil moisture content (related to the quality of the soil map and meteorological data) and the density of a CRP network. In case of a large uncertainty, like in regions with limited information about soils and a low density of meteorological stations, a sparse network of probes can already be helpful for improving soil moisture characterization. On the other hand, in regions with a high density of meteorological stations and a high resolution soil map it can be expected that a high resolution CRP network is needed to further lower the error of soil moisture characterization. Further experiments in other regions with networks of CRPs are needed to get more quantitative information about this.~~

~~A question that remains to be answered is whether it is more beneficial to assimilate neutron counts measured by CRPs directly or to assimilate CRP-SWC retrievals derived from the neutron counts, as done in this study. Fast neutron intensity measured by CRPs is also affected by vegetation. Neutron count rate decreases with increasing biomass because of the hydrogen content in vegetation (Baatz et al., 2015). Seasonal biomass changes at a single site have a rather small impact on neutron intensity compared to differences between grass land site and a forest site (Baatz et al., 2015). Therefore, using measured neutron flux directly in a data assimilation framework in a catchment with different vegetation types would require to account for the effects of vegetation types on neutron intensity. Hence, vegetation estimates for each grid cell would be necessary. At present, there are two methods that include biomass in the CRP calibration process (Baatz, Shi et al., 2015; Franz et al., 2013b) but both methods naturally require accurate biomass estimates, which are typically not available. Besides the uncertainty associated with CRP methods using biomass in the calibration process, biomass estimates also come along with high uncertainties. Therefore, in the case of a catchment with different vegetation types, it is desirable to circumvent the use of biomass estimates, and assimilate directly SWC retrievals obtained at the observation sites~~

instead of assimilating neutron intensity. Therefore, this study uses CRP SWC retrievals in the data assimilation scheme assuming that seasonal changes of biomass can be neglected.

.

## 65 Conclusions and Outlook

This real-world case study demonstrates the benefits of assimilating data from a network of nine cosmic-ray probes (CRP) neutron sensors (CRNS) soil water content (SWC) retrievals into a land surface model shows the potential of CRNS networks to improve subsurface parameterization in regional land surface models, especially if prior information on soil properties is limited. CRNS SWC retrievals were assimilated into the land surface model CLM version 4.5. Although information on neutron flux intensity was only available at few locations in the catchment, using the local ensemble transform Kalman filter (LETKF) allows updating of soil water content (SWC). SWC and subsurface parameters were updated with the LETKF at unmonitored locations in the catchment considering model and observation uncertainties. Joint state-parameter estimates improved soil moisture estimates during the assimilation and during the evaluation period. The  $E_{\text{RMS-Error}}$  and bias for the soil moisture characterization reduced strongly for simulations initialized with a biased soil map and similarly well if initialized with the FAO soil map. Simulations initialized with a biased or global soil map approached values similar to error statistics with joint state-parameter updates as the ones obtained when the regional soil map was used as input to the simulations.  $E_{\text{RMS-Error}}$  values in simulations with the regional soil map were not improved during the evaluation period, because open loop simulation results were already close to the observations. The beneficial results of joint state-parameter updates were confirmed by additional jackknife experiments. This real-world case study on assimilating CRP SWC retrievals into a land surface model shows the potential of CRP networks to improve subsurface parameterization in regional land surface models, especially if prior information on soil properties is limited, with eight and four CRNS for assimilation. In many areas of the world, less detailed only global soil maps (e.g. the FAO soil map) are available than the but no detailed high resolution regional soil map applied in this study. In has shown that in these areas, a more advanced sub-surface characterization is possible using CRP CRNS measurements and the data assimilation framework presented in this study.

For now, CRP neutron intensity observations by CRNS were not assimilated directly. In future studies it would be desirable to use the COSMIC operator for assimilating neutron intensity observations directly. However, in this case the impact of biomass on the CRP CRNS measurement signal would have to be taken into account. Therefore, it is desirable to further develop the COSMIC operator to include the impact of biomass on neutron intensities. Using the biogeochemical module of CLM would then allow to characterize model local vegetation

states as input for the measurement operator. Remotely sensed vegetation states are another option to characterize vegetation states as input for the measurement operator. Both methods require additional field measurements for the verification of vegetation state estimates. The further extension of the data assimilation framework would also enable the estimation of additional sub-land surface parameters. ~~The~~In addition, the impact of other sub-surface parameters such as subsurface drainage parameters and the surface drainage decay factor on SWC states and radiative surface fluxes has already been shown (Sun et al., 2013). Estimation of these parameters is desirable because of the inherent uncertainty of these globally tuned parameters. However, estimation of soil texture and organic matter content was demonstrated to be already beneficial for improved SWC ~~modeling~~modelling. Hence, this study represents a way forward towards the integration of ~~CRPCRNS~~ information in the calibration or real-time updating of large scale weather prediction~~land surface~~ models.

#### Data Availability

Most data presented in this study are freely available via the TERENO data portal TEODOOR (<http://teodoor.icg.kfa-juelich.de/>). Atmospheric data were licensed by the German Weather Service (DWD), and the BK50 soil map was licensed by the Geologischer Dienst Nordrhein-Westfalen.

#### 15 Acknowledgements

~~We~~The authors gratefully acknowledge the support by the SFB-TR32 "Pattern in Soil-Vegetation-Atmosphere Systems: Monitoring, Modelling and Data Assimilation" funded by the Deutsche Forschungsgemeinschaft (DFG) and TERENO (Terrestrial Environmental Observatories) funded by the Helmholtz-Gemeinschaft. The authors also gratefully acknowledge the computing time granted by the John von Neumann Institute for Computing (NIC) and provided on the supercomputer JURECA at Jülich Supercomputing Centre (JSC). Finally, the authors acknowledge and thank four anonymous referees for providing constructive comments and the Editor, Nunzio Romano, for guiding the revision process.

#### References

25 Ajami, H., McCabe, M. F., Evans, J. P., and Stisen, S.: Assessing the impact of model spin-up on surface water-groundwater interactions using an integrated hydrologic model, *Water Resour Res*, 50, 2636-2656, 10.1002/2013wr014258, 2014.  
Anderson, J. L.: An ensemble adjustment Kalman filter for data assimilation, *Mon Weather Rev*, 129, 2884-2903, Doi 10.1175/1520-0493(2001)129<2884: Aeakff>2.0.Co;2, 2001.

- Avery, W. A., Finkenbiner, C., Franz, T. E., Wang, T. J., Nguy-Robertson, A. L., Suyker, A., Arkebauer, T., and Munoz-Arriola, F.: Incorporation of globally available datasets into the roving cosmic-ray neutron probe method for estimating field-scale soil water content, *Hydrol Earth Syst Sc*, 20, 3859-3872, 10.5194/hess-20-3859-2016, 2016.
- 5 Baatz, R., Bogen, H. R., Hendricks Franssen, H. J., Huisman, J. A., Qu, W., Montzka, C., and Vereecken, H.: Calibration of a catchment scale cosmic-ray probe network: A comparison of three parameterization methods, *J Hydrol*, 516, 231-244, <http://dx.doi.org/10.1016/j.jhydrol.2014.02.026>, <http://dx.doi.org/10.1016/j.jhydrol.2014.02.026>, 2014.
- Baatz, R., Bogen, H. R., Hendricks Franssen, H. J., Huisman, J. A., Montzka, C., and Vereecken, H.: An empirical vegetation correction for soil water content quantification using cosmic ray probes, *Water Resour Res*, 51, 2030-2046, 10.1002/2014WR016443, 2015.
- 10 Bateni, S. M., and Entekhabi, D.: Surface heat flux estimation with the ensemble Kalman smoother: Joint estimation of state and parameters, *Water Resour Res*, 48, Artn W08521 10.1029/2011wr011542, 2012.
- Bell, J. E., Leeper, R. D., Palecki, M. A., Coopersmith, E., Wilson, T., Bilotta, R., and Embler, S.: Evaluation of the 2012 Drought with a Newly Established National Soil Monitoring Network, *Vadose Zone J*, 14, 10.2136/vzj2015.02.0023, 2015.
- 15 Best, M. J., Abramowitz, G., Johnson, H. R., Pitman, A. J., Balsamo, G., Boone, A., Cuntz, M., Decharme, B., Dirmeyer, P. A., Dong, J., Ek, M., Guo, Z., Haverd, V., Van den Hurk, B. J. J., Nearing, G. S., Pak, B., Peters-Lidard, C., Santanello, J. A., Stevens, L., and Vuichard, N.: The Plumbing of Land Surface Models: Benchmarking Model Performance, *J Hydrometeorol*, 16, 1425-1442, 10.1175/JHM-D-14-0158.1, 2015.
- 20 Bogen, H. R., Herbst, M., Hake, J. F., Kunkel, R., Montzka, C., Pütz, T., Vereecken, H., and Wendland, F.: MOSYRUR - Water balance analysis in the Rur basin., in: *Schriften des Forschungszentrums Jülich. Reihe Umwelt/Environment*, Jülich, 2005.
- Bogen, H. R., Huisman, J. A., Baatz, R., Hendricks-Franssen, H. J., and Vereecken, H.: Accuracy of the cosmic-ray soil water content probe in humid forest ecosystems: The worst case scenario, *Water Resour Res*, 49, 5778-5791, [Doi 10.1002/WATERWRCR.20463](http://dx.doi.org/10.1002/WATERWRCR.20463), 2013.
- 25 Bonan, G. B., Levis, S., Kergoat, L., and Oleson, K. W.: Landscapes as patches of plant functional types: An integrating concept for climate and ecosystem models, *Global Biogeochem Cy*, 16, 10.1029/2000GB001360, 2002.
- Brutsaert, W.: Hydrology : an introduction, Cambridge University Press, Cambridge : New York, xi, 605 p. pp., 2005.
- Burgers, G., van Leeuwen, P. J., and Evensen, G.: Analysis scheme in the ensemble Kalman filter, *Mon Weather Rev*, 126, 1719-1724, [Doi 10.1175/1520-0493\(1998\)126<1719:Asitek>2.0.Co;2](http://dx.doi.org/10.1175/1520-0493(1998)126<1719:Asitek>2.0.Co;2), 1998.
- 30 Chen, F., Manning, K. W., LeMone, M. A., Trier, S. B., Alfieri, J. G., Roberts, R., Tewari, M., Niyogi, D., Horst, T. W., Oncley, S. P., Basara, J. B., and Blanken, P. D.: Description and evaluation of the characteristics of the NCAR high-resolution land data assimilation system, *J Appl Meteorol Clim*, 46, 694-713, 10.1175/Jam2463.1, 2007.
- Chen, Y., and Zhang, D. X.: Data assimilation for transient flow in geologic formations via ensemble Kalman filter, *Adv Water Resour*, 29, 1107-1122, 10.1016/j.advwatres.2005.09.007, 2006.
- 35 Clapp, R. B., and Hornberger, G. M.: Empirical Equations for Some Soil Hydraulic-Properties, *Water Resour Res*, 14, 601-604, [Doi 10.1029/Wr014i004p00601](http://dx.doi.org/10.1029/Wr014i004p00601), 1978.
- Cosby, B. J., Hornberger, G. M., Clapp, R. B., and Ginn, T. R.: A Statistical Exploration of the Relationships of Soil-Moisture Characteristics to the Physical-Properties of Soils, *Water Resour Res*, 20, 682-690, [Doi 10.1029/Wr020i006p00682](http://dx.doi.org/10.1029/Wr020i006p00682), 1984.
- 40 Cosh, M. H., Ochsner, T. E., McKee, L., Dong, J. N., Basara, J. B., Evett, S. R., Hatch, C. E., Small, E. E., Steele-Dunne, S. C., Zreda, M., and Sayde, C.: The Soil Moisture Active Passive Marena, Oklahoma, In Situ Sensor Testbed (SMAP-MOISST): Testbed Design and Evaluation of In Situ Sensors, *Vadose Zone J*, 15, 10.2136/vzj2015.09.0122, 2016.
- Crow, W. T.: Correcting land surface model predictions for the impact of temporally sparse rainfall rate measurements using an ensemble Kalman filter and surface brightness temperature observations, *J Hydrometeorol*, 4, 960-973, 2003.
- 45 Crow, W. T., Berg, A. A., Cosh, M. H., Loew, A., Mohanty, B. P., Panciera, R., de Rosnay, P., Ryu, D., and Walker, J. P.: Upscaling Sparse Ground-Based Soil Moisture Observations for the Validation of Coarse-Resolution Satellite Soil Moisture Products, *Rev Geophys*, 50, Artn Rg2002 [Doi 10.1029/2011rg000372](http://dx.doi.org/10.1029/2011rg000372), 2012.
- De Lannoy, G. J. M., Reichle, R. H., Arsenault, K. R., Houser, P. R., Kumar, S., Verhoest, N. E. C., and Pauwels, V. R. N.: Multiscale assimilation of Advanced Microwave Scanning Radiometer-EOS snow water equivalent and Moderate Resolution Imaging Spectroradiometer snow cover fraction observations in northern Colorado, *Water Resour Res*, 48, Artn W01522 [Doi 10.1029/2011wr010588](http://dx.doi.org/10.1029/2011wr010588), 2012.

- Desilets, D., Zreda, M., and Ferre, T. P. A.: Nature's neutron probe: Land surface hydrology at an elusive scale with cosmic rays, *Water Resour Res*, 46, 10.1029/2009WR008726, 2010.
- Desilets, D., and Zreda, M.: Footprint diameter for a cosmic ray soil moisture probe: Theory and Monte Carlo simulations, *Water Resour Res*, 49, 3566-3575, Doi 10.1002/Wrcr.20187, 2013.
- 5 | De Lannoy, G. J. M., and Reichle, R. H.: Assimilation of SMOS brightness temperatures or soil moisture retrievals into a land surface model, *Hydrol Earth Syst Sc*, 20, 4895-4911, 10.5194/hess-20-4895-2016, 2016.
- Draper, C. S., Mahfouf, J. F., and Walker, J. P.: An EKF assimilation of AMSR-E soil moisture into the ISBA land surface scheme, *J Geophys Res-Atmos*, 114, 10.1029/2008JD011650, 2009.
- Dunne, S., and Entekhabi, D.: An ensemble-based reanalysis approach to land data assimilation, *Water Resour Res*, 41, Artn W02013  
10.1029/2004wr003449, 2005.
- Eltahir, E. A. B.: A soil moisture rainfall feedback mechanism I. Theory and observations, *Water Resour Res*, 34, 765-776, Doi 10.1029/97wr03499, 1998.
- Erdal, D., Neuweiler, I., and Wollschlager, U.: Using a bias aware EnKF to account for unresolved structure in an unsaturated zone model, *Water Resour Res*, 50, 132-147, 10.1002/2012wr013443, 2014.
- 15 | Erdal, D., Rahman, M. A., and Neuweiler, I.: The importance of state transformations when using the ensemble Kalman filter for unsaturated flow modeling: Dealing with strong nonlinearities, *Adv Water Resour*, 86, 354-365, 10.1016/j.advwatres.2015.09.008, 2015.
- Evans, J. G., Ward, H. C., Blake, J. R., Hewitt, E. J., Morrison, R., Fry, M., Ball, L. A., Doughty, L. C., Libre, J. W., Hitt, O. E., Rylett, D., Ellis, R. J., Warwick, A. C., Brooks, M., Parkes, M. A., Wright, G. M. H., Singer, A. C., Boorman, D. B., and Jenkins, A.: Soil water content in southern England derived from a cosmic-ray soil moisture observing system – COSMOS-UK, *Hydrol Process*, 30, 4987-4999, 10.1002/hyp.10929, 2016.
- 20 | Evensen, G.: Sequential Data Assimilation with a Nonlinear Quasi-Geostrophic Model Using Monte-Carlo Methods to Forecast Error Statistics, *J Geophys Res-Oceans*, 99, 10143-10162, Doi 10.1029/94jc00572, 1994.
- 25 | FAO, I., ISRIC, ISSCAS, J. Harmonized World Soil Database v1.2, Rome, Italy, 2012.
- Franz, T. E., Zreda, M., Ferre, T. P. A., Rosolem, R., Zweck, C., Stillman, S., Zeng, X., and Shuttleworth, W. J.: Measurement depth of the cosmic ray soil moisture probe affected by hydrogen from various sources, *Water Resour Res*, 48, Artn W08515  
Doi 10.1029/2012wr011871, 2012.
- 30 | Franz, T. E., Zreda, M., Ferre, T. P. A., and Rosolem, R.: An assessment of the effect of horizontal soil moisture heterogeneity on the area-average measurement of cosmic-ray neutrons, *Water Resour Res*, 49, 6450-6458, Doi 10.1002/Wrcr.20530, 2013a2013.
- Franz, T. E., Zreda, M., Rosolem, R., and Ferre, T. P. A.: A universal calibration function for determination of soil moisture with cosmic ray neutrons, *Hydrol Earth Syst Sc*, 17, 453-460, DOI 10.5194/hess-17-453-2013, 2013b.
- 35 | GmbH, s.: Digital Elevation Model 10 without anthropogenic landforms, *landforms*, 2010.
- Han, X., Li, X., Franssen, H. J. H., Montzka, C., and Vereecken, H.: Soil moisture and soil properties estimation, and Montzka, C.: Spatial horizontal correlation characteristics in the Community Land Model with synthetic brightness temperature observations, *Water Resour Res*, 50, 6081-6105, 10.1002/2013WR014586, 2014a  
land data assimilation of soil moisture, *Hydrol Earth Syst Sc*, 16, 1349-1363, 10.5194/hess-16-1349-2012, 2012.
- 40 | Han, X., Franssen, H. J. H., Rosolem, R., Jin, R., Li, X., and Vereecken, H.: Correction of systematic model forcing bias of CLM using assimilation of cosmic-ray Neutrons and land surface temperature: a study in the Heihe Catchment, China, *Hydrol. Earth Syst. Sci.*, 19, 615-629, 10.5194/hess-19-615-2015, 2015.
- Han, X., Franssen, H.-J. H., Bello, M. Á. J., Rosolem, R., Bogena, H., Alzamora, F. M., Chanzy, A., and Vereecken, H.: Simultaneous Soil Moisture and Properties Estimation for a Drip Irrigated Field by Assimilating Cosmic-ray Neutron Intensity, *J Hydrol*, <http://dx.doi.org/10.1016/j.jhydrol.2016.05.050>, <http://dx.doi.org/10.1016/j.jhydrol.2016.05.050>, 2016.
- 45 | Han, X. J., Franssen, H. J. H., Li, X., Zhang, Y. L., Montzka, C., and Vereecken, H.: Joint Assimilation of Surface Temperature and L-Band Microwave Brightness Temperature in Land Data Assimilation, *Vadose Zone J*, 12, Doi 10.2136/vzj2012.vzj2012.0072, 2013.
- Han, X. J., Franssen, H. J. H., Montzka, C., and Vereecken, H.: Soil moisture and soil properties estimation in the Community Land Model with synthetic brightness temperature observations, *Water Resour Res*, 50, 6081-6105, 10.1002/2013WR014586, 2014b2014.
- 50 | Hawdon, A., McJannet, D., and Wallace, J.: Calibration and correction procedures for cosmic-ray neutron soil moisture probes located across Australia, *Water Resour Res*, 50, 5029-5043, 10.1002/2013WR015138, 2014.

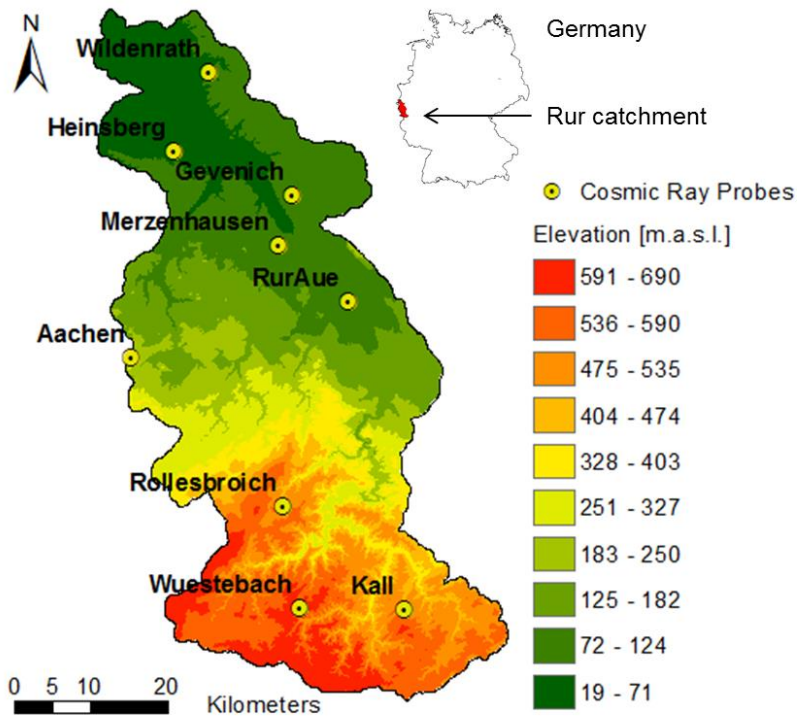
- Hendricks Franssen, H. J., and Kinzelbach, W.: Real-time groundwater flow modeling with the Ensemble Kalman Filter: Joint estimation of states and parameters and the filter inbreeding problem, *Water Resour Res*, 44, Artn W09408 Doi 10.1029/2007wr006505, 2008.
- 5 ~~Houser, P. R., Shuttleworth, W. J., Famiglietti, J. S., Gupta, H. V., Syed, K. H., and Goodrich, D. C.: Integration of soil moisture remote sensing and hydrologic modeling using data assimilation, *Water Resour Res*, 34, 3405-3420, Doi 10.1029/1998wr900001, 1998.~~
- Hunt, B. R., Kostelich, E. J., and Szunyogh, I.: Efficient data assimilation for spatiotemporal chaos: A local ensemble transform Kalman filter, *Physica D*, 230, 112-126, DOI 10.1016/j.physd.2006.11.008, 2007.
- 10 ~~Hurkmans, R., Paniconi, C., and Troch, P. A.: Numerical assessment of a dynamical relaxation data assimilation scheme for a catchment hydrological model, *Hydrol Process*, 20, 549-563, 10.1002/hyp.5921, 2006.~~
- ~~Iwema, J., Rosolem, R., Baatz, R., Wagener, T., and Bogaen, H. R.: Investigating temporal field sampling strategies for site-specific calibration of three soil moisture-neutron intensity parameterisation methods, *Hydrol Earth Syst Sc.* 19, 3203-3216, 10.5194/hess-19-3203-2015, 2015.~~
- 15 Jackson, T. J., Le Vine, D. M., Hsu, A. Y., Oldak, A., Starks, P. J., Swift, C. T., Ishak, J. D., and Haken, M.: Soil moisture mapping at regional scales using microwave radiometry: The Southern Great Plains Hydrology Experiment, *Ieee T Geosci Remote*, 37, 2136-2151, Doi 10.1109/36.789610, 1999.
- ~~Kerr, Y. H., Waldteufel, P., Richaume, P., Wigneron, J. P., Ferrazzoli, P., Mahmoodi, A., Al Bitar, A., Cabot, F., Gruhier, C., Juglea, S. E., Leroux, D., Mialon, A., and Delwart, S.: The SMOS Soil Moisture Retrieval Algorithm, *Ieee T Geosci Remote*, 50, 1384-1403, Doi 10.1109/Tgrs.2012.2184548, 2012.~~
- 20 ~~Kirkpatrick, J. B., Green, K., Bridle, K. L., and Venn, S. E.: Patterns of variation in Australian alpine soils and their relationships to parent material, vegetation formation, climate and topography, *Catena*, 121, 186-194, 10.1016/j.catena.2014.05.005, 2014.~~
- Kohli, M., Schron, M., Zreda, M., Schmidt, U., Dietrich, P., and Zacharias, S.: Footprint characteristics revised for field-scale soil moisture monitoring with cosmic-ray neutrons, *Water Resour Res*, 51, 5772-5790, 10.1002/2015WR017169, 2015.
- 25 ~~Korres, W., Reichenau, T. G., Fiener, P., Kovama, C. N., Bogaen, H. R., Comelissen, T., Baatz, R., Herbst, M., Diekkruger, B., Vereecken, H., and Schneider, K.: Spatio-temporal soil moisture patterns - A meta-analysis using plot to catchment scale data, *J Hydrol*, 520, 326-341, 10.1016/j.jhydrol.2014.11.042, 2015.~~
- Koster, R. D., Dirmeyer, P. A., Guo, Z. C., Bonan, G., Chan, E., Cox, P., Gordon, C. T., Kanae, S., Kowalczyk, E., Lawrence, D., Liu, P., Lu, C. H., Malyshev, S., McAvaney, B., Mitchell, K., Mocko, D., Oki, T., Oleson, K., Pitman, A., Sud, Y. C., Taylor, C. M., Versegny, D., Vasic, R., Xue, Y. K., Yamada, T., and Team, G.: Regions of strong coupling between soil moisture and precipitation, *Science*, 305, 1138-1140, DOI 10.1126/science.1100217, 2004.
- 30 Kumar, S. V., Reichle, R. H., Harrison, K. W., Peters-Lidard, C. D., Yatheendradas, S., and Santanello, J. A.: A comparison of methods for a priori bias correction in soil moisture data assimilation, *Water Resour Res*, 48, Artn W03515 Doi 10.1029/2010wr010261, 2012.
- 35 Kurtz, W., He, G. W., Kollet, S. J., Maxwell, R. M., Vereecken, H., and Franssen, H. J. H.: TerrSysMP-PDAF version 1.0): a modular high-performance data assimilation framework for an integrated land surface-subsurface model, *Geosci Model Dev*, 9, 1341-1360, 10.5194/gmd-9-1341-2016, 2016.
- Lawrence, D. M., and Slater, A. G.: Incorporating organic soil into a global climate model, *Clim Dynam*, 30, 145-160, 10.1007/s00382-007-0278-1, 2008.
- 40 Lee, J. H.: Spatial-Scale Prediction of the SVAT Soil Hydraulic Variables Characterizing Stratified Soils on the Tibetan Plateau from an EnKF Analysis of SAR Soil Moisture, *Vadose Zone J*, 13, 10.2136/vzj2014.06.0060, 2014.
- ~~Liu, J. J., Fung, I., Kalnay, E., Kang, J. S., Olsen, E. T., and Chen, L.: Simultaneous assimilation of AIRS Xco(2) and meteorological observations in a carbon-climate model with an ensemble Kalman filter, *J Geophys Res Atmos*, 117, Artn D05309, 10.1029/2011jd016642, 2012.~~
- 45 ~~Lv, L., Franz, T. E., Robinson, D. A., and Jones, S. B.: Measured and Modeled Soil Moisture Compared with Cosmic Ray Neutron Probe Estimates in a Mixed Forest, *Vadose Zone J*, 13, 10.2136/vzj2014.06.0077, 2014.~~
- ~~Miyoshi, T., and Kunii, M.: The Local Ensemble Transform Kalman Filter with the Weather Research and Forecasting Model: Experiments with Real Observations, *Pure Appl Geophys*, 169, 321-333, 10.1007/s00024-011-0373-4, 2012.~~
- 50 Montzka, C., Canty, M., Kunkel, R., Menz, G., Vereecken, H., and Wendland, F.: Modelling the water balance of a mesoscale catchment basin using remotely sensed land cover data, *J Hydrol*, 353, 322-334, DOI 10.1016/j.jhydrol.2008.02.018, 2008.



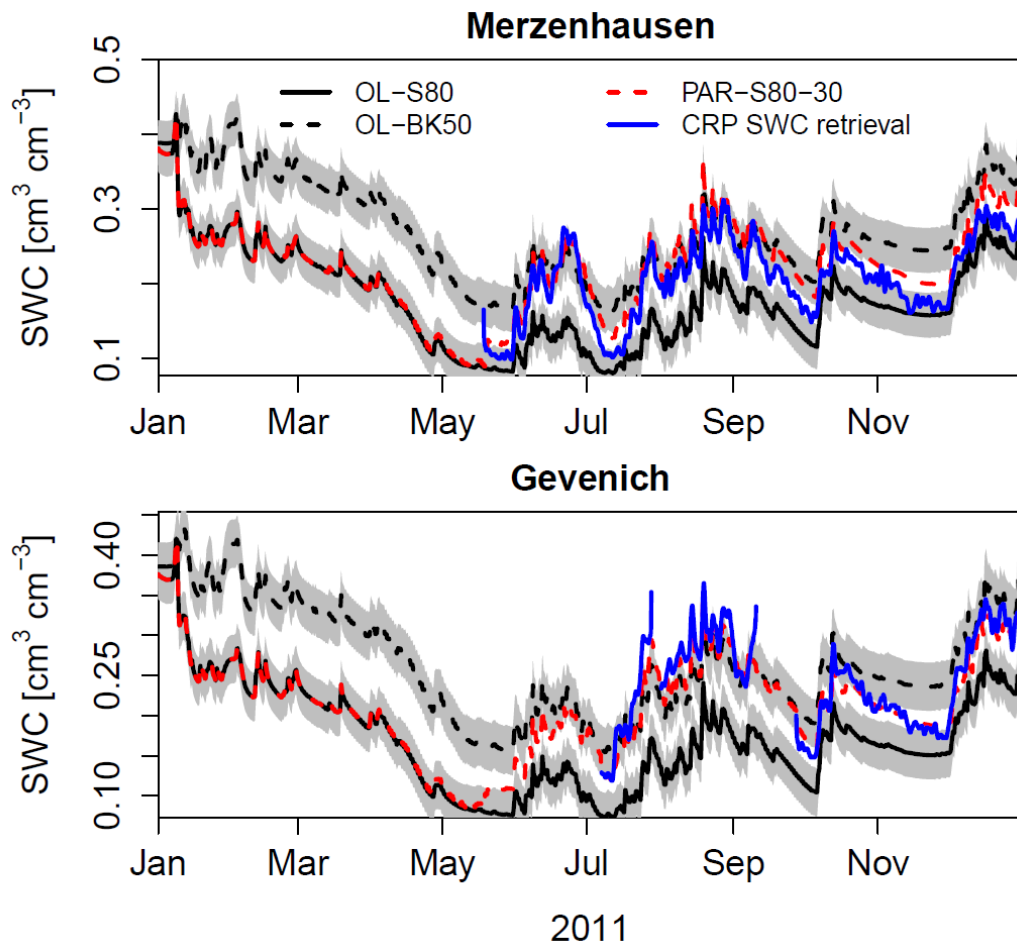
- Seneviratne, S. I., Corti, T., Davin, E. L., Hirschi, M., Jaeger, E. B., Lehner, I., Orlowsky, B., and Teuling, A. J.: Investigating soil moisture–climate interactions in a changing climate: A review, *Earth-Science Reviews*, 99, 125-161, <http://dx.doi.org/10.1016/j.earscirev.2010.02.004>, <http://dx.doi.org/10.1016/j.earscirev.2010.02.004>, 2010.
- 5 | ~~Sheffield, J., and Wood, E. F.: Global trends and variability in soil moisture and drought characteristics, 1950–2000, from observation driven Simulations of the terrestrial hydrologic cycle, *J Climate*, 21, 432–458, 10.1175/2007JCLI1822.1, 2008.~~
- Shi, Y. N., Davis, K. J., Zhang, F. Q., Duffy, C. J., and Yu, X.: Parameter estimation of a physically based land surface hydrologic model using the ensemble Kalman filter : A synthetic experiment, *Water Resour Res*, 50, 706-724, 10.1002/2013wr014070, 2014.
- 10 | Shi, Y. N., Davis, K. J., Zhang, F. Q., Duffy, C. J., and Yu, X.: Parameter estimation of a physically-based land surface hydrologic model using an ensemble Kalman filter: A multivariate real-data experiment, *Adv Water Resour*, 83, 421-427, 10.1016/j.advwatres.2015.06.009, 2015.
- Shrestha, P., Sulis, M., Masbou, M., Kollet, S., and Simmer, C.: A Scale-Consistent Terrestrial Systems Modeling Platform Based on COSMO, CLM, and ParFlow, *Mon Weather Rev*, 142, 3466-3483, 10.1175/Mwr-D-14-00029.1, 2014.
- 15 | Shuttleworth, J., Rosolem, R., Zreda, M., and Franz, T.: The COSmic-ray Soil Moisture Interaction Code (COSMIC) for use in data assimilation, *Hydrol Earth Syst Sc*, 17, 3205-3217, DOI 10.5194/hess-17-3205-2013, 2013.
- Simmer, C., Thiele-Eich, I., Masbou, M., Amelung, W., Bogen, H., Crewell, S., Diekkruger, B., Ewert, F., Franssen, H. J. H., Huisman, J. A., Kemna, A., Klitzsch, N., Kollet, S., Langensiepen, M., Lohnert, U., Rahman, A. S. M. M., Rascher, U., Schneider, K., Schween, J., Shao, Y. P., Shrestha, P., Stiebler, M., Sulis, M., Vanderborcht, J., Vereecken, H., van der Kruk, J., Waldhoff, G., and Zerenner, T.: MONITORING AND MODELING THE TERRESTRIAL SYSTEM FROM PORES TO
- 20 | CATCHMENTS The Transregional Collaborative Research Center on Patterns in the Soil-Vegetation-Atmosphere System, *B Am Meteorol Soc*, 96, 1765-1787, 10.1175/Bams-D-13-00134.1, 2015.
- Song, X. H., Shi, L. S., Ye, M., Yang, J. Z., and Navon, I. M.: Numerical Comparison of Iterative Ensemble Kalman Filters for Unsaturated Flow Inverse Modeling, *Vadose Zone J*, 13, 10.2136/vzj2013.05.0083, 2014.
- 25 | Sun, Y., Hou, Z., Huang, M., Tian, F., and Leung, L. R.: Inverse modeling of hydrologic parameters using surface flux and runoff observations in the Community Land Model, *Hydrol Earth Syst Sc*, 17, 4995-5011, 10.5194/hess-17-4995-2013, 2013.
- Temimi, M., Lakhankar, T., Zhan, X. W., Cosh, M. H., Krakauer, N., Fares, A., Kelly, V., Khanbilvardi, R., and Kumassi, L.: Soil Moisture Retrieval Using Ground-Based L-Band Passive Microwave Observations in Northeastern USA, *Vadose Zone J*, 13, 10.2136/vzj2013.06.0101, 2014.
- 30 | Vereecken, H., Huisman, J. A., Bogen, H., Vanderborcht, J., Vrugt, J. A., and Hopmans, J. W.: On the value of soil moisture measurements in vadose zone hydrology: A review, *Water Resour Res*, 44, Artn W00d06  
Doi 10.1029/2008wr006829, 2008.
- Vereecken, H., Schnepf, A., Hopmans, J. W., Javaux, M., Or, D., Roose, D. O. T., Vanderborcht, J., Young, M. H., Amelung, W., Aitkenhead, M., Allison, S. D., Assouline, S., Baveye, P., Berli, M., Bruggemann, N., Finke, P., Flury, M., Gaiser, T., Govers, G., Ghezzehei, T., Hallett, P., Franssen, H. J. H., Heppell, J., Horn, R., Huisman, J. A., Jacques, D.,
- 35 | Jonard, F., Kollet, S., Lafolie, F., Lamorski, K., Leitner, D., McBratney, A., Minasny, B., Montzka, C., Nowak, W., Pachepsky, Y., Padian, J., Romano, N., Roth, K., Rothfuss, Y., Rowe, E. C., Schwen, A., Simunek, J., Tiktak, A., Van Dam, J., van der Zee, S. E. A. T. M., Vogel, H. J., Vrugt, J. A., Wohling, T., and Young, I. M.: Modeling Soil Processes: Review, Key Challenges, and New Perspectives, *Vadose Zone J*, 15, 10.2136/vzj2015.09.0131, 2016.
- Villareyes, C. A. R., Baroni, G., and Oswald, S. E.: Inverse modelling of cosmic-ray soil moisture for field-scale soil hydraulic parameters, *Eur J Soil Sci*, 65, 876-886, 10.1111/ejss.12162, 2014.
- 40 | Vrugt, J. A., Diks, C. G. H., Gupta, H. V., Bouten, W., and Verstraten, J. M.: Improved treatment of uncertainty in hydrologic modeling: Combining the strengths of global optimization and data assimilation, *Water Resour Res*, 41, Artn W01017  
10.1029/2004wr003059, 2005.
- 45 | Waldhoff, G.: Enhanced land use classification of 2009 for the Rur catchment, in, TR32DB, 2012.
- Whan, K., Zscheischler, J., Orth, R., Shongwe, M., Rahimi, M., Asare, E. O., and Seneviratne, S. I.: Impact of soil moisture on extreme maximum temperatures in Europe, *Weather and Climate Extremes*, 9, 57-67, <http://dx.doi.org/10.1016/j.wace.2015.05.001>, <http://dx.doi.org/10.1016/j.wace.2015.05.001>, 2015.
- 50 | Wu, C. C., and Margulis, S. A.: Feasibility of real-time soil state and flux characterization for wastewater reuse using an embedded sensor network data assimilation approach, *J Hydrol*, 399, 313-325, 10.1016/j.jhydrol.2011.01.011, 2011.
- Wu, C. C., and Margulis, S. A.: Real-Time Soil Moisture and Salinity Profile Estimation Using Assimilation of Embedded Sensor Datastreams, *Vadose Zone J*, 12, 10.2136/vzj2011.0176, 2013.

- Zacharias, S., Bogen, H., Samaniego, L., Mauder, M., Fuss, R., Putz, T., Frenzel, M., Schwank, M., Baessler, C., Butterbach-Bahl, K., Bens, O., Borg, E., Brauer, A., Dietrich, P., Hajnsek, I., Helle, G., Kiese, R., Kunstmann, H., Klotz, S., Munch, J. C., Papen, H., Priesack, E., Schmid, H. P., Steinbrecher, R., Rosenbaum, U., Teutsch, G., and Vereecken, H.: A Network of Terrestrial Environmental Observatories in Germany, *Vadose Zone J*, 10, 955-973, Doi 10.2136/Vzj2010.0139, 2011.
- 5 Zreda, M., Desilets, D., Ferre, T. P. A., and Scott, R. L.: Measuring soil moisture content non-invasively at intermediate spatial scale using cosmic-ray neutrons, *Geophys Res Lett*, 35, 10.1029/2008GL035655, 2008.
- Zreda, M., Shuttleworth, W. J., Zeng, X., Zweck, C., Desilets, D., Franz, T., and Rosolem, R.: COSMOS: the COsmic-ray Soil Moisture Observing System (vol 16, pg 4079, 2012), *Hydrol Earth Syst Sc*, 17, 1065-1066, DOI 10.5194/hess-17-1065-2013, 2012.
- 10

Figures



5 | Fig. 1. Map of the Rur catchment and locations of the nine cosmic-ray probes-neutron sensors. The hilly South of the catchment is prone to more rainfall, lower average temperatures and less potential evapotranspiration than the North of the catchment.



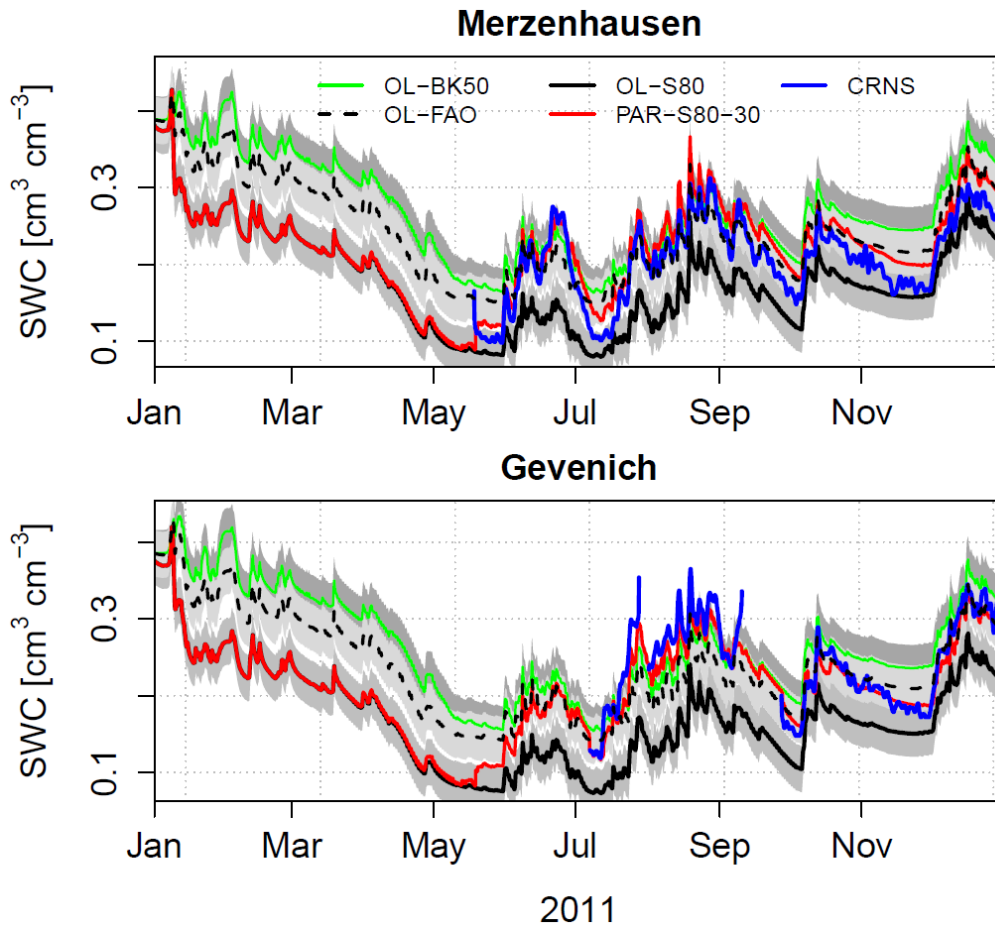
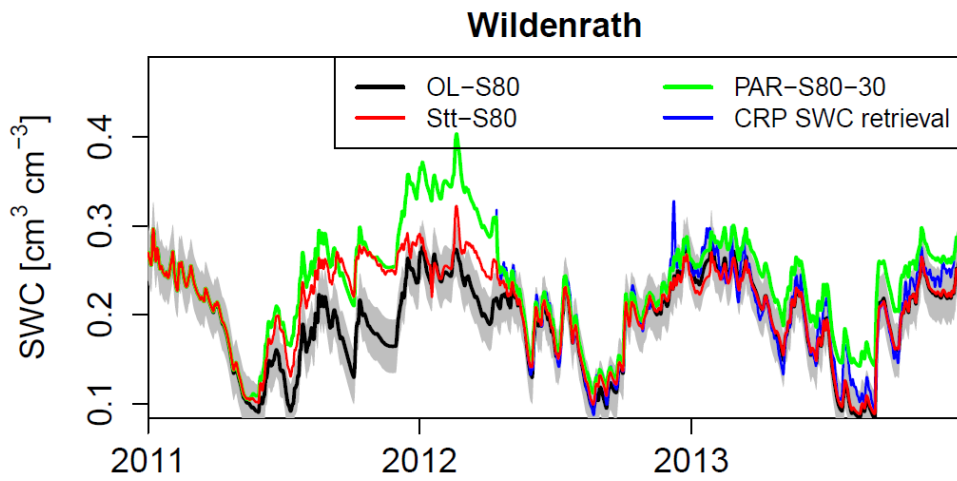
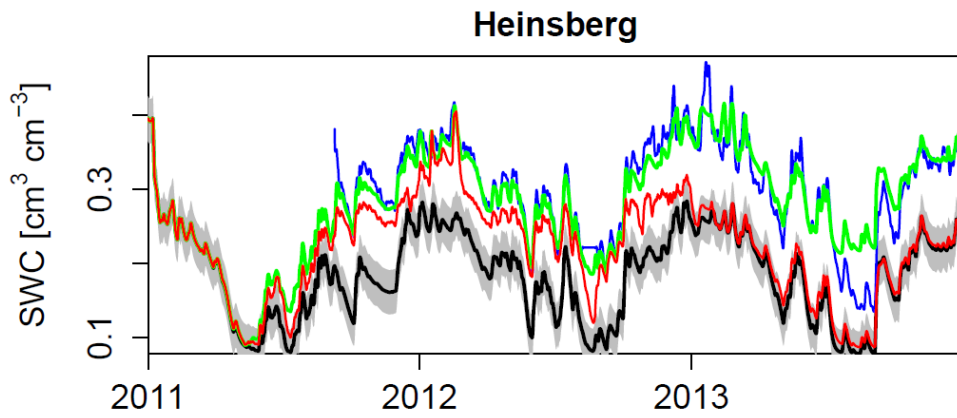


Fig. 2. Temporal evolution of simulated soil water content (SWC) retrievals, calculated with open loop (OL-\*) simulations and data assimilation including parameter updating (PAR-S80-30), together with the CRP-soil-water-content:CRNS SWC retrieval-(SWC) during the first year of simulation at the sites Merzenhausen and Gevenich. Simulated SWC was vertically weighted using the COSMIC operator to obtain the appropriate SWC corresponding to the CRP:CRNS SWC retrieval.



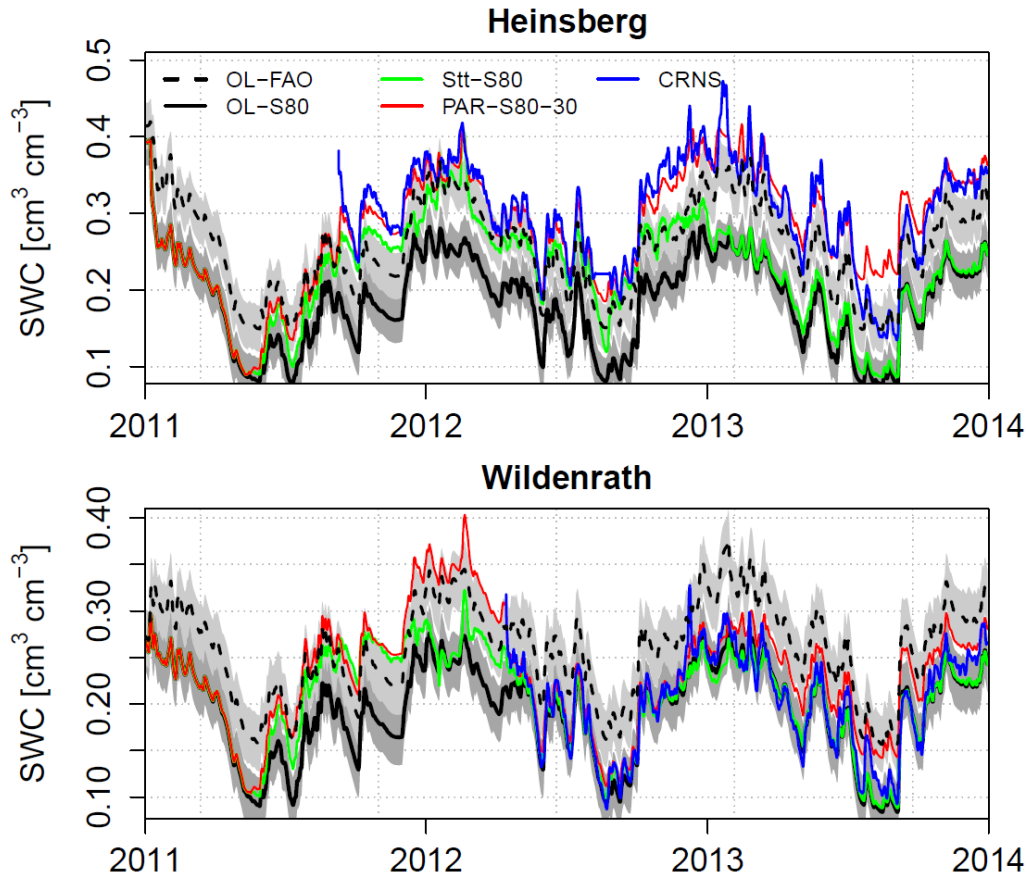


Fig. 3. Temporal evolution of simulated soil water content (SWC) retrievals, calculated with open loop (OL-S80,\*), data assimilation with state update only (Stt-BK50S80), and data assimilation including parameter updating (PAR-S80-30), together with the CRP-soil water content (SWC)CRNS SWC

5 retrieval at the sites Heinsberg and Wildenrath for the data assimilation period 2011 and 2012, and the evaluation period 2013. Simulated SWC was vertically weighted to obtain the appropriate SWC corresponding to the CRPCRNS SWC retrieval.

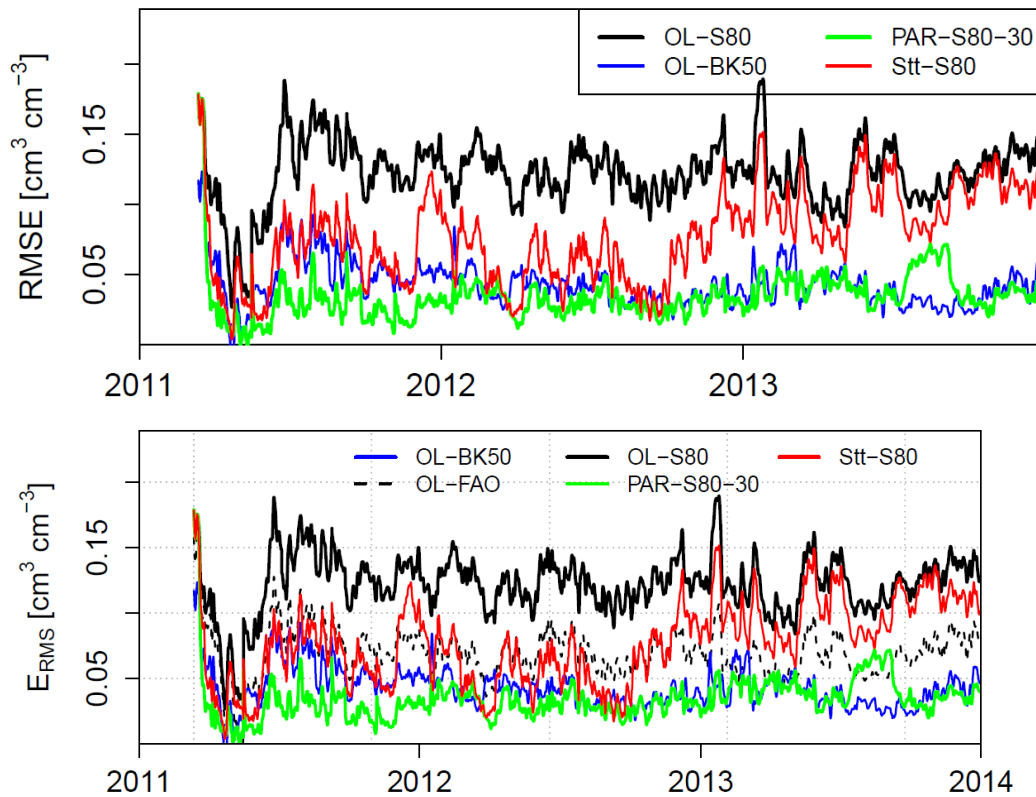
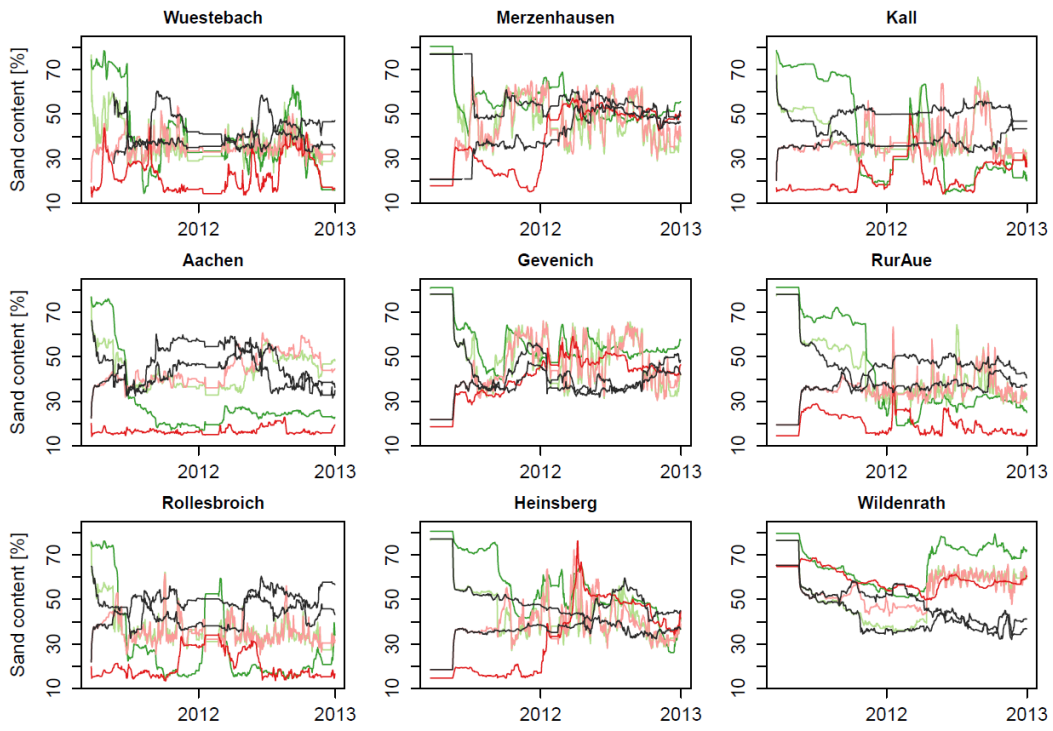


Fig. 4. Temporal evolution of root mean square error ( $E_{\text{RMS}}$ ) for hourly SWC retrievals.  $E_{\text{RMS}}$  is calculated hourly for all nine CRP's-CRNS for open loop (OL-\*) runs for soil maps S80, BK50 and BK50FAO, joint state-parameter updates (PAR-S80-30) and state updates only (Stt-S80) during the assimilation period with joint state-parameter updates (2011 and 2012) and verification period (2013).



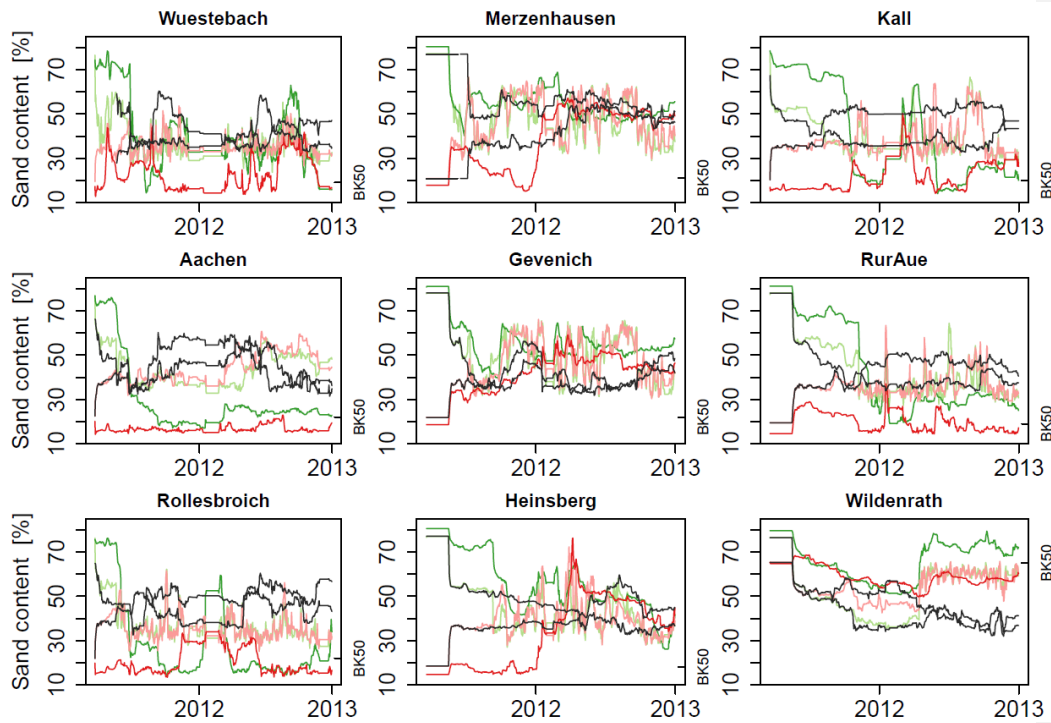
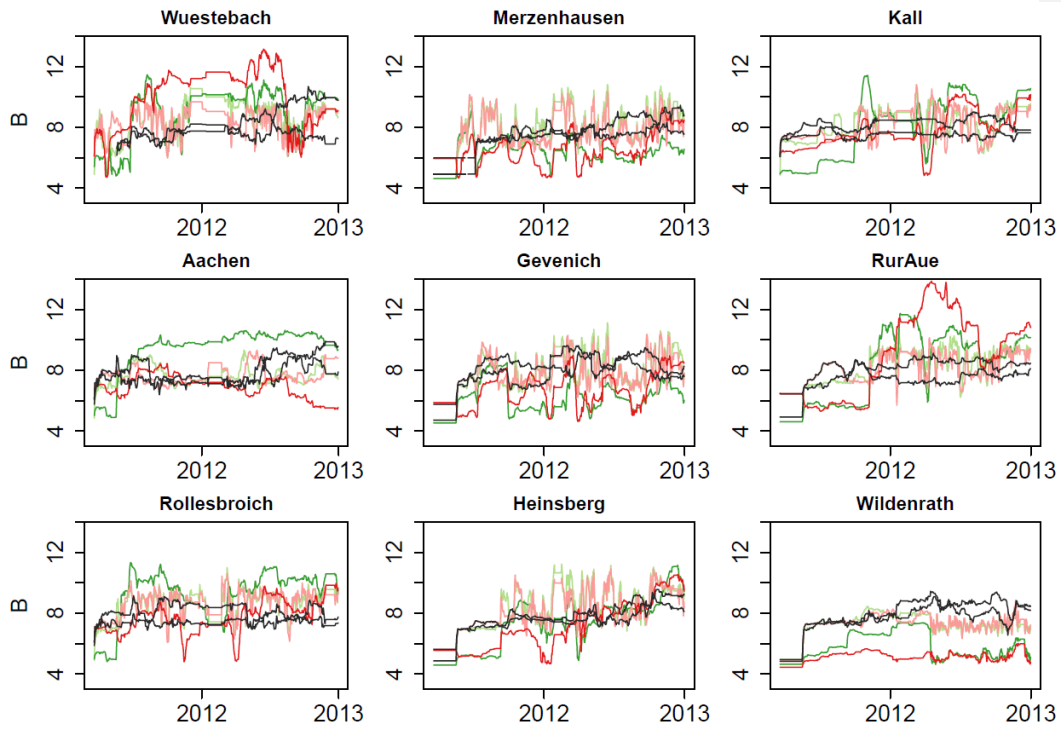


Fig. 5. Temporal evolutionAt nine sites, estimates of the percentage sand content are shown for simulations with parameter update: PAR-S80-30 (green), PAR-S80-10 (light green), PAR-BK50-30 (red), PAR-BK50-10 (light red), ~~jkk8-S80-30\*\_\*~~ (black) and ~~jkk8-BK50-30\*\_\*~~ (black). The value of the BK50 soil map is marked at the second y-axis.

5



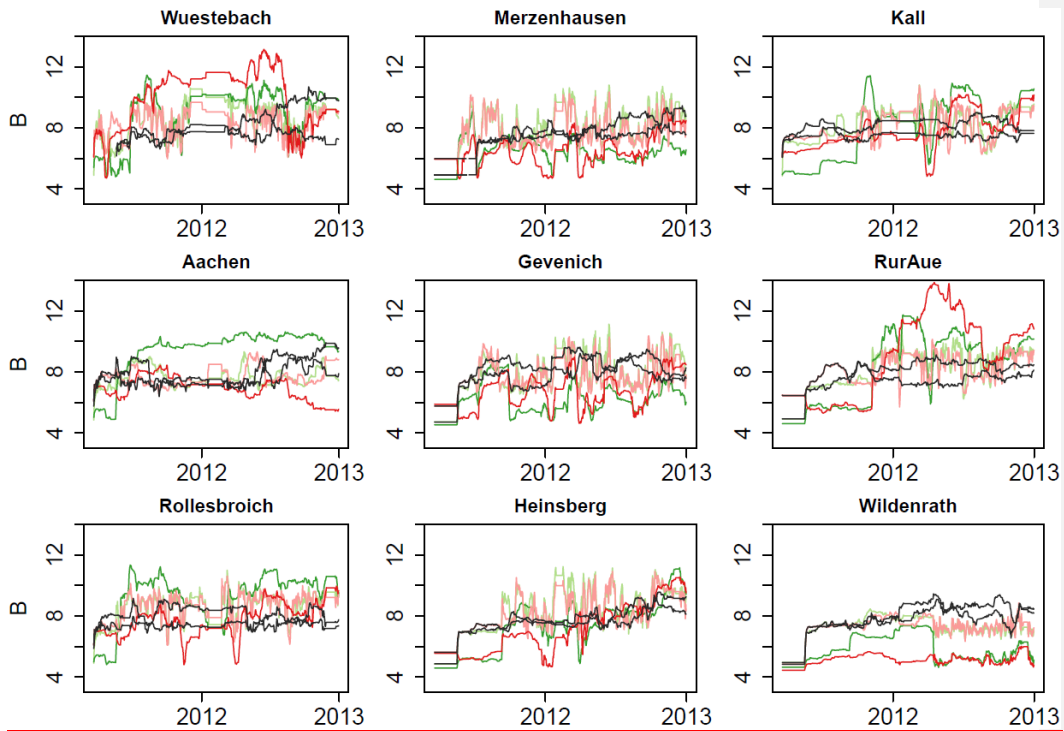
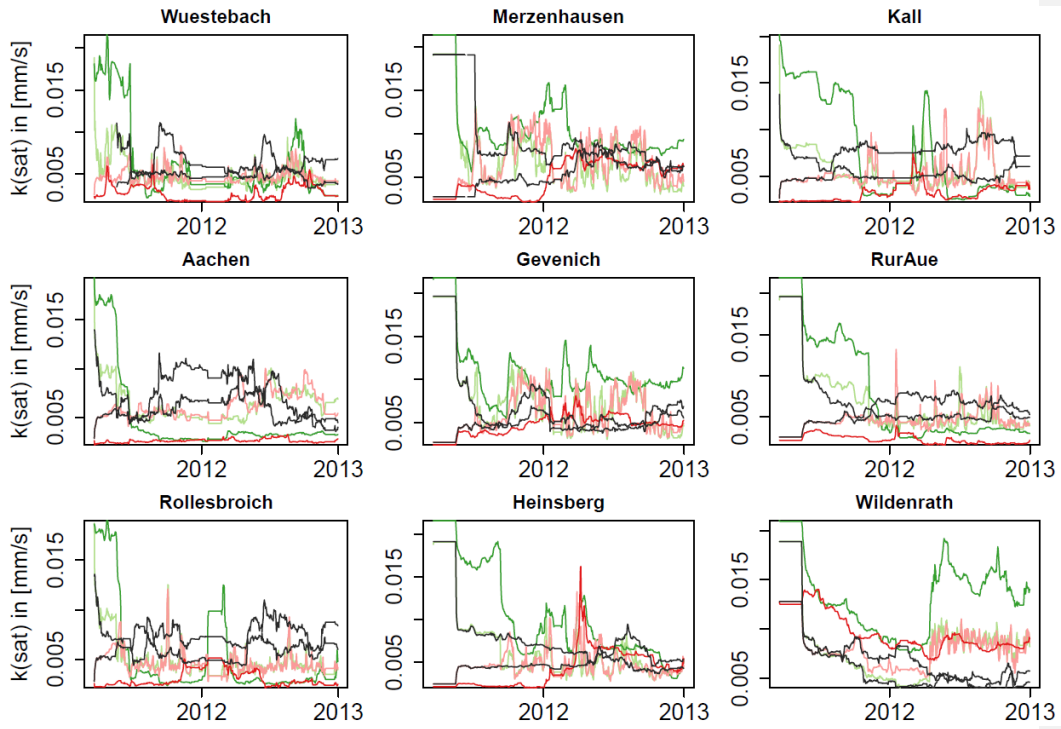


Fig. 6. Temporal evolution at nine sites, estimates of the B parameter (top 15cm) are shown for simulations with parameter update: PAR-S80-30 (green), PAR-S80-10 (light green), PAR-BK50-30 (red), PAR-BK50-10 (light red),  $\mu_{jk}k8-S80-30^{*-*}$  (black) and  $\mu_{jk}k8-BK50-30^{*-*}$  (black).



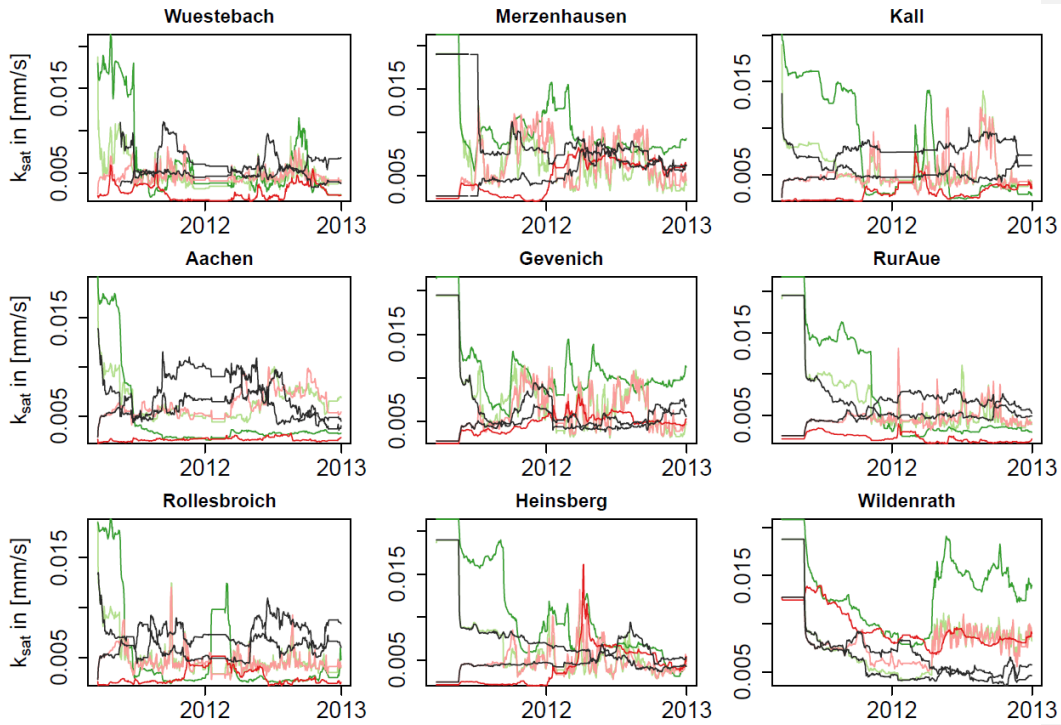
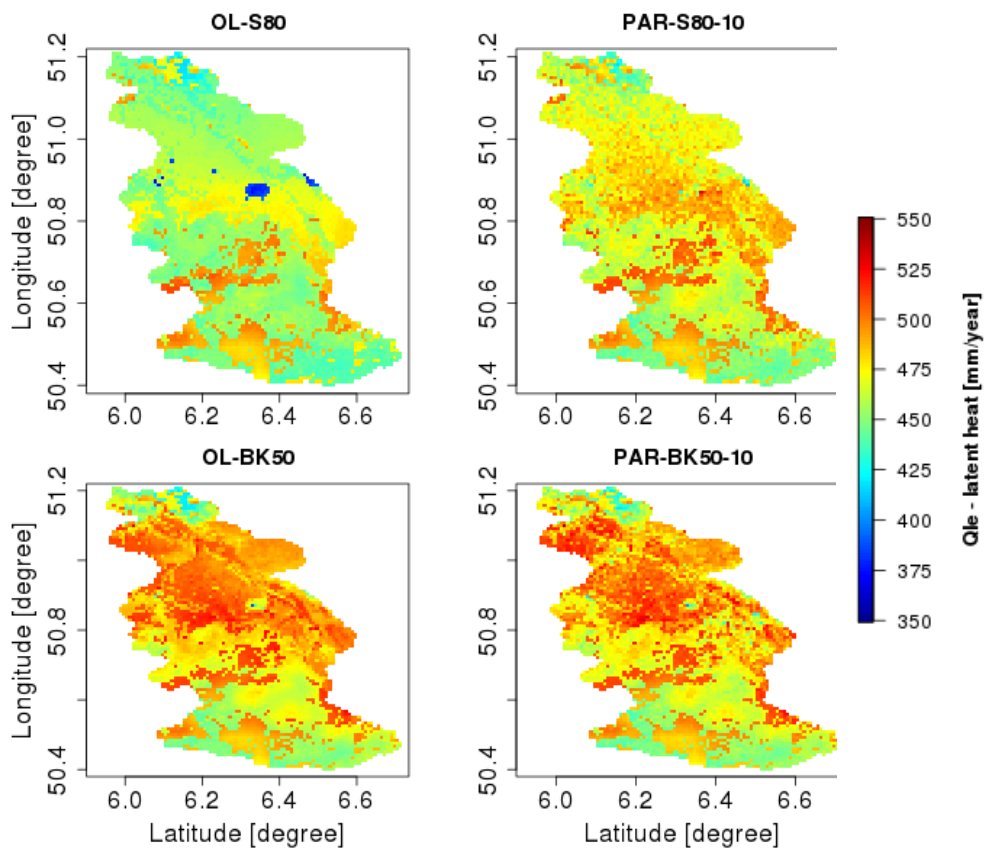


Fig. 7. Temporal evolutionAt nine sites, estimates of saturated hydraulic conductivity (top 15cm) are shown for simulations with parameter update: PAR-S80-30 (green), PAR-S80-10 (light green), PAR-BK50-30 (red), PAR-BK50-10 (light red), ~~j\_k8-S80-30\*~~ (black) and ~~j\_k8-BK50-30\*~~ (black).



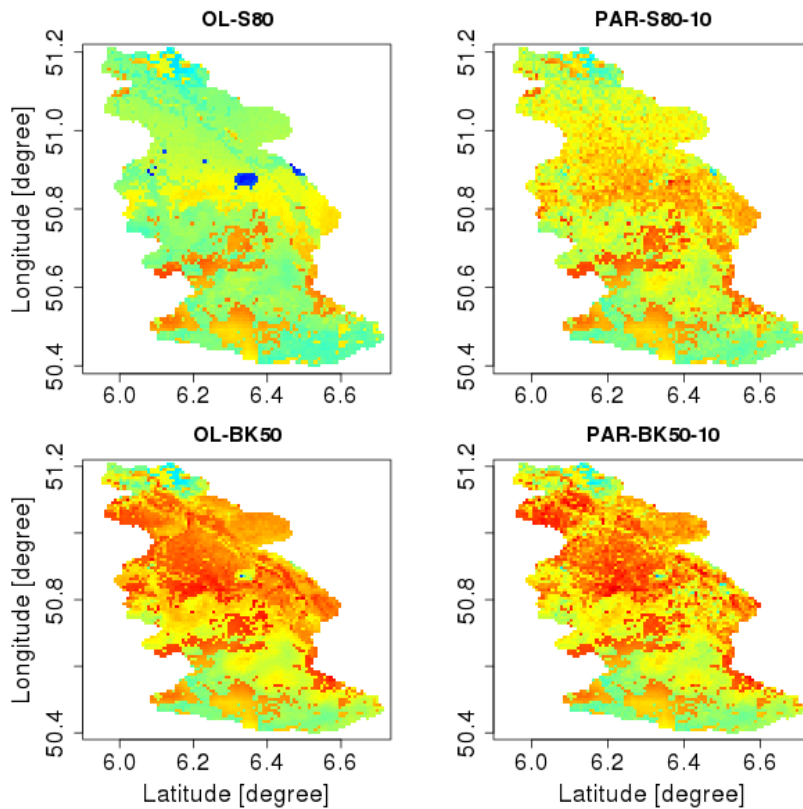


Fig. 8. Annual evapotranspiration (ET) is shown in the year 2013 (evaluation period ~~(year 2013)~~ for simulations OL-S80, OL-BK50, ~~no assimilation~~). This figure demonstrates the impact of parameter updates (PAR-S80-10 and PAR-BK50-10) in comparison to open loop (OL-S80) and reference soil map (OL-BK50). ET changes in the North but not as much in the South.

## Tables

Table 1: Site information on elevation (m.a.s.l.), average annual precipitation (mm/year), CLM plant functional type, [\(Bonan et al., 2002\)](#), sand content (%), clay content (%), and the date of the first SWC retrieval assimilated.

Name	m.a.s.l.	Precip.	Plant functional type	Sand	Clay	Date of first assimilation
Aachen	232	952	Crops	22	23	13.01.2012
Gevenich	108	884	Crops	22	20	07.07.2011
Heinsberg	57	814	Crops	18	19	09.09.2011
Kall	504	935	C3 <del>non-arctic</del> -grass	20	22	15.09.2011
Merzenhausen	94	825	Crops	21	22	19.05.2011
Rollsbroich	515	1307	C3 <del>non-arctic</del> -grass	22	23	19.05.2011
RurAue	102	743	C3 <del>non-arctic</del> -grass	19	26	08.11.2011
Wildenrath	76	856	Broadleaf deciduous temperate tree	65	12	07.05.2012
Wuestebach	605	1401	Needleleaf evergreen temperate tree	19	23	20.03.2011

5

5 Table 2: Overview of simulation scenarios: Open loop (OL-\*) with variation in the soil map BK50-~~or~~<sub>2</sub>, S80 and FAO, data assimilation run with state update (Stt) or joint state- and parameter update (PAR) with variation in the soil map perturbation (-10 ~~or~~<sub>2</sub> and -30), and jackknife evaluation runs (~~jk~~<sub>8</sub>-S80-1 to 9, and ~~jk~~<sub>8</sub>-BK50-1 to 9 and ~~jk~~<sub>4</sub>-S80-A to C).

Simulation Code	Update Soil Perturbation		Sand Content			Soil Perturbation Update	
	State	Parameter	BK50	80 % fix	FAO	Parameter	30
OL-BK50	-	+	+	-	-	-	±
OL-S80	-	+	-	+	-	-	±
<u>OL-FAO</u>					±		±
Stt-BK50	±	+	+	-	+	-	±
Stt-S80	±	+	-	+	+	-	±
PAR-BK50-30	±	+	+	-	+	+	±
PAR-BK50-10	+	±	+	-	+	+	±
PAR-S80-30	±	+	-	+	+	+	±
PAR-S80-10	+	±	-	+	+	+	±
<u>PAR-FAO-30</u>	±	±			±		±
<del>jk</del> <sub>8</sub> -BK50-1 to 9	±	+	+	-	+	+	±
<del>jk</del> <sub>8</sub> -S80-1 to 9	±	+	-	+	+	+	±
<u>jk</u> <sub>4</sub> -S80-A to C	±	±		±			±

Inserted Cells

Inserted Cells

Inserted Cells

5

Table 3--: Root mean square error ( $E_{RMS}$  in  $cm^3/cm^3$ ) and mean absolute bias ( $cm^3/cm^3$ ) for open loop simulations (OL-\*), data assimilation with state updates (Stt-\*) and joint state-parameter updates (PAR-\*) for the assimilation period (2011 and 2012) and the evaluation period (2013). Error and bias was averaged over all sites with observations. Site specific errors and biases are provided in the Annex 1 to 4.

<u>Soil map</u>	<u>Simulation</u>	<u>Site average</u>			
		<u>Data assimilation 2011 &amp; 2012</u>		<u>Evaluation period 2013</u>	
		<u><math>E_{RMS}</math></u>	<u>Absolute bias</u>	<u><math>E_{RMS}</math></u>	<u>Absolute bias</u>
<u>BK50</u>	<u>OL-BK50</u>	<u>0.04</u>	<u>0.02</u>	<u>0.04</u>	<u>0.02</u>
	<b><u>Stt-BK50</u></b>	<b><u>0.03</u></b>	<b><u>0.01</u></b>	<b><u>0.04</u></b>	<b><u>0.01</u></b>
	<u>PAR-BK50-10</u>	<u>0.03</u>	<u>0.01</u>	<u>0.05</u>	<u>0.03</u>
	<u>PAR-BK50-30</u>	<u>0.03</u>	<u>0.01</u>	<u>0.05</u>	<u>0.03</u>
<u>FAO</u>	<u>OL-FAO</u>	<u>0.07</u>	<u>0.06</u>	<u>0.07</u>	<u>0.06</u>
	<b><u>PAR-FAO-30</u></b>	<b><u>0.03</u></b>	<b><u>0.02</u></b>	<b><u>0.05</u></b>	<b><u>0.03</u></b>
<u>Biased (S80)</u>	<u>OL-S80</u>	<u>0.12</u>	<u>0.11</u>	<u>0.12</u>	<u>0.11</u>
	<u>Stt-S80</u>	<u>0.06</u>	<u>0.05</u>	<u>0.10</u>	<u>0.09</u>
	<b><u>PAR-S80-10</u></b>	<b><u>0.03</u></b>	<b><u>0.01</u></b>	<b><u>0.05</u></b>	<b><u>0.03</u></b>
	<b><u>PAR-S80-30</u></b>	<b><u>0.03</u></b>	<b><u>0.02</u></b>	<b><u>0.04</u></b>	<b><u>0.02</u></b>

5

Table 4: Root mean square error ( $E_{RMS}$  in  $cm^3/cm^3$ ) and mean absolute bias ( $cm^3/cm^3$ ) for open loop (OL-\*), jackknife simulations with eight CRNS (simulations jk8-S80-1 to 9 were averaged) and with four CRNS (simulations jk4-S80-A to C). Results were averaged over the omitted sites only. Data at omitted sites was not assimilated while at the other sites data was assimilated. At sites where data was assimilated  $E_{RMS}$  and bias was equal to the values found in simulation PAR-S80-30. Site specific errors and biases are provided in the Annex 1 to 4.

<u>Soil map</u>	<u>Simulation</u>	<u>Site average</u>			
		<u>Data assimilation</u>		<u>Evaluation period</u>	
		<u>2011 &amp; 2012</u>		<u>2013</u>	
		<u><math>E_{RMS}</math></u>	<u>Absolute bias</u>	<u><math>E_{RMS}</math></u>	<u>Absolute bias</u>
<u>BK50</u>	<b><u>OL-BK50</u></b>	<b><u>0.04</u></b>	<b><u>0.02</u></b>	<b><u>0.04</u></b>	<b><u>0.02</u></b>
-	<u>jk8-BK50-1 to 9</u>	<u>0.06</u>	<u>0.04</u>	<u>0.05</u>	<u>0.04</u>
<u>Biased (S80)</u>	<u>OL-S80</u>	<u>0.12</u>	<u>0.11</u>	<u>0.12</u>	<u>0.11</u>
-	<b><u>jk8-S80-1 to 9</u></b>	<b><u>0.06</u></b>	<b><u>0.05</u></b>	<b><u>0.06</u></b>	<b><u>0.04</u></b>
-	<u>jk4-S80-A</u>	<u>0.08</u>	<u>0.06</u>	<u>0.06</u>	<u>0.04</u>
-	<u>jk4-S80-B</u>	<u>0.06</u>	<u>0.05</u>	<u>0.06</u>	<u>0.05</u>
-	<u>jk4-S80-C</u>	<u>0.07</u>	<u>0.05</u>	<u>0.07</u>	<u>0.06</u>

**Annex**

Annex 1:  $E_{RMS}$  ( $cm^3/cm^3$ ) at CRNS  $E_{RMS}$  ( $cm^3/cm^3$ ) at CRP sites for open loop runs and different data assimilation scenarios, for the assimilation period (2011 and 2012). For jackknife experiments (21 in total) only the error of the omitted sites is reported. The best cases are marked bold.

	2011 & 2012	Rollesbroich	Merzenhausen	Geve-nich	Heins-berg	Kall	RurAue	Wueste-bach	
<b>Soil map</b>									Merged Cells
<b>BK50</b>	OL-BK50	<b>0.054058</b>	<b>0.067060</b>	0.039	<b>0.035039</b>	<b>0.042046</b>	<b>0.027034</b>	<b>0.041056</b>	Merged Cells
-	Stt-BK50	<b>0.033031</b>	<b>0.041039</b>	0.021	<b>0.022021</b>	0.030	0.024	<b>0.038039</b>	Merged Cells
-	PAR-BK50-10	<b>0.036033</b>	0.036	<b>0.020</b>	0.019	<b>0.021032</b>	<b>0.033</b>	0.025	0.035
-	PAR-BK50-30	<b>0.031030</b>	<b>0.034032</b>	0.018	<b>0.019018</b>	<b>0.027028</b>	<b>0.023024</b>	0.040	Merged Cells
-	jk8-BK50-1 to 9	<b>0.070067</b>	<b>0.058056</b>	<b>0.073065</b>	<b>0.035033</b>	<b>0.048047</b>	<b>0.050051</b>	<b>0.053062</b>	Merged Cells
<b>FAO</b>	OL-FAO	<b>0.097</b>	<b>0.033</b>	<b>0.029</b>	<b>0.056</b>	<b>0.082</b>	<b>0.096</b>	<b>0.079</b>	Inserted Cells
-	PAR-FAO-30	<b>0.029</b>	<b>0.033</b>	<b>0.018</b>	<b>0.019</b>	<b>0.028</b>	<b>0.025</b>	<b>0.042</b>	Inserted Cells
<b>Biased (S80)</b>	OL-S80	<b>0.170169</b>	<b>0.053054</b>	<b>0.081082</b>	<b>0.117119</b>	<b>0.149152</b>	<b>0.158161</b>	<b>0.065110</b>	Deleted Cells
-	Stt-S80	<b>0.104098</b>	<b>0.020019</b>	<b>0.037036</b>	<b>0.051050</b>	<b>0.082</b>	<b>0.054</b>	0.083   <b>0.056</b> <b>0.060</b>	Inserted Cells
-	PAR-S80-10	<b>0.032031</b>	<b>0.038035</b>	<b>0.024023</b>	0.023	0.033	<b>0.023024</b>	<b>0.036041</b>	Deleted Cells
-	PAR-S80-30	0.029	<b>0.035032</b>	0.018	0.019	<b>0.027028</b>	<b>0.023024</b>	<b>0.039042</b>	Deleted Cells
-	jk8-S80-1 to 9	<b>0.082081</b>	0.038	<b>0.063060</b>	<b>0.026035</b>	<b>0.062068</b>	<b>0.034043</b>	<b>0.038057</b>	Inserted Cells
-	jk4-S80-A	<b>0.064</b>	<b>0.038</b>	<b>0.059</b>	<b>0.076</b>	=	<b>0.157</b>	=	=
-	jk4-S80-B	<b>0.077</b>	<b>0.041</b>	=	<b>0.051</b>	<b>0.062</b>	<b>0.079</b>	=	=
-	jk4-S80-C	=	<b>0.073</b>	<b>0.056</b>	=	<b>0.051</b>	=	=	<b>0.078</b> <b>0.109</b> <b>0.073</b>



**Table Annex 42:**  $E_{RMS}$  ( $cm^3/cm^3$ ) at CRPCRNS-sites for open loop, data assimilation and jackknife simulations on the basis of a comparison with CRPCRNS SWC retrievals during for the verification period (2013). For each jackknife simulation experiments (21 in total) only one  $E_{RMS}$  the error of the omitted sites is reported. The  $E_{RMS}$  of the location that is meant for evaluation best cases are marked bold.

Soil map	Year 2013	Rollebroich	Merzenhausen	Gevenich	Heinsberg	Kall	RurAue	Wuestebach	Aachen	Wildenrath	Average	
											$E_{RMS}$	Merged Cells
											$E_{RMS}$	Merged Cells
BK50	OL-BK50	<u>0.04404</u>	<u>0.06507</u>	<u>0.03604</u>	<u>0.02703</u>	<u>0.04805</u>	<u>0.03804</u>	<u>0.04805</u>	<u>0.04204</u>	<u>0.01702</u>	<u>0.04104</u>	Merged Cells
-	Stt-BK50	<u>0.04104</u>	<u>0.05405</u>	<u>0.03403</u>	<u>0.02703</u>	<u>0.04905</u>	<u>0.03804</u>	<u>0.04805</u>	<u>0.04104</u>	<u>0.01802</u>	<u>0.039</u>	Merged Cells
-	PAR-BK50-10	<u>0.06807</u>	<u>0.06206</u>	<u>0.03604</u>	<u>0.03804</u>	<u>0.05606</u>	<u>0.05606</u>	<u>0.04304</u>	<u>0.05806</u>	<u>0.01702</u>	0.048	Merged Cells
-	PAR-BK50-30	<u>0.05205</u>	<u>0.06106</u>	<u>0.03504</u>	<u>0.03303</u>	<u>0.06807</u>	<u>0.04805</u>	<u>0.04304</u>	<u>0.04805</u>	<u>0.03504</u>	0.047	Merged Cells
-	jk8-BK50*-1 to 9	<u>0.03604</u>	<u>0.04705</u>	<u>0.02804</u>	<u>0.02503</u>	<u>0.04205</u>	<u>0.03104</u>	<u>0.04005</u>	<u>0.05406</u>	<u>0.10611</u>	<u>0.04505</u>	Merged Cells
FAO	OL-FAO	<u>0.08</u>	<u>0.04</u>	<u>0.04</u>	<u>0.05</u>	<u>0.09</u>	<u>0.09</u>	<u>0.07</u>	<u>0.09</u>	<u>0.07</u>	<u>0.068</u>	Merged Cells
-	PAR-FAO-30	<u>0.06</u>	<u>0.06</u>	<u>0.04</u>	<u>0.04</u>	<u>0.06</u>	<u>0.03</u>	<u>0.05</u>	<u>0.07</u>	<u>0.04</u>	<u>0.049</u>	Inserted Cells
Biased (S80)	OL-S80	<u>0.15716</u>	<u>0.06206</u>	<u>0.10611</u>	<u>0.11512</u>	<u>0.16016</u>	<u>0.15415</u>	<u>0.09910</u>	<u>0.16717</u>	<u>0.01902</u>	0.115	Inserted Cells
-	Stt-S80	<u>0.10010</u>	<u>0.06306</u>	<u>0.10711</u>	<u>0.10611</u>	<u>0.09910</u>	<u>0.14615</u>	<u>0.09710</u>	<u>0.15816</u>	<u>0.02002</u>	0.100	Inserted Cells
-	PAR-S80-10	<u>0.06006</u>	<u>0.03904</u>	<u>0.04304</u>	<u>0.04004</u>	<u>0.06406</u>	<u>0.04304</u>	<u>0.05205</u>	<u>0.06006</u>	<u>0.01902</u>	<u>0.047</u>	
-	PAR-S80-30	<u>0.04905</u>	<u>0.05906</u>	<u>0.03704</u>	<u>0.03604</u>	<u>0.05305</u>	<u>0.03203</u>	<u>0.04605</u>	<u>0.04705</u>	<u>0.03504</u>	<u>0.044</u>	
-	jk8-S80*-1 to 9	<u>0.07908</u>	<u>0.04605</u>	<u>0.04204</u>	<u>0.03604</u>	0.059	<u>0.03804</u>	<u>0.06306</u>	<u>0.04404</u>	<u>0.10511</u>	0.057	
-	jk4-S80-A	<u>0.05</u>	<u>0.03</u>	<u>0.05</u>	<u>0.04</u>	-	<u>0.16</u>	-	-	-	<u>0.065</u>	
-	jk4-S80-B	<u>0.05</u>	<u>0.07</u>	-	<u>0.04</u>	<u>0.07</u>	<u>0.07</u>	-	-	-	<u>0.061</u>	
-	jk4-S80-C	-	<u>0.05</u>	<u>0.04</u>	-	<u>0.07</u>	-	-	<u>0.06</u>	<u>0.13</u>	<u>0.069</u>	

Table



<u>jk4-S80-A</u>	<u>-0.05</u>	<u>-0.02</u>	<u>-0.03</u>	<u>-0.06</u>	=	<u>-0.16</u>	=
<u>jk4-S80-B</u>	<u>-0.07</u>	<u>0.02</u>	=	<u>-0.04</u>	<u>-0.05</u>	<u>-0.07</u>	=
<u>jk4-S80-C</u>	<u>-0.07</u>	<u>0.0304</u>	0.02	<u>0.02</u>	<u>0.04</u>	<u>-0.02</u>	=

Deleted Cells

Inserted Cells

Annex 4: Bias (cm<sup>3</sup>/cm<sup>3</sup>) at CRNS-sites for open loop, data assimilation and jackknife simulations compared to CRNS SWC retrievals for the data assimilation period (2011 and 2012). For jackknife experiments (21 in total) only the bias of the omitted sites is reported. The best cases are marked bold.

<u>- Soil map</u>	<u>2013</u>	<u>Rollebroich</u>	<u>Merzenhausen</u>	<u>Geve-nich</u>	<u>Heins-berg</u>	<u>Kall</u>	<u>RurAue</u>	<u>Wueste-bach</u>	<u>Aachen</u>	<u>Wilden-rath</u>	<u>Mean absolute bias</u>
<u>BK50</u>	<u>OL-BK50</u>	<u>-0.03</u>	<u>0.06</u>	<u>0.01</u>	<u>0.00</u>	<u>-0.02</u>	<u>0.00</u>	<u>-0.02</u>	<u>0.01</u>	<u>0.00</u>	<u><b>0.02</b></u>
-	<u>Stt-BK50</u>	<u>-0.01</u>	<u>0.04</u>	<u>0.00</u>	<u>0.00</u>	<u>-0.01</u>	<u>-0.01</u>	<u>-0.02</u>	<u>0.00</u>	<u>-0.01</u>	<u><b>0.01</b></u>
-	<u>PAR-BK50-10</u>	<u>0.06</u>	<u>0.05</u>	<u>0.01</u>	<u>0.02</u>	<u>0.04</u>	<u>0.04</u>	<u>0.02</u>	<u>-0.04</u>	<u>0.00</u>	<u>0.03</u>
-	<u>PAR-BK50-30</u>	<u>0.03</u>	<u>0.05</u>	<u>0.00</u>	<u>0.02</u>	<u>0.04</u>	<u>0.03</u>	<u>-0.01</u>	<u>-0.03</u>	<u>0.03</u>	<u>0.03</u>
-	<u>jk8-BK50-1 to 9</u>	<u>-0.02</u>	<u>0.04</u>	<u>0.01</u>	<u>-0.01</u>	<u>-0.03</u>	<u>-0.02</u>	<u>-0.04</u>	<u>-0.05</u>	<u>0.11</u>	<u>0.04</u>
<u>FAO</u>	<u>OL-FAO</u>	<u>-0.08</u>	<u>0.02</u>	<u>-0.02</u>	<u>-0.04</u>	<u>-0.08</u>	<u>-0.08</u>	<u>-0.05</u>	<u>-0.08</u>	<u>0.06</u>	<u>0.06</u>
-	<u>PAR-FAO-30</u>	<u>0.04</u>	<u>0.05</u>	<u>0.00</u>	<u>0.02</u>	<u>0.03</u>	<u>0.00</u>	<u>-0.02</u>	<u>-0.06</u>	<u>0.03</u>	<u><b>0.03</b></u>
<u>Biased (S80)</u>	<u>OL-S80</u>	<u>-0.15</u>	<u>-0.05</u>	<u>-0.10</u>	<u>-0.11</u>	<u>-0.16</u>	<u>-0.15</u>	<u>-0.09</u>	<u>-0.16</u>	<u>-0.01</u>	<u>0.11</u>
-	<u>Stt-S80</u>	<u>-0.09</u>	<u>-0.05</u>	<u>-0.10</u>	<u>-0.10</u>	<u>-0.08</u>	<u>-0.14</u>	<u>-0.09</u>	<u>-0.15</u>	<u>-0.01</u>	<u>0.09</u>
-	<u>PAR-S80-10</u>	<u>0.04</u>	<u>0.03</u>	<u>-0.03</u>	<u>0.03</u>	<u>0.05</u>	<u>0.03</u>	<u>0.03</u>	<u>-0.04</u>	<u>-0.01</u>	<u><b>0.03</b></u>
-	<u>PAR-S80-30</u>	<u>0.03</u>	<u>0.05</u>	<u>-0.01</u>	<u>0.02</u>	<u>0.03</u>	<u>0.01</u>	<u>-0.01</u>	<u>-0.03</u>	<u>0.03</u>	<u><b>0.02</b></u>
-	<u>jk8-S80-1 to 9</u>	<u>-0.07</u>	<u>0.03</u>	<u>0.02</u>	<u>0.02</u>	<u>-0.05</u>	<u>-0.02</u>	<u>-0.04</u>	<u>-0.03</u>	<u>0.10</u>	<u>0.04</u>
-	<u>jk4-S80-A</u>	<u>0.00</u>	<u>0.01</u>	<u>0.03</u>	<u>-0.03</u>	<u>=</u>	<u>-0.15</u>	<u>=</u>	<u>=</u>	<u>=</u>	<u>0.04</u>
-	<u>jk4-S80-B</u>	<u>-0.03</u>	<u>0.06</u>	<u>=</u>	<u>-0.03</u>	<u>-0.06</u>	<u>-0.06</u>	<u>=</u>	<u>=</u>	<u>=</u>	<u>0.05</u>
-	<u>jk4-S80-C</u>	<u>=</u>	<u>0.04</u>	<u>0.02</u>	<u>=</u>	<u>-0.05</u>	<u>=</u>	<u>=</u>	<u>-0.05</u>	<u>0.13</u>	<u>0.06</u>

5